MODELLING AND VALIDATION OF BEHAVIOUR OF MUSHY STATE ROLLED Al-4.5Cu-5TiB_2 COMPOSITE USING NEURAL NETWORK TECHNIQUES

Thesis

Submitted in partial fulfilment of the requirements for the degree of

DOCTOR OF PHILOSOPHY

By

NIGALYE AKSHAY VITHAL

DEPARTMENT OF MECHANICAL ENGINEERING

NATIONAL INSTITUTE OF TECHNOLOGY

KARNATAKA,

SURATHKAL, MANGALORE -575025

October, 2013

Dedicated to

My Parents, Wife and Children

D E C L A R A T I O N

by the Ph. D. Research Scholar

I hereby declare that the Research Thesis entitled **"*MODELLING AND VALIDATION OF BEHAVIOUR OF MUSHY STATE ROLLED Al-4.5Cu-5TiB_2 COMPOSITE USING NEURAL NETWORK TECHNIQUES"*** which is being submitted to **National Institute of Technology Karnataka, Surathkal** in partial fulfilment of the requirements of award of the degree **Doctor of Philosophy** in **Department of Mechanical Engineering** *is a bonafide report of the research work carried out by me.* The material contained in this Research Thesis has not been submitted to any University or Institution for the award of any degree.

Register Number: ME08P03

Name of the Research Scholar: Nigalye Akshay Vithal

Signature of the Research Scholar:

Department of Mechanical Engineering

Place: NITK- Surathkal

Date: 19-10-2013

CERTIFICATE

This is to certify that the Research Thesis entitled **"*MODELLING AND VALIDATION OF BEHAVIOUR OF MUSHY STATE ROLLED Al-4.5Cu-5TiB$_2$ COMPOSITE USING NEURAL NETWORK TECHNIQUES"*** submitted by **Mr. Nigalye Akshay Vithal (Reg. No. ME08P03)** as the record the of research work carried out by him, is accepted as the Research Thesis submission in partial fulfillment of the requirements for the award of the degree of **Doctor of Philosophy**.

Dr. M. A. Herbert Dr. S. S. Rao

Date: Research Guides Date:

Chairman DRPC:
Date:

Acknowledgement

It has been indeed a great honour for me to work under the guidance of my advisors **Dr. Mervin A. Herbert** and **Dr. Shrikantha S. Rao,** Department of Mechanical Engineering, NITK Surathkal. With deep sense of gratitude and humility, I express my sincere thanks to them for their valuable guidance, untiring perseverance and unending patience which made the research not merely educational but also enjoyable. I also take this opportunity to thank Director, NITK Surathkal and Head of Mechanical Engineering Department NITK Surathkal for allowing me to take carry out my doctoral studies.

I sincerely thank the Research Progress Assessment Committee consisting of Dr. Sitharam Nayak (Civil Engineering Department), Dr. Krishna Prasad (Head of Mechanical Engineering Department), Dr. Mervin Herbert and Dr. Shrikantha Rao for their valuable comments and constructive criticism which has helped the enrichment of this doctoral work. My heartfelt thanks to Dr. Naveen Karanth for his valuable suggestions and constant support during the course of my research work. I am indeed extremely indebted to all of them.

My sincere thanks to Dr. N. S. Reddy and my co research colleague Mr. Conel Rodrigues for rendering their support in coding for the ANN and RNN. I am immensely indebted to the unending help and support I received from my co-research colleagues Mr. Arunkumar Shettigar and Mr. Nagraj Shetty during the course of my research work. I also thank Mr. Vitlapur, Manager Guest House who made my stays at the International Hostel at NITK Surathkal possible.

Mushy state rolling experiments conducted in the Department of Metallurgical and Material Sciences at IIT Kharagpur would not have been possible without the help and guidance of Prof. R. Mitra (Dept. of Metallurgical and Material Sciences, IIT Kharagpur). I express heartfelt gratitude to Prof. R. Mitra for his invaluable guidance and support. I also thank the Head of Department (Metallurgical and material Sciences), IIT Kharagpur for allowing me to use the facilities. My gratitude and thanks also go to Mr. Kamal Kumar Saw fondly referred as *Kamalda* for helping me in conduct of melting and

casting experiments, as well as for his help in the conduct of mushy state rolling experiments. The stay at the Hostel at IIT Khatragpur would not have been comfortable without the help rendered by Mr. Anirudh Jana. I would like to express my sincere thanks to Dr. R. Maiti for providing help in SEM analysis of mushy state rolled samples.

I am indeed grateful to my colleague Prof. Siddesh Salelkar from Computer Engineering department of Goa Engineering College for rendering support in designing a GUI using Microsoft Silverlight (API) educational package. I am indebted to the constant help provided by my colleague Mr. Pushpashil Satardekar and Mr. Akash Kapdi of Computer Centre in sorting out the problems related to computer hardware.

Late Prof. Uday Amonkar, former Head of Mechanical Engineering Department at our Goa Engineering College was my close friend and colleague. Through my student days he has been my friend, philosopher and guide. I thank him for the nurturing environment he created and maintained around me that helped me to complete my research work.

I would fail in my duties if I do not remember the role my friends and close colleagues Dr. V. Mariappan. Dr. R. Prabhu Gaonkar, Dr. P. Savoicar, Prof. M. J. Sakhardande, Prof. M. N. Dhawalikar, Prof. M. Caisukar, Prof. Chetan Desai, Prof. S. Borkar, Prof. A.K.S. Bahadauria, Mr. V. B. Kamat Director of Tech Education, Goa & Ex- Principal and Dr. R. B. Lohani, Principal GEC, and my friend Mr. Rajiv Dhawalikar for their constant support. I would like to specially mention the help provided by Prof. Anant Naik during my visits to NITK Surathkal.

I am indebted to my parents for inculcating in me the right values and virtues. I am extremely grateful to my beloved wife Medha and lovely children Anukool and Akhilesh for enduring a lot of hardships caused on the domestic front due to my research priorities. I wish to express my special thanks to all my siblings, my brothers Arunkumar and Ashok, my sisters Mrs. Usha, Mrs. Shashikala and Mrs. Sudha who were a constant source of motivation and encouragement during the entire course of my doctoral work.

_____

Nigalye Akshay Vithal

Abstract

Aluminium alloy matrix composites reinforced with *in situ* formed TiB_2 particles are found to possess excellent mechanical properties as well as high stability at elevated temperatures. Forming of these composites by conventional methods is difficult due to their tendency of cracking. The problem is overcome by subjecting these composites to mushy state forming. Studies on mushy state rolling of Al-4.5Cu-5TiB_2 composite have witnessed formation of bimodal equiaxed grains having spheroidal morphology from one that is essentially dendritic in as cast condition. Resulting mechanical and wear properties of mushy state rolled Al-4.5Cu-5TiB_2 composite are also observed to be superior to that of as cast composite. The data on the grain sizes, hardness, wear and tensile properties of mushy state rolled composite has been expanded by using neural network techniques. This is done to have better understanding of the relationship between mushy state rolling process parameters and the resulting mechanical and wear properties.

Artificial Neural Networks with feed forward architecture, and trained using backpropagation algorithm have been used to predict bimodal grain sizes, hardness, tensile and wear properties of Al-4.5Cu-5TiB_2 composite rolled from mushy state in as cast and in pre hot rolled condition. The models have been validated by conducting mushy state rolling experiments. The composite samples in as cast and in pre hot rolled condition are mushy state rolled at pre set points within and outside the bounds of data used for training the ANN models. The validity of the models is established by way of comparison of the validation experiment results with the values predicted by models. The ANN models formulated for grain size, hardness, wear and tensile properties prediction are found to predict the corresponding outputs quite accurately, within the acceptable limits of prediction errors.

Artificial Neural Networks though known for non linear mapping of complex systems, are static mapping tools in the sense that the knowledge update is based on static data provided for training the network. Simple recurrent neural networks (SRN) such as the one proposed by Elman have the capacity of dynamic learning. The

computational power of Elman networks has been thought to be comparable to that of finite state machines. However, such extended simple recurrent neural networks when adopted, are found to possess severely hampered learning capabilities due to convergence problems. A novel way of overcoming the problem of convergence is proposed through this work by using a Hybrid Recurrent Neural Network (HRNN) modelled from an ANN. The HRNN is modelled by borrowing weights into an Elman Simple Recurrent Neural Network having similar architecture (devoid of context layers). Such an HRNN formulated is found to converge excellently in a significantly less time as compared to an ANN for the same value of preset MSE. The prediction errors of HRNN and prediction errors resulting from ANN predictions when subjected to statistical testing are found to be equivalent.

The predictions resulting from HRNNs modelled for prediction of duplex grain sizes, hardness, tensile and wear properties are seen to be in close agreement with the predictions made by the ANN models. However, it is seen that the overall time required for training HRNNs which includes the time required for training of partially trained ANNs, is significantly reduced. Thus it is observed that an HRNN modelled from a partially trained ANN has equivalent prediction capability and is superior to ANN in terms of computational time.

Graphical user interface (GUI) has been designed using available API libraries which include two main modules, namely, ANN and RNN. Each model has the sub components for prediction of grain size, hardness, wear rate and tensile properties. There is provision to obtain outputs by manually feeding the input values as well for plotting line graphs by varying one parameter at a time, keeping other parameters constant. The GUI is also designed to generate bar plots by varying each mushy state processing input parameter at a time. Use of GUI is made in optimising the mushy state processing parameters for obtaining the best possible hardness values and minimum wear rate for mushy state rolled Al-4.5Cu-5TiB_2 composite.

Key words: Aluminium alloy matrix composites, Mushy state forming, Artificial Neural Networks (ANN), Elman Simple Recurrent Neural Network (SRN), Hybrid Recurrent Neural Networks (HRNN).

Contents

List of Figures

List of Tables

Nomenclature

DRA	Discontinuously reinforced aluminium alloys
MMC	Metal matrix composites
FEA	Finite Element Analysis
ANN	Artificial neural networks
FFNN	Feed forward neural network
RNN	Recurrent neural network
HRNN	Hybrid recurrent neural network
GUI	Graphical user interface
API	Application programming interface
MLP	Multi layer perceptron
CI	Computational intelligence
NN	Neural networks
SSM	Semi solid metal
MHD	Magnetohydrodynamic
SIMA	Strain induced melt activation
RPA	Recrystallization and partial melting
NRC	New RheoCasting
SSR^{TM}	Semisolid rheocasting
SSTT	Semisolid thermal transformation
PM	Permanent mould casting
SLC	Sub liquidus casting
EM/ES	Electromagnetically stirred
W	Wrought
CS	Cooling slope casting
TR	Thickness reduction per roll pass
LVF	Liquid volume fraction in composite
AI	Artificial intelligence

ART	Adaptive resonance theory
RBN	Radial basis function networks
BP	Back propagation
MSE	Mean squared error
RBF	Radial basis function
SRN	Simple recurrent network
EBP	Elman back propagation
BPTT	Back propagation through time
eEBP	Extended Elman back propagation
ARMA	Autoregressive moving average
CP-Al	Commercially pure aluminium
OES	Optical Emission Spectrometer
SEM	Scanning electron microscope
EDX	Energy dispersive X-ray
H_V	Vicker's hardness number
Exptl	Experimental values
FSM	Finite state machines
LGS	Large grain size
SGS	Small grain size
YS	Yield strength in tension
UTS	Ultimate tensile strength
Pct	Percent
W_s	Weight fraction of the solid phase constituent
Q(T)	Heat absorbed from initiation of melting (J)
T	Temperature of the alloy (K)
ΔH	Heat of melting (J)
f_s	Volume fraction of solid
ρ_s	Density of the solid
ρ_l	Density of the liquid
C_0	Composition

k	Partition coefficient of alloy
m_L	Slope of the liquidus line
T_M	Melting point of the pure solvent
f_1	Liquid volume fraction in composite
X_i	Input to the i^{th} node
w_0	Squashing function
w_i	Weight to the i^{th} neuron
y	Output of a ARMA model
η	Learning rate parameter
α	Momentum term, significance level for one and two sample Kolmogorov – Smirnov test
$\mathbf{x_{min}}$	Minimum value in data range
$\mathbf{x_{max}}$	Maximum value in data range
x_n	Normalised value of input data
x	De-normalised value of input data
o^{k+1}	Output from a neuron
k	Discrete time instant
$\Delta w(t)$	Increase or decrease in weight at time instant t
$\nabla E(t)$	Gradient of error function at time instant t
$\Delta w(t-1)$	Increase or decrease in weight at time instant $(t-1)$
J	Number of hidden layers
M	Number of training input patterns
d	Diameter of indentation
b_{kp}	Targetoutput
$s_{kp}{}^0$	Network output for the k^{th} output neuron for the p^{th} pattern
$E_{tr}(x)$	Mean error in prediction of training data set for output parameter x
$b_k(x)$	Target output for k^{th} neuron
$P_k(x)$	Predicted output of k^{th} neuron for output parameter x
T_{ip}	Target output of i^{th} neuron
O_{ip}	Predicted output for the i^{th} neuron and the p^{th} pattern

$T_i(x)$	Target output for i^{th} neuron
$P_i(x)$	Predicted output of i^{th} neuron
V	Wear volume in mm^3
L	Sliding distance in m
W	Wear rate
W_R	Wear resistance
W_S	Specific wear rate
k	Wear coefficient
μ	Coefficient of friction
F_T	Tangential force in Newton
N	Normal load in Newton
H_0	Acceptance for one and two sample Kolmogorov – Smirnov test
H_1	Rejection for one and two sample Kolmogorov – Smirnov test

Chapter 1

INTRODUCTION

1.1 GENERAL BACKGROUND

The potential of metal matrix composites (MMC) as a new material for engineering use has recently been established. Commercial viability of metal matrix composites, are vigorously investigated, for use in automotives and aircrafts for structural and engine components (Viala and Bouix 1984, Huda *et al*. 1995, Hunt 2000). The recent focus though has been on discontinuously reinforced aluminium alloys (DRA) based MMCs, due to their better strength to weight ratio, high stiffness, high modulus, better thermal stability and their isotropic nature. Recent developments in the *in situ* fabrication of MMCs through chemical reactions have led to better distribution of ceramic reinforcement particles in the aluminium alloy (Herbert 2007, Siddhaligeshwar 2011).

The Al alloys based MMCs are known to encounter difficulties in conventional forming (Lasa *et al.* 2003, Herbert *et al.* 2006, Herbert 2007, Siddhaligeshwar 2011). Mushy state forming as an alternative route to material processing has provided improvement in the forming capabilities of *in* situ MMCs. The studies on mushy state rolling of Al-4.5Cu-5TiB_2 composite (Kiuchi 1989, Herbert *et al.* 2006, Siddhalingeshwar 2011) have shown improvement in the grain morphology, which is essentially dendritic in case of cast MMCs fabricated by *in situ* route. The grains, upon rolling in mushy state, revealed globular morphology and resulted in improvement in the mechanical and wear properties of the composite. Therefore, formability of MMCs in mushy state not only overcomes the difficulty in forming through conventional forming methods, but also improves the mechanical and wear properties of the alloy. In addition, requirement of lower forces in mushy state forming due to lower deformation resistances results in low energy requirements. This proposes mushy state forming as a strong contender for commercial acceptance.

The studies on Al-4.5Cu-5TiB_2 composite were carried out at preselected parameters of mushy state rolling process. Experimental studies were carried out at these conditions to determine duplex grain sizes, hardness, wear and tensile properties of the composite (Herbert 2007). However, commercial viability of manufacturing of mushy state rolled Al-4.5Cu-5TiB_2 composite and the feasibility of mushy state rolling as a manufacturing process for composites needs larger data bank of results corresponding to larger combinations of mushy state rolling conditions, than those obtained by experiments carried out in these studies. Moreover the user industry would like to optimise the process of mushy state rolling to achieve various objectives driven by market demands and select the best possible conditions for achieving the desired output, be it hardness, tensile or wear properties of the composite. Further, it would be in fact worthwhile considering in general, the in process monitoring and control (smart manufacturing) of such processes leading to optimisation of process and product properties.

The engineering approach to solve such issues is to construct a mathematical model. A mathematical model for the process of mushy state rolling of Al-4.5Cu-5TiB_2 composite will involve a number of inputs such as initial state of material, thickness reduction and the volume fraction of liquid in composite when rolling is initiated and so on. The outputs from the model would be grain size, hardness, wear and tensile properties. This results in a complex and non linear input - output relationship. It is difficult to develop such accurate complex and non linear models in the form of mathematical equations (Reddy 2004). Statistical techniques such as linear regression are not suitable for accurate modelling of data, as it exhibits a lot of noise. The method of regression analysis to model non linear data necessitates the use of an equation to transform the data to linear form. This leads to approximation which eventually results in significant error levels in predictions by model. Another method of modelling such systems has been finite element analysis (FEA), which is mathematically quite involved and therefore not user friendly.

Artificial neural networks (ANN) are a mathematical model that mimics the human way of learning the subtle relationships between the outputs and inputs and when

made to learn (trained), generalises the input - output relationship. The model can then be used to map the input - output relationship for any given input. The formulation and use of the model is quite simple but more effective as compared to more involved techniques such as developing a generic mathematical equation or developing other statistical or finite element method models.

1.2 PROPOSED WORK SUMMARY

This thesis is an effort to develop ANN models using Feed Forward Neural Network (FFNN) which can predict mechanical and wear properties of mushy state rolled Al-4.5Cu-5TiB_2 composite, for a given thickness reduction and volume fraction of liquid in the composite during mushy state rolling and to establish the relationship between these properties and input variables. Further, the predictions made by the ANN models are validated by conducting validation experiments within and outside the range of data used for training the ANN models. The predictions made by the models are then analysed with respect to the training as well as validation data to assess the suitability of the ANNs to model the mushy state rolling of Al-4.5Cu-5TiB_2 composite.

Recurrent neural networks (RNN) are known for better convergence characteristics (Elman 1990). However, the use of Elman Simple recurrent network as well as extended Elman network (Kremer 1995, Song *et al.* 2008, Gruning 2006) using back propagation training algorithm led to network getting stuck in local minima. The problem of convergence has also been noticed while modelling the process of mushy state rolling using Elman and extended Elman recurrent neural networks, to predict the grain sizes, hardness, wear and tensile properties. Various strategies were tried out to overcome the problem of Elman extended recurrent neural network which led to the formulation of a Hybrid Recurrent Neural Network (HRNN). The predictions of the HRNNs formulated are shown to be statistically equivalent to the predictions done by using FFNN model. Further, the predictions made by HRNNs modelled for mushy state rolling of Al-4.5Cu-5TiB_2 composite are analysed with those obtained using ANN models. The assessment of the performance of HRNN models with the ANN models provides the decision to accept the HRNN model as an alternative tool for

predictions and input - output mappings, with the added advantage of faster convergence.

1.3 ORGANISATION OF THE THESIS

The entire thesis has been divided into nine chapters, with each chapter devoted to a specific area of the work done while carrying out the entire study on the modelling and validation of mushy state rolled Al-4.5Cu-5TiB_2 composite using neural network techniques. The summary of discussions carried out chapter wise is detailed below.

Chapter 1 presents the historical background as well as the challenges faced and motivation to take up the present work. An overview of the proposed work with specific objectives is also enunciated in this chapter.

Chapter 2 deals with a detailed and critical review of literature in the area of semisolid processing or thixoforming of Al based alloys and composites highlighting the documented knowledge. The experimental studies carried out in mushy state rolling of Al alloy based composites which has led to establishing mushy state rolling as a process that supplements the conventional forming methods is also discussed in this chapter. The chapter also makes a critical review of the current knowledge in the area of neural network techniques as a tool for mapping input – output relationships right from the historical inventions of artificial neuron till the current literature regarding convergence in recurrent neural networks. The thorough and critical analysis of the current knowledge in semisolid or mushy state processing and neural network techniques as a modelling tool has given the direction to the current work. The inspiration obtained from the existing work in these areas has been used to model the mushy state rolling process of Al-4.5Cu-5TiB_2 composite using neural network techniques. The chapter also addresses the need for creating a Graphical User Interface using available GUI/API packages.

Chapter 3 elucidates the selection and characterisation of raw materials for conducting the experiments for validation of the model. The chapter also provides detailed description of the experimental and measurement procedures used for obtaining the

results of validation experiments on mushy state rolling of Al-4.5Cu-5TiB_2 composite. The steps involved in the casting of the alloy and its *in situ* composite, evaluation of volume fraction of liquid in composite at the initiation of rolling, specimen preparation for different experiments, mechanical testing for measurement of hardness and wear rate have also been discussed at length.

Chapter 4 deals with the prediction of bimodal grain sizes of mushy state rolled Al-4.5Cu-5TiB_2 composite, using an ANN. The chapter discusses the formulation of a multi layer perceptron (MLP) or an FFNN with two hidden layers, the outputs of the model being small and large grain sizes of the mushy state rolled composite rolled in as cast, as well as, in pre hot rolled condition. The comparison of outputs from the model with the target outputs has been carried out. The discussions on variation of the grain sizes with respect to composite condition (as cast or pre hot rolled) during initiation of rolling, thickness reduction per roll pass and volume fraction of liquid in the composite are also presented in this chapter. The chapter also discusses the validation of the ANN model by way of comparison of grain sizes obtained from validation experiments with those predicted by the model from the inputs corresponding to validation experiments.

Chapter 5 deals with the formulation and validation of ANN model with FFNN architecture for prediction of hardness of mushy state rolled Al-4.5Cu-5TiB_2 composite. The chapter addresses the performance of this neural network model being modelled for as cast, as well as, pre hot rolled composite mushy state rolled to various thickness reductions and with various liquid volume fractions. The chapter analyses the hardness predictions made by the model with respect to the target values. With the help of curvilinear plots and contour plots, variation of hardness with thickness reduction per roll pass and the volume fraction of liquid, has also been presented in this chapter. The chapter also presents the optimum values of hardness predicted by the model using Microsoft Silverlight (API) application. The chapter also demonstrates the capability of the model to interpolate and extrapolate the values of hardness within and outside the range of data used for training the model.

Chapter 6 illustrates the formulation of ANN model for prediction of tensile properties of mushy state rolled Al-4.5Cu-5TiB_2 composite, rolled in as cast and pre hot rolled condition. The chapter presents the analysis of variation of strength and elongation of mushy state rolled Al-4.5Cu-5TiB_2 composite with different thickness reductions per roll pass and volume fraction of liquid in the composite. The comparisons of model predictions with the target values are presented in the chapter to establish the suitability of the model for prediction of tensile properties of mushy state rolled Al-4.5Cu-5TiB_2 composite.

Chapter 7 is dedicated to formulation and validation of the ANN model with feed forward architecture to predict the wear properties of as cast and pre hot rolled Al-4.5Cu-5TiB_2 composite, rolled from mushy state to various thickness reductions per pass and from different temperatures (corresponding to volume fraction of liquid in composite). The variation of wear rate, wear resistance and specific wear rate of mushy state rolled composite with respect to normal load at various thickness reductions and liquid content in the composite has also been discussed at length in this chapter. The chapter also presents the optimal values of wear rate predicted by the model along with the corresponding values of mushy state rolling process parameters.

Chapter 8 deals with the formulation of an RNN model as a tool that could be used as an improvement over the ANN model. The chapter highlights the problems encountered in formulation of an RNN model to map the input – output data and the strategies to overcome this problem are discussed. The development of HRNN model is discussed at length in this chapter and the statistical analysis of the prediction errors resulting from ANN and HRNN model predictions, leading to statistical equivalence of these models has been presented. The formulation of HRNN models for prediction of grain sizes, hardness, wear and tensile parameters of mushy state rolled Al-4.5Cu-5TiB_2 composite have also been included here. The performance of HRNN models with the corresponding ANN models has also been discussed, establishing the use of HRNN models as prediction tools having capabilities equivalent to ANN models in terms of predictions but being better than ANN models in terms of convergence characteristics.

Chapter 9 presents the overall summary and the major conclusions derived from the present work.

Chapter 2

LITERATURE REVIEW

2.1 INTRODUCTION

A growing demand is being witnessed in recent years for light weight Al based alloys and composites for a large variety of automotive and aerospace applications (Hirt *et al.* 1997). However, these composites pose a challenging task in obtaining complex shapes by conventional forming and machining processes, due to the presence of hard ceramic particles in them. Semisolid processing provides an alternative route to conventional forming methods, and also results in improved mechanical properties through microstructural refinement. Researchers across the globe are doing extensive work in the semisolid processing technology, as it is found to be an excellent way to manufacture intricate shaped parts from composites to near net shapes coupled with improved mechanical properties. Generally, the research findings in the works carried out in any field, result in breakthrough technologies. However, these works mostly emphasize on the viability of a process and for this technological achievement to be commercially acceptable, a large bank of data is required. It is difficult to carry out the quantum of experiments to generate this data, as it may be too time consuming and may not be prudent economically.

Artificial Neural Network (ANN) is a mathematical model used for mapping complex, non linear input output relationships. A tool like ANN can help the research community in expanding the data of experimentations. ANN when properly trained understands the subtle relationships that exist between comparatively small volumes of experimental data available from the research work. The nicely generalized model so developed can then predict the results from unknown inputs and generate the data required for commercial harnessing.

One of the main objectives of this thesis is to present Artificial Neural Network (ANN) as a tool for modelling behaviour of complex metallurgical systems. This

involves the ANN modelling for prediction of microstructural evolution and mechanical properties of mushy state processed aluminium metal matrix composites (MMCs). The model is designed to predict the behaviour of Al-4.5% (wt. %) Cu-5% (wt. %) TiB_2 composite containing varying liquid volume fraction as it is rolled in the mushy state with varying thickness reductions. In view of this the pertinent literature reviewed has been presented in the forthcoming sections of this chapter. The literature reviewed has been categorised broadly under two heads. Firstly, history of evolution of metal matrix composites as a viable alternative to conventional metals and alloys followed by discussions on the recent trends in secondary processing of these composites. Review of mushy state processing of MMCs with in the forthcoming sections presents a strong case for its acceptance for the MMC to be commercially viable as materials for manufacturing and engineering industry. The literature related to Al-4.5Cu alloy and Al-4.5% (wt. %) Cu-5% (wt. %) TiB_2 composite has also been reviewed to underline its importance as an important emerging material. Secondly, the literature pertaining to an important component of Computational Intelligence (CI), the neural networks (NN), has been presented in respect of its invention, development, computational capability and application to engineering fields with greater emphasis on engineering metallurgy.

2.2 SEMISOLID PROCESSING

The relevance and the importance of ANN modelling for metallurgical systems are discussed in this section. In the present study the ANN is being modelled to understand the behaviour of *in situ* manufactured Al-4.5Cu-5TiB_2 composite rolled to different thickness reductions in mushy state with various volume fractions of liquid content in the composite. Therefore, this section deals with the critical review of the current literature in the field of thixoforming or mushy state forming of Al based alloys composites. The review is presented under the following detailed heads.

- Fundamentals of semisolid processing
- Evolution of thixotropy
- Microstructural evolution during partial holding and isothermal holding
- Mechanism of non dendritic microstructure formation

- Methods to form spheroidal microstructure
- Flow behaviour of mushy metal
- Volume fraction evaluation
- Semisolid processing methods
- Applications of semisolid processing
- Mechanical properties
- Wear properties

2.3 FUNDAMENTALS OF SEMISOLID PROCESSING

Processing of metals in semisolid state is a recent breakthrough in technology which involves forming of metals in semisolid state to near net shape components. The starting material in the conventional methods is either in solid state (e.g. powder metallurgy, sheet metal forming) or in liquid state (casting process). As against this, slurry of metal which contains a fraction of the metal in liquid state is used as the starting material in semisolid metal (SSM) processing as reported in the work by Fan (2002). The semisolid slurry is formed due to the dispersion of solid particles in viscous liquid matrix as reviewed in the work by Z. Fan and M. Flemings (Flemings 1991, Fan 2002).

Previously, it was believed that solidification is a natural process in metals and alloys of given composition, by rapid solidification process brought about by accelerated cooling. Discovery of semisolid processing technique has made it possible to manipulate the solidification process by using external means, so that desired microstructure can be obtained yielding improved mechanical properties (Fan 2002). The discovery of the semisolid processing route was rather more of an accident than an actual research attempt (Flemings 1991). In the year 1971 (Spencer 1972, Flemings 1991), Spencer carried out hot tearing tests on Sn – 15% Pb alloy. During the course of the experiment related to viscosity measurement of the semisolid alloy, it was observed that the shearing started above the liquidus, and continued on slow cooling in the semisolid (mushy) region, till the solidification was nearly complete as reviewed in (Flemings 1991). Due to shear thinning, the viscosity of the alloy reduced, making it behave more like a fluid, resulting in the prevention of formation

of dendrites and prevention of accompanying solute segregation (Spencer 1972, Flemings 1991). This led to the discovery of a semisolid alloy having a liquid fraction of 0.4, devoid of dendritic structure, behaving like a fluid (Spencer 1972), and having viscosity less than that of olive oil (Flemings 1991). The viscosity of the resulting semisolid was found to be significantly lower if the semisolid alloy is subjected to continuous agitation while cooling as against if the cooling was carried out without agitation (Flemings 1991, Fan 2002 and Atkinson 2005). Moreover, it has been reported (Cho and Kang 2000) that semisolid forming brings about significant refinement of microstructure, which in turn leads to better mechanical properties.

Semisolid processing is broadly classified into two routes namely 'rheocasting' and 'thixocasting'. Rheocasting was for the first time discovered by Fleming (1992) and his co-workers and was proposed as a process involving the control of rheological properties of the semisolid alloy. Rheocasting involves the agitation of the semisolid alloy which causes the breaking up of dendrites. The structure formed upon agitation consists of spheroids of solid surrounded by liquid. Further, when this alloy without dendrites is allowed to rest, the spheroids agglomerate and cause increase in viscosity of the semisolid alloy with time. Thus, a non dendritic alloy with 30-50% liquid content, containing solid phase in form of agglomerated spheroids, can support its own weight, maintain its shape and act like a solid. If on the other hand the agglomerated solid is sheared, agglomerations break up and viscosity is decreased as reviewed by Atkinson (Atkinson 2005). This continues till a steady state condition is reached for given solid fraction (Joly and Mehrabian 1976). 'Thixotropy' can be defined as the property of time dependence of viscosity at constant shear rate. The thixotropic properties are (achieved) due to the non dendritic microstructure of the alloy, once the alloy is heated in the semisolid range. The thixotropic property is made use of in semisolid processing (Kirkwood 1994, Atkinson 2005), especially for the thixocasting process. The word 'thixo' means reheating while the word casting indicates that the liquid content in the alloy is relatively high, i.e. above 50% (Moschini 1996). In 'thixocasting' the alloy with a processing prehistory of non dendritic microstructure is heated to semisolid range and is then cast in dies as reviewed in (Atkinson2005). In the first step during the thixocasting process, the feed

stock material of non dendritic microstructure is prepared. In the next step, this material which exhibits thixotropic behaviour is reheated to mushy state to produce SSM slurry. This slurry is then used for component forming. Thixoforming is the term used for the process which involves the near net shape forming from a non-dendritic alloy feed stock, which is reheated to mushy state within a metal die.

In the initial period of research, the focus was on semisolid processing of steels as steel was the major material used in engineering industries and the casting temperatures for steel could be reduced by semisolid processing. But due to oil crisis in 80's followed by environmental concerns taking centre stage in 90's and the first decade of 21st century, the need was felt for lighter materials. Therefore, the processing of Al alloys has acquired a lot of focus and attention in semisolid processing. It has taken about 40 years of extensive research and development to establish the feasibility of SSM processing. After 40 years of extensive research, the semisolid processing technology has today established itself as a commercially viable technology having strong technological background for producing metallic components, having intricate and complex shapes with high integrity, improved mechanical properties and with tight tolerances (Fan 2002). As a matter of fact, the SSM has opened the doors towards further research in technological refinement in SSM processing to be adapted commercially on a large scale.

In case of thixotropic fluids, the shear stress is not proportional to shear rate. Therefore they are termed as non-Newtonian fluids. In general, the rheological behaviour of slurries in semisolid state is a function of shear rate, solid fraction in the alloy, soaking time at high temperatures and the rate of cooling (Spencer 1972, Joly 1976, Suery *et al.*1996). The viscosity of the slurry at a given solid fraction was found to decrease with the decrease in the rate of cooling and increase in the shear rate (Joly 1976). Turng and Wang (1991) have shown that the steady state viscosity of semi-solid slurry having fixed solid fraction decreases with increase in shear rate and the variation becomes asymptotic, as the shear rate approaches infinity. This finding of the pseudo-plastic behaviour of slurries with fixed solid fraction has also been confirmed by other researchers as well (Lehuy, *et al.* 1985, Taha *et al.* 1988,

Kattamis, and Piccone 1991, Ito *et al.* 1992, Flemings *et al.* 1992). Lately, Quaak *et al.* (1996) have shown that at a given shear rate, the steady state viscosity depends on the quantum of agglomeration between solid particles. The degree of agglomeration depends on the dynamic equilibrium achieved between the agglomeration and de-agglomeration process. Now it is broadly accepted that alloys which have recrystallized prior to semisolid processing show lower viscosities than those with dendritic structures (Ferrante and DeFreitas 1999). The rate of increase of apparent viscosity with increase in solid fraction in slurry is observed to be high at high solid fraction and found to be low at low solid fraction.

Another important criterion in understanding the steady state pseudo-plastic behaviour of the semisolid alloy is "yield", which has not been understood quite clearly so far (Barnes *et al.* 1989, Harnett *et al.* 1989, Bartels *et al.* 1997). A limited data on yield strength (Sigworth 1996, Peng and Wang1996) of mushy state Mg (Sannes *et al.* 1994) and Sn-15Pb alloys (Modigell 2000) is available. There have been question marks on the ability of thixotropic material exhibiting yield stress (Mclelland *et al.* 1997). Koke and Modigell (2003) have measured the static and dynamic yield stress of Sn-15% alloy. A predominance of agglomeration has been witnessed after shear rate drop and de-agglomeration is observed after a shear rate jump (Martin *et al.* 1994, Mar, Mada, and Ajersch 1996a, 1996b, Modigell *et al.* 1999).

2.4 EVOLUTION OF THIXOTROPY

Flocculated suspensions and semi-solid systems have many things in common. In a semisolid system, the colliding particles agglomerate together. The particles with low energy boundary orientation preference will prefer agglomeration as compared to particles oriented to form high energy boundary. If a three dimensional network is formed throughout the structure, the semisolid will support its own weight and act like a solid. When shear rate is increased, the bond between the agglomerated particles breaks causing a decrease in the size of the agglomerate. The agglomerated particles sinter once the bonds are formed. Although thixotropic materials exhibit reversibility,

the evolution of particle shape and size with time of stirring is not reversible in the semisolid alloy slurry (Atkinson2005).

2.5 MICROSTRUCTURAL EVOLUTION DURING PARTIAL REMELTING AND ISOTHERMAL HOLDING

In the recent years, microstructural evolution of semisolid state during isothermal holding has received significant attention (Loue *et al*. 1992, Sannes *et al.* 1994b, Loue and Suery 1995, Braccini *et al.* 1998, Geblin *et al.* 1999, Zoqui and Robert 2001). The rate at which grain coarsening takes place increases with decreasing solid fraction with the major contribution at high solid fraction being from coalescence ripening while the major contributor at low solid fraction being Ostwald ripening (Sannes *et al.* 1994). From the studies on the effect of thermomechanical treatment of A357 alloy, it is revealed (Loue and Suery 1995) that grain density increases with increased holding time during partial remelting, provided that the initial structure is globular and that the grain density does not change in the case in which initial structure is dendritic. It is also reported that grain coarsening mechanism is accelerated with larger solidification time as well as smaller initial grain size. Blais *et al.* (1996) have reported that spheroidal grains evolve from solid phase, irrespective of the initial grain morphology. Further to this, Hong *et al.* (2000), based on their research work on Mg alloy based composites, have reported that globular grain morphology evolves from solid phase in the presence of SiC particles. Moreover, with the increase in the volume fraction of SiC particles, size of the globular grains decreases. The formation of globular grain structure during isothermal holding is dealt with further in section 2.6.

Another phenomenon observed during partial remelting and simultaneous isothermal holding is that of the entrapped liquid emerging as fine globules and dendrites in the solidified structure. Geblin *et al.* (1999) reported the evolution of globular morphology with liquid entrapment during partial remelting and isothermal soaking of grain refined AZ91 alloy. On their studies on rheocast A356 alloy, Zoqui *et al.* (2002) reported that higher holding time and inadequate stirring leads to coarser grain size and globule size. The literature on evolution of entrapped liquid during isothermal

soaking in semisolid state is not large (Seconde and Suery 1984, Braccini *et al.* 1998). From literature it seems that Ostwald ripening and dendritic arm coalescence (Seconde and Suery 1984, Annavarapu and Doherty 1995) are the factors that lead to liquid entrapment. Coalescence of complex shaped particles leads to liquid entrapment (Seconde and Suery 1984, Annavarapu and Doherty 1995, Braccini *et al.* 1998).

Lou and Surey (1995) witnessed rapid globularization in A356 alloy subjected to cold working before partial remelting. Lapkowski (1998) has reported evolution of fine grains in the microstructure in Al based alloys subjected to cold working prior to remelting. A study on the comparison of microstructures obtained by semisolid processing with Magnetohydrodynamic (MHD) stirring, Strain Induced Melt Activation (SIMA) and spray casting was carried out by Tzimas and Zavaliangos (2000a), with a conclusion that the spray cast and the SIMA processed alloys exhibit uniformly distributed equiaxed grain structures in the alloy matrix, while the same alloy when manufactured via MHD route leads to irregular spheroidal grains. Chen *et al.* (2002) reported in their work on the evolution of spheroidal grains upon partial remelting of ZA27 alloy that become coarser in size and irregular in shape due to coalescence and growth. Of late, studies on morphological analysis of Al-4.5 wt% Cu by Zoqui (2003) have revealed that grain refinement is more predominant when the alloy is subjected to deformation prior to partial remelting as compared to that in case of cast structure. The increase in strain amount not only results in grain refinement but also leads to a more uniform globular structure which is further confirmed by the work of DeFreitas *et al.* (2004) and Herbert *et al.* (2006).

The review of literature brings out that comparatively, less attention has been paid to microstructural evolution during partial remelting and isothermal holding before thixoforming than solidification from liquid state. The study leads to the understanding that microstructural reheating followed by isothermal soaking is represented by partial remelting starting at the grain boundaries, then by rapid coalescence of dendritic arms, resulting in liquid entrapment. The grain spheroidization takes place by mass transfer. Further isothermal holding leads to grain

coarsening by grain boundary migration at the cost of finer grains, which either coalesce or dissolve, with liquid entrapment. It is obvious that the holding time must be sufficiently long to cause complete transformation from dendritic to spheroidal structure but also should not be too long to cause excessive grain growth. Excessive grain growth will result in deterioration of mechanical properties of the thixoformed components.

2.6 MECHANISM OF NON DENDRITIC MICROSTRUCTURE FORMATION

There have been many mechanisms reported in literature to obtain non dendritic morphologies and fine grained structure by forced convection techniques like agitation caused by stirring. Fleming (1991) has suggested a number of mechanisms to bring about dendritic fragmentation which can be divided under three groups; (1) dendritic arm root remelting, (2) growth control mechanism, and (3) dendrite arm fragmentation. In semisolid processing, a prolonged isothermal soaking causes the particle with any morphology to attain spheroidal microstructure in order to achieve minimum interfacial free energy state, even under full diffusion control (Fan 2002). Recently, Flemings and Martinez (2006) and Martinez *et al.* (2006) have reported that the essential step in semisolid forming is to obtain a high grain density during the initial stages of solidification of an alloy melt. If the grain density is higher in the initial stages, then the grains grow to spheroidal shape in a short time. The paper claims that there are two distinct paths to achieve the desired structure, (1) coarsening of fine dendrites and (2) direct spheroidal growth. The high grain density promotes the growth of fine dendrites leading to formation of fully spheroidal grains. If there is sufficiently large number of grains, they will be of small size and isothermal holding or slow cooling will lead to fully developed structure with little or no entrapped liquid. This has been presented schematically in Figure 2.1 by the paths a-b-c-d. The intermediate structure shown at c is sometimes termed as rosette structure

At too low a grain density, even with long ripening time, the dendritic structure does not disappear as shown by b-b_2. Contrary to this, if grain density is sufficiently high,

dendrites formation can be totally prevented (Flemings and Martinez 2006, Martinez *et al.* 2006). In such situation, the grain growth will proceed along a-a_2.

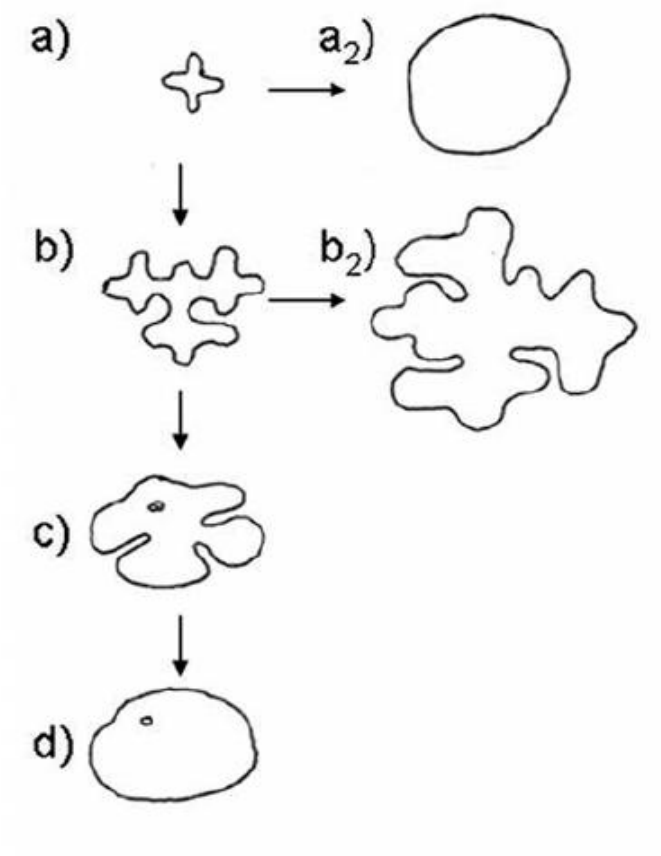

Figure 2.1 Paths for growth and coarsening of a "grain nucleus" (a) initial dendritic fragment (b) growth of dendrite (c) Ripened rosette (d) spheroid (Flemings 2006).

Martinez *et al.* (2006) in their studies involving theoretical model for diffusion-controlled spherical particle growth in semisolid alloys have suggested that spheroidal growth in semisolid alloys is favoured by high particle density, high solid fraction and low cooling rate. The predictions of this model were confirmed by experimentation on Al-4.5(wt. %) Cu alloy.

In the studies on effect of isothermal mechanical stirring on an Al-Si alloy in semisolid state, Sukumaran *et al.* (2004) has concluded that as the shear rate increases particle size decreases. Further it was found that prior addition of Ti-B grain refiner before stirring is commenced, leads to finer primary particles within a shorter

isothermal stirring duration. The boundary level model developed by Vogel and Canter (1977a) to study the effect of stirring on the growth of spherical particles from the melt has shown that stirring causes destabilization of solid/liquid interface for both low and high mobility surfaces. Further, Vogel (1977b) suggested that the non-dendritic microstructure observed in rheocasting might be the result of overlapping diffusion fields of a large number of growing particles. Another study by Hellawell (1996) shows that formation of stable diffusion field for continued evolution of dendrites is negated by vigorous stirring. The work further points out that the solute enrichment and thermosolutal convection due to remelting can detach the dendrites from their roots.

From the literature surveyed it is revealed that , in the stirred slurries, fragmentation of dendrites results in evolution of spheroidal morphology, the direct evidence for which is the work done by Spencer *et al.* (1972). It is learnt that shearing breaks up dendrites on partial solidification. Although after a lot of research is being done in this area (Spencer *et al.* 1972, Vogel and Canter 1977a, Vogel 1977b, Vogel *et al.* 1979, Apaydin *et al.* 1980, Doherty *et al.* 1984 and Hellawell 1996), the question still remains to be answered is as to how shearing can exert such a large bending moment to cause the fracture of dendritic arms, the dendritic arms being small. Vogel *et al.* (1979) have proposed a completely different theory suggesting that the dendritic arms break under the shear stress created by the stirring of melt and the plastic strain is accommodated by dislocation generation.

At low shear stress, neither the mechanism of remelting nor that of fragmentation offers perfect explanation for evolution of rosette type morphology. Mullis (1999) has proposed a theoretical model explaining how the bending of dendritic arms gives rise to rosette shaped structure, although the predicted model has not been experimentally verified so far. The Monte Carlo technique invented by Das *et al.* (2001, 2004) has shown that growth of dendrites is enhanced at low shear rates and is in agreement to the works carried out by Vogel and Canter (1977a). It is reported that turbulent type flow that penetrates into the interdendritic region appears to prevent the dendritic growth.

The literature reviewed in this section indicates that enhanced mass transfer during forced convection gives rise to rosette and spheroidal morphology. Laminar flow causes the evolution of rosette morphology from dendritic structures, while turbulent flow modifies grain morphology from rosette shaped to spheroid. A nucleation mechanism aided by uniform temperature and well distributed heterogeneous nucleation agents may be the most likely cause for structural refinement under intense stirring. Dendritic arm remelting (Flemings 1991) and fragmentation mechanisms may be significant at low shear rates.

2.7 METHODS TO FORM SPHEROIDAL GRAIN STRUCTURE

The following subsections provide a brief summary of the important routes towards obtaining non dendritic (spheroidal) structures.

2.7.1 Magnetohydrodynamic (MHD) Stirring

MHD stirring process was developed and patented by Young *et al.* (1983, 1984), to overcome the problems related to mechanical stirring (Nafisi and Ghomashchi 2005). In the MHD stirring process, electromagnetic stirring is used to break the dendrites in semisolid state (Kenney *et al.* 1988). The solidifying metal acts as the rotor and the stirring action caused shears the dendrites formed in the mushy zone to form globules. Since the invention of the MHD stirring process for production of thixotropic starting material, several citations of its use have been reported in literature (Ilegbusi and Szekely 1988, Kenney e*t al.* 1988, Naidermaier *et al.* 1988, Gabathuler *et al.* 1992, Vives 1992, Vives *et al.* 1993, Blazek *et al.* 1995, Kahn Mann *et al.* 1996, Zillgen and Hirt 1996 and Nafisi and Ghomashchi 2005). Kenney *et al.* (1988) have reported that MHD could provide the desired microstructure with a grain size of 30μm as compared to 100 μm obtained from mechanical stirring. Kirkwood (1994), Fan (2002), Atkinson (2005) and Nafisi and Ghomashchi (2005) have reviewed the existing work in this area. The review points out that the microstructures produced by MHD process are strongly affected by the design of inductive coils. Further the electromagnetic force fields in the mushy state are not uniform and can result in different degrees of

structural modification in the radial direction, incomplete spheroidization and presence of 'rosette' type grains.

2.7.2 Spray Forming (Osprey)

Spray casting (Osprey process) is a process for preparation of feedstock and involves no agitation. In this process, the molten metal is directed through a nozzle into a gas (Nitrogen or Argon gas) atomizer causing the liquid stream to be atomised in the form of different size droplets as they experience high cooling rate during the course of their flight. During atomisation, the large size droplets remain in liquid state, the intermediate size in semisolid state, while small droplets solidify (Mathur *et al.* 1989). These droplets are collected on a moving substrate and solidified to form shaped castings (Nafisi and Ghomashchi 2005). The resulting structure from Osprey process gives equiaxed microstructure with fine grains. It is reported that this material is ideal for thixoforming, if heated into semi-solid state (Elias *et al.* 1988). Spray forming method has been investigated in detail (Sukimoto *et al.* 1986, Amhold and Muller-Schwelling 1991, Sano *et al.* 1992, Annavarapu and Doherty 1995), and several methods have been proposed to describe the method in detail. This process finds wide applications which include, processing of aluminium alloys and its composites, high speed steel and copper alloys (Leatham *et al.* 1989, Mathur *et al.* 1989, Nafisi and Ghomashchi 2005). Ward *et al.* (1996) have reported that spray casting method is ideal for fabrication of Al-Si alloys containing more than 20 wt. % Silicon. The spray forming process has aroused lot of interest amongst research fraternity as witnessed in various review articles (Kirkwood 1994, Fan 2002, Atkinson 2005, Nafisi and Ghomashchi 2005).

2.7.3 Strain Induced Melt Activated/ recrystallization and partial melting

Strain Induced Melt Activation (SIMA) developed by Young *et al.* (1983) involves cold deformation or quenching of hot extruded or rolled bar into a billet, inducing sufficient residual plastic strain. Once this billet is reheated to semi-solid state, partial remelting occurs resulting in fine, uniform and non-dendritic microstructure, which can then be thixoformed in its semi-solid state (Nafisi and Ghomashchi 2005).

Kirkwood *et al.* (1989) have suggested a modification in SIMA process in which the initial heating is done below the recrystallization temperature (warm working) to ensure maximum strain hardening as reviewed in (Nafisi and Ghomashchi 2005). A thorough investigation on SIMA process by researchers (Loue and Suery 1995, Turkeli and Akbas 1996, Cho *et al.* 1996, Choi and Park 1998a, 1998b, Lapkowski 1998, Valer *et al.* 1999, Tzimas and Zavaliangos 2000a) has resulted in more insight and understanding on the effect of process parameters on the resulting microstructure. Turkeli *et al.* (1996b) have reported the possibility of obtaining non-dendritic structure with 7075 wrought aluminium alloy. Choi *et al.* (1998) have cited the conditions for obtaining globular structure using SIMA process for Al 2024 and other aluminium alloys.

Although SIMA process is a little similar to recrystallization and partial melting (RAP) route, yet there are basic differences between the two (Atkinson 2005). Recrystallization takes place when heating to semi-solid state and the recrystallized boundaries are penetrated by the liquid resulting in formation of spheroids surrounded by liquid. SIMA route (Young 1982) involves cold working while the RAP route involves warm working (Kirkwood 1992). The main advantage of SIMA and RAP route is that the extruded feedstock can directly be used and the grains are globular than those obtained by MHD route. The main disadvantage is that the variation of work stored across the section cause inhomogeneities in the grain sizes.

2.7.4 Liquidus/ near liquidus casting

Liquidus or near liquidus casting method is a recent method for developing thixotropic source material (Xia and Tausig 1998, Wang *et al.* 2000a). The technique so far has been reported for both cast (Wang *et al.* 2000a, 2000b, 2000c) as well as wrought (Xia and Tausig 1998, Yurko *et al.* 1999, Cui *et al.* 2000) aluminium alloys. The process consists of pouring the molten metal at or near the liquidus temperature in a tilted crucible and the nucleation occurs on the side of the crucible. The low pouring temperature results in fine non-dendritic microstructure. This is the principle on which the UBE New Rheo Casting (NRC) process (also known as UBE process) has been developed by UBE Industries Ltd, Japan.

2.7.5 Semi-solid rheocasting

The semisolid rheocasting (SSR^{TM}) process, developed recently is a hybrid of mechanical stirring and near liquidus casting. A team of researchers (Martinez 2001, Martinez *et al.* 2001, Flemings *et al.* 2003, Yurko *et al.* 2003) have invented this process, which produce SSM structures without liquid entrapment. The alloy is held slightly above the liquidus temperature and a stirrer, which also provides the cooling action, is inserted into it. After a few seconds of stirring, the melt temperature reaches a value corresponding to a solid fraction of few percent, and the stirrer is withdrawn.

2.7.6 Grain refinement

Grain refinement is one of the methods to obtain equiaxed grain structure (Wang *et al.* 1993) in an alloy. However, the method does not ensure uniform spheroidal and fine grain structure. The pioneering work has been carried out by Cibula (1949, 1951) on the effect of a number of elements like Ti, B, Zr, Nb, V, W, Ta, Ce on the grain refinement Aluminium. Jones and Pearson (1976) have reported that the grain refiner can be considered as effective only if the size of Al reaches below an acceptance level of 220μm. The various aspects related to grain refinement and the proposed mechanisms thereto have been reviewed in (McCullagh and Nelder 1989, Easton and St. John 1999a, 1999b and Murty *et al.* 2002).

2.7.7 Semisolid thermal transformation

It is found that if the dendritic structure is heated in the semi-solid range for a certain amount of time, spheroidal structure is obtained. The process is known as semisolid thermal transformation (SSTT) (Berry and Linoff 1997). The mechanism for formation of non-dendritic structures has already been discussed in sections 2.5 and 2.6.

A number of other techniques to obtain thixotropic feedstock have been reviewed in articles by Kirkwood (1994), Fan (2002), Atkinson (2005) and Nafisi and Ghomashchi (2005).

2.8 FLOW BEHAVIOUR OF MUSHY METAL

Tzimas and Zavaliangos (2000a) have reported that during mushy state forming, the externally induced strain is accommodated by (i) plastic deformation of the unmelted grains in contact (ii) deformation or fragmentation of bulk grains and, (iii) rearrangement of grains through sliding. Tzimas and Zavaaliangos (2000b) and Kiuchi (1989) conducted compression tests with constant strain rate and showed that the flow stress reduces with increase in liquid content. Kiuchi and co workers (Fukuoka and Kiuchi 1974, Kiuchi 1979b) have worked on determining the flow stress of Al, Cu, and Pb based alloys in mushy state, and proposed that there is substantial decrease in flow stress with decrease in solid fraction starting from 100%. Through the studies on Al-5.5% Cu and A2017 alloys, Lapkowski *et al.* have shown that plastic deformation of semisolid alloys require low forces as compared to that with traditional hot working. It is found that the flow stress is a function of liquid content, immaterial of the type of alloy (Kiuchi 1989), and that the chemical composition and the structure of the alloy have minimal effect on the flow stress. Since the deformation is fully accommodated by the viscous flow of liquid near the grain boundary, the dependence of flow stress solely on the liquid content seems justified. Hence the strain accommodation by the liquid at the grain boundaries is dependent only on the viscosity of the liquid, which of course is a function of temperature. Kiuchi (1989) has shown that the data representing the flow stress of a given alloy in the mushy state normalized by its flow stress at the solidus line temperature, if plotted against its solid fraction for different alloys, fall on the same straight line or curve. Due to the presence of liquid at the grain boundaries, the grains are free to rotate and/or slide against each other. On the other hand, the liquid flows as lubricant through intergranular gaps. As a result, the constraints in polycrystalline materials to deformation due to presence of grain boundaries are partially or completely removed. When the solid fraction in the mushy alloy is high, the liquid is trapped in the unmelted grain junctions and exerts an internal hydrostatic pressure in response to the applied load.

2.9 VOLUME FRACTION EVALUATION

The evaluation of volume fraction plays a significant role in determining the deformation process conditions (Lapkowski 1997), mainly because the flow stress is significantly dependent on the liquid fraction content. An accurate determination of liquid volume content is necessary as it determines the rheological behaviour (Joly and Mehrabian 1976, Flemings 1991, Kirkwood 1994, Lapkowski 1997, Tzimas and zavaliangos 1999 and Fan 2002) and microstructural evolution (Hardy and Voorhes 1988, Martinez 1994, Salvo *et al.*1995, Loue and Suery 1995, Tzimas and Zavaliangos 2000a). Literature review suggests three methods which are used to evaluate the volume fraction of solid (Tzimas and Zavaliangos 2000a). These methods are (a) Thermal analysis technique, (b) Quenching experiment method and (c) Use of lever rule in equilibrium phase diagram. Tzimas and Zavaliangos (2000b) have inferred that all the above methods are approximate evaluations of volume fraction and each has its own merits and limitations.

2.10 SEMISOLID PROCESSING METHODS

Semisolid processing encompasses a whole family of processes. The broad categorisation of these processes follows in the upcoming subsections.

2.10.1 Rheocasting

The process in which the alloy is cooled from the liquid state into semisolid state and injected into die without any intermediate solidification step is known as rheocasting. The non dendritic structure can be obtained by various means such as, mechanical stirring, MHD stirring, simulated nucleation of solid particles as in the new rheocasting (NRC) process patented by UBE, Japan as reviewed in (Nafisi and Ghomashchi 2005), or by electromagnetic stirring in the sleeve as in the new semi-solid metal casting process from Hitachi Ltd, Japan as reviewed in (Nafisi and Ghomashchi 2005). In the NRC process, the alloy is heated slightly above the liquidus temperature and is poured in a crucible, followed by controlled cooling resulting in spheroidal microstructure, before being taken up for forming. There is no need for a

specially treated thixo-formable feed stock for this process. The NRC method has been used for processing cast Al alloys (Kaufmann *et al.* 2000a, Wabbuseg *et al.* 2000), wrought Al alloys (Kaufmann *et al.* 2000b) and magnesium alloys (Potts 2000).

2.10.2 Rheomoulding

The first rheomoulding prototype was patented by Cornell University (Peng *et al.* 1994) which uses a vertical injection moulding and clamping single screw machine, more or less similar to that used for polymer injection moulding. The liquid alloy is fed into a barrel. The cooling s carried out while the liquid is stirred by the rotating screw. Either single (Peng e*t al*. 1994, Peng and Hsu 2000) or twin stirrer (Fan *et al.* 1999a, Fan *et al.* 2001a) can be used. The semisolid alloy is then forced into the die cavity. The process is suitable for mass production of components and does not require specially prepared feedstock. The process has been described in a number of publications (Peng *et al.* 1994, Wang *et al.* 1996) and can be applied to mould Sn-Pb and Zn-Al-Cu alloys. In the recent past, Fan and co workers (Fan *et al.* 1999a, Fan *et al.* 2001) have extended twin screw rheomoulding process to a rheomixing process for processing usually immiscible liquid alloys.

2.10.3 Thixomoulding

Thixomoulding is the process developed to fabricate the near net shaped components (Pasternak *et al.* 1992) and licensed to 'Thixomat' (Pasternak *et al.* 1992, Walukas *et al.* 2000). The raw material for the process are solid chips of 2 to 5 mm in size obtained during machining or other metal working of magnesium alloys as reviewed in (Nafisi and Ghomashchi 2005). The chips are fed into a heated injection system using a continuous rotating screw and are partially melted to thixotropic slurry under continuous shear force generated by rotating Archimedean screw (Pasternak *et al.* 1992). Spheroidal microstructure is produced during the process and the material is fed into the die. The major advantage of this process over the majority of the other SSM processing techniques is that slurry making and component forming is reduced to a single step, leading to process economy.

2.10.4 Thixoforming

Thixoforming is the name given to the process which involves heating the material to the semisolid state with liquid content in the region between 30 to 50 vol. % and subsequently forcing into a die (Kopp *et al.* 2001). Component forming in a closed die is named as 'Thixocasting' while that done in an open die is called 'Thixoforging' (Fan 2002).

Figure 2.2 shows the process map of thixoforming process in terms of the starting material routes as well as process variants. Components are manufactured using thixocasting, thixoforging and thixotransverse extrusion. Long products are manufactured using thixoextrusion and thixorolling. As a variant of thixoforming, forming could be done with an arbitrary liquid volume content which could be either more than or less than 30 volume percent. Such semisolid deformation processes are categorised as mushy state forming and a brief discussion on these is presented in the sections to follow.

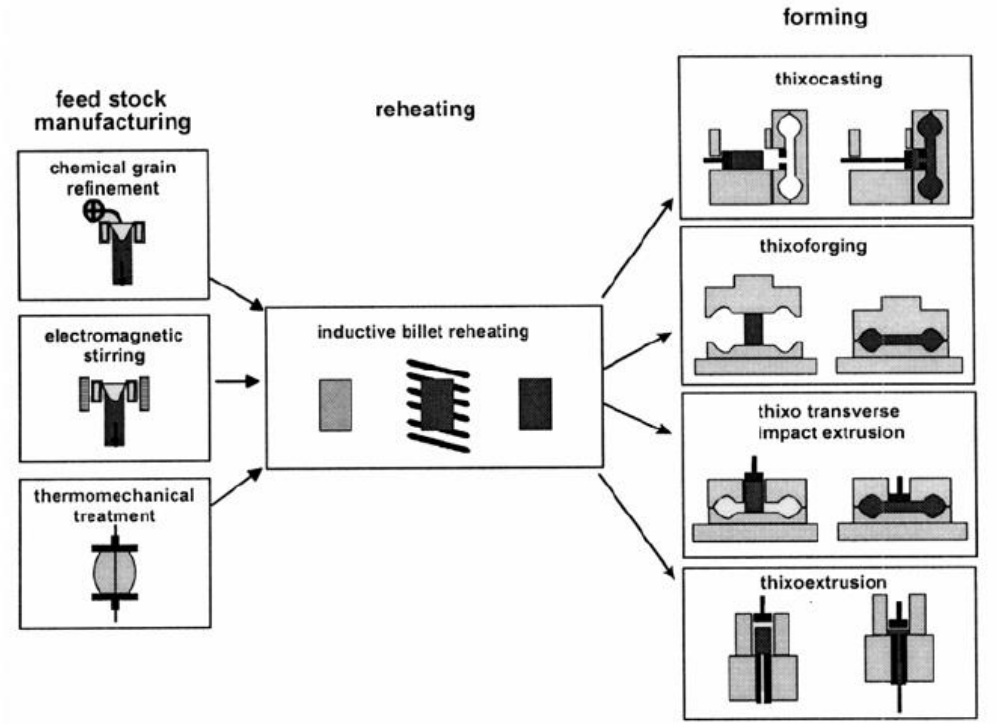

Figure 2.2 The process map of thixoforming variants (Kopp 2003)

2.10.5 Mushy state extrusion

Mushy state extrusion has been used to obtain wires, tubes and bars from billets reheated in an electric furnace (Kiuchi 1989) with the liquid weight content between 20-30%, so that the billet is able to retain its original shape and size. The extrusion pressure required in this case is only about one fourth that would be required at solidus temperature. The extrusion pressure decreases sharply when the solid content reduces from 100% to 80% and practically seen to remain constant at and below 60%. The extrusion pressure at a given solid content is a function of extrusion ratio. Higher the extrusion ratio, greater will be the extrusion pressure at a given solid content. Due to lower extrusion pressures involved with mushy state extrusion, high extrusion ratios of the order of 40:1 have been reported in case of Al-5.7 wt. % Cu alloy. As the liquid content in the billet acts as a lubricant in the container, and die and the pressure required is low, it has been possible to extrude complicated cross-sections in a single pass.

2.10.6 Mushy state rolling

Mushy state rolling is a recently developed metal forming process, which requires a stable, steady flow and homogeneous deformation of the semisolid plate or sheet, as well as rapid cooling inside the roll gap (Kiuchi 1989). Figure 2.3 depicts the schematic diagram showing the mushy state rolling of a workpiece. As the semisolid plate is in contact with the rolls during deformation of plate, the deformation zone is narrow with a wide free surface existing around it. The liquid from the deformation zone flows freely from the narrow deformation zone to the other parts of the plate or sheet. This means that a steady state condition between co-ordinated flow of solid and liquid component is difficult to be attained. Often, it is observed, that the solid and the liquid component flow independently. It has been shown that the thickness reduction is reduced at high liquid content, as the alloy flows in the gap as slurry. At the entrance to the roll gap, the liquid is likely to flow to the top and bottom surfaces under pressure created in the deformation zone. The liquid component however, does not separate out, but solidifies in contact with the comparatively cold roll surfaces and forced into the roll gap. The solid skeleton containing the unmelted grains is

compressed and is drawn into the roll gap. The grains in the solid skeleton tend to elongate at low liquid content, when the grains touch one another combined with high thickness reduction. The entire liquid solidifies in the roll gap.

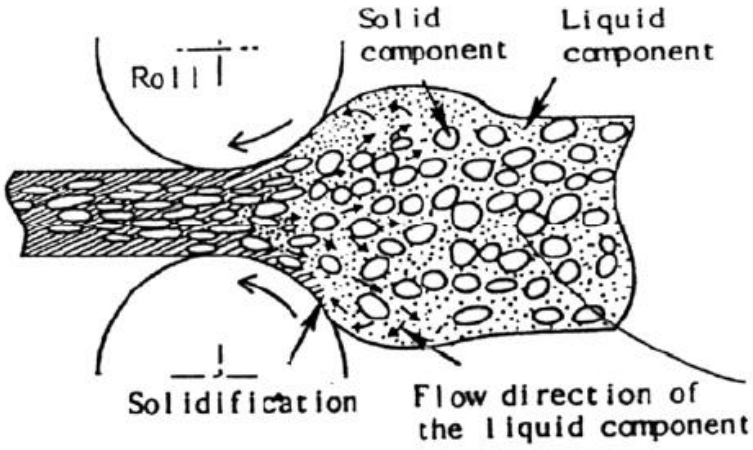

Figure 2.3 Schematic illustration of flow and solidification of a mushy workpiece inside the roll gap (Kiuchi 1991)

Mushy state rolling was first attempted by Kiuchi on AA5052 and AA7075 alloys (Kiuchi (1989). He showed that the mushy state rolled sheet provides a heterogeneous grain structure. The process yields a fine grained structure at the surfaces as compared to that at the central portion due to rapid solidification of liquid component at the surface with the rolls. Such inhomogenity is responsible for providing a gradient in hardness and yield strength across the plate and sheet thickness.

Mushy state rolling has been used to process laminated composite sheets in the form of metal ceramic composite bonded to the base alloy. Composite sheets of stainless steel diffusion bonded to composite of cast iron, deoxidised iron and Al_2O_3 particles have been processed by mushy state rolling (Kiuchi 1989). A review conducted by Fan (2002) discusses the various aspects of thixoforming process.

Recently it has been reported (Herbert 2007) that mushy state rolling of Al-4.5Cu-5TiB_2 composite at temperatures corresponding to 10-30% liquid volume, leads to refinement of rosette–shaped structure in α-Al matrix of the as-cast composite to give globular or equiaxed grains. Grain refinement is achieved in the as-cast composite due

to Zener pinning by TiB_2 particles (Zu and Luo 2001, Herbert *et al.* 2006). Rolling under similar condition resulted in grain coarsening in case of Al-4.5Cu alloy due to extensive diffusive mass transfer in presence of liquid at grain boundaries. Furthermore, in case of mushy state rolled Al-4.5Cu-5TiB_2 composite, the bimodal grain size distribution observed in the microstructure is found to have larger volume fractions of finer grains at near surface locations of the plate as compared to those at the centre. A larger volume of fine grains in the near surface locations has been attributed to the formation of fine grains due to rapid solidification of liquid being squeezed out to the surface upon being compressed within the roll gap, which is in confirmation with the results of Kiuchi (1989) and Herbert (2007). The mechanical and wear properties are found to improve dramatically on mushy state rolling of this composite due to chemical homogenisation, grain refinement and limited work hardening of the unmelted grains (Herbert e*t al.* 2008, 2010).

2.11 APPLICATIONS

2.11.1 Semisolid processing of alloys

Semisolid processing of alloys have been investigated (Kiuchi and Sugiyama 1991, Hirt *et al.* 1997, Rovira *et al.* 1999, Cho and Kang 2000, Kapranos *et al.* 2000, Kaufmann *et al.* 2000a, Rachmat *et al.* 2000, Siegert *et al.* 2000, Rice and Mendez 2001, Jung and Kang 2002, Kapranos *et al.* 2003 and Liu *et al.* 2003) with an objective towards its practical investigations over the last two decades. Kaufmann *et al.* (2000) showed that the "New RheoCasting" (NRC) process can be applied to aluminium wrought alloys (6082) to obtain better mechanical properties as against the standard casting alloys. Rice and Mendez (2001) have proposed new slurry based die casting process and have successfully used it in fabricating fuel rail, compressor heads, pistons and clutch covers for automotive applications.

Kiuchi and Sugiyama (1991) have investigated the mushy state rolling of aluminium alloys and cast iron with emphasis on the effect of thickness reduction, solid volume fraction and roll speed on the microstructure and properties of the resultant roll product. They concluded that the mushy state rolling has the potential to develop and

manufacture new functional metallic or composite sheets. Rovira *et al.* (1999) have reported the evolution of globular microstructure in the thixo-forged or thixo-extruded Al-4.5 wt. % Cu alloys. Cho and Kang (2000) have studied the effect of pressure and die temperature on microstructure and mechanical properties of thixo-forged AA2024. Rachmet *et al.* (2000) and Liu *et al.* (2003) have reported the successful filling of the die cavity with their investigations on thixoforging of high performance Al alloys suggesting the viability of near net shaping using this process. Kapranos *et al.* (2003) have successfully thixoforged a brake drum of A390 alloy for automotive application, as an alternative to cast iron, with lower weight and good wear resistance.

Investigations have been carried out by Xie *et al.* (2006)) on application of Al-6Si-2Mg alloy by fabricating water pump lid and connecting rod for automotive application using thixoforming process. Wang and Xu (2006) also successfully manufactured the water pump lid for automotive application using semisolid casting of A357 alloy. The possibility of forming light weight components using thixoforming has been explored by Hirt *et al.* (1997). A steering knuckle for a passenger car fabricated by thixoforming A356 alloy resulted in 50% saving in weight. Kapranos *et al.* (2000) proved that 'near net shaped' structures could be produced by fabricating thixoformed end plates of an electric motor from Al alloy.

2.11.2 Semisolid processing of composites

Particulate reinforced metal matrix composites (MMC) have generated a lot of interest amongst the researchers due to their high specific strength, high specific modulus, high wear resistance and stability at elevated temperatures. However, poor formability has become a hindrance to a wider use of most MMCs. A lot of research has been carried out on thixoforming of MMCs (Kiuchi and Sugiyama 1982, Lee *et al.* 1994, Ward *et al.* 1996, Youn *et al.* 2002, Zu and Luo 2001, Hamilton *et al.* 2003). Flemings and co workers were the pioneers in noting that metal slurries possessed ideal environments to incorporate ceramic particles to form composites. Moon *et al.* (1991) and Quaak *et al.* (1994b) have carried out research on castability (compocasting) and forgeability of ceramic reinforced MMCs. McLelland *et al.* (1992) have reported successful fabrication of Al-Si composites with uniform particle

distribution using thixoforming technique. Kiuchi and Sugiyama (1992) and Miwa *et al.* (1992) have proposed techniques to incorporate SiC fibres as well as whiskers into semisolid alloy. The amount of the ceramic phase that can be incorporated in the MMC depends on the liquid fraction corresponding to the SSM temperature (Hong *et al.* 2000).

Kiuchi (1987) has investigated the application of mushy state processing to manufacture various kinds of metal-ceramic composites with successful manufacture of particle reinforced cladding metal and composite sheets. Mushy state rolling has also been used to manufacture laminated composites or cladding sheets with alternate layers of base metal or alloy and composite sheets (Kiuchi 1989). Thixo-extrusion of SiC/2024Al composite was successfully carried out by Lijun Zu and Shoujing Luo (2001) with the microstructure characterised by well-densified matrix and uniform distribution of reinforcements. Minghetti *et al.* (2001) investigated the back extrusion of Al_2O_3 particle reinforced Al alloy/AA6061 matrix composite in semisolid state and observed a gradient distribution of ceramic reinforcements based on the semisolid forming parameters. Zhang and Wang (2001) carried out investigations on spray formed 6066Al/SiC composites and have shown that thixoformed composites have fine grained structure and that the process has the capability of near net shaping. Hamilton *et al.* (2003), based on their study on AA2124/SiC composites, have demonstrated the viability of the semisolid processing to achieve near net shaping of metal matrix composites.

The research activities in the semisolid processing of composites have also focussed on the manufacturing of MMC prototypes for a range of practical applications. One such remarkable achievement has been the successful fabrication of cylinder liners made with SiC reinforced MMCs using thixoforging demonstrated by Youn *et al.* (2002). Ward *et al.* (1996) have carried out investigations on thixoforming of Al-Si MMCs, wherein they have successfully manufactured oil pump housing and demonstrator components. Applications of thixoforming are continuously gaining popularity, since it is safe, clean and practical method for near net shaping.

2.12 MECHANICAL PROPERTIES

2.12.1 Alloys

Some of the data available from the literature about the mechanical properties of the thixoformed Al alloys are listed in Table 2.1. Kenney *et al.* (1988), Gabathuler *et al.* (1993) and Tietmann *et al.* (1992) have investigated the mechanical properties of the A356 and A357 cast and Al alloys. Examination of data in Table 2.1 reveals that the heat treated (T6 temper) thixocasting A356 Al cast alloy (Al-7 Si-0.5 Mg) shows better mechanical properties as against those specimens produced by permanent mould casting route. The effect of the temperature of the die and variation of applied pressure on mechanical properties during thixoforming of complex shapes using A356 alloy has been investigated by Cho and Kang (2000). It has been found that the yield strength, ultimate strength and the elongation of the alloy increase with increasing applied pressure while they are found to decrease with a little increase in temperature due to grain coarsening accompanying increase in temperature.

The thixoformed A357 alloy exhibits mechanical properties similar to that shown by permanent mould route, albeit with greater ductility (Kenney *et al.* 1988, Gabathuler et *al.* 1993). Bergsma *et al.* (1997) have compared the mechanical properties of semisolid thermal transformed (SSTT) A357 alloy with electromagnetically stirred A357 alloy, and found both exhibiting close similarity. It is observed that thermal treatment of A357 alloy provides a god alternative to EMS method in obtaining spheroidal microstructure.

The tension tests carried out by Zoqui and Robert (1998) on Al-4.5 (wt. %) Cu alloy in both as rheocast and T6 condition show that the increase in grain size results in decrease in the tensile and yield strength. It is observed that the initially an increase in grain diameter results in a slight increase in elongation but elongation decreases on higher increase in grain diameter. The increase in grain diameter is responsible for poorer tensile properties of the as rheocast Al-4.5(wt. %) Cu alloy as compared to those of it's as cast samples.

Investigations have been carried out on the mechanical properties (Kenney *et al.* 1988, Tietmann *et al.* 1992, Cho and Kang 2000, Liu *et al.* 2003 and DeFreitas *et al.* 2004) of the semisolid products produced right from wrought alloys. Cho and Kang (2000) have observed that the strength of the thixoformed AA2024 alloy increases with the pressure applied during thixoforming, while causing decrease in yield and ultimate tensile strength for a given applied pressure during thixoforming. Kiuchi and Sugiyama (1991) investigated the mechanical properties of AA2017 alloy cold worked after mushy state rolling. They concluded that the tensile strength and elongation of the rolled sheets showed improvement when subjected to cold rolling and subsequent heat treatment after mushy state rolling.

Although a lot of effort has been put in the evaluation of mechanical properties of alloys processed in semisolid condition, the literature review suggests that there is no sufficient data to analyse the processing technologies or create a design database. However, there is a pointer that semisolid processing leads to improvement in mechanical properties of alloys, generally, which may be further enhanced by heat treatment. The improvement in properties is thought to be brought about by decrease in porosity in addition to refinement of grain structure and chemical homogeneity. Quite a volume of the research work is found to be devoted to thixoforming of cast Al alloys as compared to wrought Al alloys. This is because on thixoforming wrought Al alloys do not achieve the strength levels as that of their as cast counterparts. This is due to the grain coarsening or defects in the thixoformed wrought alloys, such as hot cracks, residual porosity and oxide inclusion.

Table 2.1 Mechanical properties of some thixoformed Cast and wrought alloys

Alloy	Process*	Temper	Yield Stress MPa	Tensile Stress MPa	% El	Ref.
Casting alloys 356 (Al-7Si-0.5Mg)	SSM	T6	193	296	12.0	Kenney *et al.* (1988)
	SSM	T6	256	300	11.4	Tietmann *et al.* (1992)
	SSM	T6	240	320	12.0	Gabathuler *et al.* (1993)
	SSM	T6	260	310	9.0	Gabathuler *et al.* (1993)
	SSM	T6	172	234	11.0	Kenney *et al.* (1988)
	SSM	T6	180	225	5-10	Tietmann *et al.* (1992)

		PM	T6	186	262	5.0	Metal Hand. (1990)
		PM	T51	138	186	2.0	Metal Hand. (1990)
A356 (ALTHIX)		Thixoformed (@ 100MPA)	T6	256	298	5.7	Cho and Kang (2000)
		Thixoformed (@ 150MPA)	T6	262	313	7.8	
A356 (ALTHIX)	Applied pressure 100MPa	Thixoformed (@ T_d=300^{0}C	T6	256	298	5.7	
		Thixoformed (@ T_d=350^{0}C	T6	253	295	5.4	
		Thixoformed (@ T_d=400^{0}C	T6	247	285	3.5	
A356(0.4% Mg)		Thixocast	T5	160	250	14	Jorstad *et al.* (2005)
			T6	240	310	13	
		NRC	T5	165	265	10	
			T6	190	295	12	
		SLC	F	130	220	12	
			T5	160	265	12	
			T6	180	295	12	
A356 (0.3%Mg)		SLC	F	115	185	10	
			T5	115	190	10	
			T6	215	310	12	
B319 (0.35Mg/4% Cu)		SLC	F	140	240	9	Jorstad *et al.* (2005)
			T5	165	265	9	
			T6	225	305	9	
357, A357 (Al-7Si-0.3Mg)		SSM	T6	290	358	10.0	Kenney *et al.* (1988)
		SSM	T6	260	330	9.0	Gabathuler *et al.* (1993)
		SSM	T7	290	330	7.0	
		SSM	T5	207	296	11.0	Kenney *et al.* (1988)
		SSM	T5	200	285	5-10	Gabathuler *et al.* (1993)
		PM	T6	296	359	5.0	Metal Hand. (1990)
		PM	T51	145	200	4.0	Metal Hand. (1990)
A357 (Pechiney, RD0430)		SSTT	T6(1)	266	304	13.8	Bergsma *et al.* (1997)
		SSTT	T6(1)	260	312	11.3	
		SSTT	T6(1)	239	279	4.5	
A357 (NWA, G001-3)		ES	T6(1)	296	341	5.8	
		ES	T6(2)	330	361	9.4	
		ES	T6(3)	323	367	10.3	
		ES	T6(2)	270	314	12.2	
357		SSTT	T5[a]	219	289	5.5	Bergsma *et al.* (2001)
		Sand Cast	T5	117	179	3.0	
		SSTT	T6[b]	288	339	6.3	
		EM	T6[1]	300	341	10.8	
		Sand Cast	T6[6]	296	345	2.0	
DF53		SSTT	T5[c]	224	327	5.2	
319		EM	T5[d][8]	237	292	2.8	
		Sand Cast	T5[6]	179	207	1.5	
Modified 319 (DF53)		SSTT	T6[e]	316	387	4.8	
		SSTT	T6[f]	351	409	5.9	
		SSTT	T6[g]	299	398	10.2	
Modified 319		EM	T6[h][8]	334	379	1.6	
		EM	T6[i][10]	320	405	5.0	
		Sand Cast	T6[6]	164	250	2.0	
B319		SLC	F	140	240	9	

(0.35Mg/4% Cu)		T5	165	265	9	Jorstad *et al.* (2005)
		T6	225	305	9	
357, A357 (Al-7Si-0.3Mg)	SSM	T6	290	358	10.0	Kenney *et al.* (1988)
	SSM	T6	260	330	9.0	Gabathuler *et al.* (1993)
	SSM	T7	290	330	7.0	
	SSM	T5	207	296	11.0	Kenney *et al.* (1988)
	SSM	T5	200	285	5-10	Gabathuler *et al.* (1993)
	PM	T6	296	359	5.0	Metal Hand. (1990)
	PM	T51	145	200	4.0	Metal Hand. (1990)
A357 (Pechiney, RD0430)	SSTT	T6(1)	266	304	13.8	Bergsma *et al*. (1997)
	SSTT	T6(1)	260	312	11.3	
	SSTT	T6(1)	239	279	4.5	
A357 (NWA, G001-3)	ES	T6(1)	296	341	5.8	
	ES	T6(2)	330	361	9.4	
	ES	T6(3)	323	367	10.3	
	ES	T6(2)	270	314	12.2	
357	SSTT	T5[a]	219	289	5.5	Bergsma *et al*. (2001)
	Sand Cast	T5	117	179	3.0	
	SSTT	T6[b]	288	339	6.3	
	EM	T6[1]	300	341	10.8	
	Sand Cast	T6[6]	296	345	2.0	
DF53	SSTT	T5[c]	224	327	5.2	
319	EM	T5[d][8]	237	292	2.8	
	Sand Cast	T5[6]	179	207	1.5	
Modified 319 (DF53)	SSTT	T6[e]	316	387	4.8	
	SSTT	T6[f]	351	409	5.9	
	SSTT	T6[g]	299	398	10.2	
Modified 319	EM	T6[h][8]	334	379	1.6	
	EM	T6[i][10]	320	405	5.0	
	Sand Cast	T6[6]	164	250	2.0	
2024	Thixocast	T6	37.4kgf/mm^2	46.4kgf/mm^2	11.2	Chen *et al.* (1979)
	Squeezecast	T6	36.2kgf/mm^2	48.3kgf/mm^2	13.4	
	T6	T6	40kgf/mm^2	48.5kgf/mm^2	10	
2024 (Al-4Cu-1Mg)	SSM	T6	277	366	9.2	Tietmann *et al.* (1992)
2024	W	T6	393	476	10	Metal Hand. (1990)
2024	W	T4	324	469	19	Metal Hand. (1990)
Al2024	Thixoformed (@100MPa)	T6	233	377	20.3	Cho and Kang (2000)
	Thixoformed (@150MPa)	T6	236	387	21	
Al2024 Apllied pressure 100MPa	Thixoformed (@T_d=350^{0}C)	T6	233	377	20.3	
	Thixoformed (@T_d=400^{0}C)	T6	210	371	19.9	
AA2024	Thixoextruded	-	-	243	9	DeFreitas *et al.* (2004)
	Thixoextruded	T6	-	402	11	
	Forged	T6		420	8	
	W	T6	-	475	10	
2219 (Al-6Cu)	SSM	T8	310	352	5.0	Kenney *et al.* (1988)

2219	W	T6	260	400	8.0	Metal Hand. (1990)
6061 (Al-1Mg-Si)	SSM	T6	290	330	8.2	Kenney *et al.* (1988)
6061	W	T6	275	310	12	Metal Hand. (1990)
7075 (Al-6Zn-Mg-Cu)	SSM	T6	421	496	7.0	Kenney *et al.* (1988)
7075	SSM	T6	361	405	6.6	Tietmann *et al.* (1992)
7075	W	T6	505	570	11.0	Metal Hand. (1990)
2014 Extruded	RAP	T6[f]	399	474	3.6	Liu *et al.* (2003)
'Modified' 2014 DC cast	CS	T6[f]	270	408	19	
2014[b] Wrought	W	T6[g]	414	480	13	
6082 Extruded	RAP	T6[h]	189	303	24.4	
'Modified' 6082 DC cast	CS	T6[h]	231	302	12	Liu *et al.* (2003)
6082[i]	W	T6[h]	260	310	6	
7075 Extruded	RAP	T6[j]	420	522	13.4	
'Modified' 7075 DC cast	CS	T6[k]	499	556	4	
7075 Extruded	CS	T6[j]	397	486	8.8	
7075[b]	Wrought	T6[l]	500	570	11	
7010 Rolled	CS	T6[j]	475	524	3.3	
7010[m]	W	T6[n]	485	545	12	

SSM semisolid metal processing; PM permanent mould casting; NRC new rheocasting; SLC sub liquidus casting; SSTT semisolid thermal transformation; EM/ES electromagnetically stirred; W wrought; RAP recrystallization and partial remelting; CS cooling slope casting.

2.12.2 Composites

There have been very few publications related to the (Kang and Ku 1995, Zhang and Wang 2001 and Youn *et al.* 2002) evaluation of mechanical properties of metal matrix composites produced by thixoforming as compared to those processed conventionally. Kang and Ku (1995) have carried out studies on the mechanical properties of Al_2O_3 short fibre reinforced Al2024 components manufactured by squeeze casting. They have concluded that the ultimate tensile strength of such composites depends on the fibre volume fraction and the preform temperature. Zhang and Wang (2001) carried out studies on the evaluation of mechanical properties of SiC particle reinforced 6066Al composites manufactured by squeeze casting and semisolid extrusion. It has been observed that the ductility of the composites produced by semisolid extrusion is 50 to 100% more than those processed by conventional routes.

Studies by Kamat *et al.* (1989) on the mechanical properties of alumina particle (with different volume fractions and particle size) reinforced 2014-O and 2024-O alloy

matrix composites, produced by slurry casting, have shown increase in the yield strength with decreasing inter particle spacing. Composites though have shown limited ductility. In yet another study, Skolianos (1996) carried out mechanical testing of SiC particles reinforced Al-4.5%Cu-1.5%Mg composite processed by slurry casting and reported substantial increase in work hardening of the composite with increasing volume fraction of SiC particles. Increase in yield strength, ultimate tensile strength and the elastic modulus of the composite was observed with heat treatment and volume fraction of carbide, at the expense of elongation. Youn *et al.* (2002) have demonstrated that the thixoformed cylinder liners manufactured using SiC reinforced A380 and A390 alloys possess better mechanical properties than those manufactured from commercial composites.

Although there is an indication that the aging treatment improves mechanical properties, there have been apprehensions over the loss of their ductility. Herbert *et al.* (2010) carried out studies on mushy state rolling of cast *in situ* Al-4.5Cu-5TiB_2 composite. It was reported that mushy state rolling at temperatures corresponding to 20% volume fraction of liquid in the composite leads to significant improvement in tensile properties. In contrast, the unreinforced alloy has showed decrease in both, the strength as well as ductility, due to grain coarsening and formation of brittle eutectic and hypereutectic $CuAl_2$ phase from solidification of solute rich liquid during mushy state rolling. Thus the presence of TiB_2 particles as reinforcement has been found to inhibit grain growth and dendrite arm growth, and restricting the segregation of solute atoms during mushy state rolling. However, there is a limited data on the mechanical properties of the composites processed by mushy state rolling and extrusion. The few values of mechanical properties of thixoformed Al-alloy based metal matrix composites available from literature review are shown in Table 2.2.

Table 2.2 Mechanical properties of some thixoformed Al based MMCs

Composite	Process*		Aging time h	Yield Stress MPa	Tensile Stress MPa	%El	Ref.
Al-2024-O/ 5 vol. % Al_2O_3	Slurry cast	5μm SiC		137	280	7.3	Kamat *et al.* (1989)
		15μm SiC		118	237	4.4	
Al-2024-O/ 5 vol. % Al_2O_3		50μm SiC		107	240	9.0	
Al-2024-O/ 20 vol. % Al_2O_3		5μm SiC		114	252	4.3	

Al-2024-O/ 20 vol. % Al_2O_3			50μm SiC		92	194	2.5	
Al-2024/ Al_2O_3	673K	Squeeze cast				488		Kang and Ku (1995)
	773K					470		
	1073K					428		
Al-4.5%Cu-1.5%Mg		Slurry cast	10.7μm SiC	-	85.1	103	5.2	Skolianos (1996)
				3.5	108.2	126.1	4.8	
Al-4.5%Cu-1.5%Mg/ 4 vol.% SiC				-	101.2	114.2	5.0	
				3.5	113.3	132.2	4.3	
Al-4.5%Cu-1.5%Mg/ 12 vol.% SiC				-	118.0	123.0	5.0	
				3.5	133.1	141.1	3.1	
Al-4.5%Cu-1.5%Mg/ 25 vol.% SiC				-	143.2	161.0	2.1	
				3.5	169.0	200.3	1.5	
Spray formed 6066Al/SiC	883K	Squeeze cast		0	316	274	8.2	Zhang and Wang (2001)
				2	314	275	10.9	
				8	369	322	9.2	
				16	329	290	8.8	
	893K			0	262	220	6.8	
				2	280	250	3.6	
				8	305	265	3.9	
				16	296	262	2.6	
	903K			0	272	210	10	
				2	298	242	6.4	
				8	366	328	5.9	
				16	339	302	5.2	
6066Al Matrix		Casting + Forging		8	345	310	8	
Spray formed 6066Al/SiC	883K	Semisolid Extrusion		0	225	175	11.4	
				8	352	282	15.2	
Spray formed 6066Al/SiC	893K	Semisolid Extrusion		0	210	170	21.1	
				8	314	240	16.2	
	903K			0	233	171	15.1	
				8	362	313	13.3	
6066Al Matrix		Casting + Forging		8	345	310	8	
A380/A390		Thixo-forging	14μm SiC	-	138-159	-		Youn *et al.* (2002)
A380/10 vol. %SiC				-	290-310	-		
A380/20 vol. %SiC				-	300-325	-		
A380/A390		Thixo-forging	5.5μm SiC	-	138-159	-		
A380/10 vol. %SiC				-	300-320	-		
A380/20 vol. %SiC				-	310-330	-		

2.13 WEAR PROPERTIES

Tribological properties are one of the important factors to be considered in applications of metal matrix composites. Investigations in wear properties of composites have revealed the influence of reinforcements on the wear properties of composites. Roy *et al.* (1992) have reported that strongly bonded particle-reinforced

interface is the most significant factor causing the improvement in wear resistance of conventional composites.

Skolianos and Kattamis (1993) have evaluated the tribological properties of SiC_p reinforced Al-4.5%Cu-1.5%Mg matrix composite specimens processed by slurry casting, in both as cast and heat treated condition, using pin on disc wear testing machine. It has been observed that specific wear rate and coefficient of friction decrease with increasing volume fraction of carbide, decreasing carbide particle size, and reduction in inter-particle spacing. Kamat *et al.* (1989) in their investigation of tensile properties on composites have reported increase in yield strength with decrease in the particle spacing. Thus in other words, specific wear rate and coefficient of friction have been found to increase with increase in yield strength and therefore hardness. The solutionising and aging treatment will lead to further increase in wear resistance, and reduction in coefficient of friction.

Ward *et al.* (1996) have carried out the pin on disc and pin on plate wear testing of thixoformed Al-25Si-5Cu, Al-30Si-5Cu and Al-40Si-5Cu alloys against a nitriding steel counterface material in unlubricated condition. It has been observed that only a small difference in wear rate exists in thixoformed alloys and Al-40Si-5Cu alloy in T6 condition. Furthermore, it has been observed that wear rate increases with Si content.

Investigations by Youn *et al.* (2002) on the wear properties of thixoformed cylinder liners produced using SiC reinforced A380 and A390 alloy matrix composites were carried out using pin on disc wear testing machine. Examination of the effect of forging pressure on the wear properties has revealed that wear rate decreases with increase in the forging pressure. The wear rate of cylinder liner made by semisolid processing of A380-10 vol. % SiC_p composite has been found to be 37.5% less than that shown by commercially fabricated composite cylinder liner.

From the investigations carried out on the wear properties of semisolid processing of composites, it appears that there is a definite improvement observed in the wear properties of thixoformed products. Skolianos and Kattamis (1993) have reported that aging helps in improving the wear resistance. The reviews conducted by Kirkwood

(1994), Fan (2002) and Atkinson (2005) have not included wear properties of thixoformed alloys or composites. Hence there is need to investigate the wear properties of thixoformed alloys and composites.

The work carried out by Herbert *et al.* (2008) reported that mushy state rolling of cast *in situ* Al-4.5 Cu-5 TiB_2 composites, corresponding to 10-30 vol. % liquid, leads to significant improvement in wear properties, as compared to unreinforced alloy. The wear rates have been found to decrease with increasing hardness of the mushy state rolled composite, which in turn have been linked to grain refinement. Further, study on the variation of hardness across the section of the mushy state rolled composite revealed that the hardness variation shows an upward gradient from the centre to surface of the rolled composite.

The results of the work carried out by M.A. Herbert (2007) on mushy state rolling of Al-4.5Cu alloy and Al-4.5% (wt. %) Cu-5% (wt. %) TiB_2 composite are listed in Table 2.3 and table 2.4. Table 2.3 provides the results of microstructural evolution of mushy state rolled alloy and composite. The values of hardness of the alloy and mushy state rolled composite in as cast as well as pre hot rolled condition are tabulated at Table 2.4. Table 2.5 provides the results of the study on wear properties of the composite rolled in mushy state.

Table 2.3 Table showing grain size of mushy state rolled Al-4.5Cu alloy and Al-4.5Cu-5TiB_2 Composite

Specimen Description	Liquid Volume Fraction	Al-4.5Cu-5TiB_2 Composite Mushy state rolled in				Grain sizes of Al-4.5Cu alloy samples subjected to mushy state rolling	
		As Cast condition		Pre hot rolled condition			
		Grain size (µm)		Grain size (µm)		Grain size (µm)	
		Large	Small	Large	Small	Large	Small
As cast	--	50 ± 8		--	--	44 ± 6	
Hot rolled	--	--		52 ± 15	28 ± 9	--	
2.5% thickness reduction	f_l ~ 0.1	62 ± 14	27 ± 12	43 ± 16	27 ± 13	--	--
	f_l ~ 0.2	58 ± 18	33 ± 11	42 ± 18	26 ± 11	--	--
	f_l ~ 0.3	66 ± 15	37 ± 10	47 ± 20	25 ± 11	329 ± 204	158 ± 91
5% thickness reduction	f_l ~ 0.1	54 ± 16	25 ± 9	42 ± 16	26 ± 11	--	--
	f_l ~ 0.2	51 ± 11	31 ± 10	41 ± 15	25 ± 12	--	--
	f_l ~ 0.3	55 ± 14	32 ± 10	46 ± 17	24 ± 11	363 ± 225	157 ± 86

7.5% thickness reduction	f_l ~ 0.1	62 ± 20	32 ± 13	40 ± 15	26 ± 10	--	--
	f_l ~ 0.2	48 ± 19	26 ± 12	39 ± 15	25 ± 11	--	--
	f_l ~ 0.3	53 ± 18	27 ± 13	45 ± 17	24 ± 09	383 ± 222	158 ± 98
10% thickness reduction	f_l ~ 0.1	49 ± 17	29 ± 11	47 ± 18	32 ± 13	351 ± 218	194 ± 96
	f_l ~ 0.2	47 ± 14	30 ± 12	43 ± 16	25 ± 11	325 ± 217	176 ± 103
	f_l ~ 0.3	54 ± 12	26 ± 11	45 ± 16	27 ± 12	357± 217	155 ± 87

Table 2.4 Table showing hardness of mushy state rolled Al-4.5Cu-5TiB_2 Composite.

Specimen Description	Liquid Volume Fraction	Hardness of composite (H_v)	
		As cast	Pre hot rolled
No rolling		78±1	85±1
2.5% thickness reduction	f_l ~ 0.1	90±2	95±1
	f_l ~ 0.2	105±2	106±1
	f_l ~ 0.3	88±2.5	88±2.5
5% thickness reduction	f_l ~ 0.1	101±2	104±2
	f_l ~ 0.2	112±1.5	112±1.5
	f_l ~ 0.3	96±2	99±2
7.5% thickness reduction	f_l ~ 0.1	105±1	110±2.5
	f_l ~ 0.2	117±2	116±1
	f_l ~ 0.3	103±2	108±2
10% thickness reduction	f_l ~ 0.1	118±2	116±2
	f_l ~ 0.2	121±2	121±2
	f_l ~ 0.3	106±2.5	113±1.5

2.14 COMPUTATIONAL INTELLIGENCE

Computational Intelligence (CI) is a field which has received vast attention from the researchers and engineers working in areas such as fuzzy systems, neural networks, machine learning and evolutionary computations. CI is today, an active area of fundamental and applied research (Bezdek 1992, 1994, and Pedriyez 1998) for processing the numerical data as against the symbolic data being processed by using Artificial Intelligence (AI) techniques. The technological advancement in computing provided by CI is today being used by organisations to replicate the previously used

models as well as to solve new problems in engineering industry. Of late, there have been successful attempts in using hybrid models made from different components of CI as building blocks, to build what can be called as hybrid intelligent systems.

Intelligence is a set of specific mind capabilities which allow the individual to use the acquired knowledge efficiently to behave appropriately in the presence of continuously evolving tasks and living conditions (Szezepaniak 1999). The definition of CI (Szezepaniak 1999) states that it is a set of machine capabilities which allows it to solve evolving tasks in the presence of evolving conditions. Bezdek (1994) stated that "a system is computationally intelligent when it: deals only with numerical (low-level) data, has a pattern recognition component and does not use the knowledge in the AI sense; and additionally when it exhibits (a) computational adaptivity, (b) computational fault tolerance, (c) speed of human mind, and (d) error rates that are close to human performance.

The present work deals with the use of Artificial Neural Network i.e. the Feed Forward Neural Networks (FFNN) and Recurrent Neural Networks (RNN) for modelling the behaviour of mushy state rolling of Al matrix composites as a function of a number of process parameters, involving multiple inputs and single or multiple output(s) and hence can be termed as a complex system.

2.14.1 Artificial Neural Networks

Modern methods of computing to perform pattern recognition tasks are inspired by the structure of biological neural network in the human brain. The human brain is a complex carbon based computer which can do complex, non linear and parallel computing/processing in a matter of few milliseconds. Today's computer architectures are extremely powerful in the sense, that their speed of processing is often million times faster than that of the brain (Yegnanarayana 2008). However, since the human brain can perform massively parallel operations, each one having comparatively lesser steps, a human brain can perform certain tasks like pattern recognition, classification etc. much faster than the modern computers (Yegnanarayana 2008).

The neural networks store the information in the interconnections between the neurons. As against the computer wherein the information is stored in the memory and addressed by its location, gets overwritten in case there is new information addressed to the same location, the interconnection strengths are adjusted in case of neural networks in the event of new information received, without losing the old information (Yegnanarayana 2008, Zurada 1994).

Another important feature of neural network is fault tolerance due to parallel and distributed processing. The information is distributed in interconnections which are distributed parallely. Hence, even if some of the neurons are not functional, in course of time, the information is preserved due to its distributed nature. The distributed information storage in connections can be utilized to make the network to function as memory and therefore neural networks can perform associative memory tasks. All in all, neural networks are much more reliable and fault tolerant. An ANN is a parallel and distributed processing network, which takes the inspiration from the functioning of a human brain. ANN resembles the human brain (Zurada 1994) in following aspects:

1. A neuron in an ANN replaces the biological neuron.
2. The ANN acquires knowledge through learning.
3. Knowledge is stored in weighted connections between neurons.

The important terms in artificial neural networks are discussed in the following sub-sections.

2.14.2 Neuron: The Fundamental Unit of the Network

Muller and Reinhardt (1991) described the biological neural network in which the fundamental unit is the neuron which is the basic building block of central nervous system. Figure 2.4 shows the schematic structure of a neuron (Yegnanarayana 2008). It consists of a cell body or soma where the cell nucleus is located. Dendrites are tree like nerve fibres which originate from the soma. These dendrites receive signals from other neurons. A single and long fibre known as axon originates from the cell body or

axon and branches out into further strands and sub-strands connecting many other neurons at the synaptic junctions or synapses. The receiving ends of the junctions on the other cells may be on the cell body or on their dendrites. Typically, an axon of one cell can connect to a few thousand cells through their synapses. The synapse provides memory of the past knowledge or experience. The size of the cell is of the range of 10 to 80μm. The length of the axon ranges from 50μm to several meters and has a tubular shape having diameters of the order of few μm.

In the normal state the neuron is in the inhibited stage. The neuron is said to have fired when an electric signal traverses across the cell. The interior of the cell or protoplasm is negatively charged and is surrounded by liquid containing Na^+ ions. In the inhibited stage, protoplasm is at a potential of -70mV and is impermeable to Na^+ ions. This causes deficiency of positive ions in the protoplasm. When the potential increases above -60mV in the protoplasm, the surrounding membrane suddenly loses its impermeability against Na^+ ions which enter the protoplasm and reduce the potential difference. This sudden change in the membrane potential causes the neuron to discharge and is said to have fired. Whenever the neuron fires the ions reach the axon and from there they reach the adjacent neuron through synaptic junctions. This adjacent neuron, as mentioned in paragraph above, may be receiving connection from a number of neurons. Thus the output of a neuron is the weighted function of the inputs it receives from the connected neurons. Some of the inputs may be more decisive in deciding the outcome of the connected neuron, if its synaptic connection with the receiving neuron is stronger (Yegnanarayana 2008).

Quite similar to the biological neuron, a neuron can be created in a computer's memory (McCulloh and Pitts 1993) which can be connected to a number of other neurons to form a network of neurons. The strength of the various connections can be represented by a numeric value known as synaptic weights or just as weights. The learning is said to have occurred when the set of weights causes the network to recall or behave in a particular expected way. ANNs are much easier to design and more economical to operate as compared to their solid state hard wired neural networks (Stern 1996, Fraser 2000). A host of applications using ANNs are being witnessed in

recent times in tasks comprising pattern classification, pattern recognition and pattern mapping.

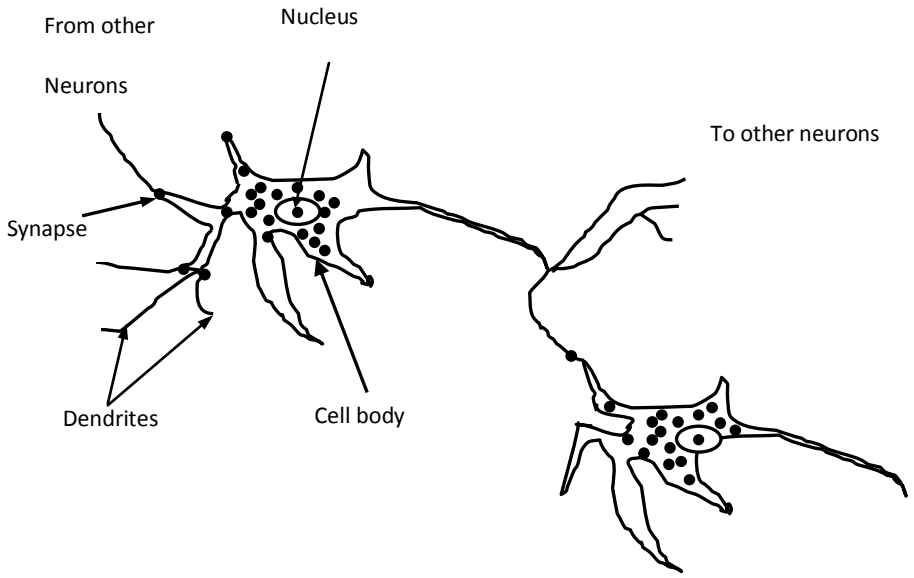

Figure 2.4 Structure of a Neuron (Yegnanarayana 2008)

2.14.3 Developments in the Field of Neural Networks

In the year 1943 McCulloch and Pitts proposed a model of a computing element called as neuron, which marked the beginning of the technique of machine learning. The McCulloch Pitts model, basically, performed the weighted sum of the inputs to the neuron followed by logic operation. The logic operation gave an output of either 1 or 0. A combination of these elements made it possible to realise a lot of logic operations. The model had the drawback that it could not learn from examples as the weights were fixed. Hebb (1949) then proposed a model in which learning was based on pre and post synaptic values and was the first and fundamental learning rule witnessed in literature relating to neural networks. Minsky (1954) further developed a machine that could learn automatically through adaption of connection weights followed by a very important invention by Rosenblatt. Rosenblatt (1958), in 1958 put forth the Perceptron model with weight adjustments being done by using Perceptron law. The Rosenblatt Perceptron model was able to solve pattern classification problems with linearly separable data. In 1960 Widrow and Hoff (1960) invented the

Adaline model. The weight adjustment was done using LMS learning algorithm. The convergence of LMS learning algorithm was proved by them and the algorithm was successfully used for adaptive signal processing applications. However, Minsky and Papert (1969) demonstrated through a number of examples, the limitations of a single layer perceptrons in solving hard problems.

Feedback neural networks by Hopfield (1982, 1984) showed that stable equilibrium states could be achieved, when the network possessed symmetric weights and the state update is done asynchronously. During the same time, their contemporaries Rumelhart and MeClelland (1986) proved that it is possible to adjust the weights of a multilayered feed forward neural network in a symmetric manner to understand the subtle and implicit relationship between input-output patterns (1986a). The multilayered network proposed by Rumelhart could solve the hard problems, i.e. problems wherein the pattern classes were not linearly separable. The convergence of Perceptron model proved by Rosenblatt ensured that the final set of weights could be reached in a finite number of steps for linearly separable data. However, Cameron (1960) and Muroga (1971) showed that the number of linearly separable functions decreased rapidly for two class problems, as the dimension of the input space is increased. In the model proposed by Rumelhart, the weight adjustments were carried out by using generalised delta rule or error backpropagation learning algorithm.

During the same time period, Ackley *et al.* (1985) proposed the Boltzmann machine, a feedback neural network with a combination of the characteristics of the Hopfield model and simulated annealing. The output function of the neurons in the Hopfield networks, which was based on deterministic update rule, was based in Boltzmann machines based on probabilistic update. In addition, in the recent few years, there have been notable developments such as, self organisation and simulated annealing. Self organisation has been useful in feature mapping while simulated annealing was effectively used in Boltzmann machine. Learning laws like competitive learning, reinforcement learning has been developed. Various architectures such as, Adaptive Resonance Theory (ART), Recurrent Neural Networks (RNN), Radial Basis Function (RBN) Networks and Counter propagation networks are being used to solve a variety

of problems related to pattern recognition, classification and pattern mapping. The ANNs are being used today in applications ranging from image processing, speech recognition, bomb detection, and robotics applications to forecasting applications. The field of neural networks has steadily yet surely made its presence and importance felt in various engineering disciplines. The field of mechanical engineering and metallurgical and material science also has not been an exception and has seen a lot of use of neural networks in various applications.

One of the most popular ways of training a Multi-Layered Perceptron (MLP) has been Back Propagation algorithm (BP). This algorithm trains the network through recursive technique and used the negative gradient descent method to decrease the error on the Mean Squared Error (MSE) v/s weights plane and adjust the weights accordingly. A completely different approach in which the curve fitting is done in a multidimensional space has emerged as another method of function approximation. This method is known as Radial Basis Function. The viewpoint here is to determine a surface in multidimensional space that best fits the training data. Thus the generalisation is brought about by a curve that interpolates the training data in a multidimensional space. RBF was first proposed by Powell (1985), while recent work by Light (1992) has generated more interest in this research area for application in numerical methods.

Recurrent networks distinguish from feed forward neural networks in that they possess one or more feedback loops. The feedback loops may be local or global. The recurrent network may contain three or more layers. The feedback from the neurons may be to all other neurons in the current layer and/or to itself. The feedback connections may start from the hidden neurons as well as from the output neurons. The presence of feedback elements is reported to have a strong influence on learning capability of the network. The feedback loops with unit time delay are known to provide non linear dynamic behaviour in case of neural networks with hidden layers (Haykin 2004).

Elman (1990, 1991) proposed the Simple Recurrent Network (SRN) which was used to discover the word boundaries in a stream of phonemes without any built-in constraints. The network contained a context layer or a temporal layer which stored

the output of hidden neurons for one time step and fed them back to the input layer. The unit time step delay in the fed back signals was reported to provide the network with ability to provide learning tasks that extend over time. As against a Jordan network (Jordan 1986, 1992), which has feedback from the output layer, the recurrent feedback in Elman network takes place in the hidden layer. Kremer (1995) showed that the computational power of the Elman simple neural network was as good as that of finite state machines.

The training of the recurrent network proposed by Elman used backpropagation algorithm with gradient descent for weight adjustment i.e. learning (Elman 1990, Jordan 1986, 1992, Li *et al.* 2002, Gruning 2006, Kremer 1995). However the problem of the network getting stuck indefinitely in a local minimum was observed (Gruning 2007). Thus there was problem of convergence while training with back propagation algorithm (Gormann and Sejnowski 1988, Bengioy *et al.*1994, Plett 2003, Yoon *et al.* 1993, Gruning 2007, Mandic and Chambers 2001, Kolen 2001, Koike 2002, Song *et al.* 2008, 2008a). Kremer (1995) stated that the power of Elman network is only partly explored. Researches in this area (Sevan-Schreiber 1988) cited that it firstly, could be because, that under the network constraints posed by Elman architecture solution may not be available. Secondly, the fault could lie with the technique of training itself, so that it does not give the solution. Mozer (1993) suggests that the Elman training technique is powerful to handle any arbitrary recurrent network. But practically it has been found that EBP training has been unable to discover the subtle relationship that exists in temporal sequences. Weight convergence in recurrent network using BP algorithm was critically analysed by Kuan *et al.* (1994). It was considered that the estimated weights were bounded and since weight estimation being a stochastic process, had considerable dependence. Some simulations, though provided weight convergence, could not be guaranteed for any arbitrary recurrent network. The implausibility of the back propagation learning was attributed to two things. Firstly, the synapses are bidirectional and secondly to the need for providing the fully specified target answer by the teacher to learner (Gruning 2007). However, not always such a fully specified target answer may be available. In this context Gruning (2007) showed that the Elman network can be reused as

reinforcement learning model (wherein signals are fed back about success or failure). The back propagation through time (BPTT) algorithm, which has given way to EBP for on line (real time) applications (Song 2010), showed convergence with low values of learning rate parameter while with high learning rates showed weight divergence. Low learning rate results in slow convergence which though is not guaranteed. Song (2009, 2010) developed an Extended EBP (eEPB) for training Elman networks using an adaptive learning rate and an adaptive dead zone, resulting in optimisation of training speed and weight convergence as well as improvement in generalisation performance. Elman recurrent network training is therefore, still a subject of active research in the area of neural computations.

The interest developed by McCulloh and Pitt's model (McCulloh and Pitts 1993) followed by resurgence in interest brought about by Rosenblatt's work continues till date. The major areas of intense research are in the fields of feed forward neural networks or multilayered perceptrons and symmetric recurrent networks.

2.14.4 Function Approximation and ANN

Function approximation from a given bunch of input-output pairs has innumerable applications in engineering and science as also in finance, medical diagnostics, weather prediction etc. In a function approximation, using statistical techniques such as regression, the specific function to which the data is to be fitted is first chosen. The data is then fitted to this function by using some methods of error minimisation such as method of least squares or by using some goodness of fit methods. An ANN when used as a function approximation model has the ability to predict the system performance which it represents and/or control it. The properties of an ANN model such as its adaptivity and non linearity are ideally suited for real world applications. The technique is mathematically less rigorous as compared to statistical and the finite element method. The mapping network does approximation in a manner similar to the generalisation that occurs with the regression technique. Any type of functional relationship between input-output pairs can be aptly represented by a three layered network (Chen and Jain 1994). In fact, function representation by a FFNN network is

more generic in nature as it encompasses many representation schemes of classical approximation method.

2.14.5 Neural Networks vs. Statistical Techniques

As a forecasting tool, ANN can be compared to Autoregressive moving Average (ARMA) class of models. ARMA methods, since ages have been used to model time series. In general, similarities do exist between the ANN and statistical techniques. An FFNN can be termed as a form of non liner regression (Ripley 1994, Potzinger *et al.* 2000). A multiple linear regression scheme, a standard statistical tool, can be thought of as a simple ANN node. For example, for a linear equation of the type, $y = w_0 + w_1x_1 + w_2x_2 + \ldots\ldots\ldots + w_nx_n$, the x_i can be taken to represent the inputs to the node, w_i can be taken as the corresponding weights and w_0 can be the threshold function.

While fitting the ARMA type of model to a time series, the data has to be stationary and must exhibit normal distribution. If indeed, that is not the case, then techniques have to be used to induce stationary data and normally distribute the data. In case of ANN, the statistical variation of data is immaterial, as the hidden neurons account for non stationarities in the data (Reddy 2004). An ANN also possesses another advantage over ARMA type models as it is a non linear model, though some non linear ARMA type models are witnessed in literature in statistics. ANNs are most ideally suited for mapping complex relationships between input-output and where the relationships are not clearly understood, either due to no proper relationship being there or inadequate data. Furthermore, ANN can make an n-step ahead forecast directly without any recursive procedure. Due to its inherent robustness in design which can be attributed to massive parallel processing, the ANNs are good modelling tools for real life problems, in which data may be inadequate, may be available with a lot of noise, and there could be distortions in data.

The ANNs have been rigorously compared with statistical methods for applications pertaining to classification and prediction (Ripley 1994). Effectiveness of ANN in time series forecasting have been examined. Lapedes and Farber (1988) have shown that in two time series prediction problems, neural networks are clearly superior to

statistical methods. Sharada and Patil (1994) analysed 75 different time series problems and inferred that the ANN and Box-Jekins forecasting system performed equally. Interestingly, it has been observed that the memory of a time series has some bearing on the performance. ANN performs slightly better than Box_Jekins model for time series with short memory while reverse is true for time series with long memory.

One of the major demerits of the artificial neural network is that unlike the statistical methods wherein the entire functioning of the model is transparent, the working of an ANN is opaque. What exactly happens inside the hidden layers is not visible although the output of the model is obviously useful. In artificial neural nets the functioning of the hidden neurons once they are trained is not clearly understood (Fraser 2000). Which of the neuron fires or why it fires is as mysterious as it was in the early days of research in neural computations. Moreover, a trained ANN serves a model for a particular problem, while there are set procedures or frameworks for selection of a fitment model in statistical techniques. Some disadvantages of ANN have been highlighted by Maier and Dandy (1999). First of all, the architecture, learning rate parameter (η) and momentum factor (α), which are functional parameters of an ANN are dependent on the problem at hand. There are no guidelines as to what architecture or what learning rate and momentum factor should be used for a particular problem. Each problem attempted by ANN is unique and all the function parameters are likely to be unique for that problem. The entire training process is a trial and error process with different combinations of number of hidden layers, number of neurons in each hidden layer, learning rate parameter and momentum factor. Another problem with ANN is that many a times, the data available to train the network isn't sufficient enough to be able to bring the generalisation of the model. Also in a system which is quite responsive to changes in the environment, ANN modelling may not be appropriate as the network may not be able to cope up to the changes taking place. For example, the networks when trained on static (past data) data may not be able to lend results for future, unless the weight matrices are updated or adjusted with suitable learning, to understand the new changes in the system.

A lot of study has been done on artificial neural networks and the regression methods to determine the suitability of these models for pattern mappings (Kim *et al.* 1993, Patuwo *et al.* 1993, Subramanian *et al.* 1993, Yoon *et al.* 1993 and Potts 2000).

Thus it can be summarised that

1. ANN can learn the relationship between input-output patterns and can generalise the relationship
2. They can handle a wide variety of data
3. They are universal approximators
4. No assumptions are required to be made in understanding relationships
5. The type or in general, the details of the process need not be known to frame an ANN model
6. Rigorous mathematical treatment is not required

All things put together, in actual practical situations, a trained ANN model has proved to be a success, complementing human brain decision making.

2.15 NEURAL NETWORKS IN MATERIAL SCIENCE

An artificial neural network is thus a parallel processing system which mimics the human style of learning through biological systems and understands the unknown process or behaviour, through prior experience. The basic unit of the network is the neuron, which passes or inhibits the signal to other neurons through connections. The knowledge is stored in the trained network by the strength of these connections, which are called as synaptic weights or simply as weights. This knowledge stored in the connections is used in predicting the behaviour of process under changed process parameters conditions. Artificial neural networks have been successfully used in the manufacturing sector as well as service sector. In the non physical sector, ANNs have been used in speech and image processing, fault detection, economy forecasting, weather forecasting, stock markets. In the manufacturing sector, use of ANN is found in steel plants, cold mill prediction, plate rolling, manufacturing of aluminium, copper, magnesium alloys and composites. The list runs quite long as far as, the use of

ANN in material science and metallurgy is concerned. The iron, steel and non ferrous metal industry is showing great interest in use of ANN in their process set up. This is to a great extent, because the system is reliable when dealing with complex and non linear relationships and does not involve rigorous mathematics. The field has also invoked a strong interest from researchers across universities and regions as it provides a good model to deal with complexities of data, non requirement of the process details, and that the model provides scope for process monitoring, control and optimization (Gormann and Sejnowski 1988, Widrow 1994, Hartley and Pillinger 2006, Su *et al.* 2007, Mousavi Anjidan 2007, Mandal *et al.* 2009).

In the recent past, a lot of applications of neural computational science are witnessed in engineering to deal with problems related to complex and non linear relationships of data. In the steel industry rolling is one of the most important forming processes. The use of ANN in rolling dates back to 1990 decade (Wang *et al.* 1995, Sun *et al.* 1995, Rao *et al.* 1995, Larkiola *et al.* 1996, 1998). Larkiola (1998) used the neural networks to optimise the mill settings to produce a product of given cross sectional dimensions and strength, and also to predict the mechanical properties of the roll strips along with the prediction of the temper force. Welding is a metal joining process used to join mostly ferrous metals and is mostly used in steel structural applications. Rao (2002) successfully used ANN for online eddy current testing of austenitic steel welds. The ANN formulated was able to evaluate the depth of the surface breaking notches within acceptable deviation. Kusiak and Kuziak (2002) proposed a new approach based on ANN to predict the volume fraction and mean size of the phase constituents after the material undergoes thermo-mechanical treatment followed by cooling. Artificial neural networks have been successfully used in predicting microstructure of 60Si2MnA rod (Jiahe *et al.* 2003), prediction of creep behaviour of 316L (N) stainless steel (Srinivasan *et al.* 2003), for simulating the forging process (Hartley and Pillinger 2006), modelling of mechanical properties of Al-Si-Cu cast alloys (Dobrazanski *et al.* 2007), optimization of flow stress in 304 stainless steels during cold and warm compression (Anijdah *et al.* 2007), and optimization of aging process for Cu-Cr-Zr-Mg alloy for aging treatment, hardness and conductivity (Su *et al.* 2007).

The deformation behaviour of AISI 304L type stainless steel was studied by Mandal *et al.* (2009) using ANN trained with standard BP algorithm. Recently, Wen *et al.* (2009) used ANN model to predict microstructural change in conventional rolling and thermo-mechanical processing of C-Mn and high strength alloy steels and were found to be capable of supplementing their counterparts using conventional classical and empirical methods. Poppe *et al.* (1995) looks at neural network as that can lead to an intelligent steel production plant, which shall include automation of processes, scheduling and management decisions being influenced by Neural Networks.

2.16 NEURAL NETWORKS IN SEMISOLID PROCESSING OF COMPOSITES

2.16.1 Procedure Involved in ANN Model Development

The development of an ANN model involves various processes and functions. To develop an ANN model one needs to know the best representative input parameters for the given output(s). The preparation of the model would require sufficient amount of training data so that network can learn. The selection of the type and amount of data is often a matter of in depth knowledge and experience about the process considered for modelling. The model developer should be in a position to determine the data which is most representative of the input-output population. Thus data generation becomes an important task in model development. Next, the input as well as output data needs to be scaled so that data is grouped in a pre-decided range. Also, the methods for weight initialisation to be used, determination of biases, deciding on the architecture etc. are not readily available and require good amount of attention during model development. The model developer should be aware that a neural network does not have any information about the metallurgical process that is being modelled. In order that the network understands the underlying relationships for the process, the network needs to be trained. Hence, neural network training is the heart of the entire ANN model development. The model developer should be sure that the data that is being used for training is authentic, devoid of any significant measurement errors. Any erroneous data used for training can lead to a situation similar to teaching

wrong things thereby, resulting in wrong learning. Wrong learning will automatically lead to erroneous outputs from the model.

2.16.2 Data Preparation

Generally the data for an NN model arrives from a variety of sources. The NN is able to process the data in a certain structured form. The network learning is affected by the form in which the data is presented to the network. Hence the right coding scheme for the data needs to be decided before hand, so that the network can learn and can perform the given task. Therefore, the coding scheme for the data has to be in place before the data collection task is taken up. Design of data coding system should be decided before data collection as one should be aware as to what he is going to do with that data. The process of data preparation involves the following steps.

2.16.2.1 Data Collection and Generation

The primary step in the ANN model development is deciding on the input and output data required. After these have been identified, the metallurgical system/process data needs to be generated. There are usually, two sources available for data generation/collection. One can get data from the hand books or data books in metallurgy and secondly from experiments. Actually, data generation means use of a data generator which will give an output for each chosen sample. The total numbers of samples are so chosen that the final model represents the actual metallurgical problem on hand accurately. The type of data generator selected, generally depends upon the type of problem being modelled. In the present work, the data is collected from the experimental work done by Herbert (2007).

2.16.2.2 Range and Distribution of Samples

In general for modelling, a neural network needs three types of data sets. They are named as training data, test data and validation data. Training data is used for training the network, that is, to update the weights as the network learns from the test samples being presented to it during training. The validation data performs the function of monitoring the quality of training and helps in decision making as regards to

terminating the training process. The test data is used to check the final performance of the trained model.

If the data being collected to develop the model lies in the range $\mathbf{[x_{min}, x_{max}]}$, the validation and the test data also needs to be generated in the range $\mathbf{[x_{min}, x_{max}]}$. The training data can also be generated in the same range. In the region near the extremes i.e. at the boundaries, it is advisable that training data may be sampled slightly beyond the bounded values of data. The reason for this is to improve the performance of the model at the boundaries of input sample space.

After deciding upon the range of the input parameters, the next step is to determine the distribution of the input samples within the range. Generally, one can adopt three methods, namely, uniform grid or equal spacing method, non uniform grid or unequal spacing method or random distribution. By default, if there is no other compulsive reason, one goes by the uniform grid method. Non uniform grid method is mostly chosen when the process requires the sampling to be dense in some regions in the input parameter space, where there is a likelihood of highly non linear process behaviour. In such cases, it is better the neural network designer has a prior knowledge of the process behaviour. In a randomised data distribution, each sample in the range $\mathbf{[x_{min}, x_{max}]}$ is a random variable and the method is used when dimension of the input parameter space is high.

2.16.2.3 Pre-Processing and Post-Processing of Data

In most of the cases, the input space consists of more than one variable. Each of the input for the data collected may have different range. Similarly the number of outputs may be more than one and each may have a different range. Hence each of the inputs and the outputs needs to be normalised by its own normalising factors. Hence there is a need for pre-processing of the raw input and output data or else the network will not perform satisfactorily. This is a critical phase in the overall model design and development.

There are two methods of data pre-processing. These are transformation method and the normalisation method. In the transformation method, the raw input data is manipulated to create a single input to a network, while normalisation transforms a single input data to be distributed evenly and scales it into a workable range that for the network (Swingler 1996, Berry and Linoff 1997, Reddy *et al.* 2005). As stated earlier, it is desirable that the knowledge of the processes and systems for which the model is developed be known, as it will help to understand the underlying features of the process. All this will help the network to be trained in a better fashion resulting in better performance of the network.

Normalisation of data is the last step in data pre-processing. The goal is to distribute the data in such a way that it is spread uniformly across the data range. This applies to both the input as well as the output data and the values should be scaled in such a way that the range of the input and output data matches the range of the summing and squashing device, the neuron. Thus, it can be seen that one may perform any other transformation, normalisation as a final pre-processing step is indispensable.

It is possible to scale the raw input data within any range. However, for our work the data is scaled between 0.1 and 0.9 using the following normalising function.

$$x_n = \frac{(x - x_{min}) * 0.8}{(x_{max} - x_{min})} + 0.1 \qquad (2.1)$$

In the above equation x_n refers to the normalised value, x_{min} is the minimum and x_{max} is the maximum value in the range.

Upon training the network to a required degree of performance, it is expected that the network will provide the output values that are well understood by the end user. In order to achieve this, the post- processing of data becomes necessary. In this step, the outputs of the network in the normalised form are de-normalised using the below mentioned equation.

$$x = \frac{(x_{max} - x_{min}) * (x_n - 0.1)}{0.8} + x_{min} \qquad (2.2)$$

2.17 STRUCTURE OF AN ANN MODEL

As of present, there is no way by which a structure of a network can be determined using some analytical formulae or any empirical methods based on the network parameters (Swingler 1996, Kang and Song 1998, Attoh-Okine 1999, Reddy 2004). Thus, the structure must be manually selected using trial and error approach. While deciding upon the network structure, several factors need to be taken into account. These can be listed as follows.

- Number of hidden layers
- Number of neurons in each hidden layer

The network is trained using standard BP algorithm. The convergence of the network depends, in addition to the above parameters, upon the following.

- Summing function
- Activation function
- Initial weights
- Learning rate
- Momentum term

2.17.1 Summing function

The non input neurons in the network receive the inputs through the weighted connections from other neurons, producing a single input known as the net input. This is known as a combination or summing function and converts a column vector into a scalar quantity (Zurada 1994, Reddy *et al.* 2005). Most neural networks such as FNNN, use linear combination functions while the argument(s) of the activation function in Radial-basis function (RBF) networks are Euclidean norm (distance) based combination functions.

2.17.2 Activation Function

Most of the applications in neural networks use bipolar continuous functions. McCulloh Pitts neuron model used the step function with binary 0 and 1 as the neuron outputs. The firing used in McCulloh Pitts model (McCulloh and Pitts 1993) is given below.

$$0^{k+1} = 1 \quad if \ \sum_{i=1}^{n} w_i {x_i}^k \geq T \qquad (2.3\ a)$$

$$= 0 \quad if \ \sum_{i=1}^{n} w_i {x_i}^k < T \qquad (2.3b)$$

Here subscript k refers to discrete time instant and w_i to the connection weight connecting the i^{th} input to the neuron. This rule is aptly followed by a step function.

However a step function and for that matter a ramp function is not suitable for understanding and learning non linear relationships of data. Hence a need was felt for continuous non linear functions. Moreover, backpropagation algorithm used for training FFNN needs a differentiable function. The capability to represent non linear relationship makes the multi layer perceptrons (MLP) powerful computational devices. For the hidden units in these MLP activation functions such as sigmoid or tan*h* (tan hyperbolic) functions are therefore more suitable. Therefore "squashed" function rather than a ramp function is preferred in modern day neural networks. The most popular function used is the sigmoid function, which is unipolar continuous. The sigmoid function is given below.

$$f(x) = \frac{1}{1+e^{-x}} \qquad (2.4)$$

For the outputs, one may select an activation function to suit the distribution of target values. For binary (0/1), the logistic function is ideally suited (Jordan 1995). Thus the logistic function (sigmoid function) has been used as the activation function.

2.17.3 Initial Weights

Typically the weights of the network are initialised at small random values. The weight initialisation has a strong bearing on the way the network learns. If one starts out with equal weights and the network solution requires that the weights be unequal, then learning will not proceed in proper direction. The network may fail to learn from the training data due to either the error stabilising or due to increase in error as training continues. If one continues training the network even when the region of low plateau has reached, it may result in drifting of weights, which is not desirable. The error then increases and the mapping quality of network suffer. To counter this, it is desirable to start with a fresh set of random weights.

2.17.4 Learning Rate

Learning rate parameter (η) determines the quantum of weight adjustment done at each step and is responsible for the rate at which the convergence of the network takes place. A poor choice of this parameter can lead to convergence problems. The selection of proper value of learning rate coefficient determines the effectiveness of the use of backpropagation algorithm. There is no information available on selection of learning rate parameter and it depends upon the type of relationship that exists in the data sets (Reddy *et al.* 2005). Thus learning rate coefficient is unique for each problem being modelled and has to be arrived at by trial and error. Use of too low a learning rate parameter will lead to very slow convergence. A too high value of η may cause the network to oscillate or diverge thereby leading to non convergence. Under this situation, no learning will take place. Rumelhart and McClelland (1986) reported that a value of $\eta = 0.25$ and $\alpha = 0.9$ gives good results for most computations. Usually η being the quantum of weight adjustment for each iteration, its value lies between 0.1 and 0.9.

2.17.5 Momentum Factor

The crux of backpropagation algorithm is the evaluation of the contribution of each weight to the error output. This is a credit assignment problem. The objective function

in NN training is a continuously differentiable function of the weights. Therefore evaluation of the credit assignment is easily possible. It therefore may appear that the use of BP training scheme is a guarantee for network convergence. But this is not the case though. This is because the error surface on the error v/s weight plane may have a number of local minimums, besides possessing a global minimum. There is quite a possibility that the training may get stuck in the local minimum and may not move on this plane. Secondly, there may be some stationary points on the error profile. The stationary points too, inhibit the learning process in the BP algorithm. The purpose of introducing the momentum term in the training scheme of an FFNN is to accelerate the convergence of the network by overcoming these issues. The method involves supplementing the current weight adjustments with a fraction of the weight adjustment in the previous time step. The current weight adjustment then takes the form shown below.

$$\Delta w(t) = -\mu \nabla E(t) + \alpha \Delta w(t-1) \qquad (2.5)$$

The arguments t and (t-1) in the above equation indicate the current and the most recent previous training step. The term α is called as the momentum term or the momentum factor. The advantage of using the momentum term is that it gives an added momentum to the downward descent movement. This process can help the network to climb out of the local minima and travel further down the slope of error profile. The larger the momentum term, as can be seen from above equation, the larger will be its impact on convergence. Typically α is chosen between 0.1 and 0.9.

2.17.6 Number of Hidden layers

There are many linear classification applications, which do not need any hidden layers. They are basically two layer perceptrons (McCullagh and Nelder 1989). In an FFNN model design, one of the most important aspects is to choose the number of hidden layers. The universal approximation theorem states that a single hidden layer or a three layered perceptron is sufficient to compute a uniform approximation to a given training set represented by the set of multidimensional inputs and desired target. The theorem does not though throw any light, whether the single hidden layer is an

optimum solution in terms of learning, implementation and most of all generalization. In feed forward networks with any of the wide variety of the continuous and non linear activation functions in the hidden layer neurons, one hidden layer with a large number of neurons gives the network a "universal approximation" property (German and Bienenstock 1992, Hornik 1993, Reddy 2004). Currently, there is no theoretical evidence on the number of hidden layers required to approximate any given function. If there is only one input, then one hidden layer is good enough to approximate and generalize the function. However, the things get more complex, when the number of inputs is two or more. Literature (Lippman 1987, Reddy 2005) suggests that a multilayer perceptron using the sigmoid function and having two hidden layers can virtually solve any problem of function approximation. The actual architecture involving the number of hidden layers and arriving at the total number of units required is problem specific and is done by trial and error method (Stern 1996, Swingler 1996).

2.17.7 Number of Hidden Neurons per Layer

The size of the number of neurons in the hidden layer(s) is one of the important considerations from the convergence viewpoint. There have been no conclusive answers thus far on the size of the hidden layers, for many tasks. The reasons for this could be the complexity of the mappings and the non deterministic nature of the many successfully completed training tasks. Thus selection of the size of the hidden layers is a challenging problem. The optimal number of hidden units depends on a number of factors, like the number of inputs, outputs, the type of activation function used, the number of training patterns available, the noise in these patterns, the net architecture and the type of training algorithm used.

Hecht-Nielsen (1991) used the network interpretation of Kolmogorov's theorem to arrive at the upper limit of the number of hidden layer units as $2(N_i+1)$, where N_i indicates the number of input units. Zurada (1994) as well as Mirchandani and Cao (1989) suggested that the relationship between number of hidden layers J and the number of training input patterns M as "$J=\log_2 M$". This relationship was based on the observations of Lippmaan (1987) and Gorman and Sejnowski (1988). Another

observation is that a three layered MLP will never require more than twice the number of neurons in the input layer (Swingler 1996, Bergsma *et al.* 1997). Too few neurons in the hidden layer can cause the problems of under fitting and high statistical bias (German, and Bienenstock 1992, Reddy 2004). This is due to high training error and statistical bias. Too high a number of neurons in the hidden layer will increase the training time.

In a majority of the situations, it is difficult to arrive at the number of neurons in the hidden layers. Again, the selection is problem specific and is obtained by trial and error approach. The hunt for the best number of hidden layer neurons is to be continued till one obtains minimum generalization error. Figure 2.5 gives a flow chart of ANN model development.

2.18 GRAPHICAL USER INTERFACE DESIGN

The medium of graphics has revolutionised the user interface design. If used appropriately, it can harness the information assimilation, processing and dissemination capabilities of the user and allow for faster interaction with computer system. Graphical User Interface (GUI) has brought about a marked change in the world of computing in terms of use of computer systems across professions. A well designed GUI will help the user to interact with the system comfortably, in the sense, that it is easier to learn, more effective to use and does not cause vision fatigue when used for long periods. The fact that they are easy to use does not imply that they are easy to design. In fact the designing medium for GUIs in modern days is so rich with so many different options of architectures, colour combinations, facilities, metaphors, patterns available that one can create an excellent GUI for a given application. However, with so much flexibility available in terms of choices in design, there is every possibility of the designer going overboard and coming out with a mediocre, lacklustre design of GUI. Therefore designing a good GUI is a challenging task.

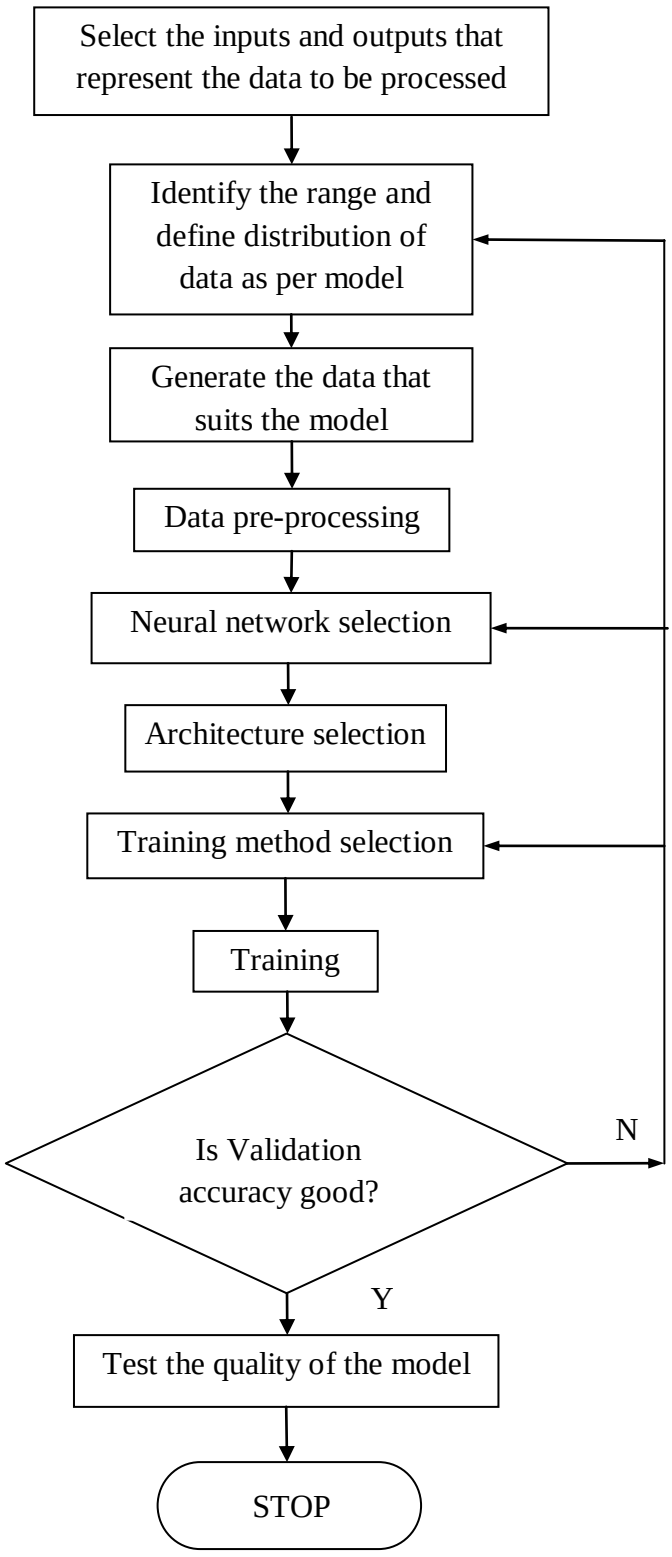

Figure 2.5 Flowchart giving the sequence of neural network model development

2.18.1 Objectives of Graphical User Interface Design

The user interface is a part of the computer system which connects the user with the internal system of the computer. In a typical information system or the systems used in offices, the user interface may include following.

- The components of the computer hardware with which the user can interact with the system such as, screen, mouse, keyboard, toggle switch, on/off switch etc.
- The images within the computer application software such as windows, task bars, pull down menus, pop ups, messages, help screens, etc.
- User documentations such as manuals, catalogues, reference cards

While the user operates on a GUI, he/she has no access to what is happening inside the computer system. The system will work in the background based on the information provided by the user in the input section and provide him/her with the processed outputs. Therefore the user is more concerned with the interface, rather than what is happening in the background. Hence the objective of the GUI design is to make it as user friendly as possible, by increasing its usability. Usability here means, making the computer system adaptable to human beings who are going to use it, and has a lot of bearing on the psychological issues relating to human memory, perception, comprehension and conceptualization.

A good interface design is important as it is the only medium that allows the user to interact with the computer internals. A lacklustre design may not be attractive to the user and he may not use it. Further a wrongly designed GUI may confuse the user and there is every possibility that one may use it wrongly or stop using it. Actually, the interface is the front end of the computer system by which the designer represents the system to the user. A good user interface can result in increase of productivity while a poorly designed one may cause stress followed by fatigue and discomfort to the user.

2.19 SUMMARY AND GAP IN KNOWLEDGE

2.19.1 Conclusions

- The near net shaping of parts by thixoforming and low weight to strength ratio, high specific modulus, high thermal stability and high wear resistance of the composites is set to bring about revolution in the engineering industry, especially the automotive and aerospace industry.
- Literature survey indicates that the data available on semisolid processing through research carried out on various composites as on date is inadequate to be viable commercially. This is because the experiments that are carried out successfully at specific predetermined points only indicate the success of the process.
- For the process to be commercially viable, a lot of other factors relating to output optimization based on the process parameters and variation of inputs is needed. This requires expansion of data available in the research literature.
- The mushy state rolling experiments are done at high temperatures. It involves a tight control of mushy state parameters, mainly the temperature which determines the mushy state i.e. the liquid content in the composite. Maintaining precise temperature ($\pm 2^{\circ}C$) during the conduct of these experiments is a challenging task. Moreover, the specimen needs to be held at that temperature corresponding to liquid volume fraction for certain period of time for homogenization. Therefore the conduct of a large number of experiments to meet the commercial requirements is not prudent, as it would be tedious, time consuming and costly.
- The survey of literature on neural networks reveals the use of artificial neural networks in various applications ranging from speech recognition and image processing to robotics and material science.
- The use of feed forward neural networks in metallurgy has been surprisingly limited in composite processing. Moreover, the author has not come across any application of recurrent neural networks in metallurgy and material science. Hence, the possibility of use of recurrent neural networks in processing of composites needs to be explored.

- The FFNN presents a powerful tool for generalisation of relationships between inputs and outputs of a metallurgical process without a need to understand the intricacies of the process, which can be used to improve the research databank. This will also help in improving the usefulness of the research work carried out in semisolid processing of composites.
- Therefore, in the present study, neural network approach, inclusive of FFNN modelling and RNN modelling, towards process/system generalisation has been demonstrated, the data for which has been taken from the results of the study carried out by Herbert (2007).

Table 2.5 Table showing the summary of the Literature review

Year	Author(s)	Findings	Remarks
1972	Spencer *et al*.	Led to the discovery of a semisolid alloy having a liquid fraction of 0.4, devoid of dendritic structure, behaving like a fluid.	Established semisolid processing as a new manufacturing process, whose commercial viability can be enhanced.
1974	Fukuoka and Kiuchi	Demonstrated that there is substantial decrease in flow stress with decrease in solid fraction in the semisolid material.	Saving in Energy requirements, which can be justified by process modelling.
1989	Kiuchi	Mushy state extrusion has been used to obtain wires, tubes and bars from billets with the liquid weight content between 20-30%.	Alternative to conventional extrusion process.
1989	Kiuchi	Demonstrated mushy state rolling on AA5052 and AA7075 alloys by stable, steady flow and homogeneous deformation of the semisolid plate or sheet, as well as rapid cooling inside the roll gap.	Alternative to conventional rolling process.
1992	Fleming *et al.*	Found a process involving the control of rheological properties of the semisolid alloy that led to a process called Rheocasting.	Better process control and prediction of flow in die cavity during forming process.
1994	Kirkwood	The property of Thixotropy can be used for Thixocasting.	Led to component manufacture by Thixoforming.

2000	Tzimas and Zavaaliangos	Showed that during mushy state forming, the flow stress reduces with increase in liquid content	Low energy requirements leading to green manufacturing, which can be further studied and analysed.
2003	Zoqui	Morphological analysis of Al-4.5 wt% Cu have revealed that grain refinement is more predominant when the alloy is subjected to deformation prior to partial remelting as compared to that in case of cast structure.	Led to the fabrication of Al-4.5 Cu alloy based composites, which can be modelled for further investigation.
2008	Herbert	Mushy state rolled Al-4.5Cu-5TiB_2 composite fabricated *in situ* by mixed salt route gives refinement in grain structure with bimodal grain size distribution resulting in improved formability and better mechanical and wear properties.	Alternative to conventional forming, with lesser energy requirements and near net forming leading to green manufacturing, whose boundaries can be extended for commercial application.
1943	McCulloh and Pitts	Invented the artificial neuron similar to a biological neuron which can be connected to a number of other neurons to form a network of neurons	Technological breakthrough.
1986	Rumelhart and MeClelland	Demonstrated the success of multilayered Perceptron model trained with back propagation algorithm to understand the subtle and implicit relationship between input-output patterns.	Ideal tool for generalisation of any process.
1990	Elman	Proposed a Simple Recurrent Neural Network using back propagation algorithm, which takes into account the dynamic changes in the input data.	Recurrent neural network of Elman type can be trained for predicting mechanical and wear properties of Al-4.5Cu-5TiB_2 composite.
2005	Reddy *et al.*	Used ANN model with Feed Forward architecture to predict grain size of Al-7Si Alloy.	ANN model with feed forward architecture can be used for modelling the mushy state rolling process.
2007	Gruning	Demonstrated that Elman network gets stuck in local minimum during training.	Scope for improving the convergence of Elman Simple Recurrent Network.

2008	Reddy *et al.*	Used Artificial Neural networks model for Prediction of flow stress in Ti-6Al- 4V alloy.	ANN model with feed forward architecture can be used to predict the mechanical and wear properties of Al-4.5Cu-5TiB_2 composite.

Thus it is seen that the FFNN presents a powerful tool for generalisation of relationships between inputs and outputs of a metallurgical process without a need to understand the intricacies of the process. A dedicated approach therefore needs to be undertaken to improve the usefulness of the research work carried out in semisolid processing of composites. Further, the possibility of use of recurrent neural networks in processing of composites needs to be explored. In the present study, neural network approach, inclusive of FFNN modelling and RNN modelling, towards process/system generalisation has been demonstrated and the data for study has been taken from the work carried out by Herbert (2007).

Aluminium alloy based Metal Matrix Composites are reinforced with ceramic particles such as TiB_2, TiC, SiC etc. which are very hard. When such composites containing hard ceramic particles are subjected to conventional forming processes, cracking is observed. This difficulty is overcome by forming of Al based alloy composites in mushy state. Further, forming of aluminium alloy based composite components in mushy state has gained importance because it requires lower flow stress compared to the working by conventional forming methods. This leads to saving in energy requirements. Moreover, mushy state forming of Aluminium based composites gives near net shaping of components leading to green manufacturing (Herbert 2007). Therefore, mushy state forming, in addition to overcoming the difficulties rendered by conventional forming of composites also leads to reduction in cost of manufacture. In this study, the concentration of Cu in the Al-Cu alloy is chosen as 4.5 wt% because of the formation of single phase α-Al at the solidus, strong age hardenability, as well as the sufficient gap between the liquidus and solidus temperatures (Herbert *et al.* 2006). Figure 2.6 and Figure 2.7 show the Al-Cu binary phase diagram and the TTT curve for Al-4.5 Cu alloy respectively. The gap between liquidus and solidus temperatures is extremely important in semisolid processing. The study of mushy state rolled Al-4.5 Cu alloy reinforced with 5 wt.% TiB_2 particles was

carried out by Herbert(2007) to explore the microstructural evolution, mechanical and wear properties. The conduct of these studies involved:

i. Casting of Al-4.5Cu-5TiB_2 composite.
ii. Preparation of specimens (as cast specimens and pre-hot rolled specimens) for rolling.
iii. Mushy state rolling experiments being carried out at temperatures in excess of 700°C, with a precise control over temperature (±2°C).
iv. Conducting SEM, XRD studies for microstructural evolution followed by Vickers hardness tests, wear tests and tensile tests.

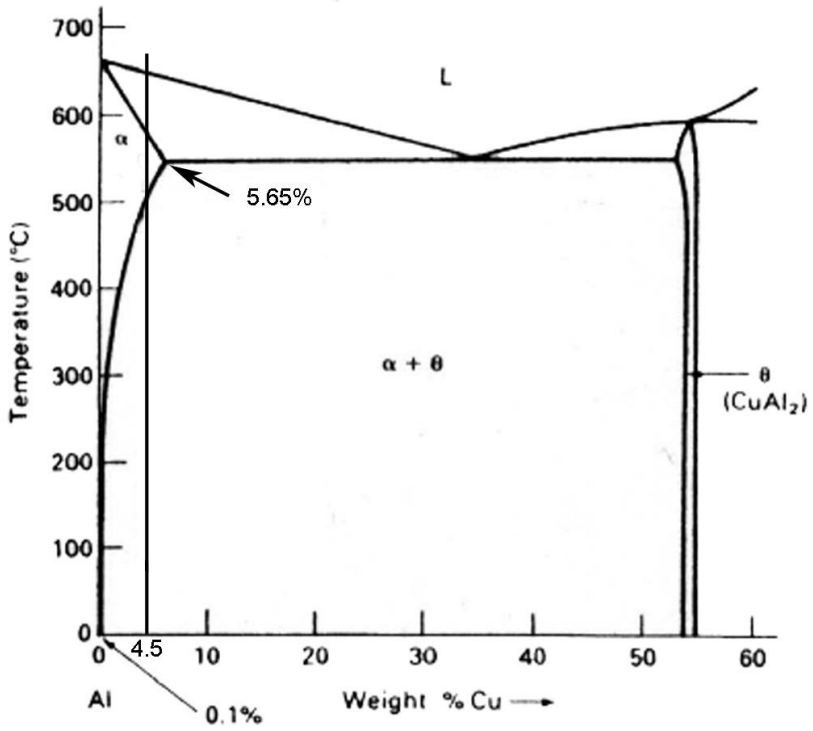

Figure 2.6 Al-Cu binary phase diagram.

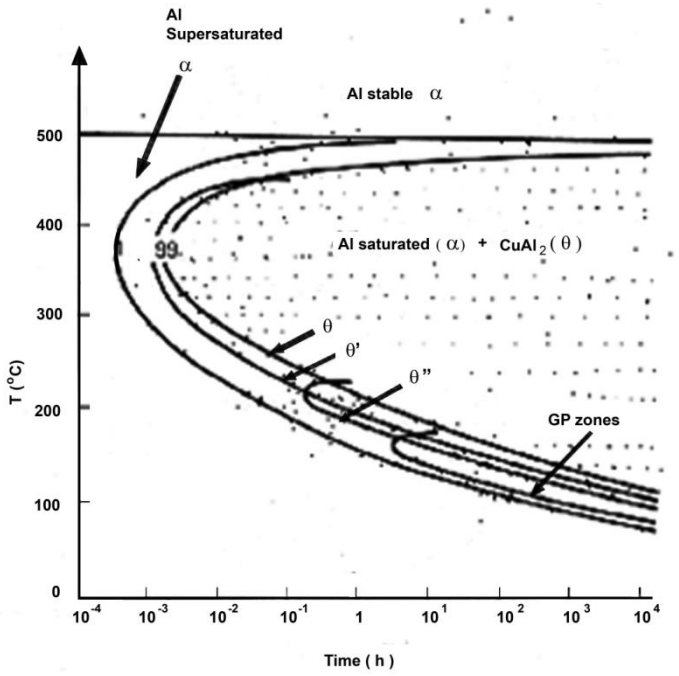

Figure 2.7 TTT diagram for Al-4.5 Cu alloy.

Thus, it can be seen that carrying out these experiments involved a large volume of time, patience and cost. The experiments were conducted at some specific combinations of input mushy state parameters and the results were reported. This though, brought out to the fore a novel research finding, yet the data required for commercial acceptance was inadequate. In order to overcome this gap, the data needs to be expanded and validated. A number of statistical techniques such as regression analysis etc. were available. But the input-output relationship in a mushy state process being non linear and being complex in nature, it is proposed to use ANN modelling for mushy state rolling of Al-4.5Cu-5TiB_2 composite, rolled in as cast and pre-hot rolled condition, which literature suggests has not been attempted earlier. Further, the use of Elman Simple RNN model is explored to improve the convergence characteristics of the neural networks proposed. Problems encountered in convergence of Elman Simple RNN model and strategies to overcome these difficulties leading to formulation of a novel Hybrid RNN are also undertaken in this study.

2.19.2 Statement of problem

As has been seen in section 2.19.1, forming of MMCs by conventional forming processes (Herbert *et al.* 2006) is difficult as MMCs do not offer themselves readily

for conventional forming. As seen earlier, this is due to the presence of hard ceramic particles, uniformly distributed in the matrix of the composite. Processing of MMCs in semisolid state offers a convenient route in overcoming this difficulty. When the MMC in semisolid state is subjected to forming upon application of an external load, the induced strain is fully accommodated by the viscous flow of the liquid entrapped at the grain boundaries and therefore the possibility of cracks originating during the forming process is prevented.

The properties exhibited by the MMCs depend upon the extent of distribution of the hard ceramic particles in the matrix of the composite. It is seen that the *in situ* fabrication of Al-4.5Cu-5TiB_2 composite via the mixed salt route(Herbert 2007) gives a uniform distribution of fine TiB_2 particles in the matrix of Al-4.5Cu alloy. The wettability of the particles due to very fine particles is known to be better. Further, the fabrication of the composite via mixed salt route offers a cleaner method of obtaining castings as the possibility of unwanted impurities entering the system is drastically reduced.

It is seen that mushy state rolling of Al-4.5Cu-5TiB_2 composite leads to nearly equiaxed grains having bimodal grain size distribution. Rolling at low liquid content with high thickness reduction leads to deformation of unmelted grains which work harden significantly, thereby causing increase in hardness of the composite. This in turn leads to higher strength and wear properties. Thus it is seen that the resulting properties of the Al-4.5Cu-5TiB_2 composite subjected to mushy state rolling depend upon the mushy state rolling parameters viz. thickness reduction and liquid volume fraction. The mushy state rolling experiments carried out by Herbert (2007) on as cast and pre-hot rolled Al-4.5Cu-5TiB_2 composite samples provided the resulting microstructural properties, mechanical and wear properties only at some predetermined combinations of input parameters viz. initial state of the composite (i.e. as cast or pre hot rolled condition), % thickness reduction and % liquid volume fraction in the composite. The excellent findings of the study provided a great potential for the mushy state rolling as a near net shaping process, resulting in decreased power requirements and saving in energy. But for commercial viability, a larger volume of input-output data of the mushy state rolling of the composite is required.

Artificial Neural Networks provide an excellent technique to generalise the relationship between inputs and outputs of process, provided that the network has been trained on such known relationships. The ANN models are especially suitable where the relationship is non linear and quite complex. Large and small grain sizes, hardness, wear and tensile properties as functions of the mushy state rolling parameters, (viz. initial state of the composite, thickness reduction and liquid volume fraction in the composite) define a non linear complex system. Thus ANN model with feed forward architecture and trained with error backpropagation algorithm provides an excellent option to predict the microstructural, mechanical and wear properties of the composite.

Elman simple Recurrent Network was proposed by Elman which exhibited faster convergence than feed forward neural networks. But generally, Elman networks were found to get stuck in local minima, resulting in convergence problems. Therefore, there is a need to explore the possibility of identifying a modification to existing Elman Simple Recurrent Network which will combine the faster convergence capability of Elman network and overcome the limitation of getting stuck in local minima.

This thesis proposes to use ANN models with feed forward architecture to predict grain sizes, hardness, tensile and wear properties of mushy state rolled Al-4.5Cu-5TiB_2 composite rolled in as cast and pre hot rolled condition with different combinations of thickness reduction (2 to 12.5%) and liquid volume fraction (5 to 35%). The work also deals with the formulation of Hybrid Recurrent Neural Network that can predict the output comparable to a feed forward neural network with better convergence characteristics, due to its inherent self looping properties.

2.19.3 Statement of objectives

Studies on mushy state rolling of cast Al- 4.5 (wt.%) - 5(wt.%)TiB_2 composite by Herbert (2007) have provided mushy state forming as an alternative route to conventional hot rolling as a forming method, yielding better mechanical and wear properties. For commercial applications, the data now needs to be made available in the entire range of parameters in which experiments were carried out and also at close

points outside the bounds of experimentation. With this in mind, the proposed work envisages the accomplishment of following specific objectives:

1. Development of ANN model to simulate the relationship of mushy state rolling process parameters and their influence on grain size and mechanical properties like hardness, wear and strength.
2. Experimental work for validation of the above ANN models for prediction of grain sizes, hardness and wear properties and analysing the results for checking the authenticity of ANN model in prediction.
3. Optimization of the process of mushy state rolling in terms of the mushy state rolling parameters to obtain the best output, by using Graphical User Interface/ Application Programmer Interface libraries.
4. Development of Hybrid Recurrent Neural Network from an Extended Elman RNN (SRN) model for mimicking the process of mushy state rolling of Al-4.5Cu-5TiB_2 composite to predict grain sizes, hardness, wear and tensile properties.
5. Comparing the performance of HRNN model with reference to ANN model for its effectiveness.

2.19.4 Scope

The scope of the work in the proposed study shall include;

a. The modelling of ANN with feed forward architecture to correlate the mushy state rolling parameters with grain sizes, hardness, tensile and wear properties of Al-4.5Cu-5TiB_2 composite.
b. The modelling of Hybrid Recurrent Neural network to correlate the mushy state rolling parameters with grain sizes, hardness, tensile and wear properties of Al-4.5Cu-5TiB_2 composite.
c. Comparing the performance of ANN with feed forward architecture and HRNN in terms of:

    i. The prediction capability and

ii. Convergence characteristics.

d. Developing a GUI based tool for studying parametric influence on the mushy state rolling of Al-4.5Cu-5TiB_2 composite.
e. Validation of the models by conducting mushy state rolling of Al-4.5Cu-5TiB_2 composite at some input parameter combinations which lie within and outside the data used for training the networks cited at (a) and (b) above.

2.19.5 Plan of work

The overall plan of work for carrying out the study is listed out hereunder:

a. To gather data from literature survey.
b. To analyse the data and apply suitable modelling technique for prediction of desired outputs, based on ANN principles.
c. Try out neural network models by error back propagation network, recurrent neural network and a hybrid option of ANN with RNN to simulate the mushy state rolling process for Al-4.5Cu-5TiB_2 composite.
d. To develop a graphics interface for observing the relationship between inputs and outputs as desired by the user instantaneously and graphically.
e. Validate the predictions by conducting suitable mushy state rolling experiments on Al-4.5Cu-5TiB_2 composite.

Chapter 3

EXPERIMENTAL DETAILS

3.1 INTRODUCTION

As reviewed in chapter 2, a large number of research is going on the in the field of mushy state forming of metals and metal matrix composites. As seen in the literature review, a fair amount of work is going on in the field of rolling of discontinuously reinforced Al alloy based composites in mushy state, with rolling initiated when the composite is in as cast condition and in pre hot rolled condition (Herbert 2007). The study (Herbert 2007, Siddalingeshwar 2011), deals with the evolution of microstructure in the mushy state rolled Al-4.5Cu-5TiB_2 composite and its effect on the mechanical properties, wear properties and creep properties. The work done by Herbert (2007) and Siddalingeshwar (2010) establishes the fact that it is possible to nearly net shape discontinuously reinforced Al alloy based *in situ* composites by subjecting the composite to mushy state rolling. In the experimentations carried out by Herbert (2007), the Al-4.5Cu-5TiB_2 composite is rolled in mushy state to thickness reductions ranging from 2.5 to 10%, with a step size of 2.5%, and with rolling being initiated when the composite has a volume fraction of liquid as 10%, 20% and 30%. The work done by them (Herbert 2007, Siddalingeshwar 2010, 2011) does establish that mushy state rolling results in improvement of grain structure, resulting in improvement in properties. The study also reveals the influence of rolling parameters such as, thickness reduction and liquid content on the resulting mechanical and wear properties. However, the investigation of microstructural details and properties with combination of inputs (thickness reduction and liquid volume content) is done at specific points of experimentation only, and therefore gives only a glimpse of the potential of mushy state rolling of the said composite. The user industry however needs more data, so that the process can be optimised based on either the input parameters control or controlling the output parameters. The commercial acceptance of the technological breakthrough is therefore the problem at hand. The data, however, if expanded to include more combinations of the input parameters providing

the corresponding microstructure and mechanical properties as outputs, will become more useful to the ultimate user, the industries. The ANN model proposed, as discussed in Chapter 1 will provide the solution for improving the database for correlation of mushy state parameters with microstructure and the resulting mechanical and wear properties. Indeed the model has to be checked to verify its authenticity as well as its correctness in prediction of outputs from an unknown set of inputs. In order to validate the ANN model, it is endeavoured to perform the investigations detailed out as under:

- Preparation of Al-4.5(wt %) Cu alloy and *in situ* Al-4.5(wt. %) Cu-5(wt. %) TiB_2 composite followed by characterization of the Al-4.5(wt. %) Cu-5(wt. %) TiB_2 composite by using Scanning Electron Microscope (SEM).
- Determining the temperature corresponding to the volume fraction of liquid selected for carrying out the mushy state rolling of the said composite, by applying the lever rule to Al-Cu equilibrium phase diagram.
- Mushy state rolling of the composite to x (x=2, 6, 11.5) percent thickness reduction containing y (y=7, 17 and 33) volume fraction of liquid followed by microstructural characterization using SEM. The mushy state rolling experiments with these values of x and y are carried out to validate the ANN model performance with values of x and y other than those used for training the model. A comparative study is then carried out between the model predictions and the experimental results at values corresponding to the values of x and y used for training of the model as well as those used for model validation.
- Study of wear behaviour of mushy state rolled Al-4.5(wt. %) Cu-5(wt. %) TiB_2 composite is carried out at x (x=2, 6 and 11.5) percent thickness reduction containing y (y=7, 17 and 33) volume percent liquid.

The work is started with the selection of raw materials followed by planning of experiments for different segments mentioned above. A schematic presentation of the overview is shown in Figure 3.1. The details of the experiments to be carried out are given in the subsequent sections.

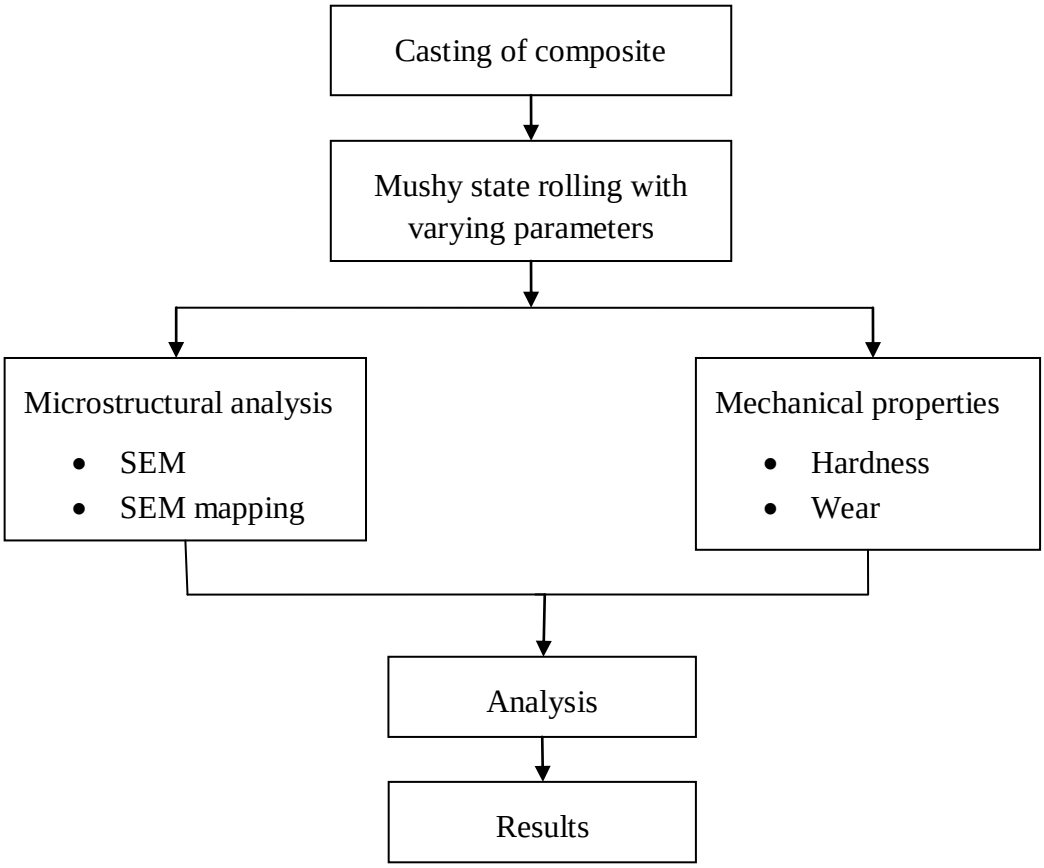

Figure 3.1 Schematic representation of experimental work

3.2 SELECTION OF RAW MATERIALS

The raw materials used for the present work consist of commercially pure metals like aluminium (CP-Al) and copper in addition to chemicals such as potassium fluoborate (KBF_4) and potassium titanium fluoride (K_2TiF_6). Al was used for the preparation of Al-33Cu master alloy, which was subsequently used to prepare Al-4.5(wt. %) Cu-5(wt. %) TiB_2 composite plates for mushy state rolling. The composition of Al and its alloy was analysed by an Optical Emission Spectrometer (OES) (Model ARL 3460 of Thermo Electron Corporation, Switzerland). The composition of Al and Al-4.5(wt. %) Cu alloy is presented in the Table 3.1. The salts used in the present work were commercial grade K_2TiF_6 and KBF_4 in the powder form (~200 mesh i.e.74μm).

Table 3.1 Chemical composition of the Al and its alloy used in the present study				
	Composition (wt %)			
Alloy	**Si**	**Fe**	**Cu**	**Al**
Al	0.11 ±0.01	0.16 ±0.02	-	Balance
Al-4.5(wt %)Cu	0.01 ±0.001	0.12 ±0.01	4.49 ±0.06	balance

3.3 SYNTHESIS OF AL BASED ALLOY AND Al-4.5(Wt. %)Cu-5(Wt. %)TiB_2 COMPOSITE

3.3.1 Preparation of Al-33 (wt. %) Cu master alloy

A master alloy of Al-33 (wt. %) Cu was prepared by melting commercially pure Al (670 gm.) in a graphite crucible placed in an induction furnace. On reaching 800°C, degassing was carried out by adding C_2Cl_6 tablets. Commercially available pure Copper (330 gm.) was then added to the molten Al and then held for some time to ensure complete dissolution of copper. The resulting molten metal is then cast by pouring into mould.

3.3.2 Preparation of Al-4.5(wt. %)Cu-5(wt. %)TiB_2 composite by mixed salt route

Al-4.5(wt. %)Cu-5(wt. %)TiB_2 composite is obtained due to an exothermic, *in situ*, reaction between K_2TiF_6 and KBF_4 salts with molten Al to create titanium diboride (TiB_2) dispersoids, based on (Mandal 2007) the results of previous studies. The technique used for generating reinforcing particles *in situ* in this study is widely referred to as the mixed salt route (Woods 1993, Bartels 1997, Lakshmi 1998). The melt processing of the composite has been schematically shown in Figure 3.2 by means of a flow chart. The process of obtaining the Al-4.5(wt. %)Cu-5(wt. %)TiB_2 composite is described in chronological sequence below:

- The Al ingots were cut to suitable size using power saw, so that they can be easily accommodated in the graphite crucible. Dilute HCl is used for pickling the Al pieces followed by thorough cleaning with acetone to remove any oil, grease or any other contaminants.

- The requisite amount of K_2TiF_6 (109 gm.) and KBF_4 (114 gm.) to achieve the required wt. % (5) of TiB_2 was weighed and subsequently dried in an oven at 150°C for around 2 hours to remove any physisorbed moisture present, as aluminium is known to be very sensitive to moisture. Simultaneously, the moulds in which the melt would be ultimately poured were also kept in a separate oven for 2 hours at around 200°C.
- The salts were removed from the oven after the requisite time and mixed thoroughly, so that a homogeneous mixture of salts was obtained.
- The mixed salts were then wrapped in aluminium foils (capsule form) in suitable quantities to form a number of batches of sizes convenient for adding to the liquid alloy.
- The master alloy (68.2 gm.) was remelted with suitable amount (431.8 gm.) of commercially pure Al in a pit type resistance furnace using a graphite crucible, to obtain 500 gm alloy of the desired composition. Once the melt attains a temperature of 800^0C, degassing of the melt with hexachloroethane (C_2Cl_6) tablets is carried out. The temperature decreases slightly upon addition of tablets.
- Once the temperature reaches 800°C again, the packets were added to the liquid alloy in batches. The melt is stirred with Zirconia coated graphite stirrer every ten minutes.
- When all the packets are added, the melt was held for duration of one hour at reaction temperature in the furnace. Intermittent stirring of the melt is carried out at every 10 minutes interval to achieve uniform distribution of salt in molten Al ensuring uniform reaction throughout the melt.

The TiB_2 particles were formed *in situ* inside the molten Al due to the exothermic reaction of K_2TiF_6 and KBF_4 salts following equation (3.1) (Mandal *et al.* 2004, Herbert 2007).

$$K_2TiF_6 + KBF_4 + Al\ alloy \longrightarrow Al\ alloy + TiB_2 + KAlF_4 \qquad (3.1)$$

(composite) (dross)

$KAlF_4$ floats on the melt as dross and is subsequently removed. The melt is then poured in the cast iron plate shaped moulds preheated to a temperature of 200°C.

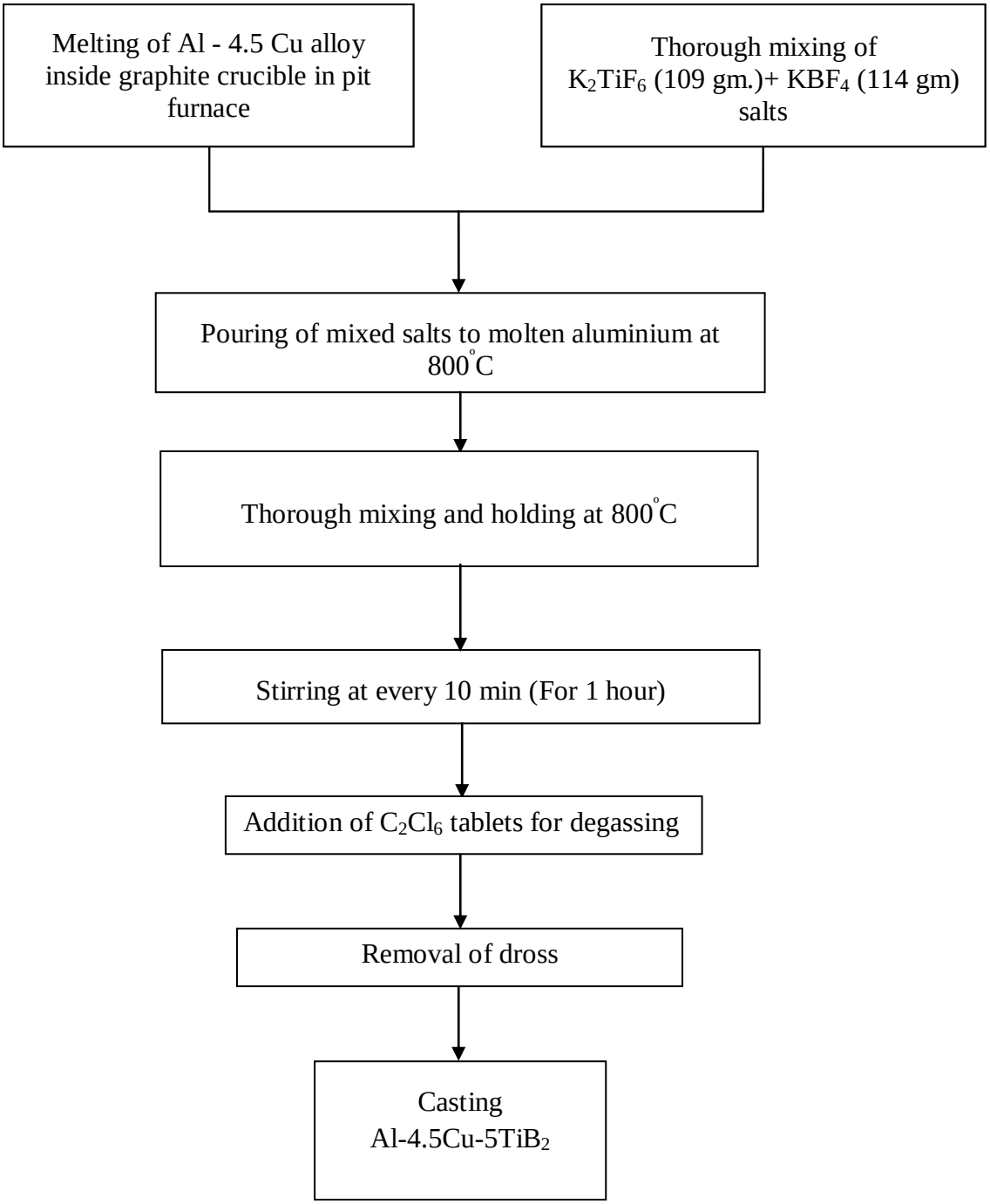

Figure 3.2 Schematic representation of Al-4.5Cu-5TiB_2 composite processing.

3.4 EVALUATION OF VOLUME FRACTION OF *in situ* Al-4.5Cu-5TiB_2 COMPOSITE IN MUSHY STATE

The volume fraction of the liquid present in Al-4.5Cu-5TiB_2 composite work piece during rolling in mushy state were chosen as 10, 20 and 30 percent for investigations carried out by Herbert (Herbert 2007) on mushy state rolling of Al-4.5Cu alloy based composites reinforced with TiB_2 particles. The ANN model proposed in this study has been trained on the investigations carried out in the above work on the Al-4.5Cu-5TiB_2 composite, rolled in mushy state, when in as cast and in pre hot rolled form. Therefore, the volume fractions of the Al-4.5Cu-5TiB_2 composite were chosen as 7, 17 and 33 percent for validation experiments proposed to be carried out. Figure 3.3 shows the chart map at locations where validation experiments are proposed. The bullet entries indicate the points at which validation experiments are proposed. The temperatures corresponding to the nominal liquid volume fractions of 7, 17 and 33 percent were obtained by applying the lever rule to the Al-Cu thermal equilibrium diagram (ASM Handbook 1997). In case of the binary Al-4.5Cu alloy, the temperature corresponding to 7, 17 and 33 volume fractions has been found to be 597°C, 618°C and 632°C respectively. For the composite, the amount of TiB_2 has to be considered as part of the solid fraction, in addition to the unmelted alloy grains (Herbert 2007). Hence the temperatures for the composites are taken to be 1°C higher than that of the binary alloy for the same volume fraction of liquid (Herbert 2007). While determining the temperatures corresponding to the volume fractions of liquid in the composite using lever rule, the densities of solid and liquid Al were assumed to be same (Herbert 2007). The temperatures corresponding to the different volume fractions of the liquid in the composite (for validation experiments to be carried out) obtained from phase diagram are shown in Table 3.2.

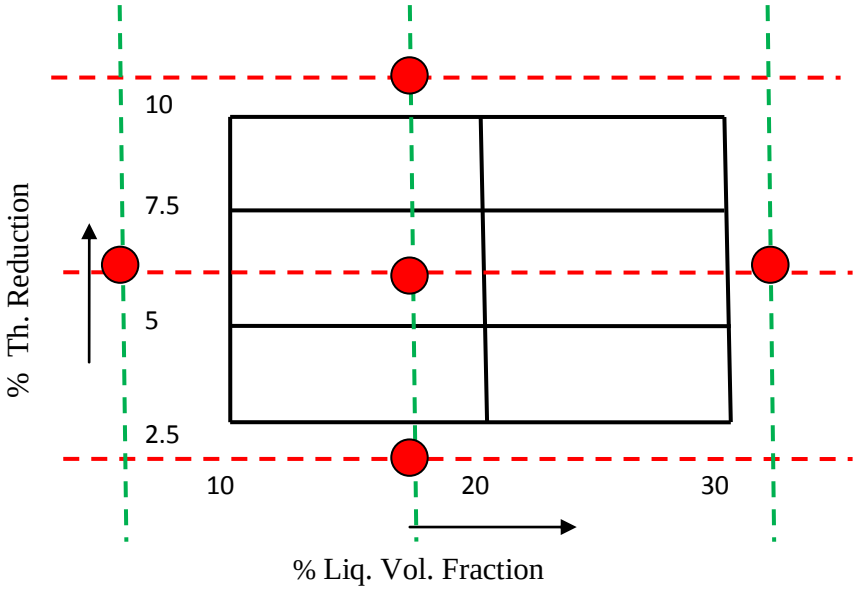

Figure 3.3 Map for proposed validation experiments

Table 3.2 Temperature corresponding to 7, 17 and 33 volume fraction of liquid in Al-4.5Cu alloy and Al-4.5Cu-5TiB_2 composite, determined from phase diagram

Liquid volume fraction	Al-4.5Cu alloy	Al-4.5Cu-5TiB_2 composite
7	597	598
17	618	619
33	632	633

3.5 MUSHY STATE ROLLING OF Al-4.5Cu-5TiB_2 COMPOSITE

A schematic representation of the experimental set up used for mushy state rolling of Al-4.5Cu-5TiB_2 composite is shown in Figure 3.4. Figure 3.5 shows the photograph of the experimental set up used for mushy state rolling of composite. The experimental setup has been specially designed to facilitate partial remelting of the composite workpiece. A two high rolling mill, having rolls of 120 mm diameter, and 12 mm barrel width was used for conducting the experiments. The mill surfaces were maintained at ambient temperature to facilitate instantaneous solidification during mushy state rolling.

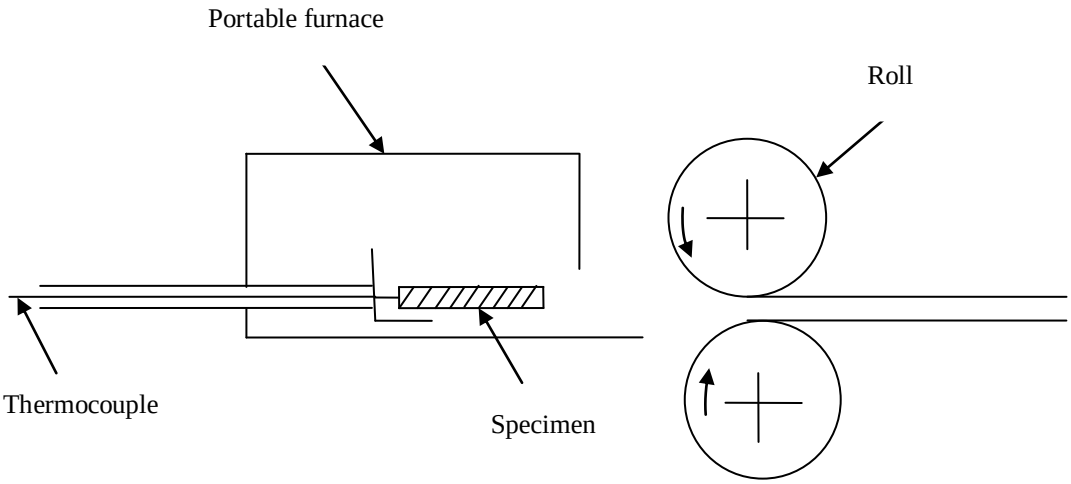

Figure 3.4 Schematic view of mushy state rolling set up

Figure 3.5 A two high roll mill used for mushy state rolling of Al-4.5Cu-5TiB_2 composite.

The specimens with dimensions of 40 mm x 25 mm x 6 mm were soaked at temperatures corresponding to mushy zone requirement inside a portable furnace (Figure 3.6). The portable furnace has inner dimensions as 100 mm x 45 mm x 35 mm and is kept and operated from very close to the rolling gap of the roll mill. The

smaller dimensions of the furnace were specifically chosen to ensure that the temperature gradient inside the furnace is minimised. The resistance heating element used in the furnace was a kanthal wire evenly spaced throughout the furnace wall from three sides, around the heating zone. The procedure was planned so as to ensure minimum loss of heat and temperature decrease between exit of workpiece from furnace and entry into roll gap.

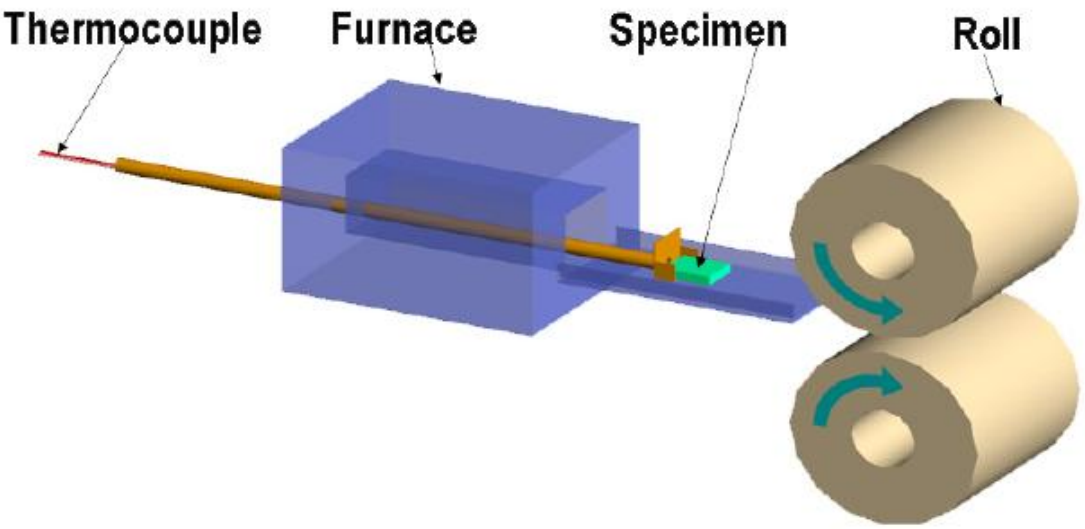

Figure 3.6 Schematic Representation of Portable Furnace (Herbert 2007)

After completion of soaking at the desired temperature, corresponding to the mushy state required, the lid of the furnace facing the roll gap is opened. Each specimen is pushed into the roll gap by using a hollow push rod connected to the sample/specimen carrying attachment. The sample carrying attachment houses a chromel-alumel thermocouple wire which runs through the hollow push rod and is connected to a temperature controller. The tip of the thermocouple was placed inside the specimen, by drilling a small hole on the rear side of specimen, so that temperature of the specimen, just before insertion into the roll gap can be ascertained and controlled. Mushy state rolling of the Al-4.5Cu-5TiB_2 composite was carried out at 598°C, 619°C and 633°C (with an accuracy of ±2°C), so as to contain 7, 17 and 33 nominal volume percents of liquid respectively (ASM Handbook 1992, Tzimus 2000). The composites were subjected to 2, 6 and 11.5 percent thickness reductions at constant roll surface velocity of 0.283 ms^{-1}. Some of the as cast Al-4.5 (wt. %) Cu -5(wt. %)TiB_2

composite samples were subjected to annealing at 370°C for 10 minutes followed by hot rolling, so as to cause 2.5 percent thickness reduction in order to homogenize the composite. These hot rolled composite specimens were then subjected to mushy state rolling. The rolling schedule is presented in Table 3.3.

Table 3.3 Rolling Schedule

Material	Thickness reduction	Liquid content
As cast Al-4.5Cu-5TiB_2 composite	Mushy state rolling @ 2%, 6% and 11.5%	7, 17 and 33%
Pre hot rolled Al-4.5Cu-5TiB_2 composite	Mushy state rolling @ 2%, 6% and 11.5%	7, 17 and 33%

In some cases, on mushy state rolling of the as cast Al-4.5Cu-5TiB_2 composite, alligatoring was observed. Alligatoring was found to occur for all combinations of liquid content and reduction in thickness, except at 633°C (corresponding to 33 volume percent liquid) to obtain 6% thickness reduction in one single pass. This is in confirmation to the investigations carried out by Herbert (2007) wherein it was reported that alligatoring is observed in all combinations of liquid content and thickness reductions other than that corresponding to 30% volume fraction of liquid giving 2.5% and 5% thickness reduction in one single pass. It is reported (Herbert 2007) that during rolling secondary tensile stresses set up by barrelling of edges, cause edge cracks. Due to barrelling or lateral deformation, greater spread occurs towards the centre than at the surfaces. Consequently, the surfaces are placed under tension while the centre is under compression. If there is any metallurgical weakness along the centreline of the specimen, fracture occurs as shown in Figure 3.7. The curling of two halves of the specimen towards the respective rolls is known as alligatoring (Dieter 1986, Herbert 2007) or split end effect or crocodiling.

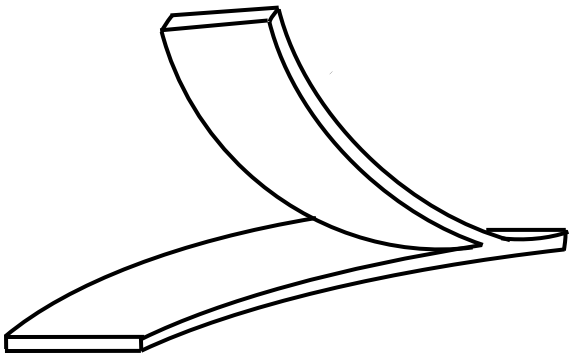

Figure 3.7 Fracture due to Alligatoring (Dieter 1986)

Figure 3.8 shows the photographs of (a) as cast composite specimen (b) specimen rolled to 6% thickness reduction with 17% liquid volume fraction and (c) specimen which has undergone alligatoring, when subjected to mushy state rolling at 598°C (corresponding to 7% volume fraction of liquid) to a thickness reduction of 6% in one pass.

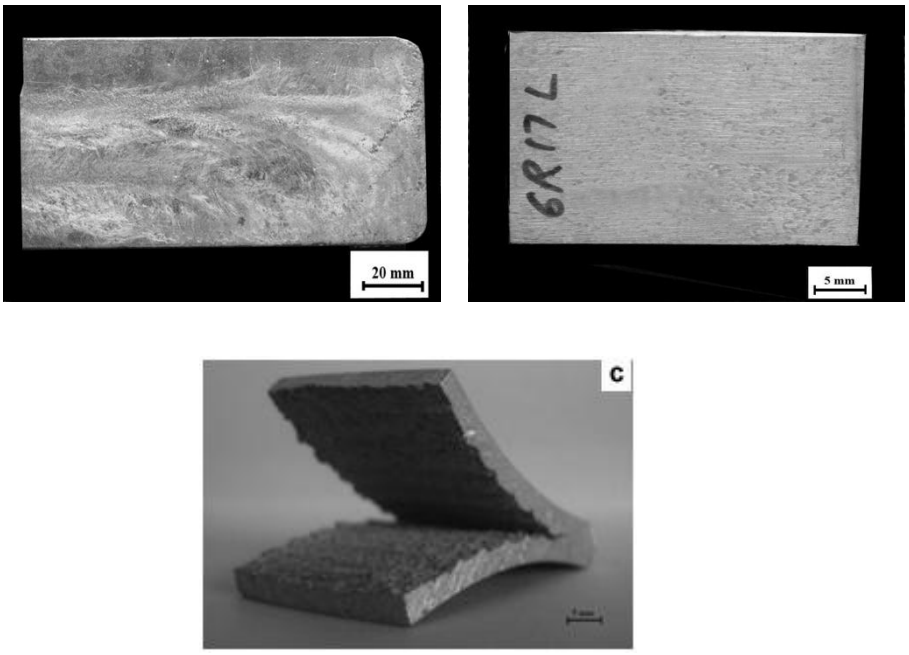

Figure 3.8 Photograph of (a) as cast Al-4.5Cu-5TiB_2 composite; (b)defect free mushy state rolled specimen and (c) fractured surface generated by alligatoring.

3.6 SECTIONING OF AS CAST AND ROLLED SPECIMENS

Figure 3.9 illustrates the way in which the plate shaped Al-4.5Cu-5TiB_2 composite was sectioned to obtain the specimens for microstructural characterization and wear studies. The surfaces selected were in the direction of rolling for both microstructural as well as wear studies. The samples were cut using Isomet 4000 Linear precision saw (Buehler Inc., IL, USA) equipped with diamond coated blades.

3.7 METALLOGRAPHIC SAMPLE PREPARATION

Sample preparations were required for studies of optical and scanning electron microscopes. Samples of size 10mm x 5mm x 5mm were cut. Both as cast as well as mushy state rolled composite samples of Al-4.5Cu-5TiB_2 composite were prepared for microstructural study by polishing using different grades of SiC papers of grades 200,320 and 600 grit until the sketches of previous grade polishing vanished completely. Subsequently, the samples were polished on a disc polishing machine (ECOMET 3000 variable speed grinder-polisher, Buehler, Germany) having polishing cloth, using water suspension of alumina powder (400 mesh size) as grinding medium. This is followed by meticulous polishing on lapping cloth fixed on a rotating disc and smeared with 1μm, 0.25μm followed ultimately with 0.05μm diamond pastes till a very fine mirror surface finish is achieved. After every stage of polishing, the samples were carefully cleaned with soap solution and alcohol after which drying followed. This was followed by etching the specimens with Keller's reagent (2.5%HNO_3, 1.5% HCl, 1% HF, and 95% H_2O) for a period of approximately 10 seconds, so that grain boundaries are delineated. Etched samples were carefully cleaned in acetone bath using ultrasonic cleaner (VS120, Vibronics Pvt. Ltd., India, 120W).

3.8 CHARACTERIZATION OF MUSHY STATE ROLLED *in situ* Al-4.5Cu-5TiB_2 COMPOSITE

3.8.1 Optical microscopy and image analysis

Optical microscopy and grain size analysis were carried out using Leica DFC320 image analyzer (Model: Q5501W) interfaced with Leica Q-win V3 Image analysis software. Optical photomicrographs of metallographically polished specimens of the

composite, as explained in section 3.7 were recorded using a digital camera attached to the microscope and were processed using the software loaded on a computer interfaced with it. Microstructures were recorded on the plane containing the rolling direction and perpendicular to the surface in contact with the rolls. The different planes involved in mushy state rolling are shown in Figure 3.10. Grain sizes of mushy state rolled Al-4.5Cu-5TiB_2 composite were measured using image analysis following the procedure of ASTM E-112-96 (ASTM 2003). A total of 100 representative grains were considered to obtain average size through image analysis software. The cross section containing the roll direction and perpendicular to the surfaces in contact with the rolls of some mushy state rolled samples were analysed by dividing the cross section in five equal zones and the average grain size along the thickness direction were measured to study the variation of grain size with respect to distance from the surface in contact with the rolls.

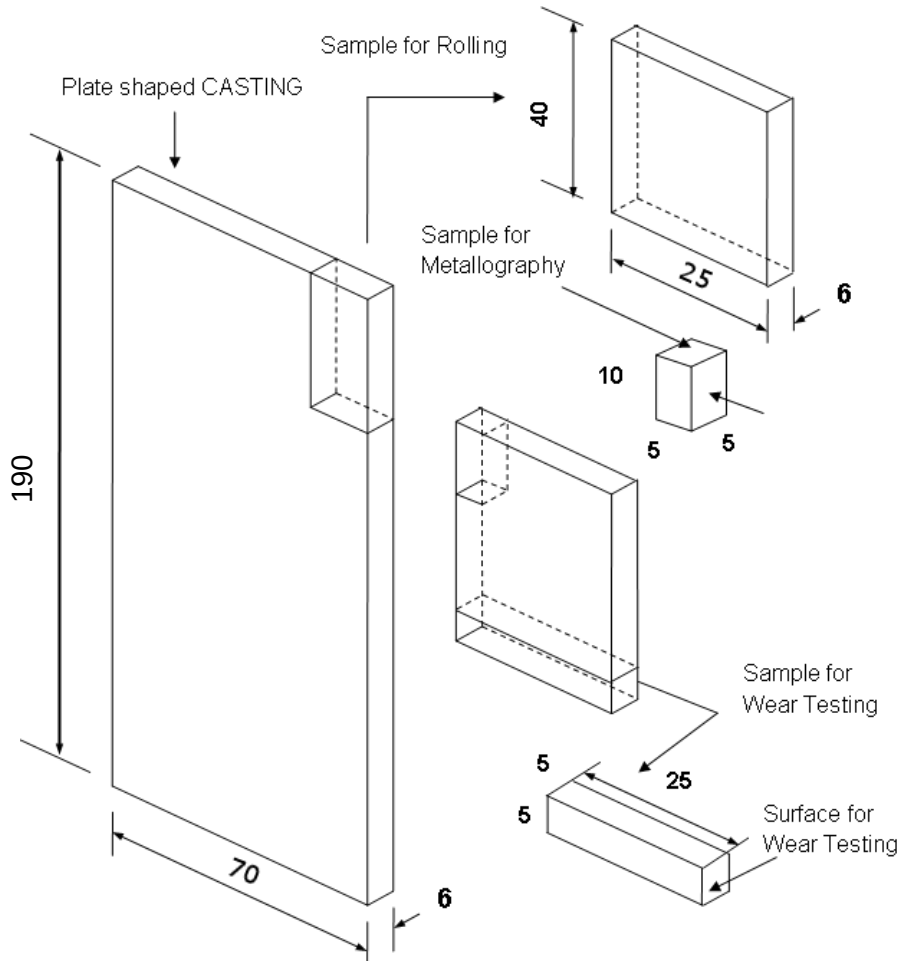

Figure 3.9 Schematic representation of sections selected for characterization.

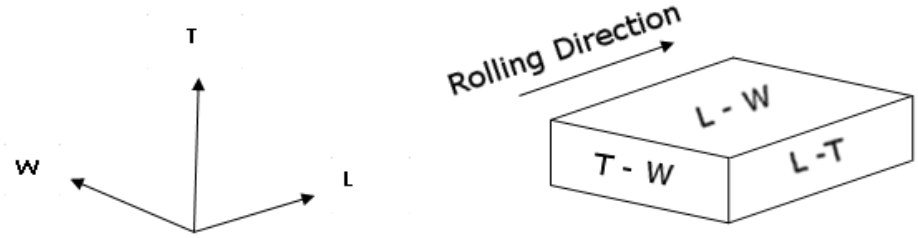

Figure 3.10 Schematic diagram of the rolled product: L-rolling direction, T-Thickness direction and W- Width direction, L-T = Longitudinal rolling plane, T-W = Transverse rolling plane, L-W = Rolling surface.

3.8.2 Scanning electron microscopy

The microstructures were also examined on a scanning electron microscope (SEM) [Model: JSM-5800, JEOL, Japan] using the secondary electron (SE) and back-scattered electron (BSE) modes accompanied by energy dispersive X-ray (EDX) [Model; ISIS 300, Oxford Instruments Ltd., UK] Analysis. The operating voltage for SEM was 20kV. The machine is interfaced with Link ISIS software for energy dispersive X-ray mapping and line-scan analysis. Samples as prepared using procedure explained in section 3.7 were then taken up for SEM investigations. A number of regions were examined in each sample in order to have an overall understanding of microstructural features. Characteristic X-ray mapping of Ti and Cu in the microstructure was carried out to study the particle distribution after mushy state rolling. The fractured surfaces generated due to alligatoring were also examined to study the features of damaged surface and origin of failure.

3.9 EVALUATION OF HARDNESS OF MUSHY STATE ROLLED Al-4.5Cu-5TiB_2 COMPOSITE

The Vickers hardness tests were conducted on mushy state rolled composite using an indentation load of 5 kg and a dwell time of 15 seconds upon indentation. Hardness measurements were carried out in the same planes in which the microstructural studies were carried out. The samples used for the hardness test were prepared as explained in section 3.7. At the end of hardness test on each sample, the diagonal

length of indentation was carefully measured. The Vickers Hardness Number is calculated using the following relation:

$$H_v = 1.854 \frac{P}{d^2} \quad (3.2)$$

where P is the indentation load (kg) and d is the mean diagonal length (mm). While taking hardness readings on a specimen, care is taken to see to it that the indentation marks are separated by at least a distance of three times the diagonal length. This is done to ensure that the accuracy of the hardness readings is not affected due to elastic deformations and to minimize the errors in measurement of diagonal length.

3.10 EVALUATION OF DRY SLIDING WEAR PROPERTIES

Dry sliding wear tests were carried out on Al-4.5Cu-5TiB_2 composite samples after the composite was subjected to mushy state rolling. The mushy state rolling of Al-4.5Cu-5TiB_2 composite was carried out as per the rolling schedule given in Table 3.3. After rolling the specimens having cross section of 5mm x 5mm and 25mm height were prepared as shown in sectioning chart in Figure 3.9. These square specimens were tested using pin-on-disc wear-testing machine (Model TR-20, DUCOM, Bangalore, India) following the ASTM G99-04 standard (ASM 1992). A schematic view of the wear testing machine is shown in Figure 3.11. The surface of the cross section in the longitudinal rolling direction was considered for wear testing. Wear specimens were cut to required size by using Isomet 4000 linear precision cutting saw (Buehler). For each case, two samples were considered and the average height loss was found out. From the average height loss, volume loss was determined and from volume loss, the wear rates were calculated. The wear tests were carried out in dry condition to obviate the effects of lubricating medium contamination. Hardened chromium steel (Rc64) was used as the counterface material. The tests were carried out with loads as 19.6N, 39.2N, 58.8N and 78.4N. For all the tests, sliding distance was maintained as 1800m, while the sliding speed was kept as 1ms^{-1} (corresponding to a constant disc speed of 240 rpm). The track radius was fixed at 40mm. The dry wear tests were carried out at ambient temperature. A computerised data acquisition system was used in this study to simultaneously monitor height loss as well as

frictional force. The plots of *height* loss against *sliding distance* were generated by the computerised system interfaced with wear testing machine. The height loss was converted to volume loss by multiplying cross sectional area of the test pin to height loss. The slope of the linear fit of the plot of *height loss* against *sliding distance* in the steady state regime (500m – 1500m) is taken as the wear rate. The reciprocal of the wear rate is reported as wear resistance. The force of friction is directly obtained as one of the outputs of the pin-on-disc wear testing machine used in this study. As we know, the coefficient of friction is calculated as the ratio of this limiting force of friction to the normal load applied (in the range of 20N to 80N). Table 3.4 shows the schedule of dry sliding wear testing experiments carried out in the present study (in terms of specimen identification and normal loads used) for validation of predictions carried out by the proposed ANN model for wear rate predictions of the Al-4.5Cu-5TiB_2 composite.

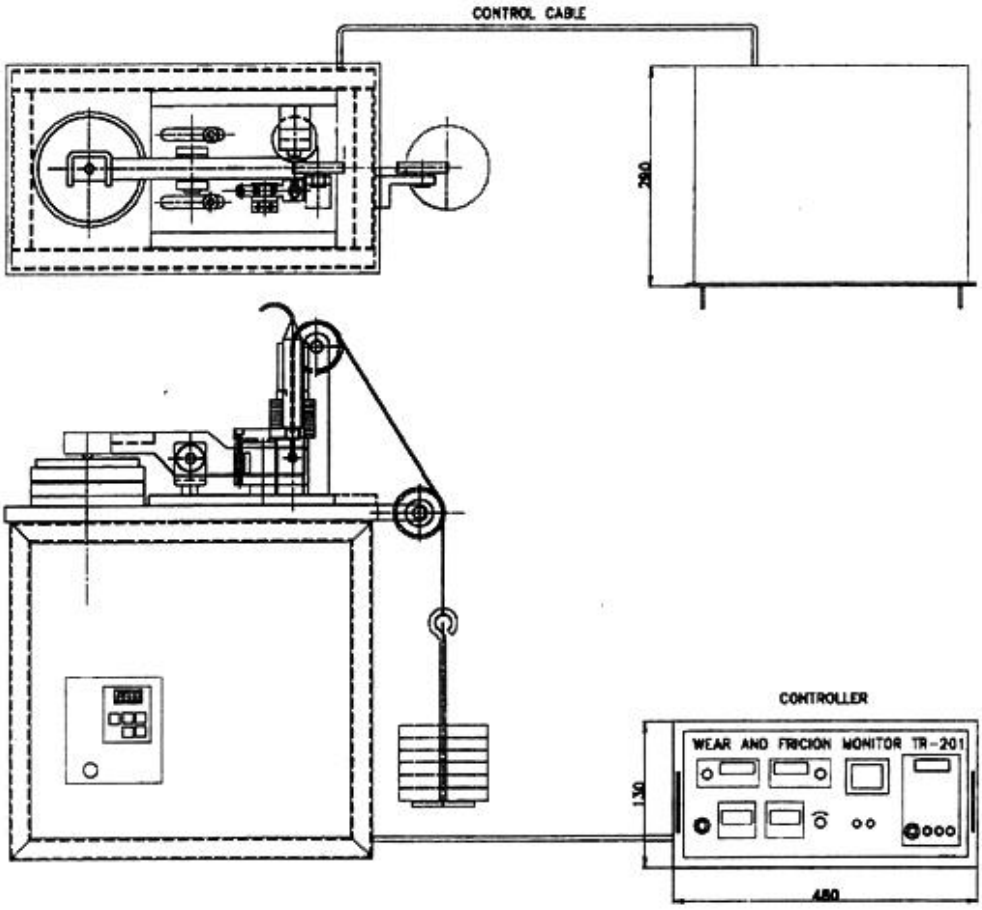

Figure 3.11 Schematic view of the Pin-on-Disc type wear testing machine

Table 3.4 Dry sliding wear studies of mushy state rolled Al-4.5Cu-5TiB_2 composite

Material*	Mushy state rolling parameters		Normal load (N)
	Thickness reduction (%)	Liquid fraction (%)	
As cast Al-4.5Cu-5TiB_2	2	17	19.6, 39.2, 58.8 and 78.4
	6	33	
Pre-hot rolled Al-4.5Cu-5TiB_2	2	17	
	6	07, 17, 33	

**All figures are in wt. %*

Chapter 4

RESULTS AND DISCUSSION (PART I)

ANN MODELLING FOR GRAIN SIZE PREDICTION

4.1 INTRODUCTION

The development of ANN model for prediction of bimodal grain sizes for as cast and pre hot rolled Al-4.5Cu-5TiB_2 composite when rolled in mushy state is discussed in the present chapter. Rolling is initiated from different mushy state temperatures (corresponding to the required liquid volume fraction in the composite) and to different thickness reductions during rolling in single pass. The model has been trained with data collected from the work carried out by Herbert (2007). The mushy state rolling data ranging from 2.5 to 10% thickness reduction per pass with 10 to 30% liquid volume content in the composite at the initiation of mushy state rolling, has been considered for training the model. The validation of the model to predict bimodal grain size in mushy state rolled Al-4.5Cu-5TiB_2 composite has been established by conducting experiments on mushy state rolling of Al-4.5Cu-5TiB_2 composite in as cast and pre hot rolled condition at pre determined input parameters. The chapter further deals with the characterization of this mushy state rolled composite using optical microscopy and SEM/EDX microanalysis. Discussion on the variation of grain sizes with different combinations of thickness reductions per roll pass and liquid volume content (mushy state parameter) during rolling initiation has also been presented. The summary of the discussions has been presented in the concluding part of the chapter.

4.2 SCOPE

In this section, it is proposed to develop a Feed Forward Neural Network model to predict the grain size as a function of input parameters namely, % thickness reduction and % volume fraction of liquid in the composite. The input parameters for the mushy

state rolling process of Al-4.5Cu-5TiB_2 composite are initial state of composite (i.e. as cast or pre hot rolled condition), % thickness reduction and % liquid volume fraction in the composite. The outputs of the process are small and large grain sizes. It is obvious that the relationship between output and input is non linear and complex. Statistical techniques like regression analysis use the technique of fitting the non linear data on a goodness of fit line. This obviously leads to errors creeping in predictions due to fitment errors. Finite element methods are mathematically too involved. The use of Feed Forward Neural Networks with one or two hidden layers is an attractive option as these networks are known to correlate complex and non linear input-output relationships without requirement of in depth mathematical knowledge to the user. The FFNN generalises the input-output relationship with a fair degree of accuracy by understanding the subtle relationships between them. This justifies the use of FFNN for prediction of grain sizes of mushy state rolled Al-4.5Cu-5TiB_2 composite.

The present work attempts to develop a FFNN model keeping in mind the following:

(a) The analysis of the effect of initial state composite material (as cast or pre hot rolled) on grain size of Al-45Cu-5TiB2 composite.
(b) The analysis of effect of the thickness reduction and liquid volume fraction during mushy state rolling and mushy state condition when rolling is initiated.
(c) Extrapolate and interpolate the average grain sizes for unknown thickness reductions and liquid volume fractions in the mushy state composite.
(d) Determining optimum condition of thickness reduction and liquid volume content to obtain desired grain sizes.

(e) Validation of the model predictions through experiments.

4.3 DATA COLLECTION AND ANN MODELLING FOR GRAIN SIZE PREDICTION

4.3.1 Data collection

The experimental data are taken from the work of Herbert (2007). The work dealt with the study of microstructural evolution of the Al-4.5(wt. %) Cu alloy and *in situ* Al-4.5(wt. %)Cu -5(wt. %) TiB_2 composite, both subjected to mushy state rolling. The condition is either as cast or pre hot rolled for single or multiple roll passes with different combinations of thickness reductions and volume fractions of liquid. Microstructural evolution in as cast and pre hot rolled Al-4.5Cu-5TiB2 composite, led to more or less equiaxed grain structure, and a modest refinement of the grain size. The matrix in the hot-rolled composite showed a bimodal or duplex grain size distribution. The finer equiaxed grains emerged through dynamic recrystallization, with finer grains appeared randomly mixed with coarser grains (Herbert *et al.* 2006).

The grain size in the α-Al matrix of the cast Al-4.5Cu-5TiB_2 was found to be 50±8μm (Herbert *et al.* 2006, Herbert 2007). The comparative study of the grain sizes in *in situ* as cast Al-4.5Cu-5TiB_2 composite and the pre hot rolled composite subjected to mushy state rolling was carried out to examine its effect on the mechanical properties.

The mean size and standard deviation of the un-melted α-Al grains in the as-cast and pre hot rolled composite subjected to mushy state rolling to various thickness reductions are listed in Table. 4.1. The average grain size was seen to be higher, for both small and large grains, in case as cast composite subjected to mushy state rolling. It is seen that that this is the least in case of the pre hot rolled composite subjected to mushy state rolling. The mean values of the large grain size vary from 47μm to 62μm in the case of as cast composite subjected to mushy state rolling and from 39μm to 47μm in the case of the pre-hot rolled composite subjected to mushy state rolling. Similarly, the mean values of the small grain size vary from 25μm to 37μm for as cast composite subjected to mushy state rolling and from 24μm to 32μm in the case of pre hot rolled composite.

Table 4.1 Experimental data on Al-4.5Cu-5TiB_2 composite mushy state rolled in as cast and pre-hot rolled conditions (Herbert 2007).

Specimen Descriptions	Liquid Volume Fraction	As cast Al-4.5Cu-5TiB_2 Composite samples subjected to mushy state rolling		Pre hot rolled Composite samples subjected to mushy state rolling	
		Grain size (μm)		Grain size (μm)	
		Large	Small	Large	Small
As cast		50 ± 8		52 ± 15 As rolled	28 ± 9 As rolled
2.5% thickness reduction	f_l ~ 0.1	62 ± 14	27 ± 12	43 ± 16	27 ± 13
	f_l ~ 0.2	58 ± 18	33 ± 11	42 ± 18	26 ± 11
	f_l ~ 0.3	66 ± 15	37 ± 10	47 ± 20	25 ± 11
5% thickness reduction	f_l ~ 0.1	54 ± 16	25 ± 9	42 ± 16	26 ± 11
	f_l ~ 0.2	51 ± 11	31 ± 10	41 ± 15	25 ± 12
	f_l ~ 0.3	55 ± 14	32 ± 10	46 ± 17	24 ± 11
7.5% thickness reduction	f_l ~ 0.1	62 ± 20	32 ± 13	40 ± 15	26 ± 10
	f_l ~ 0.2	48 ± 19	26 ± 12	39 ± 15	25 ± 11
	f_l ~ 0.3	53 ± 18	27 ± 13	45 ± 17	24 ± 09
10% thickness reduction	f_l ~ 0.1	49 ± 17	29 ± 11	47 ± 18	32 ± 13
	f_l ~ 0.2	47 ± 14	30 ± 12	43 ± 16	25 ± 11
	f_l ~ 0.3	54 ± 12	26 ± 11	45 ± 16	27 ± 12

4.3.2 Model development for Grain Size predictions

As seen in article 4.3.1 and Table 4.1, the morphology of the microstructure obtained after mushy state rolling of the composite depends on

(1) The state of the composite specimen subjected to mushy state rolling, i.e. in as cast form or pre hot rolled form from which mushy state rolling is initiated.
(2) Thickness reduction per pass during mushy state rolling
(3) Volume of liquid content (Mushy state temperature) in composite when rolling is initiated.

Hence, the grain sizes are found to be greatly influenced by the initial state of composite material, thickness reduction per rolling pass and the liquid volume fraction of the composite at the instant of initiation of mushy state rolling. Thus, the input variables for the FFNN model for grain size predictions have been identified as initial state of composite (i.e. as cast or pre hot rolled condition), % thickness reduction and % liquid volume fraction in the composite. Obviously the output variables are small grain size and large grain size.

4.3.2.1 Brief description of neural networks training

The aim of the present work is to estimate the grain sizes (small and large) of mushy state rolled Al-4.5Cu-5TiB_2 composite as a function of starting material type, thickness reduction and liquid volume fraction in the composite. Both the input and output variables have been normalized using the normalizing function (Reddy *et al.* 2005)

$$x_n = [(x - x_{min}) * 0.8 / (x_{max} - x_{min})] + 0.1 \qquad (4.1)$$

where x_n is the normalized value of x, that has the maximum and minimum value given by x_{max} and x_{min}, respectively. Once the network is trained, all the values of x acquire their original value given by (Reddy *et al.* 2005)

$$x = [(x_n - 0.1) (x_{max} - x_{min}) / 0.8] + 0.1 \qquad (4.2)$$

The main reason for standardizing the data is that it is received in terms of variables that have different units. Normalizing converts the data into non dimensional quantities and removes the arbitrary effect of similarities between the objects (Srinivasan *et al.* 2003, Reddy *et al.* 2005, 2008, Mandal *et al.* 2009). The output layer had two nodes for bimodal grain sizes. The percentage thickness reduction was varied from 2.5% to 10%, while the % volume of liquid fraction was varied from 10% to 30%.

The mushy state rolling process is a high temperature forming process. It involves a tight control of mushy state parameters, mainly the temperature which determines the

mushy state i.e. the liquid content in the composite. Secondly, this temperature is to be maintained with ±2°C accuracy (Herbert *et al.* 2006, Herbert 2007). During the conduct of experiments, each specimen is heated to above 600°C and held at that temperature corresponding to liquid volume fraction for 10 minutes for homogenization and then pushed into the roll gaps. Hence these experiments are time consuming and tedious. In addition, Herbert *et al.* (2006) have also reported the problem of alligatoring at higher thickness reductions, beyond 10%. Hence above 10% thickness reduction, experiments were not conducted and also conducting a large number of experiments at high temperatures is practically not feasible. For each starting condition of the composite (i.e. as cast and pre hot rolled condition) 12 experiments were conducted, as reported by Herbert *et al.* (2006). Thus in all 24 data sets (as cast and pre hot rolled) were available for training the neural network. However commercial application would require more data and hence prediction using neural network is an effective alternate to the time consuming and tedious nature of the experiments. The resultant grain sizes predicted by the ANN are discussed in Section 4.6.

In any FFNN application even today, the exact architecture to be used needs to be found (Reddy *et al.* 2005). More often than not, this is a trial and error exercise, as regards to the selection of a number of hidden layers and neurons in each of these layers. In this application, training was started with two hidden layers from 2 to 12 neurons in each hidden layer. The minimum mean squared error (MSE) was set as 0.00001 and the number of iterations to be executed as 1500000. Initially during training, the learning rate parameter and momentum factor were preferred as 0.5 each. The number of hidden neurons was fixed based on MSE and the mean error in prediction of training data (E_{tr}).

Single and two hidden layers were tried out to obtain the minimum MSE. It was observed that the network fails to converge with single hidden layer, when tried with different number of nodes varying from 2 to 12 in the hidden layer. This probably happens due to the fact that the input-output relationship is quite complex and non linear. Therefore, training with single hidden layer was terminated and training was

started with two hidden layers. Here the training was started with varying learning rates from 0.1 to 0.9 in steps of 0.05. The learning rate and the momentum parameters were initially taken as 0.3 and 0.9 respectively for training. For all patterns, *p*, the global error function is expressed in terms of MSE (Yagnanarayana 2008) and is given by

$$E = \Sigma E_p = (1/p)\, \Sigma\Sigma\, (b_{kp} - s_{kp}^{0})^2 \qquad (4.3)$$

where, b_{kp} is the actual output and s_{kp}^{0} is the network output for the k^{th} output neuron for the p^{th} pattern.

The mean error in the output prediction is (Reddy *et al.* 2005)

$$E_{tr}(x) = 1/N\, \Sigma\, |(b_k(x) - P_k(x))| \qquad (4.4)$$

where $E_{tr}(x)$ is the mean error in prediction of training data set for output parameter x, *N* is the number of the data sets, $b_k(x)$ is the actual output and $P_k(x)$ is the predicted output.

The following sigmoid function was used as the activation function (Reddy *et al.* 2008, Mandal *et al.* 2009, Reddy *et al.* 2005, Li, Liu and Xiong 2002, Mousavi *et al.* 2007, Haque and Sudhakar 2002).

$$F(x) = 1/ (1+\exp (-x)) \qquad (4.5)$$

Back propagation algorithm was used for training the network. It was found after a lot of trial and error that convergence of the network was obtained with 2 hidden layers with 7 neurons in the first and 4 neurons in the second hidden layer. Figure 4.1 shows the schematic diagram of the FFNN used for grain size predictions. The learning rate parameter was increased from 0.1 to 0.9 in steps of 0.05 and the momentum term was decreased from 0.9 in steps of 0.05 to observe the network behaviour with respect to MSE and number of epochs. Finally, the optimized architecture obtained with learning parameter $\eta = 0.85$ and momentum factor $\alpha = 0.65$ was found to converge

excellently after 15 lakh epochs giving a MSE of 0.00023, to predict the grain sizes in microns (μm).

.

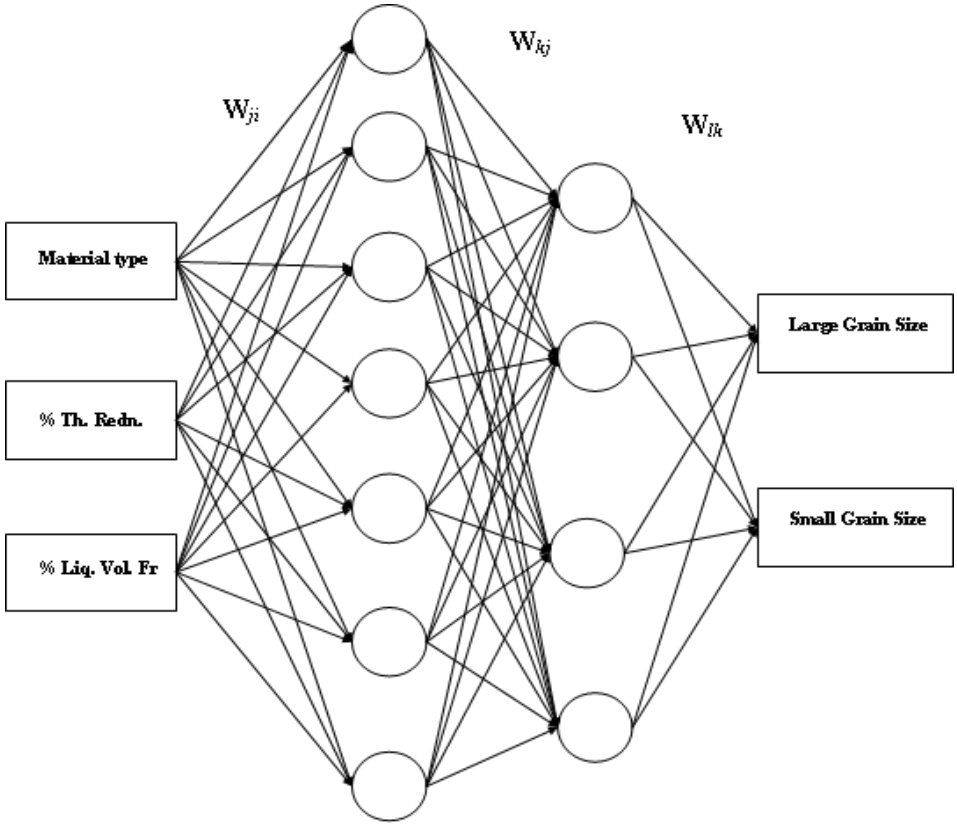

Figure 4. 1 ANN Architecture

4.4 EXPERIMENTS FOR VALIDATION OF NN MODEL

As discussed in chapter 3, mushy state rolling experiments were conducted with Al-4.5Cu-5TiB_2 composite with the composite in as cast and pre hot rolled condition. The process described for synthesis of Al-4.5Cu-5TiB_2 composite as discussed in section 3.3.3 of chapter 3 was followed. The microstructural evolution of Al-4.5Cu-5TiB_2 composite has been characterized using optical microscopy and SEM and EDX microanalysis.

4.4.1 Optical microscopy and SEM imaging

4.4.1.1 Mushy state rolled Al-4.5Cu-5TiB_2 composite from as cast state

Figure 4.2 (Herbert 2007) is the micrograph showing the characteristic microstructure of the as cast Al-4.5Cu-5TiB_2 composite. The microstructure reveals rosette like irregular grain structure with dendritic character.

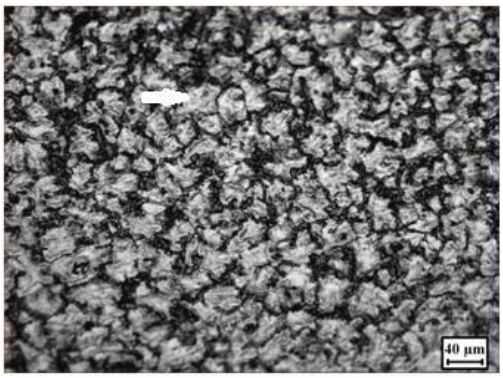

Figure 4.2 Optical micrograph showing rosette like dendritic grain structure (the dendritic arms are shown with arrow) in as cast Al-4.5Cu-5TiB_2 composite. (Herbert2007)

Figure 4.3(a) shows the optical micrographs of Al-4.5Cu-5TiB_2 rolled in mushy state with 17% volume percent liquid to a thickness reduction of 2%. The dendritic structure witnessed in Figure 4.2 in case of as cast composite has tended to modify modestly to globular shape due to tendency of α-Al grains having natural tendency to become globular with small deformation at a higher liquid content (Herbert *et al.* 2006, Herbert 2007). Figure 4.3(b) to (d) show the optical micrographs for the composite rolled to 6% thickness reduction at mushy zone temperatures corresponding to 598°C, 619°C and 633°C, while Figure 4.3(e) is the optical micrograph for the composite rolled to 11.5% thickness reduction from a temperature of 619°C. The globular shape of grains can also be witnessed in Figure 4.3(d), with 6% thickness reduction with rolling initiated at 33% liquid content in the composite. From the micrographs in Figure 4.3(c) and Figure 4.3(e), it can be observed that the grain elongation is more with higher deformation. This is because at higher deformation sufficient liquid is not available for strain accommodation, causing

elongation of the unmelted grains in the direction of rolling (Herbert *et al.* 2006, Herbert 2007). The change in the pattern of grains from globular to elongated can be seen in Figure 4.3(e). Evidence of grain fragmentation and transgranular cracks can also be seen in Figure 4.3(e).

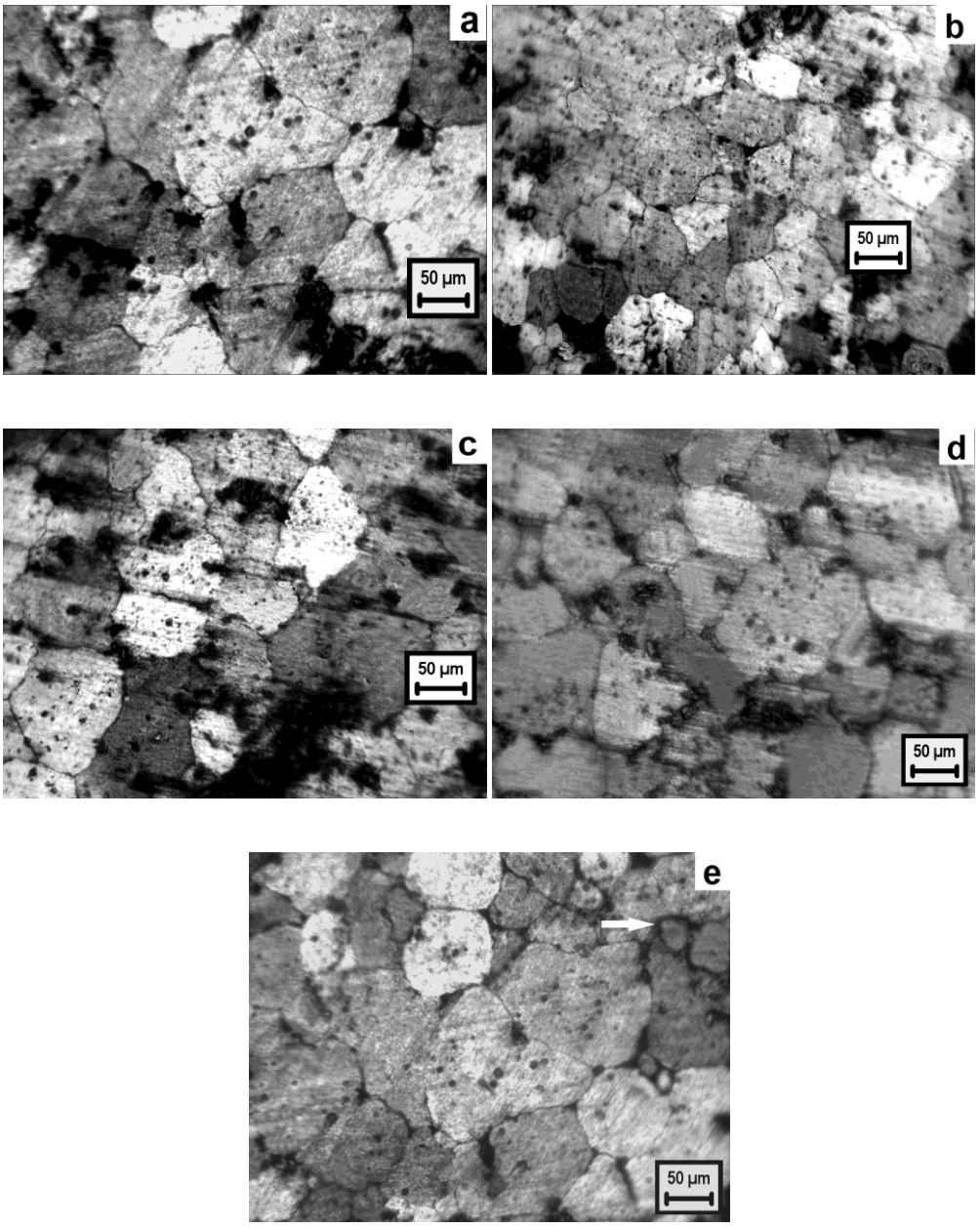

Figure 4.3 Optical micrographs showing the microstructure of Al-4.5Cu-5TiB_2 composite subjected to mushy state rolling to thickness reduction of; (a) 2% at 619°C (17% liquid), (b) 6% at 598°C (7% liquid), (c) 6% at 619°C (17% liquid), (d) 6% at 633°C (33% liquid) and (e) 11.5% at 619°C.

The SEM (BSE) images of the composite subjected to mushy state rolling in as cast condition with 6% thickness reduction and with 7, 17 and 33% liquid volume content are shown in Figure 4.4 (a) to (c). Figure 4.4(d) shows the SEM image for the mushy state rolled composite subjected to 11.5% thickness reduction with 17% liquid volume content. The grain boundaries as can be seen from the images appear dotted due to bright TiB_2 particles accumulated at grain boundaries. It can be observed that TiB_2 particles appear to be aligned along rolling direction.

Upon mushy state rolling of the composite in as cast form, alligatoring was observed in all cases except only when the composite was rolled to 6% thickness reduction and with 33% liquid volume fractions in composite.

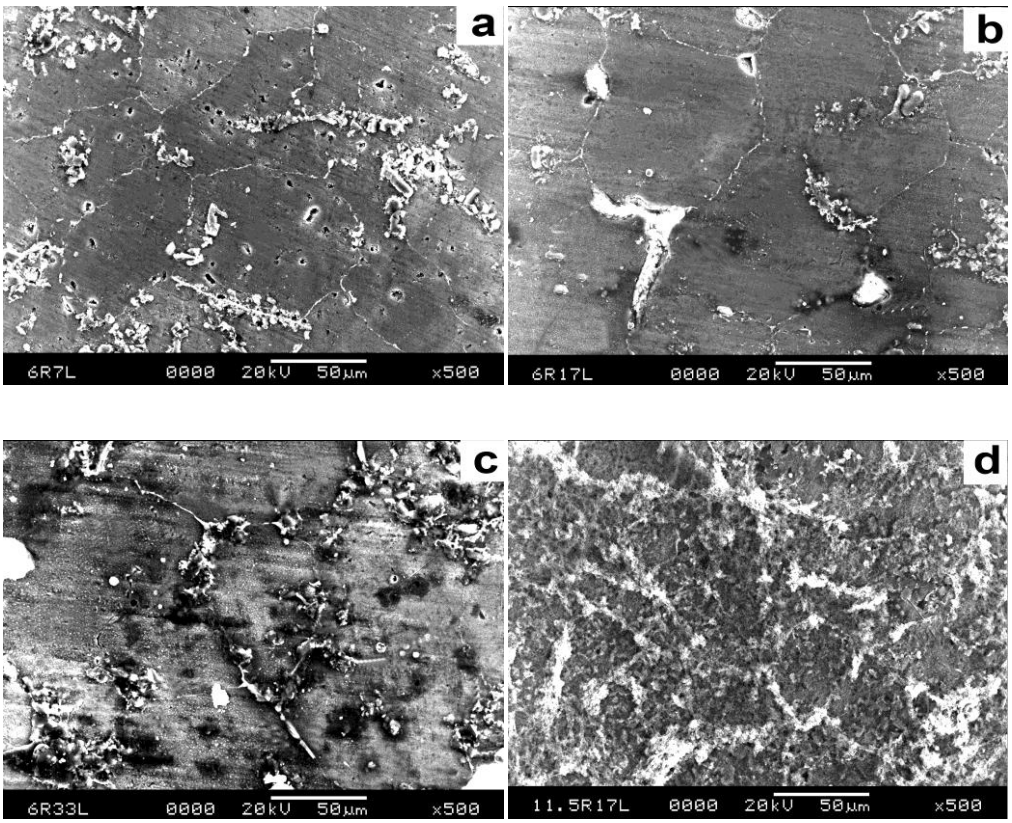

Figure 4.4 SEM images of showing the microstructure of Al-4.5Cu-5TiB_2 composite subjected to mushy state rolling to thickness reduction of: (a) 6% at 598°C (7% liquid), (b) 6% at 619°C (17% liquid), (c) 6% at 633°C (33% liquid) and (d) 11.5% at 619°C (17% liquid).

4.4.1.2 Hot rolled Al-4.5Cu-5TiB_2 composite

On subjecting the composite plates to hot rolling, the dendritic structure breaks down to a more or less equiaxed grain structure and a modest grain refinement is witnessed in the microstructure. Figure 4.5(a) is the optical micrograph and Figure 4.5(b) is the SEM image which shows the typical microstructure of the hot rolled composite when subjected to hot rolling at 370°C with a thickness reduction of 2.5%. It indicates that the cast microstructure in Figure. 4.3 is modified. The bimodal grain size distribution reported by Herbert *et al.* (2006) and Herbert (2007) is confirmed as seen in Figure 4.5(a). The finer equiaxed grains originate due to dynamic recrystallization and appear to be randomly mixed amongst the coarser grains. Dynamic recrystallization has also been confirmed in Al-4.5Cu alloy based composite when subjected to high temperature compression tests in previous studies ((Bhat *et al.* 1992, Herbert *et al.* 2006, Herbert 2007).

Upon hot rolling of the composite, prior to mushy state rolling, alligatoring was observed only when the composite was rolled to 11.5% thickness reduction with mushy state temperatures corresponding to 33% liquid volume fractions in composite. The prior hot rolling of the composite before mushy state rolling is known to inhibit alligatoring, except with very large thickness reductions (Herbert *et al.* 2006, Herbert 2007). This is due to reduction in stress concentration at grain boundaries owing to equiaxed grain morphology evolved after hot rolling. Such a phenomenon makes grain sliding easier as observed (Raj & Ashby 1971, Sherby & Wadsworth 1989) in super plastic deformation involving much finer grains. In addition, large amounts of diffusion during annealing in hot rolling leads to redistribution of the solute, Cu in the composite matrix (Herbert 2007). This in turn leads to more uniform accumulation of liquid near grain boundaries. It is reported (Herbert *et al.* 2006, Herbert 2007) to result in more uniform distribution of strain and strain accommodation by inter-grain sliding, in line with the observations made in this study. Tzimas and Zavalnigos (1999) have reported much lower flow stress during the compression tests on previously deformed (strain induced melt activated) 2014 alloy specimens, compared to that seen with as cast specimens having dendritic microstructure.

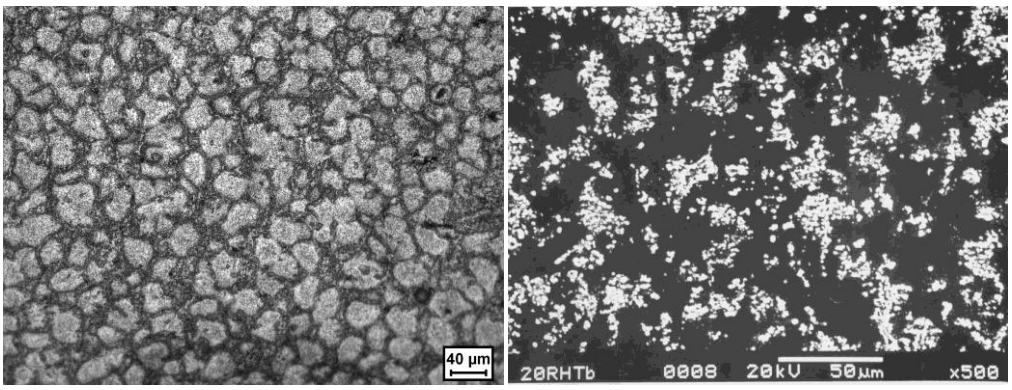

Figure 4.5 Typical microstructure of Al-4.5Cu-5TiB_2 composite subjected to hot rolling at 370°C with a thickness reduction of 2.5%: (a) optical micrograph (b) SEM image.

4.4.1.3 Mushy state rolled Al-4.5Cu-5TiB_2 composite from pre hot rolled condition

Figure 4.6 (a) to (e) show the optical micrographs of pre hot rolled composite rolled in mushy state to various thickness reductions and at various mushy zone temperatures. Figure 4.6(a) is the optical micrograph for specimen rolled in mushy state with 17% liquid volume content to 2% thickness reduction. Figure 4.6(b) to (d) show the optical micrographs of mushy state rolled composite to 6% thickness reduction with 7, 17 and 33% liquid volume content, respectively. Optical micrograph depicted in Figure 4.6(e) is for the specimen mushy state rolled to 11.5% thickness reduction with 17% liquid volume content. The grains are found to be globular with low reduction and high liquid content as observed in Figure 4.6(a). Grains appear to be elongated with higher thickness reduction and low liquid content as seen in Figure 4.6(e), as was the case observed in mushy state rolled composite in as cast form in Figure 4.3(e). It can also be seen from Figure 4.6(a) through (e) that the overall morphology of the microstructure in mushy state rolled specimens rolled in pre hot rolled condition gets more refined, with the bimodal grain size morphology being maintained.

Figure 4.7 (a) to (e) show the SEM (BSE) images of the composite rolled in mushy state when in pre hot rolled condition with various liquid volume contents and at various thickness reductions. Figure 4.7(a) shows image for 2% thickness reduction with 17% liquid volume content of the composite. Figure 4.7(b) to (d) are the images for 6% thickness reduction of composite with 7, 17 and 33% liquid volume content while Figure 4.7(e) shows the SEM image for the pre hot rolled composite, mushy

state rolled to 11.5% thickness reduction with 17% liquid volume content. It can be seen that the TiB_2 particle distribution in the matrix is more refined as compared to TiB_2 particle distribution in as cast composite. Also it can be observed that TiB_2 particles are aligned in the direction of rolling.

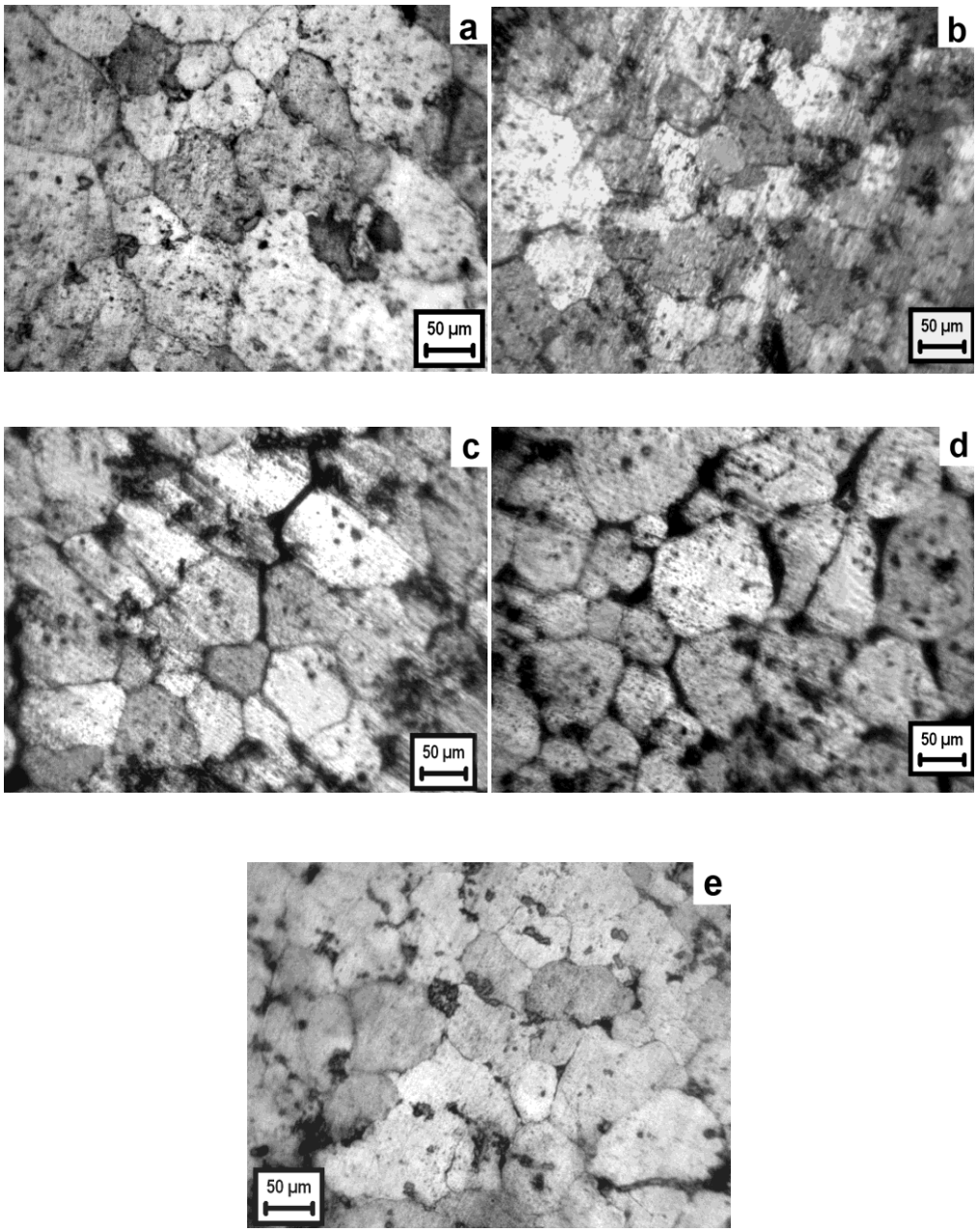

Figure 4.6 Optical micrographs showing the microstructure of Al-4.5Cu-5TiB_2 composite subjected to mushy state rolling to thickness reduction of; (a) 2% at 619°C (17% liquid), (b) 6% at 598°C (7% liquid), (c) 6% at 619°C (17% liquid), (d) 6% at 633°C (33% liquid) and (e) 11.5% at 619°C.

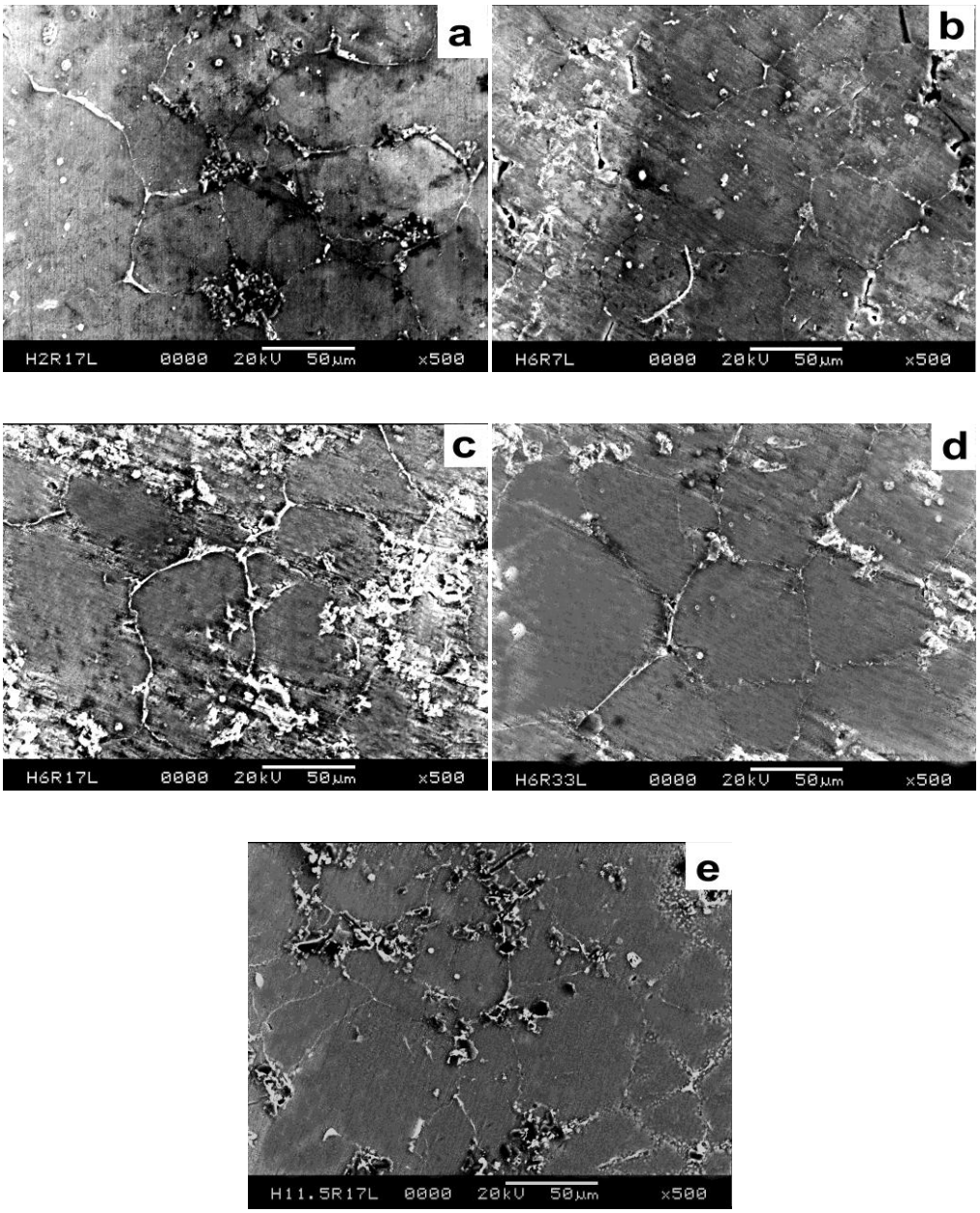

Figure 4.7 SEM images showing the microstructure of Al-4.5Cu-5TiB_2 composite subjected to mushy state rolling to thickness reduction of: (a) 2% at 619°C (17% liquid), (b) 6% at 598°C (7% liquid), (c) 6% at 619°C (17% liquid), (d) 6% at 633°C (33% liquid) and (e) 11.5% at 619°C.

4.5 GRAIN SIZE ANALYSIS OF MUSHY STATE ROLLED Al-4.5Cu-5TiB_2 COMPOSITE

4.5.1 Grain size analysis of mushy state rolled as cast and pre hot rolled Al-4.5Cu-5TiB_2 composite

The average grain size value 50±8μm has been reported in the α-Al matrix of cast Al-4.5Cu-5TiB_2 composite by Herbert (2007), using image analysis. The Al-4.5Cu-5TiB_2 composite exhibits bimodal grain size distribution as discussed in 4.4.1.1 to 4.4.1.3. Table 4.2 lists the values of large and small grain size for mushy state rolled as cast Al-4.5Cu-5TiB_2 composite for the input parameters of mushy state rolling selected for validation experiments. The cause for bimodal distribution and presence of fine grains mixed in coarser grains has been discussed in section 4.4.1. The mean grain sizes of both the large as well as small grains are found to be much smaller than those reported for the Al-4.5Cu alloy in the work of Herbert (2007). This is because the grain coarsening is caused by uninhibited grain boundary migration which is inhibited by Zener pinning of grain boundaries by TiB_2 particles (Kiuchi 1989, Herbert 2007). Furthermore, the TiB_2 sites act as heterogeneous nucleation sites during solidification of liquid. Also, these sites act as triggers for particle induced recrystallization of unmelted grains, thus helping creation of fine α-Al grains (Herbert *et al*. 2006). Table 4.3 shows the listing of grain sizes for mushy state rolled pre hot rolled Al-4.5Cu-5TiB_2 composite. Again it can be seen that the grain sizes exhibit bimodal distribution. It can also be seen that both, the coarse as well as fine grain sizes in case of pre hot rolled composite are smaller as compared to that for mushy state rolled as cast composite. This can also be seen from Figure 4.8(a) and Figure 4.8(b) which show the bar graphs for grain sizes for mushy state rolled Al-4.5Cu-5TiB_2 composite rolled in as cast and in pre hot rolled condition, respectively. Zoqui (2003) in his study on the cast Al-4.5Cu alloy subjected to cold work and partial remelting at 635°C obtained small rheocast α-Al grain size through large prior deformation and this was attributed to recrytallization during heating. Thus reduction in grain size after mushy state rolling in case of coarse as well as fine grains can therefore be attributed to refinement in grain structure as well as recrystallization during prior hot rolling.

Table 4.2	Grain sizes of Al-4.5Cu-5TiB_2 composite samples subjected to mushy state rolling in as cast state. (along longitudinal rolling plane).			
Sr. No.	**Thickness Reduction (%)**	**Liquid Volume Fraction (%)**	**Large Grain size (µm)**	**Small Grain size (µm)**
1	2	17	63	30
2	6	7	66	29
3	6	17	49	26
4	6	33	55	28
5	11.5	17	46	30

Table 4.3	Grain sizes of Al-4.5Cu-5TiB_2 composite samples subjected to mushy state rolling in pre hot rolled condition. (along longitudinal rolling plane).			
Sr. No.	**Thickness Reduction (%)**	**Liquid Volume Fraction (%)**	**Large Grain size (µm)**	**Small Grain size (µm)**
1	2	17	43	25
2	6	7	41	26
3	6	17	40	26
4	6	33	46	24
5	11.5	17	46	30

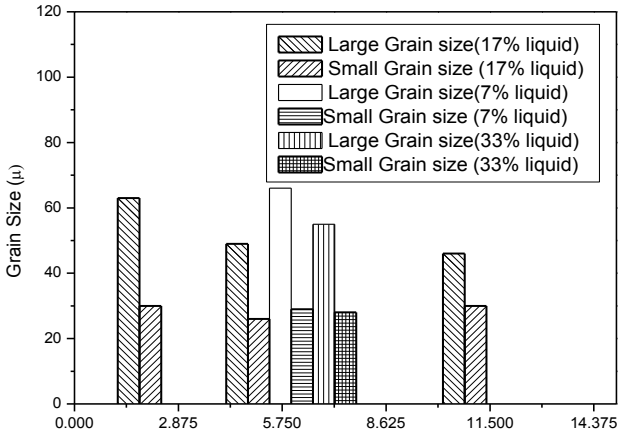

Figure 4.8(a) Bar diagram showing the grain sizes (along longitudinal rolling plane for as cast Al-4.5Cu-5TiB_2 composite samples subjected to mushy state rolling.

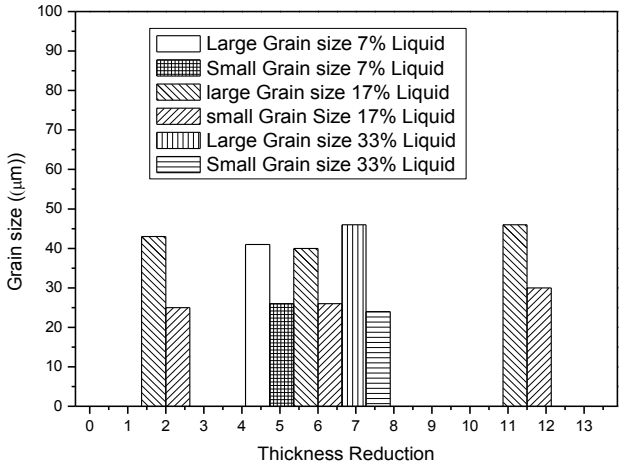

Figure 4.8(b) Bar diagram showing the grain sizes (along longitudinal rolling plane for pre hot rolled Al-4.5Cu-5TiB_2 composite samples subjected to mushy state rolling.

4.6 GRAIN SIZE PREDICTION USING ARTIFICIAL NEURAL NETWORKS (ANN)

The values of grain size predicted by ANN are compared in the next sub-section with the corresponding experimentally obtained values listed at Table 4.1, to check the suitability of the model within the purview of experimentation. Further, the model is checked for its capability to extrapolate and interpolate the values of grain size with the outcome of validation experiments. A detailed analysis of the variation of the values of grain sizes with respect to amount of thickness reduction during rolling and with liquid volume fraction at the beginning of rolling is also presented in this section.

4.6.1 Comparison of Grain sizes obtained by experimentation and ANN prediction

4.6.1.1 Rolling of as cast Al-4.5Cu-5TiB_2 composite in mushy state

Table 4.4 shows the values of experimentally obtained large and small grain sizes as well as those predicted by ANN for as cast Al-4.5Cu-5TiB_2 composite in mushy state containing varying liquid volume fractions (10% corresponding to 610°C, 20% corresponding to 626°C and 30% corresponding to 631°C) and rolled to 2.5%, 5%,

7.5% and 10% thickness reductions per pass. The experimental values used for training the network are taken from the PhD work of Herbert (2007), for experiments carried out at 10%, 20% and 30% liquid volume fractions to 2.5%, 5%, 7.5% and 10% thickness reductions while the ANN predictions have been extended beyond the upper and lower limits of experimentation. Table 4.4 lists the values of large and small grain sizes predicted by the trained ANN for the data used for training the network as well as the data corresponding to validation experiments.

From Table 4.4, it can be seen that the percentage error between the experimental values used for training the network and corresponding ANN predicted values ranges from -3.0987% to +1.99% for large grain size, with the maximum errors corresponding to 10% liquid volume fraction at 5% thickness reduction and 20% liquid volume fraction at 5% thickness reduction, respectively. Similarly, for small grain size, the maximum % error is between -5.3307% corresponding to 10% liquid volume fraction at 10% thickness reduction and 4.8529% corresponding to 20% liquid volume fraction at 5% thickness reduction.

The percentage error between experimental values and values predicted by ANN at various percent liquid volume fractions for entire range of percentage thickness reduction are within |5.4%|. This suggests that the model has learnt the relationship between the mushy state parameters and the grain sizes quite adequately and has generalized it to predict the large and small grain sizes for any values of input parameters viz. the material type, % thickness reduction and % liquid volume fractions supplied to it, within an error of 5.4%. Kusiak and Kuziak (2002) have reported a maximum error of 8% in ANN predictions, while Jiahe *et al.* (2003) reported a maximum error of 5.7% in the prediction of average ferrite grain size of 60Si2MnA stainless steel rod based on controlled rolling and cooling process parameters.

Figure 4.9 and 4.10 show the variation of grain sizes (coarse and small) with change in % thickness reduction as predicted by ANN at 5% and 35% liquid volume fractions, respectively. It can be seen from Figure 4.9 that size of coarse grain size increases gradually till 7% thickness reduction but subsequently falls drastically

beyond 7.5% liquid volume fraction. Marginal increase in grain size up to 7% thickness reduction may be due to enhanced diffusion across unmelted grains, probably due to mushy state deformation (Aikin1997, Tzimas and Zavaliangos 1993, Herbert 2007) of solid grains or dendritic arms during rolling due to increased contact between them. Beyond 7%, especially after 7.5% thickness reduction, the coarse grain size decreases rapidly, which could be due to the dominant effect of fragmentation of grains and dendritic arms, overtaking the effect of grain coarsening (Aikin1997).

At higher values of liquid volume fraction of 35%, corresponding to higher mushy state temperature at which rolling is started, as seen in Figure 4.10, the coarse grain size predicted decreases up to 7.5% thickness reduction. The decrease in the coarse size in this region can be attributed to the compressive force during rolling operation, which may cause the liquid in inter granular spaces of α- Al grains to rush to the surface and cool more rapidly in contact with the rolls, giving rise to fine grain formation (Aikin 1997). As the % thickness reduction increases, the rate of escape of the liquid from the inter-granular spaces also increases. At the same time, due to higher degree of deformation grains undergo fragmentation (Herbert *et al.* 2006, Herbert 2007). As a result the grain size decreases. Beyond 7.5% thickness reduction, a momentary steep rise in coarse grain sizes is observed. Firstly, this could be due to the fact that larger liquid fraction being present at higher temperature corresponding to 35% liquid volume fraction, and secondly, that rolling speed being maintained constant for all cases, there is more scope for grain growth at higher temperature (Herbert *et al.* 2006, Herbert 2007). Therefore grain size increases between 7.5% thickness reduction and 10% thickness reduction overriding the effects of compressive force and more rapid cooling rate of liquid in inter granular spaces Beyond 10% thickness reduction a steep fall in the ANN predicted coarse grain size is observed. Again this could be probably be attributed to higher compressive forces causing the breaking of dendritic/columnar structures (Aikin1997) giving rise to finer grain fragmentation. This coupled with larger rate of liquid escaping from intergranular regions and coming in contact with cooler rolls, gives rise to smaller grains overriding the effect of higher temperatures during initiation of rolling.

TABLE 4.4 Comparison of Experimental values of grain sizes of as cast Al-4.5Cu- 5TiB_2 composite samples subjected to mushy state rolling with ANN predicted values.

Specimen descriptions		Experimental		ANN		%Error	
		Grain size(μm)		Grain size (μm)		Grain size	
		Large	Small	Large	Small	Large	Small
As cast		50		49.9944	49.9944	0.0112	0.2106
** 2% thickness. Reduction	**f_l~ 0.17	63	30	61.5498	30.2633	2.3019	-0.8777
2.5% thickness reduction	f_l ~ 0.05			66.7204	27.2855		
	af_l ~ 0.1	62	27	60.7838	27.4532	1.9616	-1.6785
	af_l ~ 0.2	58	33	59.338	33.8438	-2.3069	-2.557
	$_{afl}$ ~ 0.3	66	37	64.776	35.8221	1.8545	3.1835
	f_l ~ 0.35			66.6396	30.0602		
5% thickness reduction	f_l ~ 0.05			69.5573	27.2271		
	af_l ~ 0.1	54	25	55.6733	25.8852	-3.0987	-3.5408
	af_l ~ 0.2	51	31	49.9853	29.4956	1.9896	4.8529
	af_l ~ 0.3	55	32	55.5784	33.4465	-1.0516	-4.5203
	f_l ~ 0.35			61.1633	28.4914		
*6% thickness reduction	**f_1~ 0.07	66	29	66.9744	28.032	-1.476	3.3379
	*f_1~0.17	49	26	48.496	25.793	1.0286	0.7962
	**f1~0.33	55	28	56.3759	28.2583	-2.5016	-0.9255
7.5% thickness reduction	f_l ~ 0.05			71.394	32.4656		
	af_l ~ 0.1	62	32	61.5025	30.92	0.8024	3.375
	af_l ~ 0.2	48	26	47.299	27.3059	1.4604	-5.0227
	af_l ~ 0.3	53	27	52.922	26.4012	0.1471	2.2177
	f_l ~ 0.35			56.2987	24.2107		
10% thickness reduction	f_l ~ 0.05			48.5162	30.514		
	af_l ~ 0.1	49	29	49.2457	30.5459	-0.5014	-5.3307
	af_l ~ 0.2	47	30	48.0792	30.494	-2.2962	-1.6467
	af_l ~ 0.3	54	26	54.1504	26.2361	-0.2785	-0.9081
	f_l ~ 0.35			59.3253	21.9236		
** 11.5% thickness reduction	**f_1 ~ 0.17	46	30	47.0124	30.4498	-2.2008	-1.4993
12.5% thickness reduction	f_l ~ 0.05			46.7048	30.4369		
	f_l ~ 0.1			46.7111	30.3472		
	f_l ~ 0.2			46.7789	30.44		
	f_l ~ 0.3			46.8364	30.391		
	f_l ~ 0.35			48.8614	29.249		

* Validation experiments carried out in the present study within range of training data.

** Validation experiments carried out in the present study outside training data range.

a Experimental data.

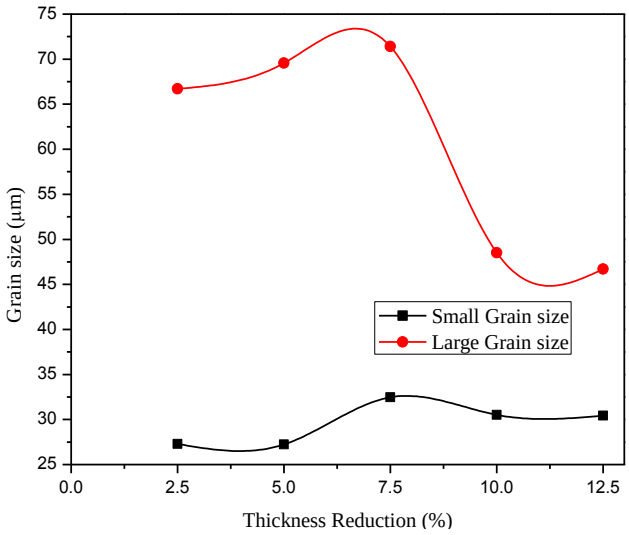

Figure 4.9 Plots showing variation of ANN predicted values of large grain and small grain size with % thickness reduction at 5% liquid volume fraction when as cast Al-4.5Cu-5TiB_2 composite is rolled in mushy state.

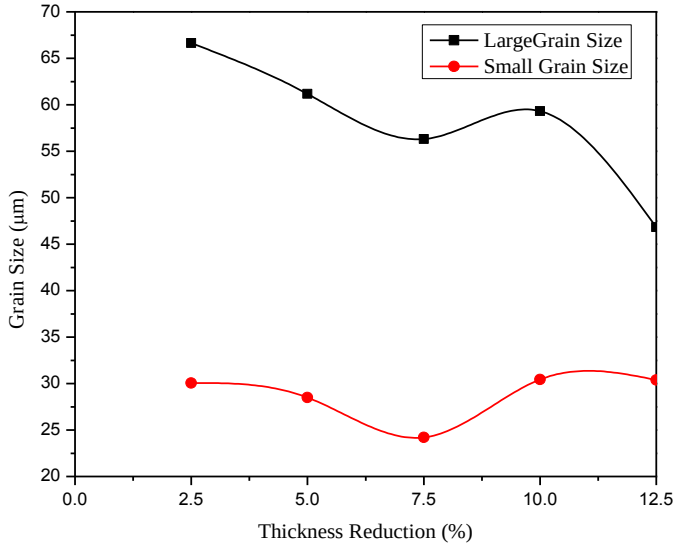

Figure 4.10 Plots showing variation of ANN predicted values of large grain and small grain size with % thickness reduction at 35% liquid volume fraction when as cast Al-4.5Cu-5TiB_2 composite is rolled in mushy state.

Further in Table 4.4, the ANN model predictions are compared with the results of validation experiments for data beyond the range used for training the ANN model. This data is indicated with ** in Table 4.4. It can be seen from Table 4.4 that in case of large grain size, the maximum error of |2.5016| % in ANN model prediction occurs when the as cast composite is mushy state rolled to 6% thickness reduction in mushy state condition corresponding to 33% liquid volume fraction in the composite. The maximum error of |3.3379|% is observed at 6% thickness reduction in case of small grain size, when as cast composite is rolled at temperature corresponding to 7% liquid volume fraction. The errors in prediction obtained outside the range of data used for training are less than errors reported in literature (Kusiak and Kuziak 2002, Jiahe *et al.* 2003, Selvakumar *et al.* 2007*)*. The trained ANN model can be therefore be used for extrapolation also and can predict the large and small grain sizes for as cast Al-4.5Cu-5TiB_2 composite rolled in mushy state to 2 to 11.5% thickness reduction and with 7 to 33% liquid volume fraction.

Figure 4.11 to 4.13 show the variation of coarse and small grain sizes at 10%, 20% and 30% liquid volume fraction, respectively, with experimentation and as predicted by ANN. For rolling carried out with 10% liquid volume fraction in mushy state, the coarse grain size decreases continuously at a modest rate up to 5% thickness reduction, and then increases gradually till about 9% thickness reduction, while fine grain size initially decreases at a marginal rate up to 5% thickness reduction and then increases slowly till around 9% thickness reduction. Both, the coarse and fine grain sizes are then seen to decrease beyond 9% reduction in thickness. More or less similar trends are exhibited for samples with 20% and 30% liquid volume fractions. Thus, it can be seen that variation of grain sizes following rolling operation carried out for different mushy state temperatures corresponding to respective liquid volume fractions do not show any definite trend with respect to % thickness reductions, which may be due to randomly occurring grain fragmentation and grain boundary pinning by the TiB_2 particles opposing the natural process of grain growth (Aikin1997). However, the overall behaviour is in between the extreme cases discussed for 5% and 35% liquid volume fractions.

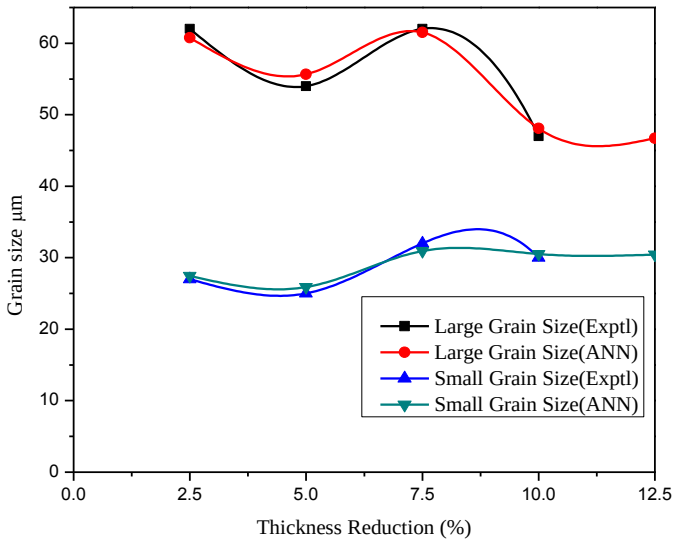

Figure 4.11 Plot showing comparison of variation of large grain and small grain size with % thickness reduction at 10% liquid volume fraction when as cast Al-4.5Cu-5TiB_2 composite is rolled in mushy state, with that predicted by ANN.

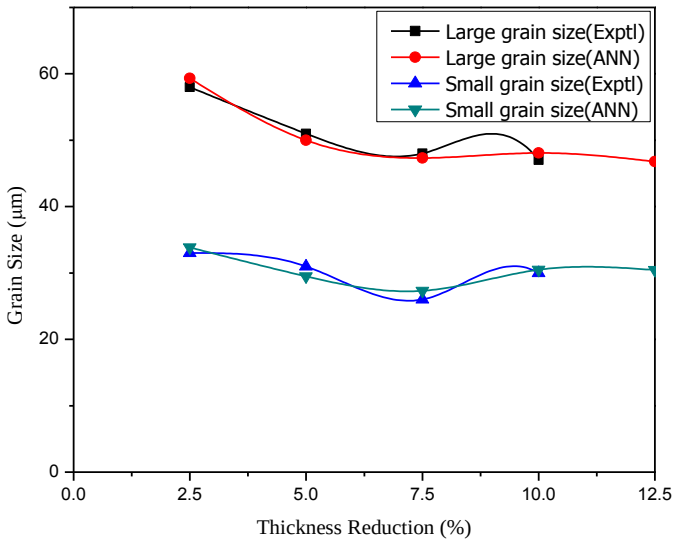

Figure 4.12 Plots showing comparison of variation of large grain and small grain size with % thickness reduction at 20% liquid volume fraction when as cast Al-4.5Cu-5TiB_2 composite is rolled in mushy state, with that predicted by ANN.

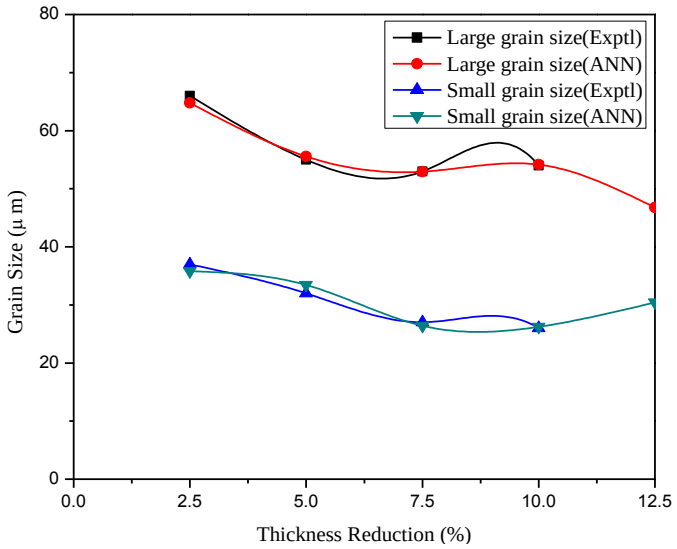

Figure 4.13 Plots showing comparison of variation of large grain and small grain size with % thickness reduction at 30% liquid volume fraction when as cast Al-4.5Cu-5TiB_2 composite is rolled in mushy state, with that predicted by ANN.

4.6.1.2 Pre-hot rolled composite rolled in mushy state

Table 4.5 lists the values of grain sizes predicted by ANN for mushy state rolled Al-4.5Cu-5TiB_2 composite rolled in pre hot rolled condition. Here the model, predicts the grain sizes for the entire range of mushy state rolling from 2.5% to 10% thickness reduction and the composite containing liquid volume fractions from 10% to 30% within an error of |6.1|%. Figure 4.14 and 4.15 show the variation of grain sizes predicted by ANN, while those in Figure 4.16, 4.17 and 4.18 show comparison of grain sizes obtained experimentally and those predicted by ANN model, when pre hot rolled Al-4.5 Cu- 5TiB_2 composite is rolled to different % thickness reductions, (i.e. 2.5%, 5%, 7.5%, 10% and 12.5%) with varying % liquid volume fractions (i.e. 5%, 10%, 20%, 30% and 35%).

The comparison of experimental and ANN predicted graphs in Figure 4.16, 4.17 and 4.18 shows that there is a very small variation between these values. The values predicted by ANN are plotted in Figure 4.14 and 4.15, and show the expected values of coarse and small grain size for the Al-4.5Cu-5TiB_2 composite in pre hot rolled condition, rolled in mushy state containing 5% liquid volume fractions and 35% liquid volume fractions, respectively.

Table 4.5 Comparison of Experimental values of grain size and hardness for pre hot rolled Al-4.5Cu-5TiB2 composite samples subjected to mushy state rolling with ANN predicted values.

Specimen descriptions		Experimental		ANN		% Error	
		Grain size (µm)		Grain size (µm)		Grain size	
		Large	Small	Large	Small	Large	Small
Hot rolling		52	28	51.9851	28.514	0.0286	-1.8382
**2% thickness reduction	**f_l~0.17	43	25	42.6188	25.461	0.8866	-1.8444
2.5% thickness reduction	f_l ~ 0.05			43.635	25.404	--------	--------
	[a]f_l ~ 0.1	43	27	42.2821	25.385	1.6695	5.9807
	[a]f_l ~ 0.2	42	26	42.4751	25.524	-1.1312	1.8307
	[a]f_l ~ 0.3	47	25	47.6159	24.558	-1.3104	1.7664
	f_l ~ 0.35			47.7306	23.813	--------	--------
5% thickness reduction	f_l ~ 0.05			42.016	25.276	--------	--------
	[a]f_l ~ 0.1	42	26	40.9082	25.235	2.5995	2.9415
	[a]f_l ~ 0.2	41	25	40.6746	25.300	0.7937	-1.2008
	[a]f_l ~ 0.3	46	24	45.474	24.349	1.1435	-1.4554
	f_l ~ 0.35			46.7005	23.605	--------	--------
* 6% thickness reduction	**f_l ~ .07	41	26	41.1357	25.247	-0.3309	2.8946
	*f_l ~ .17	40	26	40.5689	25.226	-1.4222	2.9742
	**f_l ~0.33	46	24	46.7183	23.807	-1.5615	0.8038
7.5% thickness reduction	f_l ~ 0.05			47.0957	30.340	--------	--------
	[a]f_l ~ 0.1	40	26	40.7523	25.337	-1.8807	2.5484
	[a]f_l ~ 0.2	39	25	40.5014	25.211	-3.8497	-0.846
	[a]f_l ~ 0.3	45	24	45.1837	24.371	-0.4082	-1.5467
	f_l ~ 0.35	-------	-------	46.7293	23.5	--------	--------
10% thickness reduction	f_l ~ 0.05	-------	-------	46.7033	30.4	--------	--------
	[a]f_l ~ 0.1	47	32	46.6879	30.414	0.6640	4.9546
	[a]f_l ~ 0.2	43	25	42.0928	26.524	2.1098	-6.0972
	[a]f_l ~ 0.3	45	27	44.7634	26.82	0.5258	0.6666
	f_l ~ 0.35	-------	-------	45.7546	24.422	--------	--------
**11.5% thickness reduction	**f_l ~ .17	46	30	46.6799	30.418	-1.478	-1.3937
12.5% thickness reduction	f_l ~ 0.05	-------	-------	46.6958	30.432	--------	--------
	f_l ~ 0.1	-------	-------	46.6916	30.428	--------	--------
	f_l ~ 0.2	-------	-------	46.6995	30.435	--------	--------
	f_l ~ 0.3	-------	-------	46.7157	30.425	--------	--------
	f_l ~ 0.35	-------	-------	46.5245	29.605	--------	--------

[*] Validation experiments carried out in the present study within range of training data.
[**] Validation experiments carried out in the present study outside the range of training data.
[a] Experimental data.

From all the Figure 4.16, 4.17 and 4.18, it can be seen that the variation does not show any definite continuous increase or decrease with increase in % thickness reduction. As we have seen earlier, this may be again due to randomly occurring fragmentation of grains and grain boundary pinning by TiB_2 particles which restrict grain growth (Aikin1997). However, it can be seen that, coarse grain sizes have higher values in the composite with 30% liquid volume fractions rolled to 10% thickness reduction.

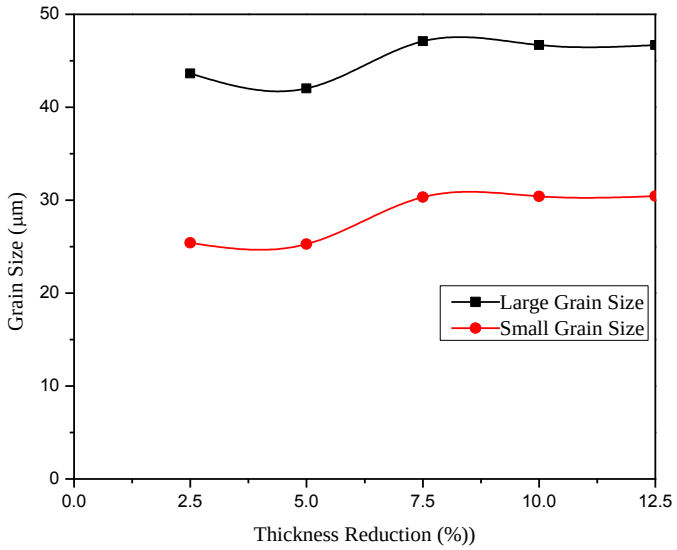

Figure 4.14 Plots showing variation of ANN predicted values of large grain and small grain size with % thickness reduction at 5% liquid volume fraction when pre hot rolled Al-4.5Cu-5TiB_2 composite is rolled from mushy state.

It can be seen from Table 4.5 that the trained ANN model for grain size prediction predicts the large grain sizes within an error of |1.5615|% outside the bounds of data range used for training the model. The maximum error of |1.5615|% is observed at 6% thickness reduction when pre hot rolled composite is mushy state rolled with 33% liquid volume fraction. Similarly, the model predicts the small grain size within an error of |2.8946|% with this maximum error observed at 6% thickness reduction and 7% liquid volume fraction. Thus the model extrapolates the large and small grain sizes within an error of |2.9|% for mushy state rolled composite rolled to 2 to 12% thickness reduction and with 7 to 33% liquid volume fraction. These observed errors

are less than the errors reported in literature related to NN modelling (Kusiak and Kuziak 2002, Jiahe *et al.* 2003, Selvakumar *et al.* 2007). Thus the trained ANN model for mushy state rolled Al-4.5Cu-5TiB_2 composite rolled in pre hot rolled condition has capabilities to model the variation of large and small grain sizes within as well as outside the bounds of data used for training the model.

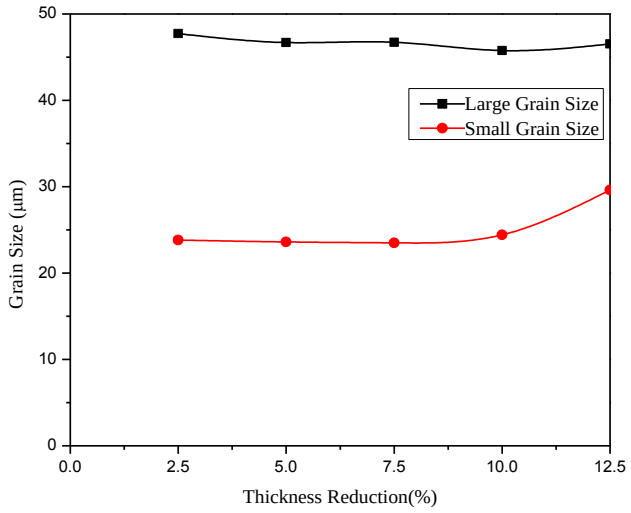

Figure 4.15 Plots showing variation of ANN predicted values of large grain and small grain size with % thickness reduction at 35% liquid volume fraction when pre hot rolled Al-4.5Cu-5TiB_2 composite is rolled from mushy state.

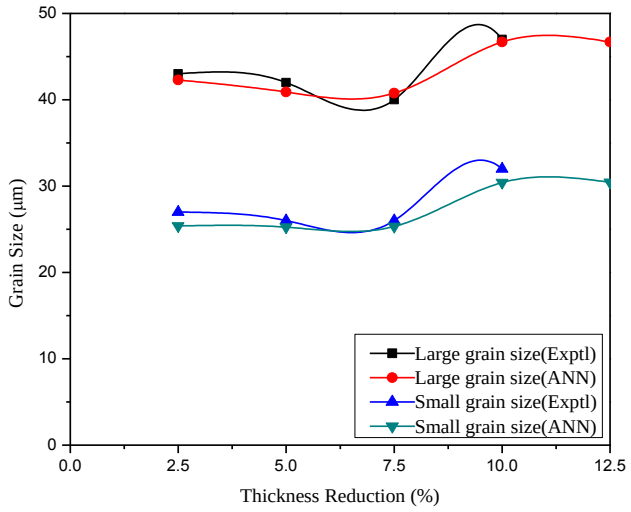

Figure 4.16 Plots showing comparison of variation of large grain and small grain size with % thickness reduction at 10% liquid volume fraction when pre hot rolled Al-4.5Cu-5TiB_2 composite is rolled from mushy state, with that predicted by ANN.

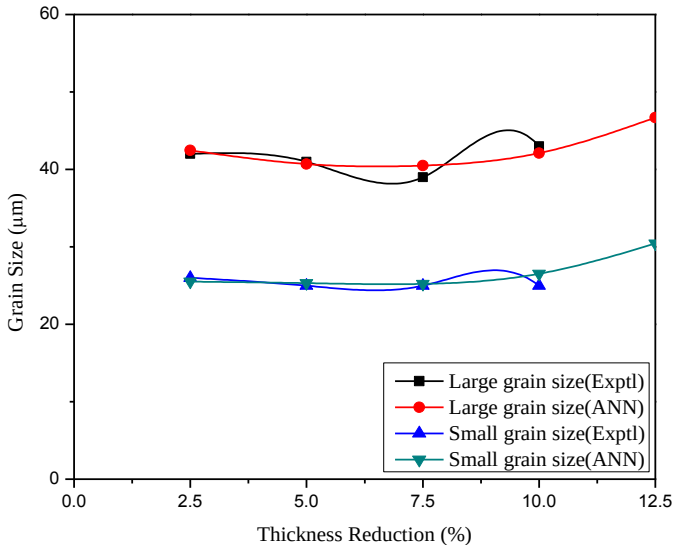

Figure 4.17 Plots showing comparison of variation of large grain and small grain size with % thickness reduction at 20% liquid volume fraction when pre hot rolled Al-4.5Cu-5TiB_2 composite is rolled from mushy state, with that predicted by ANN.

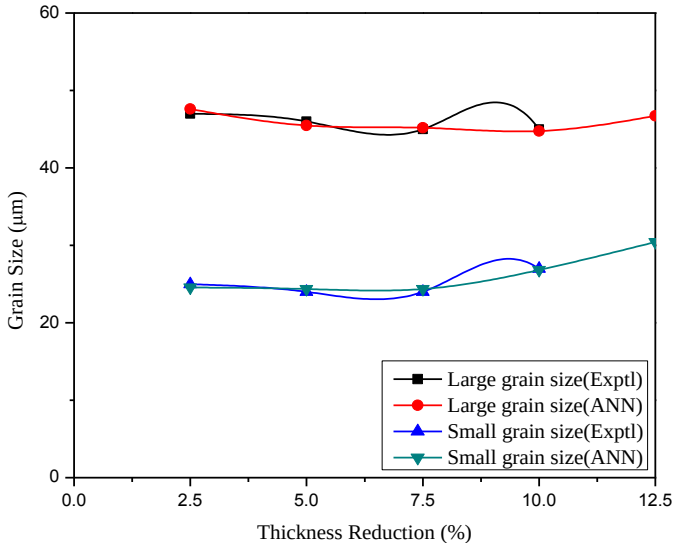

Figure 4.18 Plots showing comparison of variation of large grain and small grain size with % thickness reduction at 30% liquid volume fraction when pre hot rolled Al-4.5Cu-5TiB_2 composite is rolled from mushy state, with that predicted by ANN.

Figure 4.19(a) and (b) show the contour graphs of the distribution of large grain sizes and small grain sizes for as cast composite with variations in % thickness reduction and % liquid volume fractions. In the contour plot shown in Figure 4.19(b) it is seen that low values of small grain size are concentrated in the region between 2.5% and

7.5% thickness reduction and 5% and 12.5% liquid volume fractions. High values of small grain size are concentrated near 2.5% thickness reduction and 35% liquid volume fraction. High values are also seen around 7.5% thickness reduction and low values of liquid volume fraction. Figure 4.19(a) shows high values of large grain size near 7.5% thickness reduction and 5% liquid volume fraction and low values in higher % thickness reduction and medium values of % liquid volume fractions.

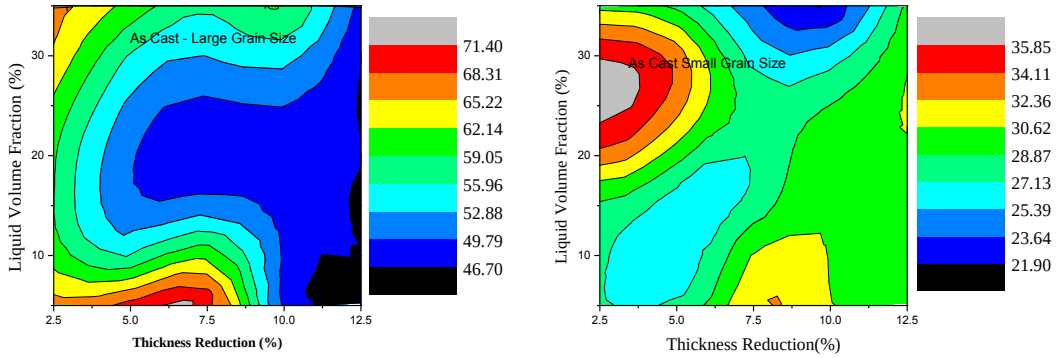

Figure 4.19 Contour maps showing (a) large grain size and (b) small grain size spectrum when as cast Al-4.5Cu- 5TiB_2 composite is rolled in mushy state to different thickness reductions and with different Percentage Liquid fractions.

Similarly Figure 4.20(a) and (b) show the contour graphs for similar variations for hot rolled composite. Here it can be seen that low values of small grain size are present in a wider spectrum and so also the low values of large grain size, thus providing a larger quantities of low values of grain sizes.

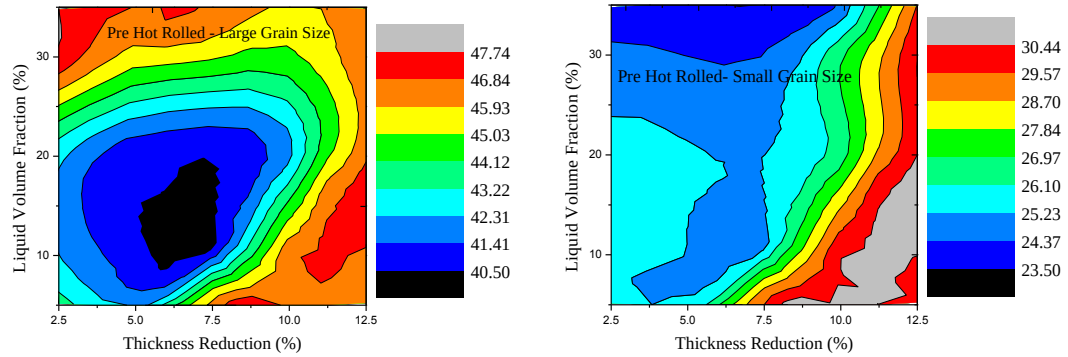

Figure 4.20 Contour maps showing (a) Large grain size and (b) Small grain size spectrum when pre Hot Rolled Al-4.5Cu- 5TiB_2 composite is rolled in mushy state to various thickness reductions and with different liquid volume fractions.

4.7 PARAMETRIC STUDY

4.7.1 Variation of grain sizes of mushy state rolled composite with respect to thickness reduction at given liquid fraction.

Figure 4.21 shows the variation of grain sizes with thickness reduction when Al-4.5Cu-5TiB_2 composite is rolled in mushy state from temperature corresponding to 30 % liquid volume fraction. It is seen that, the predicted coarse grain size decreases up to 7.5% thickness reduction.

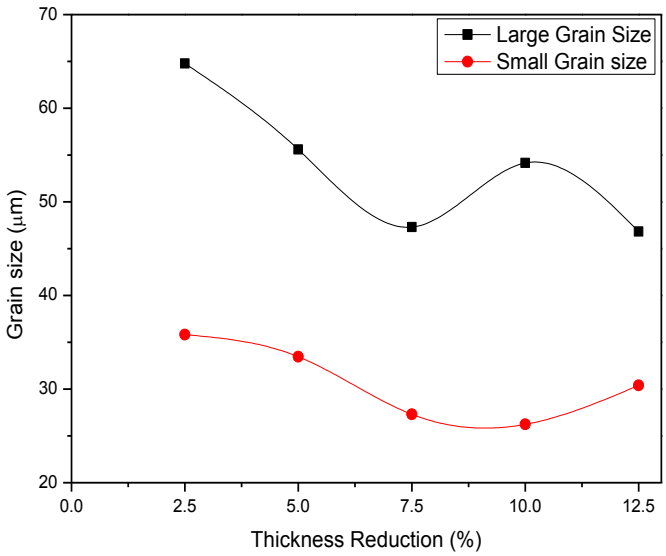

Figure 4.21 Plot showing variation of large and small grain sizes with % thickness reduction at 30% liquid volume fraction, as predicted by ANN, when Al-4.5Cu-5TiB_2 composite is rolled in mushy state.

The decrease in the coarse size in this region can be attributed to the compressive force during rolling operation, which may cause the liquid in intergranular spaces of α-Al grains to flow to the surface and cool more rapidly in contact with the rolls, giving rise to fine grain formation (Herbert *et al.* 2006). As the % thickness reduction increases, the amount of liquid shifted to the surface by the squeezing action of the rolls also increases. Rapid solidification of this liquid, together with greater degree of fragmentation decreases the grain size. Beyond 7.5% thickness reduction, a momentary steep rise in coarse grain sizes is observed. Probably, grain growth could have been promoted by coalescence of unmelted grains on application of higher roll

pressure for ≥7.5 thickness reduction. Again, beyond 10% thickness reduction, a steep fall in the ANN predicted coarse grain size is observed. This is attributed to higher compressive forces causing the fragmentation of dendritic/columnar structures (Herbert 2007) giving rise to finer grains, along with dynamic recrystallization of the unmelted deformed grains.

Besides this mechanism, larger amount of liquid escaping to the surface and coming in contact with cooler rolls could also be responsible for the formation of smaller grains. In case of small grain sizes, grain growth is observed beyond 10% thickness reduction. This is probably because at high temperature (632ºC) corresponding to 30% liquid volume fraction, grain growth could have been promoted by coalescence of unmelted grains (on application of higher roll pressure) overriding the effects of higher compressive force due to 12.5% thickness reduction.

4.8 CONCLUSIONS

1. Artificial neural network with feed forward architecture is successfully modelled to predict large and small grain sizes in mushy state rolled Al-4.5Cu-5TiB_2 composite.
2. The values of grain sizes (small and coarse) predicted by the ANN model proposed give an error less than |5.53%| and |6.1%| for as cast and pre hot rolled Al–4.5Cu-5TiB_2 composite respectively rolled in mushy state, with thickness reduction in the range from 2.5% to 10% per pass and % liquid volume fraction in the mushy state ranging from 10% to 30%. Therefore, the model characterizes the process of mushy state rolling very much within the reasonable limits in this range and therefore can be used as an alternative to costly and time consuming experimentation.
3. The ANN model has been validated by conducting experiments on mushy state rolling of Al-4.5Cu-5TiB_2 composite with predefined starting parameters i.e. (a) with thickness reduction of 2% at 619°C, (b) with 6% thickness reduction at 598°C, 619°C and 633°C respectively and (c) 11.5% thickness reduction at 619°C. In case of mushy state rolled as cast composite, the relative error between validation experiment values of grain sizes and ANN predicted

values lies within |2.51|% and |3.4|% for large and small grain sizes respectively. Similarly the corresponding relative errors are within |1.6|% and |2.9|% respectively for large and small grain sizes, in case of mushy state rolled pre hot rolled composite. The validity of the model to predict the grain sizes has therefore been established.

4. It can be concluded that the ANN model can extrapolate grain sizes values beyond the experimental range, which is proved by a small error of |3.4|% in prediction by ANN in case of cast composite and less than |2.9|% in case of pre hot rolled composite. Thus, the model can characterize effectively, with a very low degree of variation, the mushy state rolling of as cast as well as pre-hot rolled Al–4.5Cu-5TiB_2 composite with low to high liquid content that is with 5 to 35% liquid content and from 2.5% to 12.5% thickness reduction per pass.
5. *In situ* Al-4.5(wt. %) Cu-5(wt. %) TiB2 composite was synthesized using mixed salt route. Alligatoring was observed in samples of the composite for all conditions other than those corresponding to 6% thickness reduction at 633°C (corresponding to 33% liquid) in case of mushy state rolling of composite in as cast form. Alligatoring results from strain localization at shrinkage porosities or due to solute rich intergranular locations with constraints or intergranular sliding due to presence of TiB_2 particles, culminating in intergranular fracture. However alligatoring is seen to be prevented by prior hot rolling of composite leading to homogenization and refinement of dendritic microstructure to one which has equiaxed grains before subjecting to mushy state rolling.
6. On mushy state rolling the irregular rosette shaped dendritic grains of α-Al in the matrix of as cast Al-4.5Cu-5TiB_2 composite gets modified to one having globular shaped equiaxed grains. The matrix of the composite shows bimodal distribution of grains on mushy state rolling.

Chapter 5

RESULTS AND DISCUSSION (PART II)

ANN MODELLING FOR HARDNESS PREDICTION

5.1 INTRODUCTION

The formulation of ANN model for prediction of hardness of *in situ* fabricated Al-4.5Cu-5TiB_2 composite has been discussed in this chapter. The microstructural evolution was discussed in the previous chapter. It is seen that the original dendritic morphology present in the cast composite gets modified to one which has globular grains on being subjected to hot working and mushy state rolling. It was also seen in chapter 4 that mushy state rolling led to bimodal grain size distribution along with a refinement in grain structure. It is well known that the hardness is vastly influenced by grain morphology and size distribution. In general, the surface of the mushy state rolled composite contains higher volume of fine grains (and therefore hard grain boundary volume) as compared to that at the interior of the composite (Herbert *et al.* 2006, Herbert 2007). This therefore, leads to higher surface hardness in the composite. The present study involves the formulation of the ANN model for hardness prediction, which is treated as a function of grain sizes in addition to the initial state of material, thickness reduction per pass and liquid volume fraction in composite during mushy state rolling. The study also presents the results of the experiments on Al-4.5Cu-5TiB_2 composite performed to validate the ANN model for hardness and compares them with the hardness values predicted by the model. It involves, as was the case with the work (Herbert 2007) from which data is collected, measurement of Vickers hardness of *in situ* Al-4.5Cu-5TiB_2 composite samples rolled in mushy state in as cast and pre hot rolled condition. The data for training the network has been taken from previous work related to studies on mushy state processing of Al-4.5Cu-5TiB_2 composite (Herbert 2007).

5.2 SCOPE

In this section, it is proposed to formulate an Artificial Neural Network model with Feed Forward architecture to predict the hardness of Al-4.5Cu-5TiB_2 composite rolled in mushy state in as cast as well as pre hot rolled condition with the input parameters being, % thickness reduction, % volume fraction of liquid, large and small grain sizes. The present work attempts to develop the ANN model with following:

(a) The analysis of the effect of initial state of composite material (as cast or pre hot rolled) on hardness of Al-4.5Cu-5TiB_2 composite.

(b) The analysis of effect of thickness reduction during mushy state rolling and mushy state condition from where rolling is initiated.

(c) Extrapolation and interpolation of hardness for unknown thickness reductions and liquid volume fractions in the mushy state composite.

(d) Optimisation of the input parameters for achieving best possible hardness within the range of permissible thickness reduction per pass and permissible mushy state from where rolling is initiated.

(e) Validation of the model predictions by hardness measurements on Al-4.5Cu-5TiB_2 composite samples subjected to mushy state rolling.

The input parameters for predicting the hardness of mushy state rolled Al-4.5Cu-5TiB_2 composite are initial material state, % thickness reduction, % liquid volume fraction, large and small grain sizes. The relationship being complex and non linear necessitates the use of neural network techniques. ANN with feed forward architecture and trained with error back propagation technique offers a powerful method to predict the outputs from a given input parameter combinations and hence is proposed to be used in prediction of hardness of mushy state rolled Al-4.5Cu-5TiB_2 composite.

5.3 HARDNESS

Hardness is defined as resistance to plastic deformation by indentation. It is therefore related to yield strength of its material (Sahoo and Koczak 1991). The hardness of the material provides an approximate assessment of tensile strength of the material. Thus, hardness provides a means for comparative assessment of strength of materials in the absence of data on strength properties of material.

5.4 DATA COLLECTION

The data for training the ANN network proposed for hardness prediction of mushy state rolled Al-4.5Cu-5TiB_2 composite is collected from previous studies done on mushy state rolling of as cast as well as pre hot rolled Al-4.5Cu-5TiB_2 composite (Herbert 2007). This data is listed in Table 5.1. The hardness of the material also depends upon the grain size distribution, in addition to the parameters of mushy state rolling. Table 5.1 also includes the grain sizes corresponding to the inputs of mushy state rolling (viz. Initial state of the material, % thickness reduction and % liquid content) which shall be used for training the network.

From Table 5.1, it can be seen that the hardness increases with increase in thickness reduction during rolling per pass. Also, it is observed that for a given thickness reduction during mushy state rolling, the hardness values increase with increase in liquid volume fraction above 10% and up to 20% and then found to decrease at 30% liquid volume. This phenomenon is observed both in case of as cast as well as pre hot rolled mushy state rolled composite. It is of interest to know the initial state of the composite which will give the maximum value of hardness, as hardness is not only an indicator of strength, but also a determinant of the wear properties of the material. The determination of optimised parameters of mushy state rolling for maximum hardness is therefore the prime objective of ANN formulation, in addition to understanding the variation of hardness with different conditions of mushy state rolling.

Table 5.1 Vickers hardness (H_V) of *in situ* Al-4.5Cu-5TiB_2 composite rolled in mushy state in as cast as well as pre hot rolled condition (Herbert 2007).

Material	Specimen descriptions		Experimental		
			Grain size (μm)		Hardness (Hv)
			Large	Small	
As Cast Al-4.5Cu-5TiB_2	As cast		50		78±1
	2.5% thickness reduction	f_l ~ 0.1	62 ± 14	27 ± 12	90±2
		f_l ~ 0.2	58 ± 18	33 ± 11	105±2
		f_l ~ 0.3	66 ± 15	37 ± 10	88±2.5
	5% thickness reduction	f_l ~ 0.1	54 ± 16	25 ± 9	101±2
		f_l ~ 0.2	51 ± 11	31 ± 10	112±1.5
		f_l ~ 0.3	55 ± 14	32 ± 10	96±2
	7.5% thickness reduction	f_l ~ 0.1	62 ± 20	32 ± 13	105±1
		f_l ~ 0.2	48 ± 19	26 ± 12	117±2
		f_l ~ 0.3	53 ± 18	27 ± 13	103±2
	10% thickness reduction	f_l ~ 0.1	49 ± 17	29 ± 11	118±2
		f_l ~ 0.2	47 ± 14	30 ± 12	121±2
		f_l ~ 0.3	54 ± 12	26 ± 11	106±2.5
Pre Hot Rolled Al-4.5Cu-5TiB_2	Hot rolled		52±15	28±9	85±1
	2.5% thickness reduction	f_l ~ 0.1	43 ± 16	27 ± 13	95±1
		f_l ~ 0.2	42 ± 18	26 ± 11	106±1
		f_l ~ 0.3	47 ± 20	25 ± 11	88±2.5
	5% thickness reduction	f_l ~ 0.1	42 ± 16	26 ± 11	104±2
		f_l ~ 0.2	41 ± 15	25 ± 12	112±1.5
		f_l ~ 0.3	46 ± 17	24 ± 11	99±2
	7.5% thickness reduction	f_l ~ 0.1	40 ± 15	26 ± 10	110±2.5
		f_l ~ 0.2	39 ± 15	25 ± 11	116±1
		f_l ~ 0.3	45 ± 17	24 ± 09	108±2
	10% thickness reduction	f_l ~ 0.1	47 ± 18	32 ± 13	116±2
		f_l ~ 0.2	43 ± 16	25 ± 11	121±2
		f_l ~ 0.3	45 ± 16	27 ± 12	113±1.5

5.5 HARDNESS EXPERIMENTS FOR MODEL VALIDATION

The experimental details of hardness measurements used for validation of the ANN model have already been described in section 3.9. Each hardness data is generated as an average of 10 readings taken from indentations made at different locations of the specimen surface. Care is taken to see to it that the successive indentations are taken at least at a distance of three times the length of the diagonal of the indentation mark obtained in Vickers indentation. As seen in the map chart of Figure 3.3 in chapter 3, a

total of 5 experiments each were planned for mushy state rolling of Al-4.5Cu-5TiB_2 composite in as cast and pre hot rolled condition, respectively. Thus, a total of 10 samples were taken up for hardness validation experiments.

5.5.1 Hardness measurement of *in situ* Al-4.5Cu-5TiB_2 composite mushy state rolled in as cast condition

Table 5.2 shows the hardness values of mushy state rolled *in situ* Al-4.5Cu-5TiB_2 composite, rolled in as cast condition.

Table 5.2 Vickers hardness (H_V) of *in situ* Al-4.5Cu-5TiB_2 composite rolled in mushy state in as cast condition.

Condition of rolling	Liquid fraction, f_i	Vickers hardness
2% thickness reduction	619^0C ~ 0.17	94±2
6% thickness reduction	598^0C ~ 0.07	89±2.5
6% thickness reduction	619^0C ~ 0.17	114±1
6% thickness reduction	633^0C ~ 0.33	92±1
11.5% thickness reduction	619^0C ~ 0.17	123±1

From Table 5.2, it can be observed that hardness increases with increase in reduction of thickness during mushy state rolling. Furthermore, it is observed that with thickness reduction remaining constant, hardness increases with increase in liquid fraction until 17% liquid fraction and then is seen to decrease beyond that limit. A detailed analysis of the variation of hardness with thickness reduction and liquid fraction based on predictions from the model will be presented in section 5.7.

5.5.2 Hardness measurement of *in situ* Al-4.5Cu-5TiB_2 composite mushy state rolled in pre hot rolled condition

The resulting Vickers hardness values of hardness measurements for *in situ* Al-4.5Cu-5TiB_2 composite rolled in mushy state in pre hot rolled condition for the inputs corresponding to experiments planned for model validation are listed at Table 5.3.

Table 5.3 Vickers hardness (H_V) of *in situ* Al-4.5Cu-5TiB_2 composite rolled in mushy state in pre hot rolled condition.

Condition of rolling	Liquid fraction, f_i	Vickers hardness
2% thickness reduction	619^0C ~ 0.17	102±2.5
6% thickness reduction	598^0C ~ 0.07	101±2
6% thickness reduction	619^0C ~ 0.17	114±1.5
6% thickness reduction	633^0C ~ 0.33	101±1.5
11.5% thickness reduction	619^0C ~ 0.17	122±1.5

The variation of hardness with respect to thickness reduction and volume fraction of liquid in the composite during mushy state rolling of composite in pre hot rolled condition presents a scenario similar to that seen in case of mushy state rolling of as cast composite as can be observed by comparing values of hardness from Table 5.2 and Table 5.3.

5.6 ANN MODEL DEVELOPMENT FOR HARDNESS PREDICTION

In this section, the development of ANN model using FFNN for prediction of hardness for mushy state rolled Al-4.5Cu-5TiB_2 composite rolled in as cast as well as pre hot rolled condition is discussed. As discussed in section 5.1 and also subsequently in section 5.4, the input variables/nodes for the model are taken as initial material state, % thickness reduction, % liquid volume fraction, large and small grain sizes, while the output node of the network is dedicated to hardness.

5.6.1 Neural Network training

As discussed in chapter 4 for grain size description, the ANN was modelled with FFNN architecture. Both single as well as two hidden layers were tried out. Before training the network, both the input as well as the output variables were normalised between values 0.1 to 0.9 using the normalising function given in equation (4.1) of chapter 4. Once the network is trained, all the values acquire their original values provided by the de-normalising function stated at equation (4.2) in chapter 4. Back propagation algorithm was used for training the network. With single hidden layered network (i.e. three layered perceptron network), the network was trained with different values of learning rate parameter (η) and momentum factor (α). The learning was started with 5 hidden nodes, with an initial value of η as 0.1 and with α=0.9. The value of η was increased while that of α was decreased in steps of 0.05 in each subsequent iteration. The MSE which is an indicator of network convergence, discussed earlier in chapter 4 and given by equation (4.3) was set at 0.0001 while the number of epochs (iterations) was fixed at 5 lakhs. With repeated trials involving different values of hidden nodes ranging from 2 to 9, different values of η and α as

well as by changing the order of the input vector presentation to the network, the network failed to converge towards the set MSE. This probably is due to the non linear correlation between the input output relationships of data (Reddy *et al.* 2005). The network was then tried with two hidden layers following the same procedure used for three layered perceptron. The network converged satisfactorily with 5 nodes in the first hidden layer and 3 nodes in the second hidden layer with η=0.5 and α=0.5, with a MSE of 9.76 x 10^{-5} after 3.25 lakh iterations. The sigmoid function in equation (4.4) of chapter 4 used to train the ANN model for grain size predictions is reproduced below as the activation function for training the network:

$$F(x) = \frac{1}{1+e^{-x}} \tag{5.1}$$

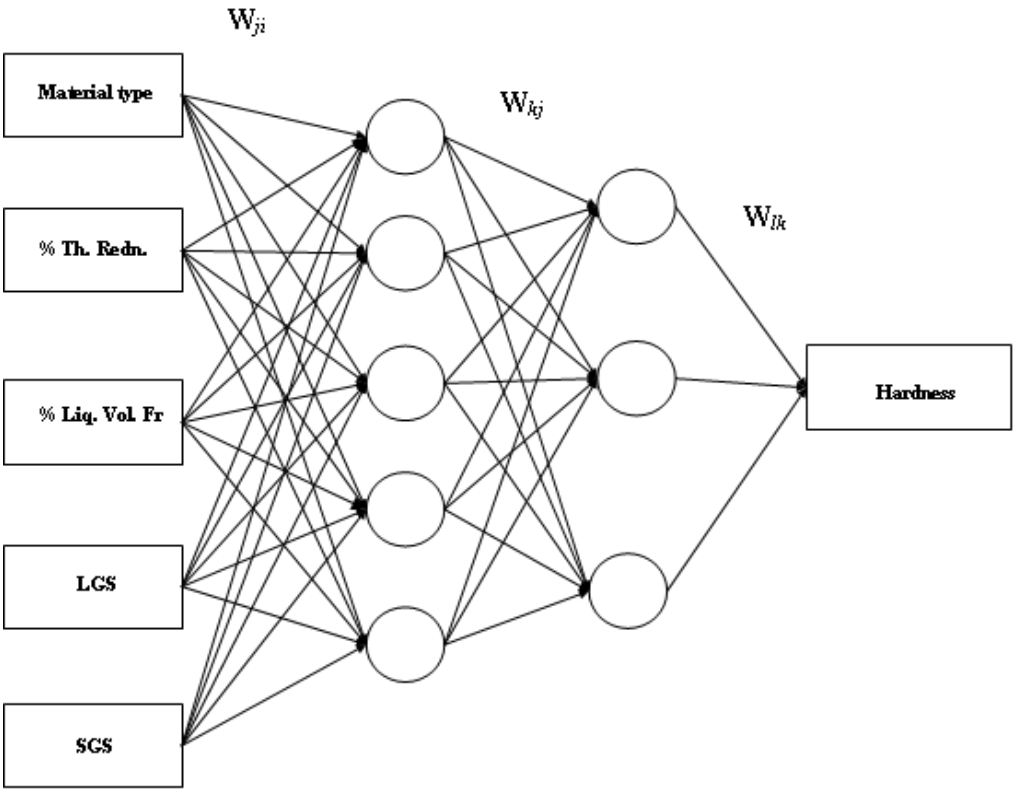

Figure 5. 1 ANN Architecture

5.7 HARDNESS PREDICTION THROUGH ANN MODEL

Table 5.4 and Table 5.5 respectively provide the values of hardness predicted by the trained ANN model for mushy state rolled Al-4.5Cu-5TiB_2 composite, rolled in as

cast and pre hot rolled state, respectively, to a thickness reduction ranging from 2 to 12.5% and liquid volume fraction ranging from 5 to 35%. The table lists the values predicted by the model for the training data represented by superscript [a], while the validation data within training data range is represented by the superscript [*] while that outside the range is represented by superscript [**].

5.7.1 Comparison of hardness obtained by experimentation and prediction by ANN model

5.7.1.1 Rolling of as cast Al-4.5(wt.%)Cu-5(wt.%)TiB_2 composite in mushy state

The values of hardness obtained by experimentation (Herbert 2007) and those predicted by the trained ANN model are presented in Table 5.4. The percentage error in prediction by the ANN model, as can be seen from the Table 5.4, is between -2.436% and +2.6323%, which is very much within the acceptable limits of accuracy for any prediction system. Further, the hardness of cast composite obtained experimentally is $78H_V$. While using the ANN model, the hardness value for the as cast composite is obtained by using zeros as inputs for % thickness reduction and % liquid volume fractions in the model. The value so predicted by ANN model is 77.66 H_V resulting in an error of 0.4359% over experimental result.

Kusiak & Kuziak (2002) have reported a maximum percentage error of 8% in prediction of ultimate tensile and yield strength of steel, while Mandal *et al.* (2009) have reported a Gaussian distribution of percentage error of prediction within ±10% in prediction of flow stress using Resilient Propagation algorithm which has been reported to perform better than Back Propagation algorithm. Selvakumar *et al.* (2007) have reported a maximum error of 5% in the prediction of axial stress, hoop stress , hydrostatic stress and the axial strain in their work on modelling the effect of particle size and iron content on forming of Al-Fe preforms using ANN. Considering that the network has been trained with experimental values between 10% to 30% liquid volume fraction and rolling with 2.5% to 10% thickness reduction, a percentage error of 2.6323% within and 1.4234% outside the range of training data values is quite reasonable.

Table 5.4 Comparison of Experimental values of Hardness of as cast Al-4.5Cu-5TiB_2 composite samples subjected to mushy state rolling with ANN predicted values.

Specimen descriptions		Experimental			ANN	%Error
		Grain size (µm)		Hardness (Hv)	Hardness (Hv)	Hardness
		Large	Small			
As cast		50		78	77.66	0.436
**2% thickness reduction	*f_l~ 0.17	63	30	94	92.662	1.4234
2.5% thickness reduction	f_l ~ 0.05	--	--	--	83.212	--
	[a] f_l ~ 0.1	62	27	90	87.89	2.3444
	[a] f_l ~ 0.2	58	33	105	105.45	-0.4286
	[a] f_l ~ 0.3	66	37	88	90.144	-2.4364
	f_l ~ 0.35	--	--	--	97.32	--
5% thickness reduction	f_l ~ 0.05	--	--	--	83.4	--
	[a] f_l ~ 0.1	54	25	101	100.13	0.8614
	[a] f_l ~ 0.2	51	31	112	112.28	-0.25
	[a] f_l ~ 0.3	55	32	96	93.473	2.6323
	f_l ~ 0.35	--	--	--	99.702	--
* 6% thickness reduction	** f_l ~ 0.07	66	29	89	88.22	0.8764
	* f_l ~0.17	49	26	114	112.18	1.5965
	** f_l~0.33	55	28	92	92.431	-0.4685
7.5% thickness reduction	f_l ~ 0.05	--	--	--	83.397	--
	[a] f_l ~ 0.1	62	32	105	104.63	0.3524
	[a] f_l ~ 0.2	48	26	117	116.31	0.5897
	[a] f_l ~ 0.3	53	27	103	101.05	1.8932
	f_l ~ 0.35	--	--	--	105.29	--
10% thickness reduction	f_l ~ 0.05	--	--	--	109.62	--
	[a] f_l ~ 0.1	49	29	118	117.15	0.7203
	[a] f_l ~ 0.2	47	30	121	121.14	-0.1157
	[a] f_l ~ 0.3	54	26	106	104.63	1.2925
	f_l ~ 0.35	--	--	--	111.73	--
**11.5% thickness reduction	** f_l ~ 0.17	46	30	123	122.4	0.4878
12.5% thickness reduction	f_l ~ 0.05	--	--	--	117.79	--
	f_l ~ 0.1	--	--	--	121.72	--
	f_l ~ 0.2	--	--	--	122.86	--
	f_l ~ 0.3	--	--	--	102.3	--
	f_l ~ 0.35	--	--	--	103.73	--

* Validation experiments carried out in the present study within the range of training data.

** Validation experiments carried out in the present study outside the range of training data.

[a] Experimental data.

Table 5.5 Comparison of Experimental values hardness for pre hot rolled Al-4.5Cu-5TiB_2 composite samples subjected to mushy state rolling with ANN predicted values.

Specimen descriptions		Experimental			ANN	%Error
		Grain size (μm)		Hardness (Hv)	Hardness (Hv)	Hardness
		Large	Small			
Hot rolling		52	28	85	85.264	-0.31
**2% thickness reduction	** f_l ~0.17	43	25	102	103.49	-1.461
2.5% thickness reduction	f_l ~ 0.05	--------	--------	--------	90.7	--------
	[a] f_l ~ 0.1	43	27	95	95.93	-0.9789
	[a] f_l ~ 0.2	42	26	106	105.01	0.934
	[a] f_l ~ 0.3	47	25	88	88.114	-0.1295
	f_l ~ 0.35	--------	--------	--------	96.338	--------
5% thickness reduction	f_l ~ 0.05	--------	--------	--------	94.764	--------
	[a] f_l ~ 0.1	42	26	104	102.21	1.7212
	[a] f_l ~ 0.2	41	25	112	111.92	0.0714
	[a] f_l ~ 0.3	46	24	99	100.15	-1.1616
	f_l ~ 0.35	--------	--------	--------	105.59	--------
*6% thickness reduction	** f_l~0.07	41	26	101	99.724	1.2634
	* f_l ~ 0.17	40	26	114	115.57	-1.3772
	** f_l~ 0.33	46	24	101	103.3	-2.2772
7.5% thickness reduction	f_l ~ 0.05	--------	--------	--------	99.646	--------
	[a] f_l ~ 0.1	40	26	110	110.33	-0.3
	[a] f_l ~ 0.2	39	25	116	117.27	-1.0948
	[a] f_l ~ 0.3	45	24	108	108.12	-0.1111
	f_l ~ 0.35	--------	--------	--------	111.7	--------
10% thickness reduction	f_l ~ 0.05	--------	--------	--------	107.83	--------
	[a] f_l ~ 0.1	47	32	116	116.44	-0.3793
	[a] f_l ~ 0.2	43	25	121	120.44	0.4628
	[a] f_l ~ 0.3	45	27	113	112.35	0.5752
	f_l ~ 0.35	--------	--------	--------	114.51	--------
**11.5% thickness reduction	** f_l~0.17	46	30	[122]	122.31	-0.2541
12.5% thickness reduction	f_l ~ 0.05	--------	--------	--------	115.95	--------
	f_l ~ 0.1	--------	--------	--------	121.18	--------
	f_l ~ 0.2	--------	--------	--------	123.06	--------
	f_l ~ 0.3	--------	--------	--------	112.64	--------
	f_l ~ 0.35	--------	--------	--------	113.9	--------

[*] Validation experiments carried out in the present study within the range of training data.

[**] Validation experiments carried out in the present study outside the range of training data.

[a] Experimental data.

This suggests that the ANN model is quite capable of extrapolating the grain sizes and hardness of the composite beyond 10% & below 2.5% thickness reduction and beyond 30% liquid volume fraction and below 10% liquid volume fraction respectively, when as cast Al-4.5Cu-5TiB_2 composite is rolled in mushy state. One of the prime objectives of the present study is to obtain the optimised values of thickness reduction per roll pass and volume fraction of liquid in the composite that provides a maximum value of hardness. It is desirable to know the conditions leading to maximum hardness since hardness is a measure not only of strength but also of wear properties of the composite. To achieve the optimised mushy state rolling parameters for maximum hardness, a small optimisation code was written in the front end designed for ANN and RNN model in the present study. The code written in C++ (included at APPENDIX II) is interfaced with Microsoft Silver light software, which is a web based application, to provide hardness by continuous variation of one input parameter selected at a time, with the help of slider button provided on the screen. By alternately varying the % thickness reduction from 2 to 12.5% and liquid volume fraction from 5 to 35%, the maximum hardness was recorded for data within and outside the training range of the model. Table 5.6 shows the maximum value of hardness predicted by the ANN model within the training range as 121.324 H_V corresponding to 19% liquid volume fraction at 10% thickness reduction. The maximum value of hardness predicted by the model is 123.1 H_V corresponding to 17.4% liquid volume fraction at 12.5% thickness reduction for the entire range of study carried out i.e. rolling at mushy state temperatures corresponding to 5% liquid volume fraction to 35% liquid volume fraction at various thickness reductions ranging from 2 % thickness reduction to 12.5% thickness reduction. Figure 5.2 shows a screen capture at an instance when the hardness of the as cast composite is 121.3 H_V.

The comparison of ANN predicted values of hardness with the values obtained from validation experiments reveals errors in prediction within |1.43%|, as seen from Table 5.4. This vindicates the generalisation of hardness relationship of the composite, mushy state rolled in as cast state, to 2 to 12.5% thickness reduction and with 5 to 35% volume fraction of liquid in composite.

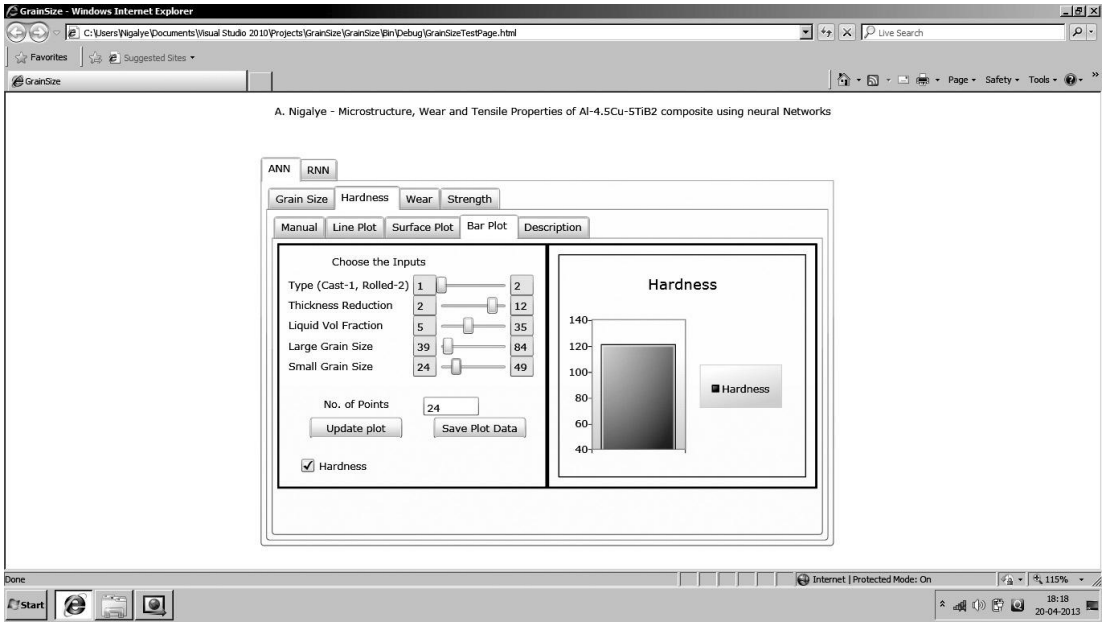

Figure 5.2 Screen capture of GUI designed for ANN model.

Table 5.6 Optimal values of Grain size and Hardness as predicted by ANN for as cast Al-4.5Cu-5TiB2 composite samples subjected to mushy state rolling with ANN predicted values.

Description of Mushy State Rolled Composite		ANN Predicted Values of		
		Grain Size (μm)		Hardness (Hv)
		Large	Small	
10% thickness reduction	19% liquid volume fraction	48.3	30.5	121.3
12.5% thickness reduction	17.4% liquid volume fraction	46.8	30.4	123.1

It can be seen from Table 5.4 and Figure 5.3 and Figure 5.4 that hardness of the composite increases with increase in thickness reduction. Also from Table 5.4 and Figure 5.5 it is observed that from 2.5% thickness reduction to 10% thickness reduction, the variation of hardness is much more when the as cast composite is rolled in mushy state corresponding to 10% liquid volume fraction as compared to that at 20% liquid volume fraction, with the variation in the former being 50%, more than that in case of latter. Further it is seen from experimental values in Table 5.4, that for a particular thickness reduction, hardness increases up to 20% liquid volume fraction and then decreases. But the ANN model predicts that hardness at a particular thickness reduction increases up to 19% liquid volume fraction and then gradually

decreases until the liquid volume fraction is increased to 35%. The optimal values of hardness for corresponding grain sizes as predicted by ANN for as cast Al-4.5Cu-5TiB_2 composite samples subjected to mushy state rolling are tabulated in Table 5.6. This variation in the result by ANN model is a consequence of training data used from the experimentations which were being carried out only at discrete values i.e.at 10%, 20% and 30% liquid volume fractions.

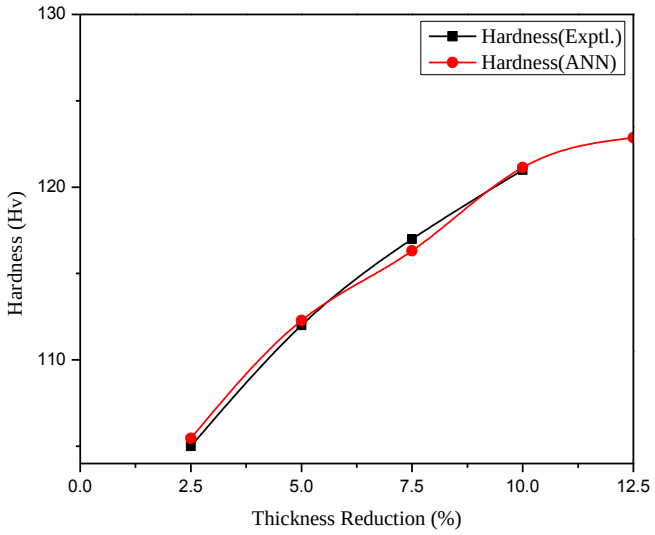

Figure 5.3 Plot showing comparison of variation of experimental values of hardness with ANN predictions at varied % thickness reduction when as cast Al-4.5Cu-5TiB_2 containing 20% liquid volume fraction composite is rolled in-mushy state.

Figure 5.3 shows the plot depicting the variation of hardness with thickness reduction at a constant volume percent of liquid of 20%, for values obtained experimentally and those predicted by ANN model. The values, as can be seen from the plot match very closely. It is also observed that the hardness increases with increasing thickness reduction, at a given liquid volume fraction of 20%. There are two phenomena which take place simultaneously, when the composite is rolled in mushy state. First one is due to rolling work hardening taking place in the composite because of induced plastic strains (Herbert *et al.* 2006, Herbert 2007). Secondly, since the temperatures involved during mushy state forming are above recrystallization temperature, the time elapsed in rolling operation in the recrystallization temperature zone allows for grain

growth which tends to reduce hardness (Aikin1997, Herbert *et al.* 2006, Herbert 2007). At 20% liquid volume fraction, as seen from Figure 4.12 in chapter 4, it is observed that the grain sizes for both coarse and small grain sizes decrease slightly with increase in % thickness reduction. The smaller average grain size results in increased hardness. As can be observed from the plots shown in Figure 5.3, the hardness of the composite increases continuously with increase in % thickness reduction initially due to decrease in average grain size and secondly due to strain induced work hardening. Also the increased reduction in thickness increases the rate of escape of liquid from inter granular regions of un-melted α–Al grains to the surface, which cools faster and inhibits grain growth, yielding finer grains. Grain fragmentation associated with high thickness reduction also causes decrease in large grain size. This consequently increases the hardness (Aikin 1997, Herbert *et al.* 2006, Herbert 2007).

Plots in Figure 5.4 show the variation of experimental values with ANN predicted values of hardness when as cast Al-4.5Cu-5TiB_2 composite is rolled in mushy state containing 30% liquid volume fraction to various thickness reductions. Referring back to Figure 4.10 in chapter 4, it is seen that the average grain sizes decrease up to 7.5% thickness reduction and then increase marginally beyond, up to 10% thickness reduction when composite is rolled with 35% liquid volume fraction in mushy state. Consequently, it can be seen from Figure 5.4 that the hardness increases quite steeply up to 10% thickness reduction and then the rate of increase decreases marginally. The average decrease in grain size up to 7.5% thickness reduction and consequent increase in hardness can be attributed to the effect of work hardening, grain boundary pinning, compressive stresses resulting in squeezing of liquid from inter granular spaces to the surface, overriding the effect of grain growth (Aikin 1997, Herbert *et al.* 2006, Herbert 2007).

However, beyond 10% thickness reduction, the average grain size increases (due to higher contribution in size due to small grains) resulting in lowering of hardness, which can be seen from the plot in Figure 5.4. This invariably, may be due to the greater sliding of liquid through the inter-granular spaces of un-melted α–Al grains at higher temperature, greater than corresponding to 30% liquid volume fraction in

mushy state. The lower viscosity decreases the effect of grain boundary pinning by TiB_2 as % thickness reduction increases (Aikin1997), thereby causing grain growth.

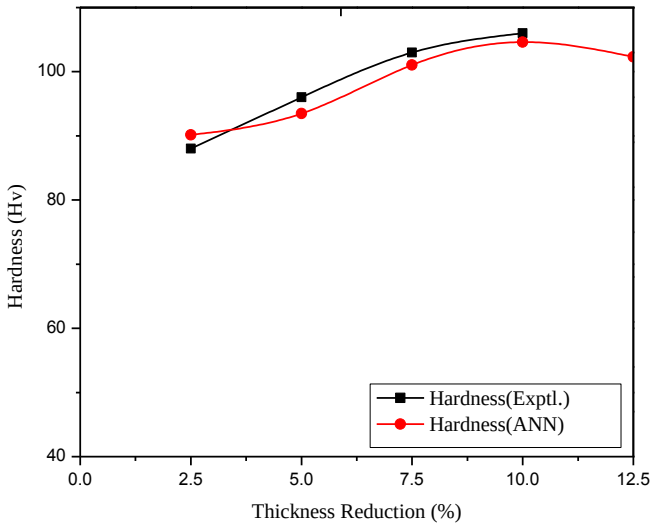

Figure 5.4 Plot showing comparison of variation of experimental values of hardness with ANN predictions at varied % thickness reduction when as cast Al-4.5Cu-5TiB_2 composite containing 30% liquid volume fraction is rolled in mushy state.

Graph plotted in Figure 5.5 shows variation of hardness obtained experimentally for 10%, 20% and 30% liquid volume fraction and that obtained from ANN computations for 5%, 10%, 20%, 30% and 35% liquid volume fractions at varying % thickness reductions. It can be seen that in both the cases of experiment and ANN predictions, the hardness value increases steeply with increase in thickness reduction, for 10% liquid volume fractions, compared to those cases with higher liquid content, as the unmelted α-Al grains are more likely to touch one another, and the work hardening of unmelted grains causes increase in hardness. With increase in % liquid volume fractions from 10 to 20%, the hardness values are observed to increase. But with higher % liquid volume fractions namely at 30% liquid volume fractions, the hardness falls. In all cases i.e. 10%, 20% and 30% liquid volume fractions, it is seen that the maximum hardness is obtained at 20% liquid volume fractions.

The reduction in values of hardness at higher liquid volume fractions is quite expected, as greater amount of fluidity associated with higher liquid content in mushy state (Aikin 1997), over rides the effect of work hardening. In addition at higher temperature, strain accommodation by intergranular liquid lowers degree of deformation of solid skeleton. This decreases the rate of work hardening rate significantly (Herbert *et al.* 2006, Herbert 2007). Figure 5.6 shows the variation of hardness in the form of the plot generated by the ANN model. It can be seen that the maximum hardness occurs at around 19% liquid volume fractions when rolled at a thickness reduction of 10%.

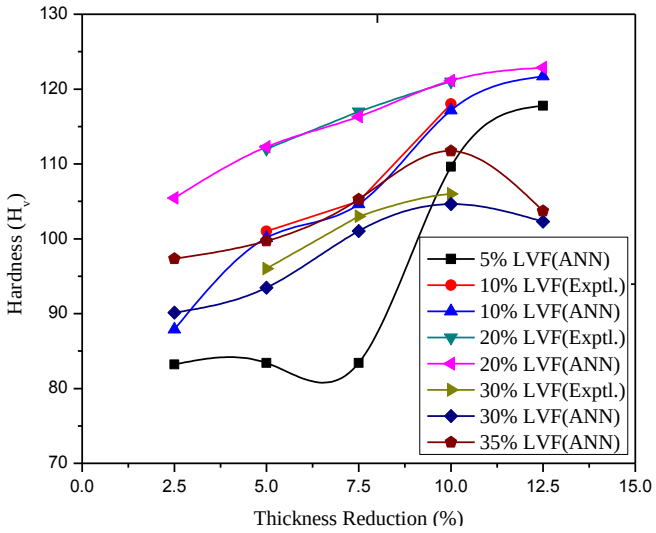

Figure 5.5 Plot showing the variation of hardness with thickness reduction at different volumes of liquid fraction for Al-4.5Cu-5TiB2 composite, mushy state rolled in as cast state.

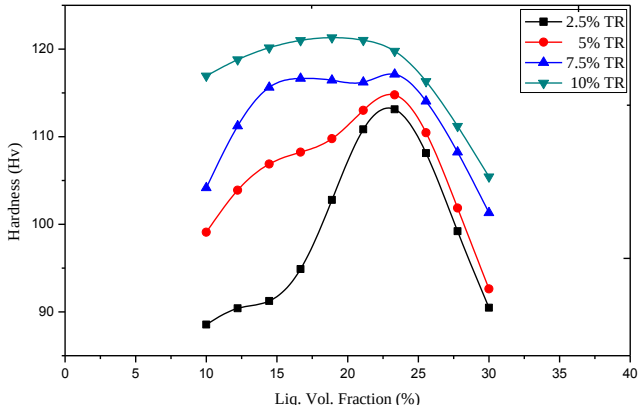

Figure 5.6 Graph showing the variation of hardness for as cast Al-4.5Cu-5TiB_2 composite rolled in mushy state to various thickness reductions (TR) with different volume fractions of liquid.

Figure 5.7 shows the contour graph of the distribution of hardness for as cast composite with variations in % thickness reduction and % liquid volume fractions. From the contour plot of Figure 4.19(b) in chapter 4, it is observed that low values of small grain size are concentrated in the region between 2.5% and 7.5% thickness reduction and 5% and 12.5% liquid volume fractions, while higher values are concentrated near 2.5% thickness reduction and 35% liquid volume fraction and also near 7.5% thickness reduction and low values of liquid volume fraction. Higher values of large grain size near 7.5% thickness reduction and 5% liquid volume fraction and lower values in higher % thickness reduction and medium values of % liquid volume fractions are also seen in Figure 4.19(a) discussed in chapter 4. The higher values of hardness seen from plot 5.7 are therefore obtained for mushy state rolling with high % thickness reduction and 5 - 25% liquid volume fractions.

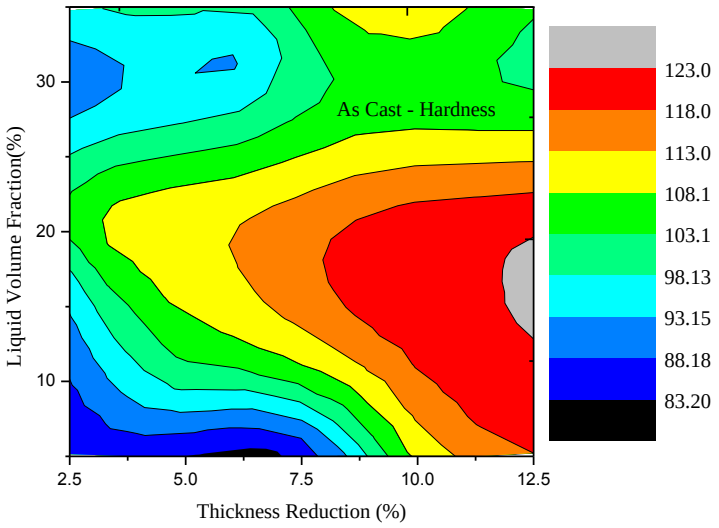

Figure 5.7 Contour maps showing Hardness Spectrum when as cast Al-4.5Cu-5TiB_2 composite is rolled from mushy state to different thickness reductions with various liquid fractions.

5.7.1.2 Rolling of pre hot rolled Al-4.5(wt. %)Cu-5(wt. %)TiB_2 composite in mushy state

The behaviour of pre hot rolled composite shows similar pattern as discussed in the previous section. The only difference being slight change in the individual values at various % thickness reduction corresponding to various % liquid volume fractions, as

seen from Table 5.1 and 5.2. Table 5.2 indicates that the % error in prediction of hardness by ANN ranges between -1.1616% at 5% thickness reduction and 30% liquid volume fractions and + 1.7212% at 5% thickness reduction at 10% liquid volume fractions. This variation is over the entire range of experimentally obtained results. The hardness predicted by the model for hot rolled composite is 85.264 H_v as against the experimental value of 85 H_v resulting in prediction error of -0.31%.

This suggests that the ANN model has learnt the input output relationships and has exhibited good generalization to predict hardness of the pre hot rolled Al-4.5 (wt. %)Cu-5(wt. %) TiB_2 composite rolled in mushy state.

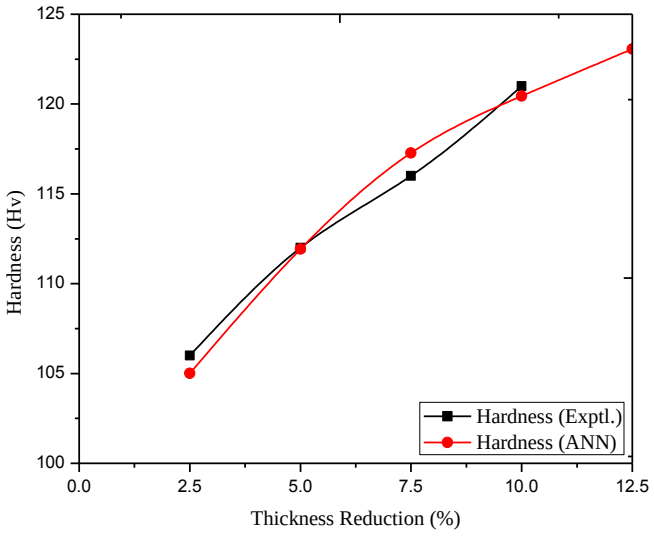

Figure 5.8 Plots showing comparison of variation of experimental values of hardness with change in % thickness reduction when pre-hot rolled Al-4.5Cu-5TiB_2 composite containing 20% liquid volume fraction is rolled from mushy state, with that predicted by ANN.

The error in prediction of hardness by the ANN model as against the values determined in experiments conducted for validation of the model lies within |2.28%|. The prediction error of |2.2772|% occurs at 6% thickness reduction and 33% liquid volume fraction, which is a case of input data lying outside the data used for training the network. This confirms that the predictions done by the model not only stand validated within the entire range of model predictions done by the model but also possesses the capability to extrapolate the mushy state rolling process.

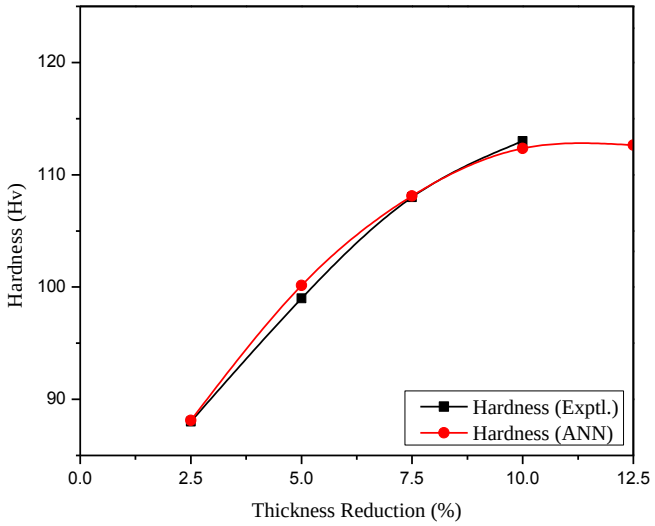

Figure 5.9 Plots showing comparison of variation of experimental values of hardness with change in % thickness reduction when pre-hot rolled Al-4.5Cu-5TiB_2 composite containing 30% liquid volume fraction is rolled from mushy state, with that predicted by ANN.

Figure 5.8 and 5.9 show the variation of hardness of the pre-hot rolled composite rolled in mushy state with % liquid volume fractions of 20% and 30%, respectively. The plots are similar to those seen in Figure 5.3 and 5.4 for as cast Al-4.5Cu-5TiB_2 composite, with similar reasoning for variation in hardness.

Table 5.7 shows the maximum hardness values and the corresponding grain sizes predicted by ANN model for pre hot rolled Al-4.5Cu-5TiB_2 composite samples subjected to mushy state rolling. As noticed from Table 5.7, within the range of experimentation, between 10% to 30% liquid volume fractions and 2.5% to 10% thickness reduction, the maximum hardness of 120.9 H_V is predicted by ANN model for mushy state rolling with 18% liquid volume fraction causing 10% thickness reduction. The model also predicts a maximum hardness of 123.1 H_V at 18.6% liquid volume fractions and 12.5% thickness reduction. Figure 5.10 shows, the variation of hardness for pre-hot rolled Al-4.5Cu-5TiB_2 composite rolled in mushy state with thickness reduction between 2.5% and 12.5% at various liquid volume fractions. As expected, this plot is similar to Figure 5.5. As discussed in the previous section,

reduction in hardness is expected for mushy state rolling at higher values of % liquid volume fractions.

TABLE 5.7 Optimal values of Grain size and Hardness as predicted by ANN for pre hot rolled Al-4.5Cu-5TiB$_2$ composite samples subjected to mushy state rolling.

Description of Mushy State Rolled Composite		ANN Predicted Values of		
		Grain size (µm)		Hardness (Hv)
		Large	Small	
10% thickness reduction	18% Liquid volume fraction	43.261	27.4832	120.9
12.5% thickness reduction	18.6% liquid volume fraction	46.6982	30.4346	123.1

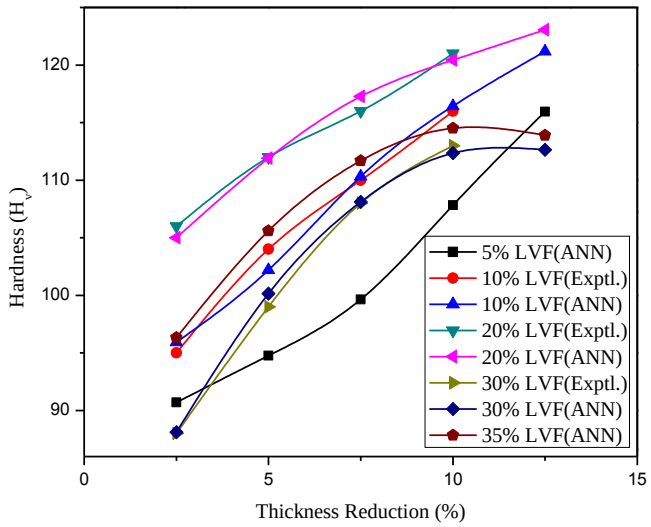

Figure 5.10 Plot showing the variation of hardness with thickness reduction at different % volume fractions of liquid (LVF) for pre hot rolled Al-4.5Cu-5TiB2 composite rolled in mushy state.

Figure 5.11 plots the variation of hardness based on the ANN model within the range of experimentation, with maximum value of hardness of 120.9 H_V occurring at 18% liquid volume fractions and 10% thickness reduction. Figure 5.12 shows the contour plot generated for hardness variation, with respect to thickness reduction per pass during mushy state rolling of pre hot rolled composite and volume fraction of liquid in the composite at the initiation of rolling. It can be seen that as compared to the contour plot in Figure 5.7 for as cast composite, this plot provides a larger region depicting higher values of hardness.

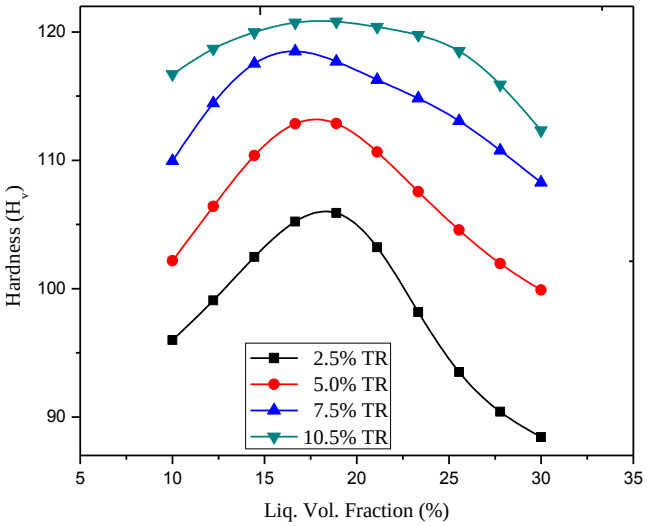

Figure 5.11 Graph showing the variation of ANN predicted values of hardness for pre hot rolled Al-4.5Cu-5TiB_2 composite rolled from mushy state to various Thickness Reductions (TR) with different percent volume of liquid in the composite.

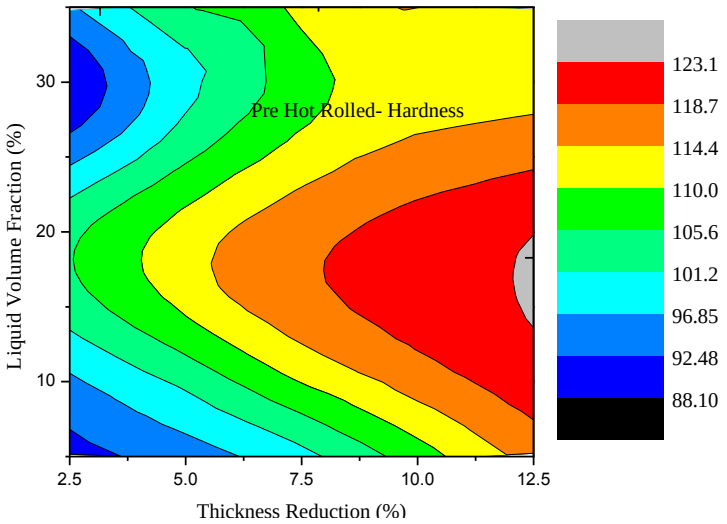

Figure 5.12 Contour maps showing hardness spectrum when pre hot rolled Al-4.5Cu-5TiB_2 composite is rolled from mushy state to different thickness reductions with different liquid volume fractions.

5.8 PARAMETRIC STUDY

5.8.1 Variation of hardness of mushy state rolled composite with respect to thickness reduction at given liquid fraction.

Figure 5.13 shows the plots depicting the variation of hardness, predicted by ANN model, with thickness reduction at a constant liquid fraction of 20%. It is observed that the hardness increases with increasing thickness reduction during mushy state rolling with liquid volume fraction of 20%. There are two mechanisms operating simultaneously during mushy state rolling of the composite: work hardening caused by plastic deformation of unmelted grains, and coarsening of the unmelted grains due to applied stress and increased mass transport in presence of liquid phase (Herbert *et al.* 2006, Herbert 2007). Whereas the hardness is increased due to work hardening, it is expected to decrease due to grain growth. On mushy state rolling with 20% liquid volume fraction, as seen from in Table 4.4 of chapter 4, the grain sizes for both coarse and small grain sizes decrease slightly with increase in % thickness reduction, and therefore hardness is increased. As can be observed from the plots shown in Figure 5.13, the hardness of the composite increases continuously with increase in % thickness reduction due to the plastic strain induced work hardening.

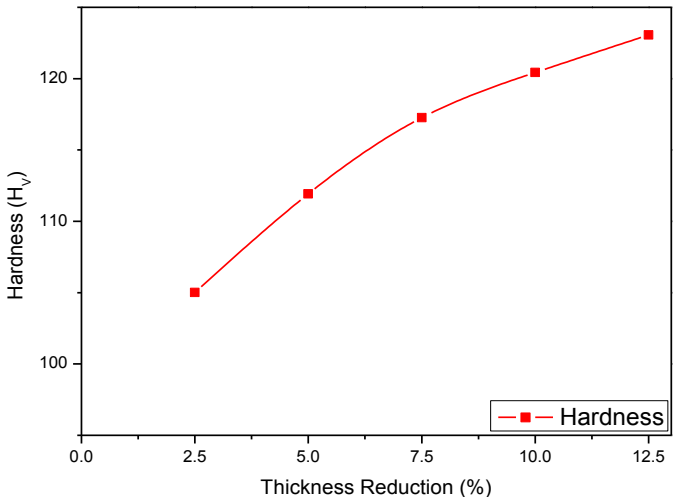

Figure 5.13 Plot showing variation of hardness predicted by ANN at varied % thickness reduction when as cast Al-4.5Cu-5TiB_2 composite is rolled in mushy state with 20% liquid volume fraction.

5.9 SUMMARY

1. The ANN model for prediction of hardness of Al-4.5Cu-5TiB_2 composite rolled in mushy state in as cast and Prehot rolled condition was successfully formulated. Within the data used for training the model, the values of hardness predicted by the ANN model proposed give an error less than |2.65%| and |1.8%| for as cast and pre hot rolled Al – 4.5Cu- 5TiB_2 composite respectively rolled in mushy state, with thickness reduction in the range from 2.5% to 10% per pass and % liquid volume fraction in the mushy state varying from 10% to 30%. Therefore, the model characterizes the process of mushy state rolling very well within the reasonable limits in this range and therefore can be used as an alternative to tedious, costly and time consuming experimentation. Further, within the range of data used to train the model, the ANN model reveals that the hardness of the mushy state rolled composite containing any liquid volume fraction shows highest value for a thickness reduction of 10% per roll pass, both in case of as cast as well as pre hot rolled composite.

2. It can be concluded that the ANN model proposed for predicting hardness can extrapolate hardness values beyond the experimental range, which is proved by a small error of |1.43|% in prediction by ANN in case of cast composite and less than |2.3|% in case of pre hot rolled composite. Thus, the model can characterize effectively, with a very low degree of variation, the mushy state rolling of as cast as well as pre-hot rolled Al – 4.5 Cu -5TiB_2 composite with liquid content varying from 5 to 35% and thickness reduction per pass varying from 2% to 12.5%.

3. The study of variation of hardness of mushy state composite predicted by ANN model within the range of data used to train the model (i.e. experimental range), with reduction in thickness per roll pass at a given liquid volume fraction indicates that the highest hardness values for any thickness reduction are obtained for a liquid volume fraction of 20%. This information along with the conclusion at point 1 above indicates that the highest value of hardness of the composite lies somewhere in the range of 10% thickness reduction and

20% liquid volume fraction, for both as cast as well as pre hot rolled composite rolled in mushy state. This conclusion can also be arrived by the study of contour plots shown in Figure 5.7 and Figure 5.12.

4. The experimental values show the maximum hardness for mushy state rolling causing all thickness reductions with 20% liquid volume fraction, while the maximum hardness depicted by the ANN model in experimental range is 121.3 H_V at 19% liquid volume fraction and 10% thickness reduction for as cast composite and 120.9 H_V at 18 % liquid volume fraction and 10% thickness reduction for pre hot rolled composite.
5. The maximum hardness predicted for the mushy state rolled composite by the ANN model for entire range with 2 to 12.5% thickness reduction and with 5 to 35% liquid volume fractions is 123.1 H_V at 17.4% liquid volume fraction and 12.5% thickness reduction for as cast composite. For pre hot rolled composite, for the corresponding range, the maximum value of hardness predicted is 123.116 H_V when composite containing 18.6% liquid volume fraction is mushy state rolled to 12.5% thickness reduction per pass.
6. The errors in prediction of hardness by ANN model compared with the hardness values obtained from experiments carried out for validation of model are within |2.28%|. This ensures that the generalisation of relationship of hardness variation with respect to thickness reduction, mushy state of the composite and initial material state of composite rolled in mushy is validated within an error of |2.28%|.

Chapter 6

RESULTS AND DISCUSSION (PART III)
ANN MODELLING FOR PREDICTION OF TENSILE PROPERTIES

6.1 INTRODUCTION

In the previous chapter, the details of ANN modelling and prediction of hardness of Al-4.5Cu-5TiB_2 composite were presented. The predictions from the validated model were used to analyse the variation of hardness with the mushy state rolling parameters. Along with hardness, which is a very important property in any engineering application, strength and ductility too are equally important. The determinants of the strength of the material obviously have its roots related to grain morphology. Grain morphology, in turn can be affected to ones requirement by subjecting the material to pre treatment, including conventional hot working in case of conventional materials. However, as we have seen in chapter 2, literature survey indicates that MMCs do not offer themselves conveniently to traditional methods of forming. Mushy state rolling of Al-4.5Cu-5TiB_2 composite led to bimodal grain distribution (Herbert *et al.* 2006, Herbert 2007). Investigation of tensile properties of Al-4.5Cu-5TiB_2 composite was carried out by Herbert (2007). Since the mushy state rolled composite led to duplex grain size distribution, it would be of interest to possess knowledge about the variation of tensile properties with respect to mushy state rolling parameters. It is seen from previous work (Herbert *et al.* 2010, Herbert 2007), that the tensile properties of the composite are a function of mushy state rolling parameters as well as grain sizes and hardness, leading to a complex and non linear relationship between input and output parameters. The use of ANNs is known to map complex and non linear input output relationships. ANN can therefore be used as a system to predict these properties of the composites. Once it has been trained, it understands the subtle and underlying relationships of tensile properties with mushy

state rolling parameters, hardness and the grain morphology of the mushy state rolled composite. The data on the tensile properties of Al-4.5Cu-5TiB_2 composite being inadequate, the present work has also considered the published data (Herbert 2007) on tensile properties of Al-4.5Cu alloy. The present chapter deals with the ANN modelling for prediction of tensile properties viz. yield strength, ultimate tensile strength and percentage elongation of mushy state rolled Al-4.5Cu-5TiB_2 composite as well as Al-4.5Cu alloy.

6.2 SCOPE

The tensile properties (Ultimate Tensile Strength, Yield Strength and percentage elongation) of mushy state rolled Al-4.5Cu-5TiB_2 composite depend on the initial material state, % thickness reduction, % liquid volume fraction, large and small grain sizes, %TiB_2 and hardness of the composite. Therefore the relationship between inputs and outputs is quite complex apart from being non linear. Hence, it is proposed to formulate the Artificial Neural Network model with Feed Forward architecture to predict the tensile properties which include, yield strength, ultimate strength and elongation of Al-4.5Cu-5TiB_2 composite rolled in mushy state in as cast as well as pre hot rolled condition with the input parameters being, % thickness reduction, % volume fraction of liquid, large and small grain sizes, hardness and the % wt. content of TiB_2 (which is fixed as 5%) in the composite. The present work describes the development of the ANN model with following:

(a) The analysis of the effect Initial state of composite material during mushy state rolling (as cast or pre hot rolled) on yield strength, ultimate tensile strength and elongation of Al-4.5Cu-5TiB_2 composite mushy state rolled in as cast as well as pre hot rolled state.

(b) The analysis of effect of thickness reduction during mushy state rolling and mushy state condition when rolling is initiated.

(c) Interpolate and thereby expand the data on tensile properties of mushy state rolled composite for a wider range of thickness reductions and liquid volume fractions in the composite.

6.3 TENSILE PROPERTIES

The yield strength, ultimate tensile strength and elongation until failure are important properties of the material from the view of applications in structural engineering. The tensile properties are a function of the microstructure as well as flaws present in the material. The following tensile properties of interest are considered in this section:

6.3.1 Strength

6.3.1.1 Yield strength (YS)

It is defined as the stress at which the material starts deviating from the straight line relationship on the stress strain curve. In case of structural steel, the yield point is obvious. However in case of non ferrous materials, since the yielding is not obvious, 0.2% proof stress is considered as yield stress and is denoted as 0.2% yield stress. (Dieter 1986). The data taken in the present development of model refers to the 0.2% yield strength of Al-Cu alloy and Al-4.5Cu-5TiB_2 composite.

6.3.1.2 Ultimate tensile strength (UTS)

This refers to the maximum strength resisted by the material before undergoing failure by breaking and as in case of yield strength, is expressed in MPa (Dieter 1986).

6.3.1.3 Percentage (pct) elongation

Percentage elongation is the elongation to failure expressed as a fraction of the original length of the specimen tested in tension test. It is a measure of the ductile properties of the material and therefore is an important property from material formability point of view (Dieter 1986).

6.4 DATA COLLECTION

The data for developing ANN model for prediction of tensile properties has been taken from previous work done on studies of mushy state rolling of Al-Cu alloy and Al-4.5Cu-5TiB_2 composite (Herbert 2007). The tensile properties being dependent on

grain morphology, grain sizes have been adopted as input parameters for the model, in addition to initial state of material (as cast or pre hot rolled), thickness reduction during mushy state rolling and volume fraction of liquid in composite, which are the mushy state rolling parameters. Hardness of the material is related to the tensile properties of the material and therefore has also been considered as input parameter. In addition, the fixed weight percentage of TiB_2 (5%) is considered as an input parameter to the model. The tensile testing (Herbert *et al.* 2010, Herbert 2007) on the specimens prepared from Al-4.5Cu alloy and Al-4.5Cu-5TiB_2 composite rolled in mushy state were carried out on a Hounsfeld Material Testing Machine (Model: THE/S-Series H10KS/05, England) fitted with a non contacting type Laser Extensometer (Model: 500LC, Tenius Olsen Ltd., England) for measurement of elongation. Table 6.1 (Herbert 2007) shows the details of the testing conducted on the alloy and the composites.

Table 6.1 Tensile testing details of mushy state rolled alloy and composite (Herbert2007).

Material	Mushy state rolling parameters		Crosshead speed (mm/min)
	Thickness reduction (%)	Liquid content (%)	
Al-4.5Cu alloy	0 (as cast), 2.5, 5	30	3.8
As cast Al-4.5Cu-5TiB_2	0 (as cast), 2.5, 5	30	
Pre-hot rolled Al-4.5Cu-5TiB_2	5	10,20,30	

The data relating to tensile properties and considered for training the model is presented in Table 6.2. From Table 6.2, it can be seen that, in general, the yield and the ultimate tensile strength as well as pct elongation exhibited by the mushy state rolled Al-4.5Cu alloy are much lower than that exhibited by Al-4.5Cu-5TiB_2 composite with the lowest value recorded for alloy mushy state rolled to 5 pct thickness reduction with 30 pct liquid content. The composite recorded much higher values with the maximum strength exhibited by as cast composite rolled to 5 pct thickness reduction with 30 pct liquid content. The highest ductility was reported with pre hot rolled composite containing 30 pct liquid content mushy state rolled to 5 pct thickness reduction.

Table 6.2 Table showing the Tensile properties of as cast Al-4.5Cu alloy and Al-4.5Cu-5TiB_2 composite rolled in mushy state in as cast and pre hot rolled condition (Herbert2007).

Material	% TR	%. LVF	Pct TiB_2	LGS	SGS	Hardness	YS MPa	UTS MPa	Pct Elong.
Al-4.5Cu alloy	0	30	0	44	44	72	116	169	7.2
	2.5	30	0	329	158	77	124	174	6.3
	5	30	0	363	157	63	97	147	5.1
As cast Al-4.5Cu-5TiB_2 composite	0	30	5	50	50	78	178	236	9.7
	2.5	30	5	66	37	88	195	264	12.1
	5	30	5	55	32	96	224	277	14.1
Pre-hot rolled Al-4.5Cu-5TiB_2	5	10	5	42	26	104	189	239	11.3
	5	20	5	41	25	112	219	276	13.5
	5	30	5	46	24	99	214	273	14.4

TR - thickness reduction; LVF- liquid volume fraction; LGS - large grain size; SGS - small grain size; Pct Elong. – percent elongation

6.5 NEURAL NETWORK TRAINING DESCRIPTION

The aim of the study in this chapter is to estimate the strength and ductility characteristics (output) as a function of % liquid volume fraction of Al-4.5Cu-5TiB_2 composite, % thickness reduction during mushy state rolling, small and large grain size and hardness (inputs) when the composite is rolled in mushy state in the as cast and pre hot rolled condition. Both the inputs and the output were first normalised within the range 0.1 to 0.9. The main reason for standardizing the data has already been discussed in section 4.3.2.1 in chapter 4. The normalizing and de-normalizing functions used in chapter 4 are reproduced here for convenience.

$$x_n = [(x - x_{min}) * 0.8 / (x_{max} - x_{min})] + 0.1 \quad (6.1)$$

$$x = [(x_n - 0.1) (x_{max} - x_{min}) / 0.8] + 0.1 \quad (6.2)$$

The neural network training refers to the process of fitting the neural network to the data obtained from experimentation. During the course of this process, the synaptic weights connecting the each individual neuron are continuously updated, as each input vector is presented to the network over and over again, till the error function, in this case, the mean squared error (MSE) becomes equal to or less than some

predefined value or the training is stopped at some specified number of iterations. In the present model development, FFNN model with an input layer and an output layer with a single hidden layer was tried with different values of η and α and with number of nodes ranging from 2 to 15 in the hidden layer (Reddy *et al.* 2005), with a MSE of 0.00001 and number of iterations as 5 lakhs. But the network failed to converge. This was expected since the relationship between input and output parameters is obviously quite complex and probably non linear. The FFNN was then tried with two hidden layers. The training of the model was started with 2 to 15 neurons in each hidden layer (Reddy *et al.* 2005). The minimum MSE was set at 0.0001 and the number of iterations was limited to 500000. At the beginning, the starting values of the learning rate parameter (η) and the momentum factor (α) were taken as 0.1 and 0.9 respectively. For all patterns p_s the global error function MSE is given by Reddy *et al.* (2005),

$$MSE = \sum_p E_p = \frac{1}{p}\sum_p \sum_i \left(T_{ip} - O_{ip}\right)^2 \qquad (6.3)$$

where, T_{ip} is the target output and O_{ip} is the predicted output, for the i^{th} neuron and the p^{th} pattern presented to the network. The mean error in the output prediction is given by Reddy *et al.* (2005),

$$E_{tr}(x) = \frac{1}{N}\sum_1^N |(T_i(x) - p_i(x))| \qquad (6.4)$$

where $E_{tr}(x)$ is the mean error in prediction of data set for the output parameter x, N is the number of data sets, $T_i(x)$ is the target output and $p_i(x)$ is the predicted output. The learning rate η was then varied from 0.1 to 0.9 in steps of 0.05 to start with the training. The learning rate was selected for the model based on the MSE and E_{tr} of the training. Now, the learning rate was fixed for the model and the momentum factor was varied from 0.9 to 0.1 in steps of 0.05. Again based on the MSE and E_{tr} the momentum was selected and the FFNN architecture was finalised for predicting the yield strength, ultimate tensile strength and pct elongation for the Al-4.5Cu alloy rolled in the as cast form and Al-4.5Cu-5TiB_2 composite in the as cast and pre hot rolled condition when rolled in mushy state to various % thickness reductions and with various % liquid volume fractions. Sigmoid function stated at equation (4.5) (Reddy *et al.* 2005, Yagnanarayana 2007, Zurada 1994, 2003) and reproduced here at

equation (6.5) was used for activating the neurons and back propagation algorithm was used for training the network.

$$F(x) = \frac{1}{[1+\exp(-x)]} \quad (6.5)$$

An extensive analysis of different combinations of the learning rate parameter, momentum factor and the number of neurons in each hidden layer was done. The number of neurons in each hidden layer was varied from 2 to 15. Learning rate was varied from 0.1 to 0.9 and momentum term varied from 0.9 to 01 in steps of 0.05 in each of these cases. The network was found to excellently converge with 9 and 6 neurons in the first and second hidden layer respectively with η=0.85 and α=0.7. The MSE was reset at 0.0001692 and E_{tr} = 8 x 10^{-6} and the epochs were restricted to 500000. Training was decided to be stopped either when MSE reached 0.00017 or when the number of iterations reached 500000, whichever occurred earlier. Here the targeted MSE was achieved after 490000 iterations. The inputs to the model were material type (as cast alloy, as cast or pre hot rolled composite), pct thickness reduction, pct liquid content, large grain size, small grain size and hardness. The outputs predicted were the yield strength, ultimate tensile strength and pct elongation of the alloy in cast and mushy state rolled form and of the composite in the as cast as well as pre hot rolled form when it is rolled in mushy state. The prediction of the strength and ductility parameters carried out for the range of experimental values tabulated in Table 6.2 for the cases listed in Table 6.1 are shown in Table 6.3.

6.6 DISCUSSION

The resulting values of strength parameters, namely, yield strength and ultimate tensile strength and the ductility characteristic represented by pct elongation predicted by Artificial Neural Network are compared with the corresponding experimentally obtained values to check the suitability of the ANN model within the perview of experimentation. A detailed analysis of the variation of the values of strength and pct elongation with respect to percentage thickness reduction during rolling and with percent liquid volume fraction at which the rolling is initiated is also presented in this section.

Table 6.3 Table showing the comparison of Tensile properties of as cast Al-4.5Cu alloy and Al-4.5Cu-5TiB_2 composite rolled in mushy state in as cast and pre hot rolled condition.

Material	% TR	% LVF	% TiB_2	LGS (µm)	SGS (µm)	Hardness (H_v)	Yield strength MPa		Pct Error	UTS MPa		Pct Error	Pct elongation		Pct Error
							Exptl	ANN		Exptl	ANN		Exptl	ANN	
Al-4.5Cu alloy	0	30	0	44	44	72	116	118.9	-2.55	169	167	1.20	7.2	6.95	3.44
	2.5	30	0	329	158	77	124	120.4	2.86	174	176.6	-1.48	6.3	6.39	-1.40
	5	30	0	363	157	63	97	99.4	-2.46	147	145.5	1.03	5.1	5.12	-0.45
As cast Al-4.5Cu-5TiB_2	0	30	5	50	50	78	178	175.8	1.23	236	238.3	-0.96	9.7	10.4	-7.65
	2.5	30	5	66	37	88	195	197.9	-1.52	264	260.3	1.39	12.1	11.8	2.22
	5	30	5	55	32	96	224	223.4	0.27	277	278.2	-0.44	14.1	14.1	0.01
Pre-hot rolled Al-4.5Cu-5TiB_2	5	10	5	42	26	104	189	185.1	2.06	239	242.9	-1.64	11.3	11.5	-1.94
	5	20	5	41	25	112	219	220.6	-0.71	276	273.3	0.97	13.5	14.3	-6.24
	5	30	5	46	24	99	214	215.2	-0.58	273	271.2	0.65	14.4	13.6	5.57

TR - thickness reduction; LVF- liquid volume fraction; LGS - large grain size; SGS - small grain size.

It can be seen from Table 6.3 that the maximum error in prediction by the ANN model is 7.65%, while the majority of the predictions are within 3.5% error in predictions. Jiahe *et al.* (2003) have reported prediction of microstructure of 60Si2MnA rod within a prediction of 3.2% error. Selvakumar *et al.* (2007) have modelled the effect of particle size and iron content on forming of Al-Fe composite preforms within an error of 5%. Peng *et al.* (2002) in their work on semisolid processing of steel-Al-7 graphite binding plate have formulated an ANN model for relationship of the bonding parameters and interfacial shear strength of bonding plate within a prediction error of 3.9%. Microstructural evolution model of TA15 titanium alloy based on BP algorithm trained ANN model has been reported by Zhicago *et al.* (2010), with an estimation error of 5%. Kusiak & Kuziak (2002) have reported a maximum percentage error of 8% in prediction of ultimate tensile and yield strength of steel, while Mandal *et al.* (2009) in their paper reported a Gaussian distribution of % error of prediction within ±10% in prediction of flow stress using Resilient Propagation algorithm which has been reported to perform better than Back Propagation algorithm. In light of these findings in similar contemporary works, the

proposed network trained by using back propagation algorithm for modelling mechanical behaviour of Al-4.5Cu alloy and its composites reinforced by (*in situ* synthesised) TiB_2 particles subjected to rolling in mushy state having varying fractions of liquid content and rolled to varying pct thickness reductions per pass can be considered to be suitable for predicting the strength and ductility properties.

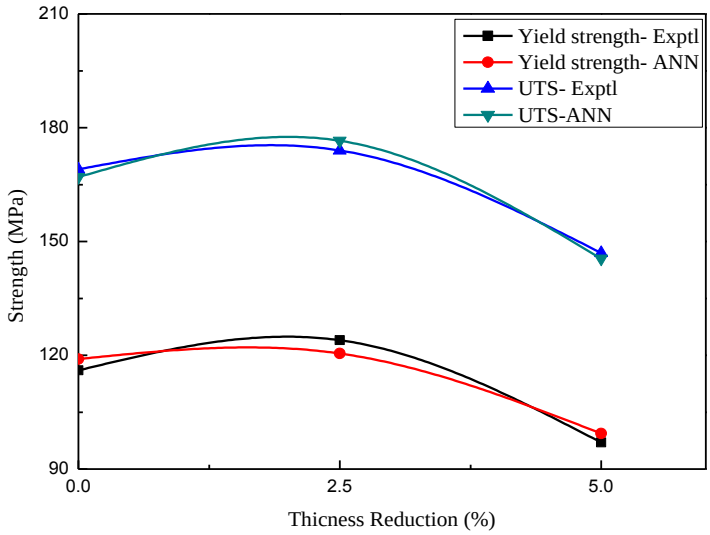

Figure 6.1 Plot showing comparison of variation of experimental and ANN predicted values of yield strength and UTS of as cast Al-4.5-Cu alloy containing 30% liquid volume fraction, rolled from mushy state to various thickness reductions.

6.6.1 Comparison of ANN predictions and experimental values of Yield strength and UTS

6.6.1.1 Rolling of as cast Al-4.5Cu alloy in mushy state

From Table 6.2, it can be seen that when Al-4.5Cu alloy containing 30% liquid volume fraction is rolled from this mushy state, the maximum values of yield and ultimate strength in tension are recorded at 2.5 % thickness reduction. Plot in Figure 6.1 indicates that these values gradually increase with increase in thickness reduction during rolling up to 2.5 % thickness reduction but then decrease steeply beyond. The increase in the YS and UTS is found to be 7% and 2.9% respectively at 2.5 % thickness reduction as compared to the unrolled alloy. However, the decrease in the

YS and UTS is found to be 21.77% and 17.24% respectively at 5 % thickness reduction as compared to that at 2.5 %. This steep decrease in strength with increase in thickness reduction beyond 2.5 % thickness reduction, which can also be seen from Table 6.2, is attributed to grain growth (Herbert *et al.* 2010, Herbert 2007).

6.6.1.2 Rolling of as cast Al-4.5Cu-5TiB_2 composite in mushy state

Table 6.3 shows the experimentally obtained values of YS and UTS as well as those predicted by Neural Network for cast Al-4.5Cu-5TiB_2 composite rolled in mushy state containing 30 % liquid volume fraction corresponding to 632°C temperature and rolled to 2.5% and 5% thickness reductions per pass.

It can be seen that the percentage error between the experimental values for yield strength in tension and ANN predicted values ranges from -1.5221% to +1.2348%, with these maximum errors occurring at 2.5 % thickness reduction. Similarly, for ultimate tensile strength, the % error is between -0.4458% and +1.3943% under same conditions of rolling. The percentage error between experimental values and values predicted by ANN at various percent liquid volume fractions for entire range of percentage thickness reduction are within |1.6%|. The errors in prediction by proposed ANN model are comparable with those reported in literature (Peng *et al.* 2002, Kusiak and Kuziak 2002, Zhicago *et al.* 2010).

Plot in Figure 6.2 shows the variation of YS and UTS of as cast composite when rolled in mushy state with temperature corresponding to 30 % liquid volume fraction at various thickness reductions. The values predicted by ANN are observed to closely match with the corresponding experimental values. It can be seen from the plots that both, the YS as well as the UTS increase with increase in thickness reduction. From Table 6.3, it is seen that the grain size decrease is modest at 2.5 % thickness reduction while it is quite significant when the thickness reduction is 5 %. This is manifested in modest increase of yield strength at 2.5 % thickness reduction followed by a steeper increase beyond. However, in case of UTS the increase is more in the beginning and modest beyond. The increase in the strength properties are in good agreement with the hardness values as can be seen from Table 6.2 and 6.3.

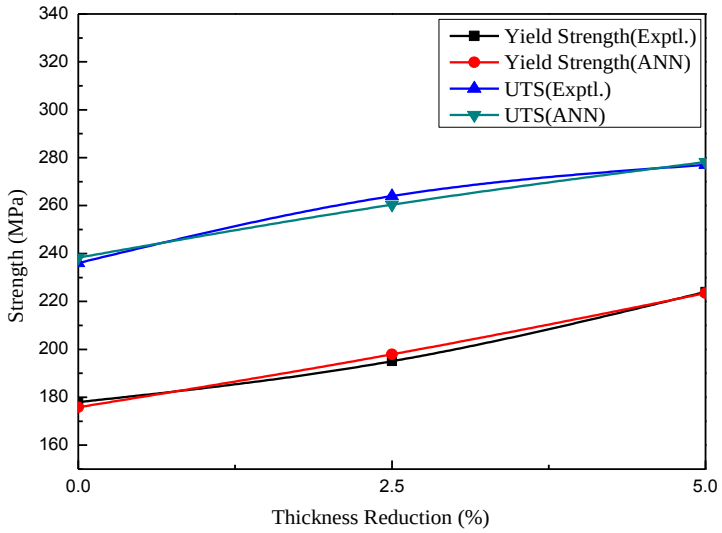

Figure 6.2 Plot showing comparison of experimental and ANN predicted values of yield and ultimate strength in tension for as cast composite containing 30% liquid volume fraction, rolled in mushy state to various thickness reductions.

6.6.1.3 Rolling of pre-hot rolled Al-4.5Cu-5TiB_2 composite in mushy state

Table 6.3 shows the experimentally obtained values of YS and UTS as well as those predicted by Neural Network for pre-hot rolled Al-4.5Cu-5TiB_2 composite rolled in mushy state containing 10, 20 or 30 % liquid volume fraction (corresponding to 610°C, 626°C or 632°C temperatures respectively) and rolled to 5% thickness reductions per pass. The percentage error in prediction in case of UTS is found to vary from -1.6448% to 0.9783% while that for YS varied from -0.7128% to 2.0571% with maximum error in prediction exhibited at 10% liquid volume fraction, in both the cases. The errors in prediction by the model are in agreement with predictions done by ANN models in various applications in material science (Kusiak and Kuziak 2002, Jiahe *et al.* 2003, Selvakumar *et al.* 2007). Therefore it can be concluded that the ANN model proposed has generalised the relationship between the inputs to the network and is able to predict the YS and UTS for the composite rolled in mushy state in pre hot rolled condition within acceptable levels of accuracy.

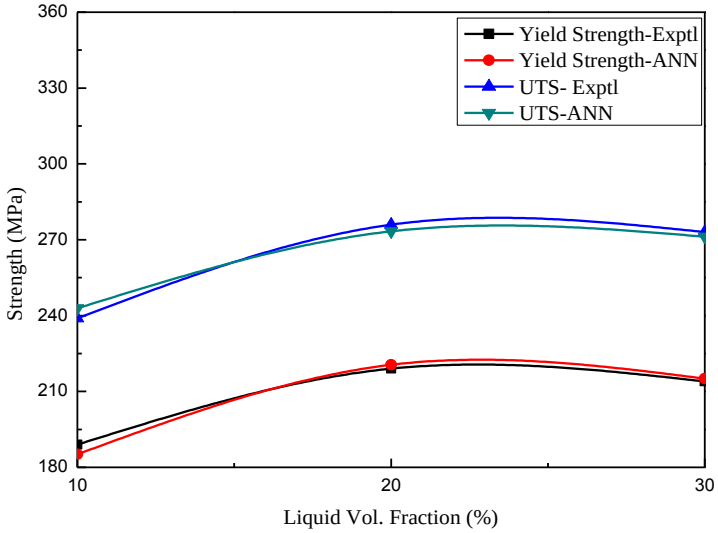

Figure 6.3 Plot showing comparison of experimental and ANN predicted values of yield and ultimate strength for pre hot rolled composite rolled in mushy state to 5% thickness reduction at different liquid volume fractions.

The plots of YS and UTS v/s liquid volume fraction depicted in Figure 6.3 indicate that the strength properties increase initially with increase in % volume fraction of liquid in the pre-hot rolled composite but decrease modestly beyond. This is because the average grain size decreases till the rolling is initiated with mushy state temperature of 626°C corresponding to 20 % liquid volume fraction, mainly due to grain globulisation. Secondly as the rolling progresses, some liquid tends to push out towards the roller periphery, thereby coming in contact with atmosphere, resulting in rapid cooling, giving finer grains. Then there is strain induced work hardening (Kiuchi 1989, Herbert *et al.* 2006, Herbert 2007) associated with rolling operation which results in increase in strength of the composite. Beyond 20 % liquid volume fraction, the mushy state temperatures at the initiation of rolling increase. Since the rolling speed is maintained constant for all cases, there is more time available for grain growth when rolling is initiated from higher temperatures overriding the effects of strain induced work hardening and grain globulisation (Kiuchi 1989, Herbert *et al.* 2008). This perhaps, is the reason why the strength properties as indicated by plot in Figure 6.3 fall beyond 20 % liquid volume fraction.

6.6.2 Comparison of Percentage Elongation obtained by experimentation and ANN prediction

6.6.2.1 Al-4.5Cu alloy

From Table 2 it can be seen that the maximum value of 7.2 pct elongation for the Al-4.5Cu alloy is exhibited when the mushy state alloy is rolled with 30 % liquid volume fraction. Plot in Figure 6.4 shows the comparison of the ANN predicted values with experimentally obtained values of pct elongation for the alloy. It can be seen that that values predicted by ANN match closely with the corresponding experimental values and that the pct elongation decreases with increase in thickness reduction. This decrease can be attributed to increase in the average grain size as well as increased strain induced work hardening associated with increase in thickness reduction during the rolling of mushy state alloy (Herbert 2007). From Table 6.3 as well as graphs in Figure 6.4, it can be observed that the error in prediction of pct elongation varies between -0.4529 % at 5 % thickness reduction to +3.4458 % corresponding to as cast condition i.e. 0 % thickness reduction.

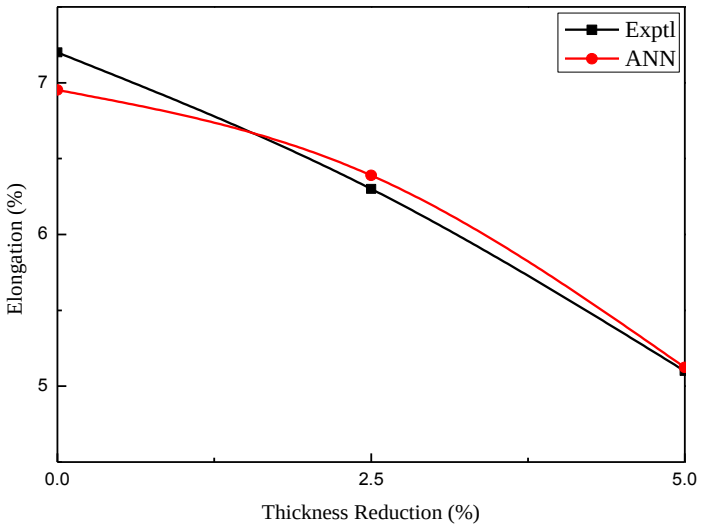

Figure 6.4 Plot showing comparison of experimental and ANN predicted values of pct elongation for Al-4.5Cu alloy containing 30% liquid volume fraction, rolled from mushy state to various thickness reductions.

6.6.2.2 Mushy state rolling of as cast Al-4.5Cu-5TiB_2 composite

Table 6.2 indicates that the maximum of pct elongation is obtained when mushy state composite in as cast form is rolled in mushy state at temperature corresponding to 30 % liquid volume fraction to 2.5 % thickness reduction. Table 6.3 indicates that the error in prediction varies from -7.6546% to +2.215% corresponding to 5 % thickness reduction. Plots depicted in Figure 6.5 as well as Table 6.3 show the comparison of the variation of pct elongation of as cast composite containing 30 % liquid volume, rolled in mushy state to varying thickness reductions. It can be concluded from the plots that the values predicted by the model are in close agreement with the experimentally achieved values. The plots in Figure 6.5 show that there is a continuous increase in the ductility of the as cast composite mushy state rolled with increased thickness reduction during rolling. The continuous increase is attributed to grain globulisation that follows mushy state rolling and decrease in average grain size which probably overcomes the effect of work hardening (Herbert *et al.* 2006, Herbert 2007). The errors observed between the experimental values and those predicted by the proposed ANN model are within |7.66|%. Kusiak and Kuziak (2002) in their work on estimation of YS and UTS using ANN model have reported an error of 8%. Therefore the errors in estimation of YS and UTS by proposed ANN model for as cast composite rolled in mushy state can be considered to be reasonable.

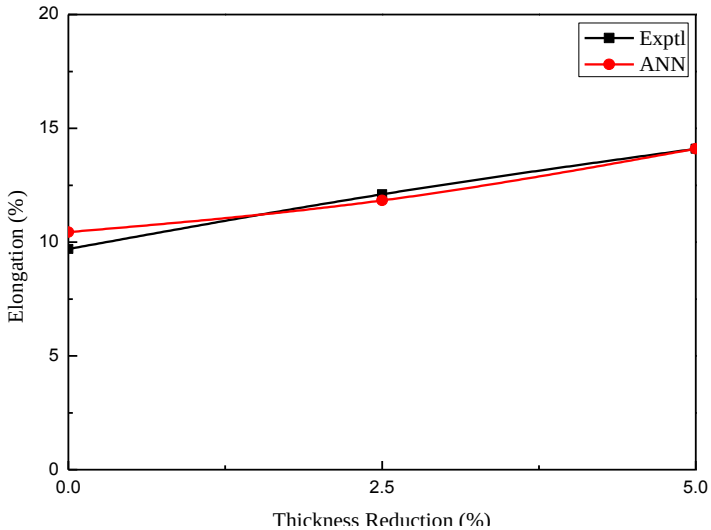

Figure 6.5 Plot showing comparison of experimental and ANN predicted values of pct elongation for Al-4.5Cu-5 TiB_2 composite having 30% liquid volume fraction, rolled from mushy state to various thickness reductions.

6.6.2.3 Mushy state rolling of pre-hot rolled Al-4.5Cu-5TiB_2 composite

Plot of comparison of pct elongation for pre-hot rolled Al-4.5Cu-5TiB_2 composite with 5% thickness reduction with rolling initiated at temperatures corresponding to various liquid volume fractions is shown in Figure 6.6. It can be seen from these plots, that the ANN predicted values closely follow the values from experimentation. The maximum error in prediction of pct elongation equal to -6.2% is observed corresponding to the prediction made when the pre-hot rolled composite is rolled with 20% liquid volume fraction. The errors in prediction of pct elongation of pre hot rolled composite by ANN model are in agreement with those reported in literature on applications of ANN model in material science (Kusiak and Kuziak 2002, Jiahe *et al.* 2003, Selvakumar *et al.* 2007, Peng *et al.* 2002, Zhicago *et al.* 2010). The pct elongation, as noted in the case of strength properties of pre-hot rolled composite discussed at section 6.6.1.3 is found to increase initially till 20% liquid volume fraction and then decrease modestly. The same reasons as those discussed for variation of strength properties do apply for this trend of variation observed in ductility of pre-hot rolled composite also.

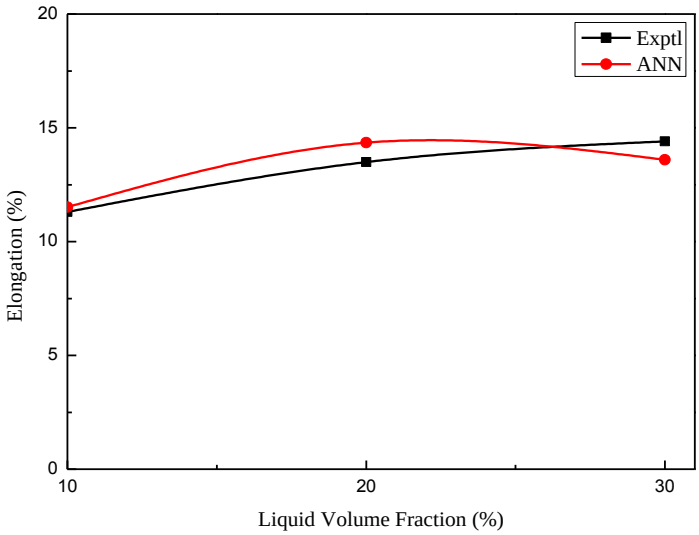

Figure 6.6 Plots showing comparison of experimental and ANN predicted values of pct elongation for pre hot rolled composite rolled in mushy state to 5% thickness reduction at different liquid volume fractions.

6.7 PARAMETRIC STUDY

6.7.1 Variation of Tensile Properties with respect to liquid fraction for pre hot rolled Al-4.5Cu-5TiB_2 composite rolled in mushy state to 5 pct. thickness reduction.

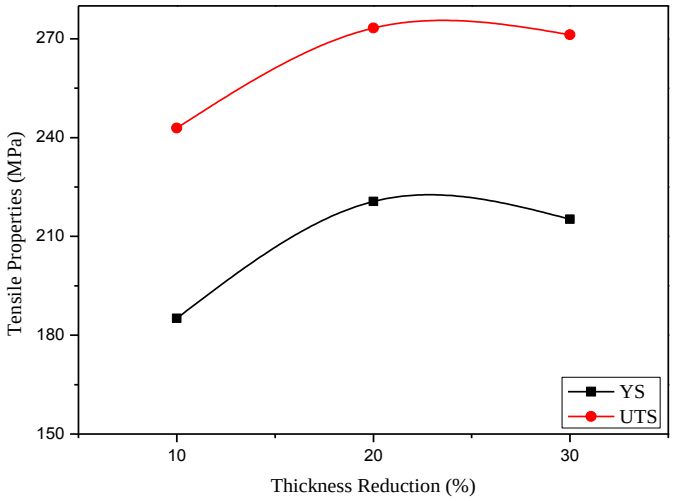

Figure 6.7 Plot showing variation of tensile properties as predicted by ANN

From Table 6.3, it is seen that there is improvement in yield as well as ultimate tensile strength in case of mushy state rolled composite as compared to Al-4.5 Cu alloy. The improvement in properties is mainly due to the refinement in grain structure and size distribution that occurs during mushy state rolling. Plots in Figure 6.7 indicate that the yield strength and ultimate tensile strength increase as the volume fraction of liquid increases from 10 to 20% and decreases slightly as the liquid volume fraction increases to 30%. This is similar to the trend shown by hardness (Figure 5.11). This variation of yield strength and ultimate strength with liquid content in the composite can be explained as follows. During mushy state rolling, the solid skeleton in sample containing least liquid content i.e. 10% volume fraction of liquid undergoes more deformation as compared to those samples with higher liquid content, as the unmelted grains are likely to touch one another. The work hardening of the α-Al grains in the composite is expected to enhance hardness and therefore, the yield and ultimate tensile strength. With further increase in liquid content from 20 to 30%, there is

decline in the strength properties, due to the grain coarsening phenomena occurring at higher temperature (632ºC) corresponding to 30% liquid volume fraction. For a given thickness reduction, the composite mushy state rolled with 20% liquid volume fraction (Figure 5.11) exhibits the maximum value of hardness and therefore shall exhibit high values of strength in the same region. The maximum value of hardness and therefore the strength properties at 20% liquid volume fraction is due to the optimum combination of the effects of work hardening of solid skeleton and the fine grains formed by rapid solidification of the liquid.

6.8 SUMMARY

1. The ANN model proposed for prediction of tensile properties of Al-4.5Cu alloy and its composite reinforced with 5 wt. % TiB_2 has very well generalised the relationship with the mushy state rolling parameters. The values of yield strength in tension predicted by the ANN model proposed give an error less than |2.1%| while the prediction of tensile strength is within an error of |1.5%|, for the entire range of data within which the ANN has been trained
2. The predictions done by the trained ANN model for pct elongation at various thickness reductions and starting state of Al-4.5Cu alloy and its composite reinforced with 5 wt.% TiB_2 during mushy state rolling, are within an error of |7.65%|, with the majority of the predictions being within |2.3%| error as compared to experimental results.
3. The ANN model proposed, therefore characterizes the process of mushy state rolling very much within the reasonable limits in the range of experimentation carried out and therefore can be used as an alternative to costly and time consuming experimentation.
4. The model can be used to make predictions of tensile properties at any point within 0 to 5% thickness reduction with mushy state rolling initiated at $632^{\circ}C$ (corresponding to 30% liquid volume fraction) in case of as cast Al-4.5Cu-5TiB_2 composite.
5. For mushy state rolling of pre hot rolled composite, the model can make predictions at any intermediate point between 10 and 30% volume fractions of liquid (i.e. from $610^{\circ}C$ until $632^{\circ}C$).

Chapter 7

RESULTS AND DISCUSSION (PART IV)

ANN MODELLING FOR PREDICTION OF WEAR PROPERTIES

7.1 INTRODUCTION

This chapter reports the modelling of ANN for prediction of dry sliding wear properties of Al-4.5Cu-5TiB_2 composite rolled from mushy state conditions. Literature (Caracostas *et al.* 1992, Roy *et al.* 1992) reports that the metal matrix composites have superior wear properties in comparison to monolithic alloys. Studies have revealed that Al based MMCs undergo adhesive wear (Deuis *et al.* 1997, Herbert 2007, Herbert *et al.* 2008), strongly influenced by hardness. Hardness in a particulate reinforced MMC is a function of grain morphology, hardness of particles and their distribution. The hardness of mushy state rolled Al-4.5Cu-5TiB_2 composite, as was seen in chapter 5, varies with the matrix grain size, volume content of liquid in the composite and thickness reduction per roll pass. Herbert (2007) and Herbert *et al.* (2008) carried out study on dry sliding wear properties of Al-4.5Cu-5TiB_2 composite as a function of mushy state rolling parameters and analyzed the tribological properties using adhesive wear model. The outcome of this study has been used as the data for training the ANN model to predict the wear rates of mushy state rolled Al-4.5Cu-5TiB_2 composite with respect to various combinations of thickness reductions and volume content of liquid in the composite. The proposed ANN model is validated by conducting validation experiments within and outside the bounds of data used for training the network. Thus the trained ANN model will be able to predict the wear properties of the mushy state rolled Al-4.5Cu-5TiB_2 composite within and outside the bounds of training data set. The proposed ANN model along with the user friendly GUI designed for the purpose will serve as a useful tool for optimization of wear properties based on the parameters specified by the user.

7.2 WEAR PARAMETERS

Figure 7.1 is the plot of wear volume loss with respect to sliding distance, which shows the regions of transient and steady state sliding wear. As seen from Figure 7.1, initially, the volume loss is seen to vary in curvilinear fashion and the rate of volume loss with sliding distance is observed to decrease at point B, beyond which it is found to vary in linear trend along line BC. Yang (2003) has reported that the wear in the region given by portion AB is known as unsteady state or transient wear, while the wear in the portion provided by BC regime is termed as steady state wear. In the steady state wear condition, the wear volume loss occurs at a constant rate over an extended duration of time. For this reason, the wear rate in the first 600 m was ignored in his work by Herbert (2007). Generally, the steady state wear behaviour of materials is expressed in terms of some key parameters, namely, wear rate, wear resistance, wear coefficient, specific wear rate and coefficient of friction. In the subsections to follow, these parameters are further discussed in more detail.

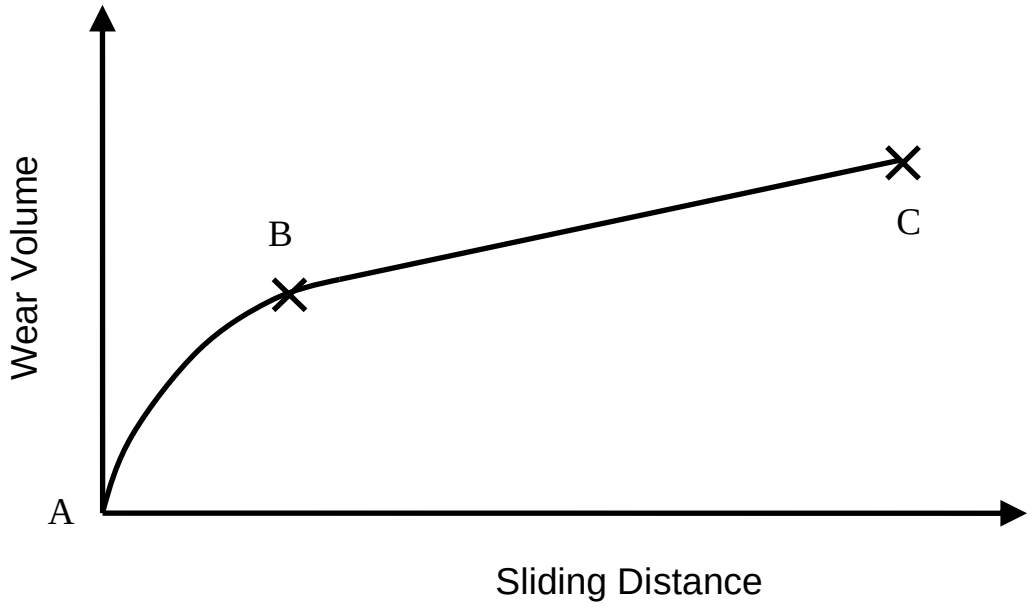

Figure 7.1 Schematic plot of wear volume loss against sliding distance showing transient and steady state wear regime

7.2.1 Wear rate

The wear rate (Yang 2003, Mandal 2007, Herbert 2007, Herbert *et al.* 2008) is defined as the volume loss per unit sliding distance. The pin on disc machine provides the data on loss of height during the wear test. The product of the height loss during the test and the cross sectional area of the specimen, which remains unchanged during the test, help to determine the volume loss at any specified sliding distance. The sliding distance is computed from the sliding speed and the time elapsed in sliding test from the beginning of wear test. The slope of the line which represents the best fit line for the volume loss data plotted against sliding distance gives the wear rate. In the steady state regime represented by portion BC in Figure 7.1, wear rate, W is given by the expression

$$W = \frac{V_c - V_B}{L_C - L_B} \qquad (7.1)$$

In other words,

$$W = \frac{\Delta V}{\Delta L} \qquad (7.1a)$$

where V is the wear volume and L is the sliding distance. The wear rate is reported (Herbert 2007) to be independent of sliding distance, but is dependent on the normal load applied during the dry sliding wear test.

7.2.2 Wear resistance

Wear resistance has been defined as the reciprocal of wear rate (Mandal 2007, Herbert 2007, Herbert *et al.* 2008). Wear resistance W_R is given by the expression

$$W_R = \frac{L_C - L_B}{V_C - V_B} \qquad (7.2)$$

$$W_R = \frac{\Delta L}{\Delta V} \qquad (7.2a)$$

Wear resistance being reciprocal of wear rate, it decreases as wear rate increases and vice versa. As in case of wear rate, wear resistance is independent of sliding distance, but depends on normal load applied during wear test.

7.2.3 Specific wear rate

The specific wear rate signifies the load bearing capacity of the material. It is defined as the wear rate per unit normal load (Mandal 2007, Herbert 2007, Herbert *et al.* 2008). Specific wear rate, W_S is given by the expression

$$W_S = \left(\frac{V_C - V_B}{L_C - L_B} \right) \frac{1}{P} \tag{7.3}$$

where, P is the normal load applied during the wear test.

7.2.4 Wear coefficient

Wear volume is observed to be a function of applied normal load, sliding distance and hardness. Archard (1953) and Rabinowicz (1965) proposed the relationship for wear volume as follows:

$$V = \frac{kPL}{3H} \tag{7.4}$$

where, H is the hardness and *k* is a dimensionless constant known as wear coefficient. Moreover, *k* can be expressed as

$$k = \frac{3H}{P} * \frac{V}{L} \tag{7.5}$$

It has been established by Yang (2003) that the steady state wear parameter is a better way of expressing the sliding wear behaviour of material tested on pin on disc machine, as all the parameters affecting wear are being considered in its calculation.

7.2.5 Coefficient of friction

It is defined as the ratio of the limiting tangential force needed to produce sliding to the normal load between the mating surfaces (Rabinowicz 1965). Coefficient of friction, μ is given by the relation

$$\mu = \frac{F_T}{N} \tag{7.6}$$

where, F_T is the tangential force reported in the steady state regime and N is the normal load.

7.3 SCOPE

We have seen that ANN is a mathematical model for solving complex relationships between inputs and outputs, wherein the model mimics the human brain in solving the relationships (Reddy *et al*. 2005, 2008). The Neural Network has the ability to compute these complex relationships by virtue of their similarity to the activities carried out by biological neurons in the human brain by way of parallel and distributed processing. This parallel and distributed processing adapts to the subtle relationships between the inputs and outputs and generalizes the functional relationship between them, even from a limited number of samples provided to it for training. The experiments carried out leading to any formidable conclusion always rely on a specific and limited number of readings at which the results are obtained or proved. Although this brings to the fore a very important research outcome, the information can be more useful for commercial applications when this experimental data is available over a wider range, within and outside the range of experimentation. ANN is an efficient tool to predict the output for any input within and in close locations outside the range of experimentation. Wear properties of mushy state rolled Al-4.5Cu-5TiB_2 composite depend on a number of parameters such as initial material state, % thickness reduction, % liquid volume fraction, large and small grain sizes, hardness and % TiB_2 in of the composite. The relationship as discussed earlier in section 6.2 is very complex and exhibits non linearity. Various ANN architectures and

training algorithms are available, but the most widely used architectures use FFNN with Back Propagation learning algorithm. FFNN is trained using supervised learning through the use of generalised delta rule in which the mean squared error is minimised step by step over the error surface by adjustment of weights, as each sample pattern is offered to the network (Zurada 2003, Reddy *et al.* 2005, 2008, Yagnanarayana 2008).

In this chapter it is proposed to model ANN with FFNN architecture and trained using BP algorithm to predict the wear properties of Al-4.5(wt. %)Cu-5(wt. %)TiB_2 composite rolled from mushy state with various volume content of liquid in the composite and to various thickness reductions during rolling. The scope of the work to be achieved through this chapter is outlined as follows:

a) To model ANN with FFNN architecture using BP algorithm to predict wear properties of Al-4.5Cu-5TiB_2 composite rolled in mushy state at various volume content of liquid in the composite and to various thickness reductions per pass during rolling.
b) To compare the predictions of the model with the target values used for training the network.
c) To validate the model through experimentations planned at specific points within and outside the bounds of data used for proposed training the ANN model.
d) To analyse the variation of wear properties of mushy state rolled Al-4.5Cu-5TiB_2 composite with respect to mushy state parameters.
e) To optimise the mushy state rolling process for wear parameters (wear rate) using proposed ANN model.

7.4 DATA COLLECTION

The data collected for training the ANN model proposed for prediction of wear properties of Al-4.5Cu-5TiB_2 composite is taken from previous study carried out by Herbert (2007) on wear properties of mushy state rolled Al-4.5Cu alloy and its composite reinforced with TiB_2 particles. The work involved the study of the behaviour of Al-4.5Cu alloy and Al-4.5Cu-5TiB_2 composite when rolled from mushy

state with various thickness reductions and temperatures corresponding to portion of the volume of liquid content in the semisolid composite. The behaviour of the composite was analysed for microstructural evolution, hardness and wear properties in addition to strength. The behaviour of the composite rolled in mushy state, at temperatures corresponding to 10%, 20% and 30% liquid volume fraction (corresponding to mushy state temperatures of 610°C, 626°C and 632°C respectively) with thickness reduction of 2.5, 5, 7.5 and 10% has been studied. The composite is rolled in mushy sate with initial state being in as cast and prior hot-rolled form. The parameters which represent the wear of the composite such as wear rate, wear resistance i.e. reciprocal of wear rate (Mandal *et al.* 2004), specific wear rate which is defined as wear rate per unit normal load (Mandal *et al.* 2004, Mandal 2007) have been determined. The dry sliding test was conducted on the composite in cast, pre hot rolled and mushy condition. Square specimens of 5mm x 5mm x 25mm height were tested using pin on disc wear testing machine (Model: TR-20, DUCOM, Bangalore, India). ASTM G99-04 standard was followed for conducting the test (ASM 1992). From the height loss, volume loss was calculated as product of cross sectional area and height loss. From these, the wear rates were calculated. Dry tests were conducted at normal loads of 19.6N, 39.2N, 58.4N and 78.4N at an ambient temperature to avoid the effects of lubricating medium. Hardened chromium steel (Rc64) was used as the counter face material. For all the tests, the sliding distance was kept as 1800m and the sliding speed was maintained at $1ms^{-1}$. The track radius was fixed as 40mm. Plots of volume loss v/s sliding distance were constructed. The slope of this graph in the steady state wear regime (sliding distance of 500m to 1500m) (Herbert 2007, Herbert *et al.* 2008) is taken as the wear rate.

Table 7. 1. Dry sliding wear studies of mushy state rolled Al-4.5Cu-5TiB_2 composite

Material#	**Mushy state rolling parameters**		**Normal Load (N)**
	Thickness reduction (%)	**Liquid content (%)**	
As cast Al-4.5Cu-5TiB_2	As cast 2.5, 5	30	19.6, 39.2, 58.8 and 78.4
Pre hot rolled Al-4.5Cu-5TiB_2	2.5, 5	30	
	7.5	10, 20 and 30	

 # All figures are in weight %.

Table 7.1 provides the details related to the specimen identification and the normal loads used to carry out experiments on the wear studies of Al-4.5Cu-5TiB_2 composite when rolled in mushy state to various thickness reductions and at various temperatures corresponding to the volume of liquid content in the semisolid composite in as cast and pre hot rolled condition (Herbert 2007). The wear rates obtained from the plot of volume loss v/s sliding distance obtained for the composite for the cases listed in Table 7.1 (by fitting the best fit line using regression analysis) are tabulated in Table 7.2 (Herbert 2007). Listed further, in Table 7.2, are the calculated values of wear resistance and specific wear rate.

From Table 7.2, it can be seen that the wear rate is maximum in case of as cast Al-4.5Cu-5TiB_2 composite when rolled in mushy state to 2.5% thickness reduction corresponding to 30% liquid volume fraction with 19.6 N normal load, while it is minimum in case when rolled to 5% thickness reduction from mushy state with 30% liquid volume fraction with 78.4 N normal load. Similarly, it can be seen that the maximum and minimum wear rates occur for pre hot rolled composite when it is mushy state rolled from 10% and 20% liquid volume fractions, with 7.5% thickness reduction and with 78.4N and 19.6N normal load respectively.

7.5 WEAR TEST EXPERIMENTS FOR MODEL VALIDATION

Experiments were planned to validate the proposed ANN model for prediction of wear properties of mushy state rolled Al-4.5Cu-5TiB_2 composite, as per the schedule shown in Table 7.3. As can be seen from Table 7.3, the experiments are planned within, as well as outside the bounds of experimental data given at Table 7.2, which is used for training the model. Validation experiments were carried out for the cases listed in Figure 3.4 of chapter 3. Wear testing experiments have not been conducted with 6% thickness reduction at 7 and 17% volume fractions of liquid and with 11.5 % thickness reduction during mushy state rolling in as cast composite. Similarly, in case of pre hot rolled composite, experiments are not planned with 11.5% thickness reduction. This is because, in all the cases mentioned, alligatoring was observed (Herbert 2007, Herbert *et al.* 2006).

Table 7.2 Wear rate, wear resistance and specific wear rate of mushy state rolled Al-4.5Cu-5TiB_2 composite in as cast and pre hot rolled condition.

Specimen description	% TR	% LVF	LGS	SGS	Hardness (H_V)	Load (N)	Wear rate	Wear resistance	Specific wear rate
As cast Al-4.5Cu-5TiB_2 Composite	2.5	30	66	37	88	19.6	0.00392	0.25510	0.00020
						39.2	0.00525	0.19048	0.00013
						58.8	0.00595	0.16807	0.00010
						78.4	0.00651	0.15361	0.00008
	5.0	30	55	32	96	19.6	0.00360	0.27778	0.00018
						39.2	0.00421	0.23753	0.00011
						58.8	0.00539	0.18553	0.00009
						78.4	0.00601	0.16639	0.00008
Pre hot rolled Al-4.5Cu-5TiB_2 Composite	2.5	30	47	25	88	19.6	0.00308	0.32468	0.00016
						39.2	0.00517	0.19342	0.00013
						58.8	0.00574	0.17422	0.00010
						78.4	0.00605	0.16529	0.00008
	5.0	30	46	24	99	19.6	0.00298	0.33557	0.00015
						39.2	0.00407	0.24570	0.00010
						58.8	0.00518	0.19305	0.00010
						78.4	0.00592	0.16892	0.00008
	7.5	10	40	26	110	19.6	0.0027	0.37037	0.00014
						39.2	0.00454	0.22026	0.00012
						58.8	0.00516	0.19380	0.00009
						78.4	0.00644	0.15528	0.00008
		20	39	25	116	19.6	0.00217	0.46083	0.00011
						39.2	0.00263	0.38023	0.00007
						58.8	0.00401	0.24938	0.00007
						78.4	0.00501	0.19960	0.00006
		30	45	24	108	19.6	0.00233	0.42918	0.00012
						39.2	0.00405	0.24691	0.00010
						58.8	0.00444	0.22523	0.00009
						78.4	0.00581	0.17212	0.00007

TR – Thickness reduction; LVF – Liquid volume fraction; LGS – large grain size; SGS – Small grain size

Table 7.3 Dry sliding wear studies of mushy state rolled Al-4.5Cu-5TiB_2 composite planned for model validation.

Material#	Mushy state rolling parameters		Normal Load (N)
	Thickness reduction (%)	Liquid content (%)	
As cast Al-4.5Cu-5TiB_2	2	17	19.6, 39.2, 58.8 and 78.4
	6	33	
Pre hot rolled Al-4.5Cu-5TiB_2	2	17	
	6	7, 17 and 33	

 # All figures are in weight %.

Table 7.4 shows the results of wear test experiments conducted to validate the model, for the cases listed in Table 7.3. The outcome of the experiments from wear testing of samples is the wear rate in mm^3/m. The values of wear resistance are calculated as reciprocal of wear rate, while specific wear rate is calculated as wear rate per unit normal load.

Table 7.4 Validation experiment results for wear rate, wear resistance and specific wear rate of mushy state rolled Al-4.5Cu-5TiB_2 composite.

Specimen description	% Thickness reduction	% Liquid volume fraction	Load (N)	Wear rate (mm^3/m)	Wear resistance (km/mm^3)	Specific wear rate (mm^3/m-N)
As cast Al-4.5Cu-5TiB_2 Composite	2	17	19.6	0.00266	0.37594	0.00014
			39.2	0.00508	0.19685	0.00013
			58.8	0.00703	0.14225	0.00012
			78.4	0.00831	0.12034	0.00011
	6	33	19.6	0.00464	0.21552	0.00024
			39.2	0.00617	0.16207	0.00016
			58.8	0.00632	0.15823	0.00011
			78.4	0.00744	0.13441	0.00009
Pre hot rolled Al-4.5Cu-5TiB_2 Composite	2	17	19.6	0.00260	0.38462	0.00013
			39.2	0.00170	0.58824	0.00004
			58.8	0.00464	0.21552	0.00008
			78.4	0.00541	0.18484	0.00007
	6	7	19.6	0.00412	0.24272	0.00021
			39.2	0.00586	0.17065	0.00015
			58.8	0.00605	0.16529	0.0001
			78.4	0.00719	0.13908	0.00009
		17	19.6	0.00208	0.48077	0.00011
			39.2	0.00199	0.50251	0.00005
			58.8	0.00388	0.25773	0.00007
			78.4	0.00503	0.19881	0.00006
		33	19.6	0.00273	0.3663	0.00014
			39.2	0.00456	0.2193	0.00012
			58.8	0.00496	0.20161	0.00008
			78.4	0.00563	0.17762	0.00007

7.6 ANN MODELLING FOR PREDICTION OF WEAR RATE

The aim of the proposed ANN model is to estimate the wear rate(output) as a function of liquid volume fraction in mushy state Al-4.5Cu-5TiB_2 composite, thickness reduction during mushy state rolling, small and large grain size and hardness (inputs) when the composite is rolled in mushy state in the as cast and pre hot rolled condition. Both the inputs and the output were as usual, first normalised within the range 0.1 to 0.9. Neural network training is the process of fitting the NN to the experimental data. In this process, the synaptic weights connecting each neuron are continuously updated as each input vector is being presented to the network. The adjustment of these weights is continued till the mean squared error (MSE) is minimised to a predefined value or the number of iterations are predefined. The model developed for the present application is FFNN model with input, output and hidden layer(s). The training of the model was started with, a single hidden layer with 2 to 15 neurons in hidden layer (Reddy *et al.* 2005, 2008). The minimum MSE was set at 0.000001 and the number of iterations was limited to 300000. The initial values of the learning rate (η) and the momentum factor (α) were taken as 0.1 and 0.9 respectively for training. Subsequently, two hidden layers with 2 to 15 neurons in each hidden layer had to be attempted, as the network failed to converge with single hidden layer prescription for all combinations attempted with η and α.

As discussed in previous paragraph, single and two hidden layers were attempted to obtain the least MSE. The learning rate η was varied from 0.1 to 0.9 in steps of 0.05 to start with the training. The learning rate was selected for the model based on the MSE and E_{tr} of the training. Now, the learning rate and the number of hidden layers were fixed for the model and the momentum factor was varied from 0.1 to 0.9 in steps of 0.05. Again based on the MSE and E_{tr} the momentum was selected and the FFNN architecture was finalised for analysis of wear rate for the Al-4.5Cu-5TiB_2 composite when rolled from mushy state in the as cast or pre hot rolled condition at various % thickness reductions and % liquid volume fractions. Sigmoid function was used for activating the neurons, while back propagation algorithm was used for training the network.

Extensive analysis of various combinations of learning rate parameter and momentum factor was done to understand the criterion of convergence. It is found to exhibit convergence with 7 neurons in first and 4 neurons in second hidden layer, with η=0.25 and α=0.9 after 300000 iterations. Back propagation learning was carried out starting with these fixed values of η and α. For our model, the best combination was found to be η=0.5 and α=0.5. Training was stopped when MSE reaches 29 x 10^{-5} with E_{tr} = 3.44 x 10^{-6} or when the number of iterations reached 2000000, whichever occurred earlier. Here the targeted MSE was achieved after 18 lakh iterations.

The prediction of wear rate is carried out for the range of experimentation tabulated in Table 7.2 and 7.4, respectively, for as cast composite and pre hot rolled composite for the cases listed in Table 7.1 and 7.3. Alligatoring has been reported to be absent (Herbert 2007, Herbert *et al.* 2006) for combinations of thickness reductions and liquid content, while mushy state rolling of Al-4.5Cu-5TiB_2 composite in as cast as well as pre hot rolled condition, at temperature of 632°C (30% liquid volume fraction) with thickness reduction of 2.5 and 5 percent in one single pass. Again, in case of pre hot rolled composite at 7.5% thickness reduction with temperatures corresponding to 10, 20 and 30% liquid volume fraction, alligatoring is not observed. Therefore, the model is used to predict the values within the range of experimentation where the phenomenon of alligatoring is absent and to determine the optimal values of wear rate and the corresponding parameters of the composite yielding optimal wear rate. The predicted values of wear rate for as cast composite and pre hot rolled composite are compared with the experimentally obtained values and the same are presented in Table 7.5 and 7.6 respectively. The relative error in Table 7.5 and 7.6 is calculated using the following relation:

$$Relative\ Error = \left(\frac{Value_{Exptl} - value_{ANN}}{Value_{Exptl}} \right) * 100 \qquad (7.7)$$

It can be seen from Table 7.5 that within the data range used for training the model, a maximum error of 3.06 % occurs with 2.5 % thickness reduction when composite is rolled with 30 % liquid volume fraction, for19.6 N normal load. A minimum (i.e. zero) error occurs when composite is rolled to 5 % thickness reduction from same

conditions of liquid volume fraction and for same normal load. From Table 7.6, it is observed that for mushy state rolling in pre hot rolled condition of the composite, the maximum error of 6.17 % occurs with 7.5 % thickness reduction when rolled from temperature corresponding to 30 % liquid volume fraction, for 39.2 N normal load. Zero error is obtained with 7.5 % thickness reduction rolled from mushy state containing 10 % volume fraction of liquid in the composite, for 19.6 N normal load.

The prediction by ANN model proposed, as can be seen from Table 7.5, for cases where validation experiments are carried out, exhibit a maximum error of 5.51 %, in the as cast composite rolled from mushy state to 6 % thickness reduction with 33 % liquid volume fraction in the composite, for 78.4 N normal load. Table 7.6 reveals that the ANN model predicts the wear rate in case of pre hot rolled composite within an error of |4.13|% corresponding to the data used for validation of the model. This indicates that the model has properly generalised the relationship for mushy state rolling of Al-4.5Cu-5TiB_2 composite rolled in as cast and pre hot rolled condition from 2 to 7.5 % thickness reduction, rolled from temperatures corresponding to 7 to 33 % liquid volume fraction and that the validation of model is established.

The optimisation of the mushy state rolling process for wear rate prediction is achieved by using the GUI or front end for ANN model designed for this purpose. The GUI provides for graphical viewing of variation of wear rate with respect to variation of one mushy state rolling parameter, keeping other parameters constant. By varying one parameter at a time, minimum wear rate is determined and the mushy state rolling process parameters corresponding to these values of optimised wear rate are noted for composite rolled in as cast and pre hot rolled condition. The model predicts the minimum wear rate for the composite mushy state rolled in as cast condition to 10 % thickness reduction at temperature corresponding to 16.88 % liquid volume fraction. For the composite rolled from mushy state in pre hot rolled condition, the minimum value of wear rate is obtained for 10 % thickness reduction at temperature corresponding to 18.9202 % liquid volume fraction. These optimal values obtained from the ANN model along with the range of normal loads are presented in Table 7.7. Figure 7.2 shows a capture of the graphical user interface screen when the

optimum value of wear rate is achieved using the GUI designed with Microsoft SilverLight API package, in case of as cast Al-4.5Cu-5TiB_2 composite rolled in mushy state.

Table 7.5 Comparison of Wear rate predicted by ANN with the experimentally obtained values of wear rate for mushy state rolled Al-4.5Cu-5TiB_2 composite in as cast condition.

Specimen description	% Thickness reduction	% Liquid volume fraction	Load (N)	Wear rate (mm^3/m)		Relative Error (%)
				Experimental	ANN	
As cast Al-4.5Cu-5TiB_2 Composite	2*	17*	19.6	0.00266	0.00258	3.01
			39.2	0.00508	0.00499	1.77
			58.8	0.00703	0.00676	3.84
			78.4	0.00831	0.00797	4.09
	2.5	30	19.6	0.00392	0.0038	3.06
			39.2	0.00525	0.0052	0.95
			58.8	0.00595	0.0058	2.52
			78.4	0.00651	0.0064	1.69
	5.0	30	19.6	0.00360	0.0036	0.00
			39.2	0.00421	0.0042	0.24
			58.8	0.00539	0.0053	1.67
			78.4	0.00601	0.006	0.17
	6+	33*	19.6	0.00464	0.00457	1.51
			39.2	0.00617	0.00612	0.81
			58.8	0.00632	0.00621	1.74
			78.4	0.00744	0.00703	5.51

* validation experiments

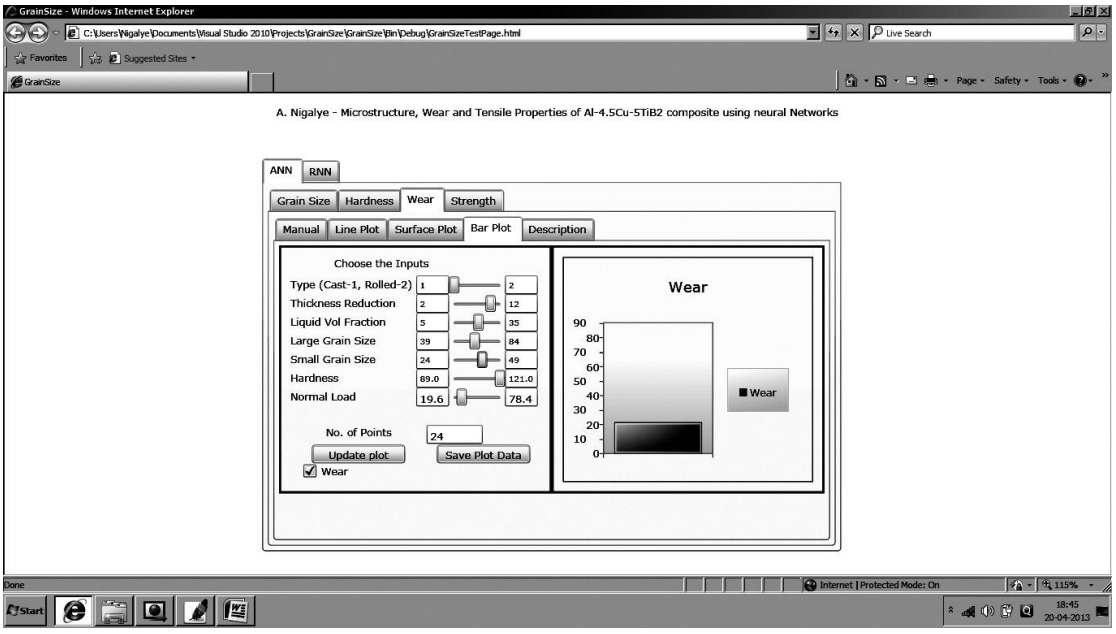

Figure 7.2 Screen capture showing optimal value of wear rate

Table 7.6	**Comparison of Wear rate predicted by ANN with the experimentally obtained values of wear rate for mushy state rolled Al-4.5Cu-5TiB$_2$ composite in pre hot rolled condition.**					
Specimen description	**% Thickness reduction**	**% Liquid volume fraction**	**Load**	**Wear rate (mm^3/m)**		**Relative Error**
			(N)	**Experimental**	**ANN**	**(%)**
Pre hot rolled Al-4.5Cu-5TiB$_2$ Composite	2*	17*	19.6	0.00260	0.00255	1.92
			39.2	0.00170	0.00168	1.18
			58.8	0.00464	0.00452	2.59
			78.4	0.00541	0.00536	0.92
	2.5	30	19.6	0.00308	0.00300	2.60
			39.2	0.00517	0.00500	3.29
			58.8	0.00574	0.00580	-1.10
			78.4	0.00605	0.00590	2.48
	5	30	19.6	0.00298	0.00300	-0.70
			39.2	0.00407	0.00400	1.72
			58.8	0.00518	0.00520	-0.40
			78.4	0.00592	0.00590	0.34
	6*	7*	19.6	0.00412	0.00407	1.21
			39.2	0.00586	0.00582	0.68
			58.8	0.00605	0.00597	1.32
			78.4	0.00719	0.00703	2.23
		17*	19.6	0.00208	0.00217	-4.33
			39.2	0.00199	0.00195	2.01
			58.8	0.00388	0.00395	-1.80
			78.4	0.00503	0.00500	0.60
		33*	19.6	0.00273	0.00271	0.73
			39.2	0.00456	0.00450	1.32
			58.8	0.00496	0.00484	2.42
			78.4	0.00563	0.00575	-2.13
	7.5	10	19.6	0.0027	0.00270	0.00
			39.2	0.00454	0.00450	0.88
			58.8	0.00516	0.00510	1.16
			78.4	0.00644	0.00640	0.62
		20	19.6	0.00217	0.00210	3.23
			39.2	0.00263	0.00280	-6.5
			58.8	0.00401	0.00390	2.74
			78.4	0.00501	0.00500	0.2
		30	19.6	0.00233	0.00220	5.58
			39.2	0.00405	0.00380	6.17
			58.8	0.00444	0.00440	1.67
			78.4	0.00581	0.00560	3.61

*validation experiments

Table 7.7 Optimal values of wear rate predicted by the ANN model.				
Specimen description	**% Thickness reduction**	**% Liquid volume fraction**	**Load (N)**	**Wear rate mm^3/m (ANN)**
As cast Al-4.5Cu-5TiB_2 Composite	10	16.88	25.7 to 54.09	0.0021
Pre hot rolled Al-4.5Cu-5TiB_2 Composite	10	18.9202	19.2 to 39.89	0.0022

It can be seen from Table 7.7, that in case of as cast composite rolled from mushy state, the model prediction of minimum wear rate is obtained at 10 % thickness reduction when the composite is rolled with 16.88 % liquid volume fraction, while it is minimum in case of pre hot rolled composite mushy state rolled with same reduction at 18.9202 % liquid volume fraction. In case of former, the minimum wear condition is obtained when normal load is between 25.7 and 54.09N while in the latter case it occurs when the normal load is between 19.2 and 39.89N.

Figure 7.3 is the plot showing variation of experimental and ANN predicted values of wear rates as a function of normal load for the Al-4.5Cu-5TiB_2 composite mushy state rolled in as cast condition subjected to different thickness reduction at 30 % liquid content. It can be seen that the wear rate increases as the normal load increases from 19.6N to 78.4N. The rate of increase of wear rate is steeper, in the case of 2.5 % thickness reduction in the region from 19.6N to 39.2N, beyond which the increase is only marginal. In case of 5 % thickness reduction, the wear rate increase is a maximum in the region from 39.2N to 58.8N. The plot also reveals close proximity between the experimentally obtained and ANN predicted values of wear rate. Similarly, Figure 7.4 shows the comparison of experimental and ANN predicted variation of wear rates as a function of normal load for the Al-4.5Cu-5TiB_2 composite mushy state rolled in pre-hot rolled condition, subjected to different thickness reductions at 30 % liquid content. It is observed that the predicted values closely follow the experimental values of wear in almost all the cases displayed in the plot, with the maximum variation of 6.17 % seen in case of 7.5 % thickness reduction for

the composite pre hot rolled from 30 % liquid volume fraction with 39.2N normal load.

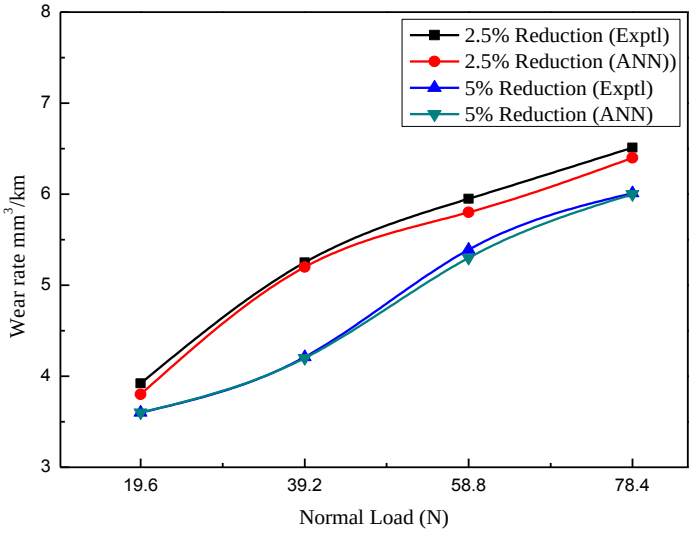

Figure 7.3 Plots showing comparison of experimental and ANN predicted variation of wear rates as a function of normal load for the Al-4.5Cu-5TiB_2 composite mushy state rolled in as cast condition subjected to different thickness reduction at 30 % liquid content.

The variation between the experimental values and those predicted by ANN are found to be the least i.e. 0.34 % in case of composite mushy state rolled with 5 % thickness reduction, while the maximum variation of 6.17 % is observed in case of pre hot rolled composite mushy state rolled with 7.5 % thickness reduction from 30 % liquid volume fraction. Although there appears to be only a minor variation in the wear rates based on whether mushy state rolling was performed after casting or prior hot rolling, it is obvious that the wear rates tend to decrease with increase in thickness reduction. The decrease in wear rate with increase in thickness reduction is more pronounced for wear tests at lower normal loads, and is less obvious for tests under the normal load of 78.4N. It can be seen from Figure 7.3 and 7.4 that the wear rates of the mushy state pre hot rolled composites are lower than those rolled as cast, when tested under the same load.

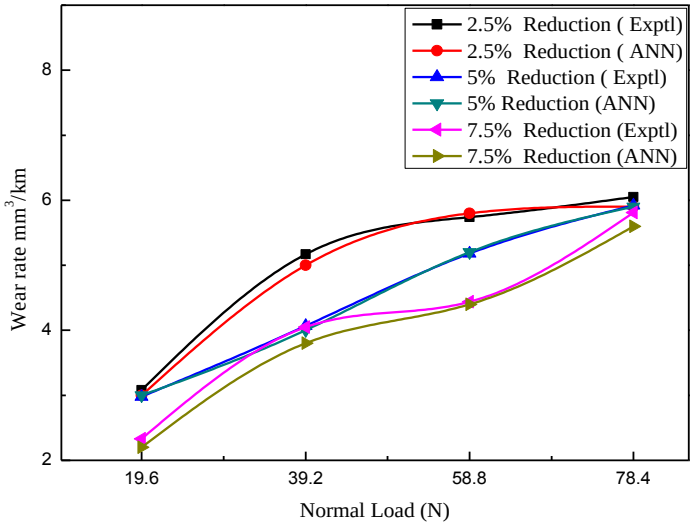

Figure 7.4 Plots showing comparison of experimental and ANN predicted variation of wear rates as a function of normal load for the Al-4.5Cu-5TiB_2 composite mushy state rolled in pre-hot rolled condition subjected to different thickness reductions at 30 % liquid content.

Figure 7.5 shows the comparison of experimental and ANN predicted variation of wear rates as a function of normal load for the Al-4.5Cu-5TiB_2 composite mushy state rolled in pre-hot rolled condition to 7.5 % thickness reduction with different liquid volume fractions. For composite rolled from 10 and 30 % volume fractions of liquid, it can be seen that the wear rate increase is quite steep in the region between 19.6N to 39.2N and between 58.8N and 78.4N normal loads, while it is marginal between 39.2N and 58.8N normal loads. In case of 20% liquid volume content, the increase is maximum between 39.2N and 58.8N normal loads, while is minimum between 19.6N to 39.2N normal loads. The path of ANN predicted values of wear rate and that obtained by experimentation closely follow one another, in case of 2.5 % reduction, while it differs maximum with 7.5 % reduction. At 39.2N normal load, for mushy state rolled composite containing 30 % liquid volume fraction, a maximum error of 6.17% is observed from Fig. 7.5. It is obvious from Fig. 7.5, that the wear rate is minimum in the composite mushy state rolled with 20% volume liquid, followed by those with samples rolled at temperatures corresponding to 30 and 10 volume percent liquid in pre hot rolled composite.

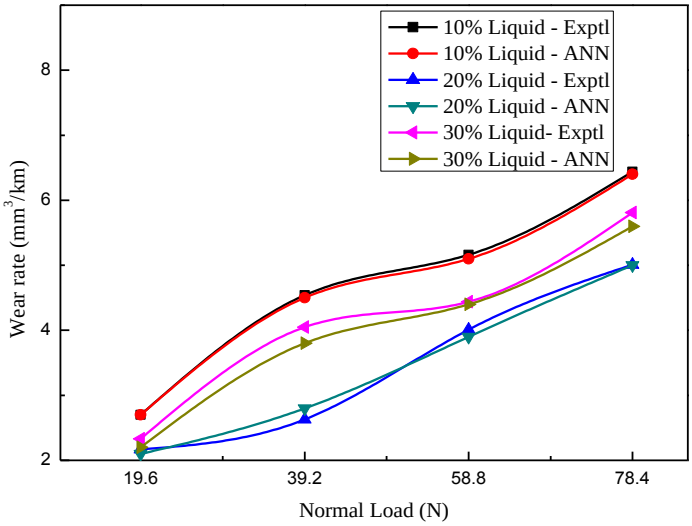

Figure 7.5 Plots showing comparison of experimental and ANN predicted variation of wear rates as a function of normal load for the Al-4.5Cu-5TiB_2 composite mushy state rolled in pre-hot rolled condition to 7.5% thickness reduction with different liquid volume fractions.

7.7 WEAR RESISTANCE

Table 7.8 shows the comparison of wear resistance obtained from experimental values of wear rates with those obtained from ANN predicted values of wear rates. It can be seen that wear resistance being reciprocal of wear rates, the absolute value of variation (i.e. absolute % error) between the experimental and ANN predicted values remain more or less same. However, there is a change in the sign of % error variation as expected, wear resistance being reciprocal of wear rate. The plots shown in Figure 7.6 compare ANN predicted values of wear resistance with those obtained experimentally for the Al-4.5Cu-5TiB_2 composite mushy state rolled in as cast condition to different thickness reduction with 30 % liquid content, as a function of normal loads. It can be seen that while the ANN predicted variation of wear resistance closely follows that obtained experimentally, the wear resistance is maximum in case of 5 % reduction for all values of normal loads as compared to 2.5 % reduction.

Table 7.8 Values of wear resistance predicted by ANN with the experimentally obtained values of wear resistance for mushy state rolled Al-4.5Cu-5TiB_2 composite rolled in as cast and pre hot rolled condition.

Specimen description	% Thickness reduction	% Liquid volume fraction	Load (N)	Wear Resistance (km/mm^3)		Relative Error (%)
				Experimental	ANN	
As cast Al-4.5Cu-5TiB_2 Composite	2.0*	17*	19.6	0.3759	0.3876	-3.10
			39.2	0.1969	0.2004	-1.80
			58.8	0.1423	0.1479	-3.99
			78.4	0.1203	0.1255	-4.26
	2.5	30	19.6	0.2551	0.2632	-3.16
			39.2	0.1905	0.1923	-0.96
			58.8	0.1681	0.1724	-2.59
			78.4	0.1536	0.1563	-1.72
	5.0	30	19.6	0.2778	0.2778	0.00
			39.2	0.2375	0.2381	-0.24
			58.8	0.1855	0.1887	-1.70
			78.4	0.1664	0.1667	-0.17
	6.0*	33*	19.6	0.2155	0.2188	-1.53
			39.2	0.1621	0.1634	-0.82
			58.8	0.1582	0.1610	-1.77
			78.4	0.1344	0.1423	-5.83
Pre hot rolled Al-4.5Cu-5TiB_2 Composite	2.0*	33*	19.6	0.3846	0.3922	-1.96
			39.2	0.5882	0.5952	-1.19
			58.8	0.2155	0.2212	-2.65
			78.4	0.1848	0.1866	-0.94
	2.5	30	19.6	0.3247	0.3333	-2.67
			39.2	0.1934	0.2000	-3.40
			58.8	0.1742	0.1724	1.03
			78.4	0.1653	0.1695	-2.54
	5.0	30	19.6	0.3356	0.3333	0.67
			39.2	0.2457	0.2500	-1.75
			58.8	0.1931	0.1923	0.38
			78.4	0.1689	0.1695	-0.34
	6.0*	7*	19.6	0.2427	0.2457	-1.23
			39.2	0.1707	0.1718	-0.69
			58.8	0.1653	0.1675	-1.34
			78.4	0.1391	0.1423	-2.28
		17*	19.6	0.4808	0.4608	4.15
			39.2	0.5025	0.5128	-2.05
			58.8	0.2577	0.2532	1.77
			78.4	0.1988	0.2000	-0.60
		33*	19.6	0.3663	0.3690	-0.74
			39.2	0.2193	0.2222	-1.33

			58.8	0.2016	0.2066	-2.48
			78.4	0.1776	0.1739	2.09
	7.5	10	19.6	0.3704	0.3704	0.00
			39.2	0.2203	0.2222	-0.89
			58.8	0.1938	0.1961	-1.18
			78.4	0.1553	0.1563	-0.63
		20	19.6	0.4608	0.4762	-3.33
			39.2	0.3802	0.3571	6.07
Pre hot rolled Al-4.5Cu-5TiB_2 Composite	7.5	20	58.8	0.2494	0.2564	-2.82
			78.4	0.1996	0.2000	-0.20
		30	19.6	0.4292	0.4545	-5.91
			39.2	0.2469	0.2632	-6.58
			58.8	0.2252	0.2273	-0.91
			78.4	0.1721	0.1786	-3.75

*validation experiments

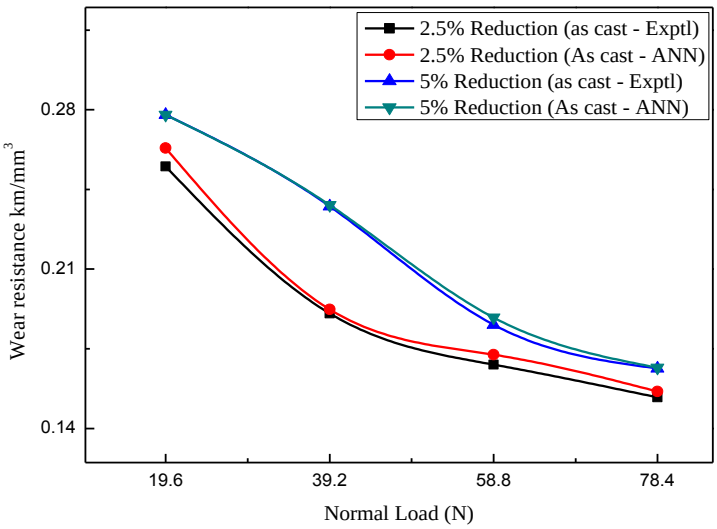

Figure 7.6 Plots showing comparison of experimental and ANN predicted variation of wear resistance as a function of normal load, for the Al-4.5Cu-5TiB_2 composite mushy state rolled in as cast condition to different thickness reductions with 30 % liquid content.

The reduction in wear resistance with increase in normal load is more in case of 2.5 % reduction as compared to 5 % reduction, quite evident in portion between 19.6N to 39.2N range. Figure 7.7 shows comparison of experimental and ANN predicted variation of wear resistance as a function of normal load, for the Al-4.5Cu-5TiB_2 composite mushy state rolled in pre hot rolled condition to different thickness reduction at 30 % liquid content. The ANN predicted values and experimentally obtained values follow each other quite closely. A steep decrease in wear resistance is

seen in case of 7.5 % and 2.5 % reduction, especially in the range between 19.6N to 39.2N of normal load. The wear resistance, in general, is seen to decrease with increase in normal load as well as decrease in thickness reduction. Increase in thickness reduction during rolling results in increase in hardness caused due to strain hardening (Herbert *et al.* 2006, Herbert 2007). Hardness as reported earlier (Herbert *et al.* 2006, Herbert 2007) is proportional to the wear resistance. However, as seen in Figure 7.7, at higher loads, the wear resistance becomes increasingly less sensitive to thickness reduction.

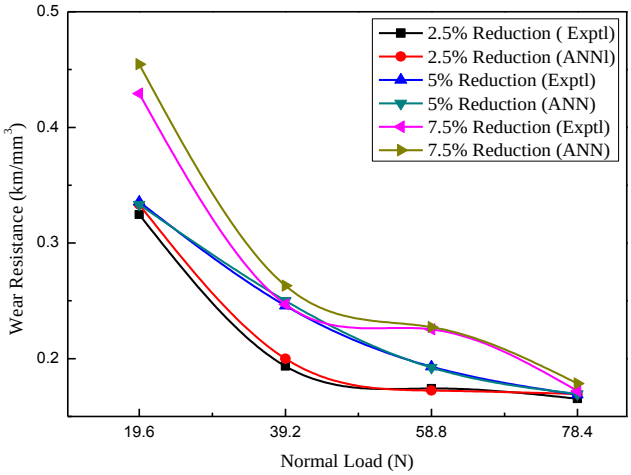

Figure 7.7 Plots showing comparison of experimental and ANN predicted variation of wear resistance as a function of normal load, for the Al-4.5Cu-5TiB_2 composite mushy state rolled in pre hot rolled condition to different thickness reduction with 30% liquid content.

The plots in Figure 7.8 show comparison of experimental and ANN predicted variation of wear resistance as a function of normal load, for the Al-4.5Cu-5TiB_2 composite mushy state rolled in pre hot rolled condition to 7.5 % thickness reduction with different liquid content. The variation between the ANN predicted and experimentally derived values is slightly higher in case of composite rolled in mushy state with 20 % and 30 % liquid volume fractions, at lower loads, as compared to composite rolled from temperature corresponding to 10 % liquid volume fraction. The plots show that at any normal load, the highest wear resistance is observed in the composite rolled with 20 % liquid volume fraction, followed by that in the samples rolled with 30 and 10 % volume fraction of liquid.

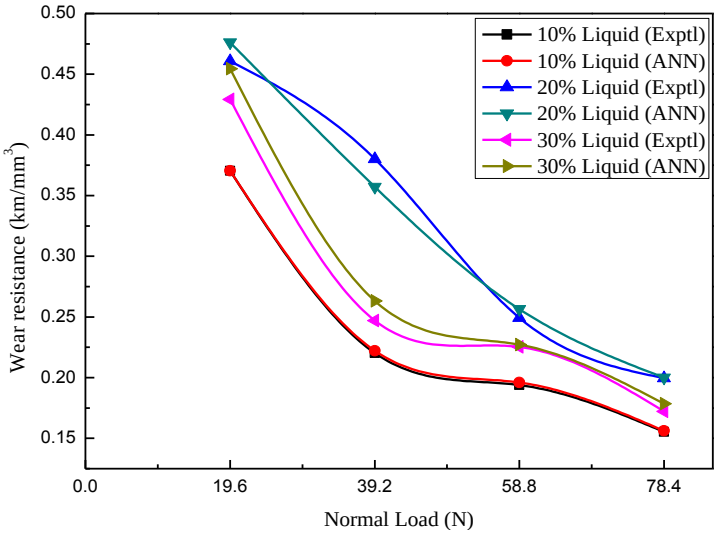

Figure 7.8 Plots showing comparison of experimental and ANN predicted variation of wear resistance as a function of normal load, for the Al-4.5Cu-5TiB_2 composite mushy state rolled in pre hot rolled condition to 7.5% thickness reduction with different liquid content in composite.

7.8 SPECIFIC WEAR RATE

Table 7.9 shows the values of specific wear rate calculated from training as well as validation data presented in Table 7.5 and 7.6. The table also shows the values of specific wear rates, calculated from ANN predicted values of wear rates presented in Table 7.5 and 7.6. The specific wear rate represents the load bearing capacity of the material. Being the ratio of wear rate to unit load applied during wear test, it is interesting to see the variation of specific wear rate with respect to mushy state parameters at various normal loads. The error in prediction of specific wear rate values when compared with training and validation data values will not vary from that for wear rate since the denominator is constant for both.

Figure 7.9 shows the plot depicting comparison of experimental and ANN predicted variation of specific wear rate as a function of normal load for the Al-4.5Cu-5TiB_2 composite mushy state rolled from 632°C (30 vol.% liquid) in as cast condition. Plots indicate that the specific wear rate decreases drastically in case with 2.5 as well as 5 % reduction until 39.2 N normal load. While it continues to decrease at more or less same rate with 2.5 % reduction, the rate of fall is greatly reduced with 5 % reduction. The plot in Figure 7.9 further indicates that in as cast condition, the variation of

specific wear rate with respect to thickness reduction is very marginal for very high and very low loads. The plot in Figure 7.10 shows the comparison of variation of specific wear rate as a function of normal loads for the Al-4.5Cu-5TiB_2 composite rolled in mushy state to different reductions from temperature corresponding to 30 % liquid volume fraction, while plot in Figure 7.11 depicts variation of specific wear rate as a function of normal loads, when rolled with different liquid volume fractions with respect to ANN prediction and experimental values.

Table 7.9 Table showing values of specific wear rate predicted by ANN with the experimentally obtained values for mushy state rolled Al-4.5Cu-5TiB_2 composite rolled in as cast and pre hot rolled condition.

Specimen description	% Thickness reduction	% Liquid volume fraction	Load (N)	Specific Wear rate (mm^3/km-N)		Relative Error (%)
				Experimental	ANN	
As cast Al-4.5Cu-5TiB_2 Composite	2.0*	17*	19.6	0.13571	0.13163	3.01
			39.2	0.01296	0.01273	1.77
			58.8	0.11956	0.11497	3.84
			78.4	0.10599	0.10166	4.09
	2.5	30	19.6	0.2	0.19388	3.06
			39.2	0.01339	0.01327	0.90
			58.8	0.10119	0.09864	2.52
			78.4	0.08304	0.08163	1.70
	5.0	30	19.6	0.18367	0.18367	0.00
			39.2	0.01074	0.01071	0.28
			58.8	0.09167	0.09014	1.67
			78.4	0.07666	0.07653	0.17
	6.0*	33*	19.6	0.23673	0.23316	1.51
			39.2	0.01574	0.01561	0.83
			58.8	0.10748	0.10561	1.74
			78.4	0.0949	0.08967	5.51
Pre hot rolled Al-4.5Cu-5TiB_2 Composite	2.0*	17*	19.6	0.13265	0.1301	1.92
			39.2	0.00434	0.00429	1.15
			58.8	0.07891	0.07687	2.59
			78.4	0.06901	0.06837	0.93
	2.5	30	19.6	0.15714	0.15306	2.60
			39.2	0.01319	0.01276	3.26
			58.8	0.09762	0.09864	-1.04
			78.4	0.07717	0.07526	2.48
	5.0	30	19.6	0.15204	0.15306	-0.67
			39.2	0.01038	0.0102	1.73
			58.8	0.0881	0.08844	-0.39
			78.4	0.07551	0.07526	0.33

Pre hot rolled Al-4.5Cu-5TiB_2 Composite	6.0*	7*	19.6	0.2102	0.20765	1.21
			39.2	0.01495	0.01485	0.67
			58.8	0.10289	0.10153	1.32
			78.4	0.09171	0.08967	2.22
		17	19.6	0.10612	0.11071	-4.33
			39.2	0.00508	0.00497	2.17
			58.8	0.06599	0.06718	-1.80
			78.4	0.06416	0.06378	0.59
		33	19.6	0.13929	0.13827	0.73
			39.2	0.01163	0.01148	1.29
			58.8	0.08435	0.08231	2.42
			78.4	0.07181	0.07334	-2.13
	7.5	10	19.6	0.13776	0.13776	0.00
			39.2	0.01158	0.01148	0.86
			58.8	0.08776	0.08673	1.17
			78.4	0.08214	0.08163	0.62
		20	19.6	0.11071	0.10714	3.22
			39.2	0.00671	0.00714	-6.41
			58.8	0.0682	0.06633	2.74
			78.4	0.0639	0.06378	0.19
		30	19.6	0.11888	0.11224	5.59
			39.2	0.01033	0.00969	6.20
			58.8	0.07551	0.07483	0.90
			78.4	0.07411	0.07143	3.62

*validation experiments

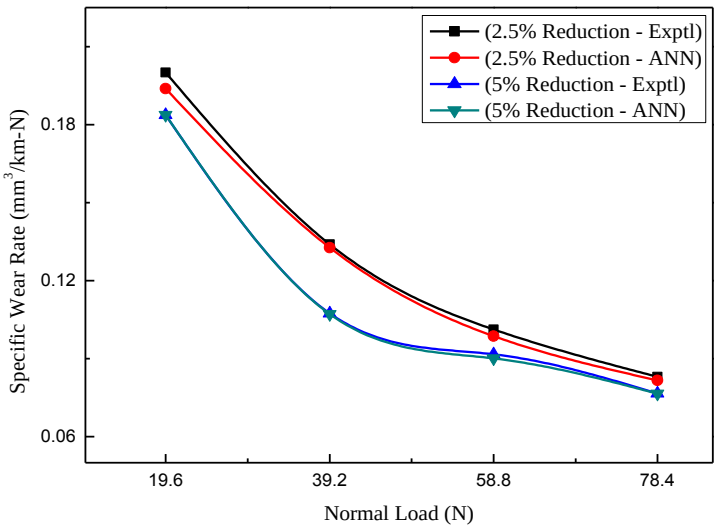

Figure 7.9 Plots showing comparison of variation of experimental and ANN predicted values of specific wear rate for the Al-4.5Cu-5TiB_2 composite rolled from mushy state in as cast condition to different thickness reductions from 632°C (30 vol.% liquid).

The difference between the ANN predicted and experimental (training data) values of specific wear rates at different normal loads with various thickness reductions as seen through Figure 7.10 and from liquid volume fraction in Figure 7.11 is high at low loads. The variation of specific wear rate is a maximum with 39.2N normal load. The variation of specific wear rate as seen from Figure 7.10 for the pre hot rolled composite mushy state rolled with 30 % liquid volume fraction is more at lower loads, with specific wear rate being minimum at 7.5 % reduction. The specific wear rate is insensitive to reduction at very high loads, since much of the higher load is utilised in plastic deformation rather than wear (Herbert 2007, Herbert *et al.* 2008).

From Figure 7.11, it is seen that, when the pre hot rolled composite is mushy state rolled with 20 % liquid volume content in composite, the specific wear rate initially decreases at a rapid rate till 39.2N load. Then it is seen to rise till 58.8N load and then gradually decreases. In the case of 10 % liquid volume fraction, the decrease is, more or less, at constant rate till 58.8N and then remains constant.

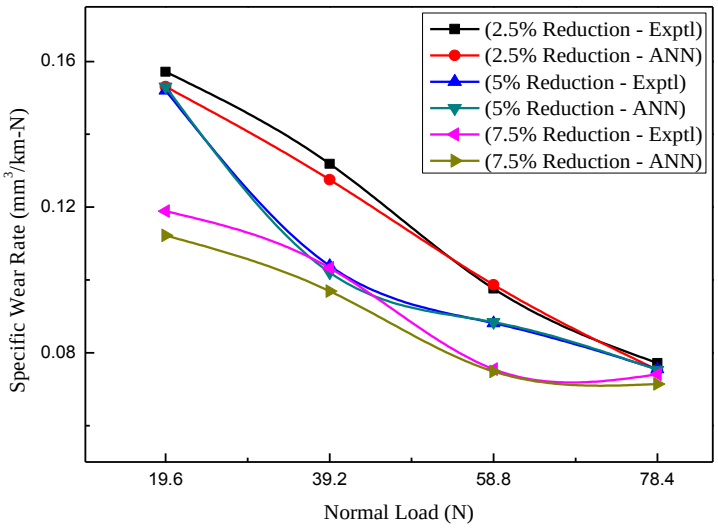

Figure 7.10 Plots showing comparison of experimental and ANN predicted variation of specific wear rate as a function of normal load, for the Al-4.5Cu-5TiB_2 composite rolled from mushy state to different thickness reductions from 632°C (30 vol.% liquid) in pre hot rolled condition.

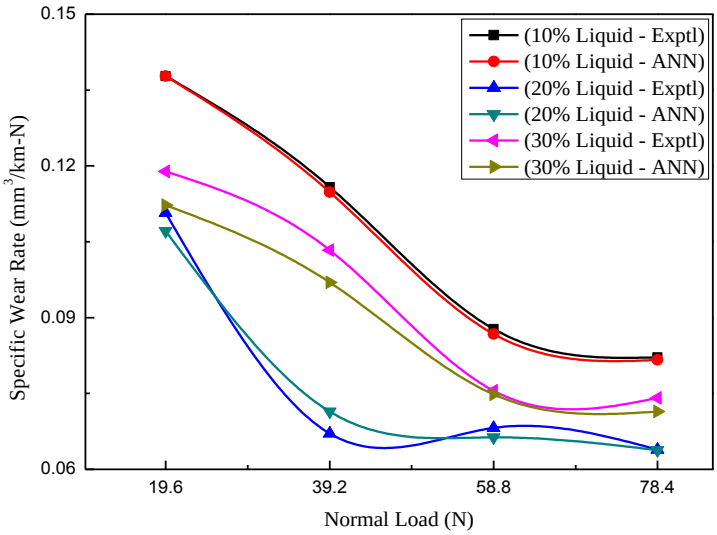

Figure 7.11 Plots showing comparison of experimental and ANN predicted variation of specific wear rate as a function of normal load, for the Al-4.5Cu-5TiB_2 composite rolled from mushy state rolled in pre hot rolled condition to 7.5% thickness reduction, with various liquid contents.

With 30 % liquid fraction in composite, a steep decrease in specific wear rate is observed from 39.2N to 58.8N load and thereon it remains practically constant. From Table 7.7, the minimum (optimal) specific wear rate based on the wear rate predicted by the model works out to 0.039 mm^3/km-N for as cast composite and 0.055 mm^3/km-N for pre hot rolled composite rolled from mushy state with 10 % thickness reduction from temperatures corresponding to 16.88 and 18.92 % volume fraction of liquid in composite, respectively.

Obvious from the plots in Figure 7.11 also is the fact that specific wear rate is minimum for composite mushy state rolled from 20 % liquid volume fraction at any given normal load. This indicates that the load bearing capacity of composite rolled in mushy state from around 20 % liquid volume fraction is going to yield highest values for any given normal load situation, which is in agreement with the studies on hardness in chapter 5.

7.9 PARAMETRIC STUDIES

7.9.1 Variation of wear rate with normal load at different thickness reductions.

From plots in Figure 7.4 we can see the variation of wear rates as a function of normal load for the Al-4.5Cu-5TiB_2 composite mushy state rolled in pre-hot rolled condition subjected to different thickness reductions at 30 % liquid content. It is obvious that the wear rates decrease with increase in thickness reduction at a given normal load. The decrease in the wear rate is more pronounced at lower normal loads and is less obvious at the normal load of 78.4N. It is also seen that for a given thickness reduction, the wear rate increases as normal load increases.

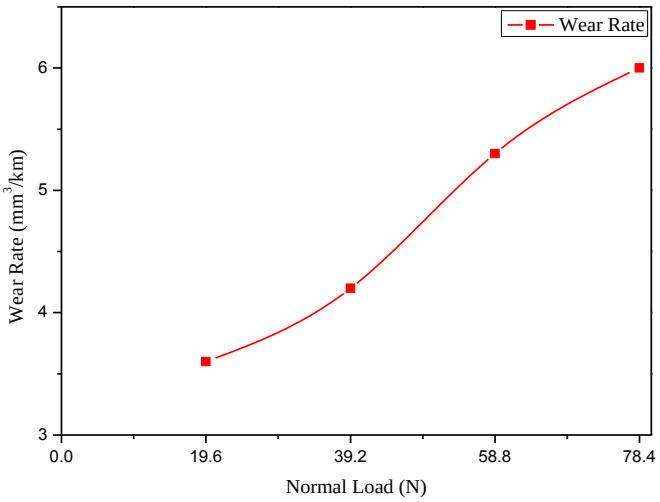

Figure 7.12 Plot showing the variation of wear rate as a function of normal load for mushy state rolled Al-4.5Cu-5TiB_2 composite rolled to 5% thickness reduction with 30% liquid volume fraction.

Figure 7.12 shows the variation of wear rate as a function of normal load for mushy state rolled Al-4.5Cu-5TiB_2 composite rolled to 5% thickness reduction with 30% liquid volume fraction in the composite. It is seen from the figure that the wear rate increases with the normal load up to 78.4 N. During the wear process, the TiB_2 particles in the composite tend to align themselves in the sliding direction. At higher normal loads, plastic deformation and material removal occurs exposing the TiB_2

particles (Herbert 2007). The material displaced due to cutting or deformation gets embedded on either side of the cut grooves. As the wear process continues, further sliding causes both the reinforcement and the matrix to be ironed flat, forming deformation tongues (Herbert *et al.* 2008). These deformation tongues then gets detached as debris resulting in material loss. This explains the reason as to why wear rate increases as normal load increases, even though it may appear that high normal loads cause strain induced work hardening and therefore should result in low wear rates.

7.10 SUMMARY

1. ANN model has been successfully designed and validated to predict the wear rate, with the experimental data adopted from the studies already carried out on mushy state rolling of Al-4.5Cu-5TiB_2 composite being used for training.
2. The ANN model successfully predicts the values within an overall error of |6.5| percent for wear rate. However for majority of the predictions, the error is between ±3.6 percent. The proposed model is validated within a prediction error of |5.51 |percent within and outside the bounds of data used for training the model.
3. The wear rate and the specific wear rate are seen to decrease with increase in thickness reduction as the composite is rolled from mushy state in as cast as well as in pre hot rolled condition. The variation is more pronounced at lower values of normal loads. The wear resistance being reciprocal of wear rate, it increases with thickness reduction during mushy state rolling and again the maximum variation is observed at lower loads, i.e. at 19.6N and 39.2N.
4. At higher loads, the wear rate, specific wear rate and the wear resistance variations are insensitive to normal load as compared to that at lower loads.
5. Considering the region of mushy state rolling in which the phenomenon of alligatoring is absent, the load bearing capacity of composite rolled in pre hot rolled condition from mushy state containing 20 % liquid volume fraction is found to be maximum for any given normal load situation. The specific wear rate for Al-4.5Cu-5TiB_2 composite at all normal loads is found to be least when

mushy state rolling with 7.5 % thickness reduction is carried out from temperature corresponding to 20 % liquid volume fraction.

Chapter 8

RESULTS AND DISCUSSION (PART V)

RECURRENT NEURAL NETWORK MODELLING

8.1 INTRODUCTION

ANN as a prediction tool has been vastly discussed in chapters 4 through 7 in terms of formulation, training as well as predictions done by these trained networks to provide outputs like grain sizes, hardness, strength and wear rate respectively. An attempt has been made here to develop an improvised neural network solution over the feed forward neural networks (FFNN). The objective here may mean either better predictions with equal training time for the model or at least comparable predictions with a decrease in the time required for training the model.

It is well known (Reddy *et al.* 2005, Selvakumar *et al.* 2007) that a major issue in use of multilayered perceptron or FFNN to be used as a mapping tool is the problem of the model getting stuck while training, on the gradient descent curve of MSE v/s weight planes, in areas of local minima. The momentum factor (α) helps the model to jump over the local cliffs and the training proceeds further, and disturbances are encountered and overcome, till the training has reached a stage where the neural network reaches the bottom of the bowl. At this point, the training is stopped and the MSE of the network is checked with the set error. If the set error is significantly smaller as compared to the FFNN mean squared error (MSE), the parameters of the network (η and α) are changed and the training is started all over again. The FFNN model is trained with various combinations of η and α and also with different architectures (i.e. number of hidden layers and number of nodes per hidden layer), till the near about of the set MSE is achieved. As seen in the case of FFNN training for grain size predictions, the number of epochs required to obtain the set MSE were

500000. It would be therefore viable to attempt a reduction in this training time and make the prediction more efficient.

Recurrent Neural Networks (RNN) has been proposed in the recent past as a mathematical tool to map the inputs with outputs. The underlying principle which differentiates it from FFNN is that unlike in case of FFNN, the outputs in case of RNN are fed back to itself as well as other neurons of the same and/or other layer. It is believed that corrected weights which had provided output at time (t-1) if fed to the neurons during the subsequent epoch along with the current output from neurons of previous layer at time t, would result in a better output and it would make the training faster. A lot of research is going on in the field of convergence characteristics of Elman Simple NN known as Simple Recurrent Network (SRN) and it is being actively studied for varying conditions of input-output data relationships (Lang *et al.* 1990, Narendra and Parthasarathy 1990, Guler *et al.* 2005).

In this chapter, it is proposed to formulate RNN model for the various cases for which ANN was formulated in Chapters 4 through 7 considering the difficulties in convergence spotted in Elman's SRN for these applications and overcoming them. These problems related to Elman SRN for the applications under study are presented in section8.4.

8.2 SCOPE

It is proposed to model recurrent neural networks to predict grain sizes, hardness, tensile and wear properties for which ANN models have been presented in Chapters 4, 5, 6 and 7. The inputs for the models are kept same as that for the corresponding ANN models. The current chapter is written with the following objectives:

1. To formulate Elman Simple Recurrent Network for grain size prediction, hardness prediction, and prediction of tensile and wear properties from same data from which ANN models were formulated.
2. To highlight the problems faced by SRN model in mapping the input-output relationship for the applications under study.
3. To propose Hybrid Recurrent Neural Network (HRNN) as an improvement over SRN overcoming the convergence related problems faced by SRN.

4. Application of HRNN models to predict grain sizes, hardness, tensile and wear properties.
5. Analysis of predictions done by HRNN and its comparison with FFNN and establishing the usefulness of HRNN as a prediction system.

8.3 ELMAN SIMPLE NEURAL NETWORK

In the recent past quite a few Recurrent Neural Network (RNN) architectures have been studied (Elman 1990, Lang *et al.* 1990, Frasconi *et al.* 1992, Giles *et al.* 1992, Tesauro *et al.* 1995). Recurrent networks are neural networks with one or more feedback loops, in which the loops may be local or global. RNN can be divided into two broad categories depending on whether the states of the network are guaranteed and observable or not. Observable state is one in which the state of the network can be derived by observing only the inputs and outputs (Giles *et al.* 1992). A model which falls into this class was proposed by Narendra and Parthasarathy (1990) and had time delayed outputs as well as inputs fed to a Multi Layer Perceptron (MLP) which computed the output using the recent state dynamics. However, network having hidden dynamic states are not observable (Giles *et al.* 1992). Single layered and multi layered recurrent networks are being extensively studied in recent times. A typical single layered RNN was the one proposed by Elman in 1990 (Elman 1990). In this network, the hidden layer is copied in a virtual or context layer and the feedback is given back to the same layer along with the next set of inputs in the next time step as seen in Figure 8.1.

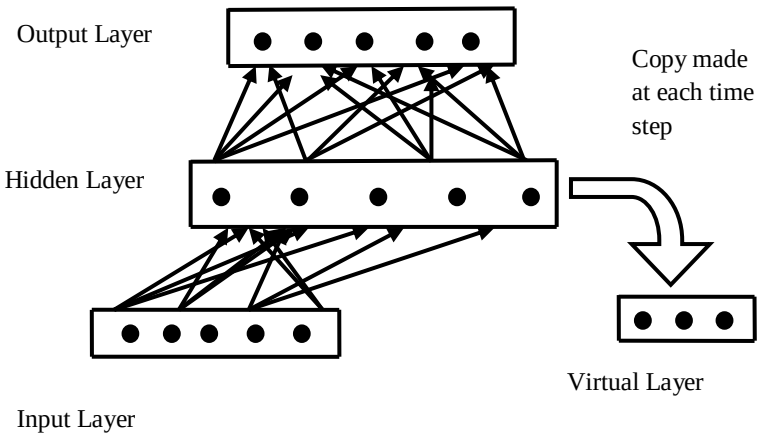

Figure 8.1 A simple RNN proposed by Elman (1990)

The Elman network can be extended for a multilayered network with the temporal context layer providing feedback at each subsequent time step. Such a network is shown in Figure 8.2. The convergence of a Simple Elman Recurrent Neural Network (SRN) has been established. The computational power of Elman networks is as good as that of finite state machines (FSM) (Kremer 1995). In addition, it is reported that any network having additional layers between input and output layer than that of Elman network, possesses the same computational power exhibited by FSM (Kremer 1995). The convergence of RNN has been active subject of research in machine learning. An extended back propagation algorithm for Elman networks reported a better convergence, faster training and better generalization (Song *et al.* 2009). In this algorithm, use is made of adaptive learning scheme coupled with adaptive dead zone to improve convergence speed.

In this study we try to develop a novel way of improving the convergence of Elman network (SRN) using the borrowed weights of a partially trained FFNN into an Elman network with single hidden layer or an extended Elman network having more than one hidden and context layer. The study further highlights the fact that the recurrent neural network so formulated performs the task of predictions comparable to that performed

by the fully trained FFNN, from which the weights were borrowed to formulate the RNN, with better convergence.

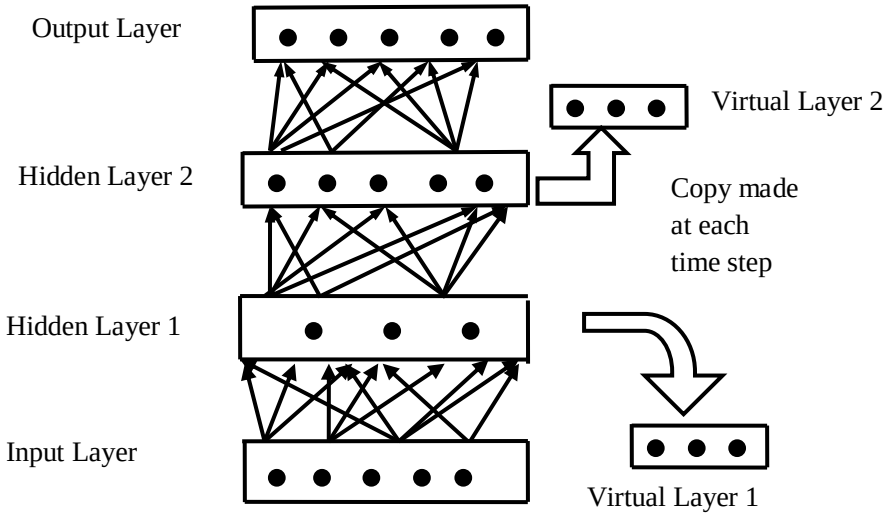

Figure 8.2 An extended simple RNN

8.4 RNN MODELLING

In this section, it is proposed to model the Elman Simple neural Network (SRN) to predict the grain sizes of Al-4.5Cu-5TiB_2 composite for the data used for training the FFNN for grain sizes prediction shown at Table 4.1. This table is reproduced again for convenience of the reader in Table 8.1.

Elman Simple Recurrent Network (SRN) was modelled for grain sizes as well as hardness predictions. The SRN with two context layers were tried with two hidden layer and with different combinations of number of neurons in each layer for different combinations of η and α. The networks failed to converge for a variety of combinations mentioned above. The SRN with Elman architecture uses a context layer that contains the same number of neurons as that in the hidden layer. The output of each hidden neuron which is being copied in the context layer will contain neurons with exciting as well as inhibiting signals. These neurons then pass on the signals through weighted connections to each neuron in the current hidden layer in the next time step. Also these neurons receive signals from the neurons in the previous layer during this time step. Due to this, the previously excited neuron or the neuron which

otherwise would have received a consistent excited signal from previous layer neurons may get inhibiting signals from the context layer neurons or vice versa. This probably, does not allow the network to move progressively along the path of negative gradient on the MSE weight plane. Such a phenomenon is likely to cause an oscillatory profile on the MSE synaptic weight plane, as witnessed while training the simple Elman recurrent network.

In order to overcome this shortcoming, various strategies discussed hereunder were tried:

a. The networks with single hidden layer were trained for the same architectures mentioned earlier with different combinations of η and α. During training, it was observed that the network does not converge. The system learns smoothly during initial phase. But as the training progresses, the network starts oscillating randomly. Further it is observed that the oscillations decrease and the network stops learning and MSE reaches a value much higher than the pre set value which in our case is selected as 0.0001, thus indicating that the network has not been able to map the input output pattern.

b. In the next instance, the neural network model was modified with each neuron in the hidden layer giving feedback only to itself. The networks were modelled for each of the case with similar architectures discussed at (a) above with different combinations of η and α. It was observed that the networks still oscillate during training and fail to converge to the pre-set value, but a better convergence is seen as indicated by slightly lower MSE indicating that learning capability of the network has slightly improved. But the convergence obtained is nowhere near the pre-set value of MSE. Hence, this strategy, though could not be discarded totally, was found to be ineffective.

c. In the modified model stated at (b) above, the weight vectors of a partially trained ANN with similar architecture were borrowed. The ANN network is partially trained till a steep negative gradient is identified on the MSE weights plane indicating the downward movement of MSE. The SNN with single context layer for second hidden layer, with each neuron giving feedback to itself in layer 2 is modeled with similar architecture as that of partially trained ANN. The weight vectors of the SNN from input layer to hidden layer 1,

hidden layer1 to hidden layer 2 and from hidden layer 2 to output layer are replaced by the corresponding weight vectors of partially trained ANN. The biases for different layers except the context layers of the SNN are also replaced by the corresponding biases from the partially trained ANN. The weight vector from the context layer neurons to hidden layer neurons (each neuron to itself) is taken as a zero vector (unbiased). Once the architecture is finalized this way, the network is trained. Upon training with the same values of η and α as that used for partially trained ANN, the SNN so formulated is found to converge excellently. The convergence of SNNs so modeled is found to be better as compared to the parent ANNs from which these have been modelled. The performance of the SNNs modelled from the parent ANNs is demonstrated using the following cases. The SNN so developed has been named as Hybrid RNN (HRNN), since the RNN incorporates the weights from the partially trained FFNN for its processing. Figure 8.3 shows the block diagram for such an HRNN model formulation.

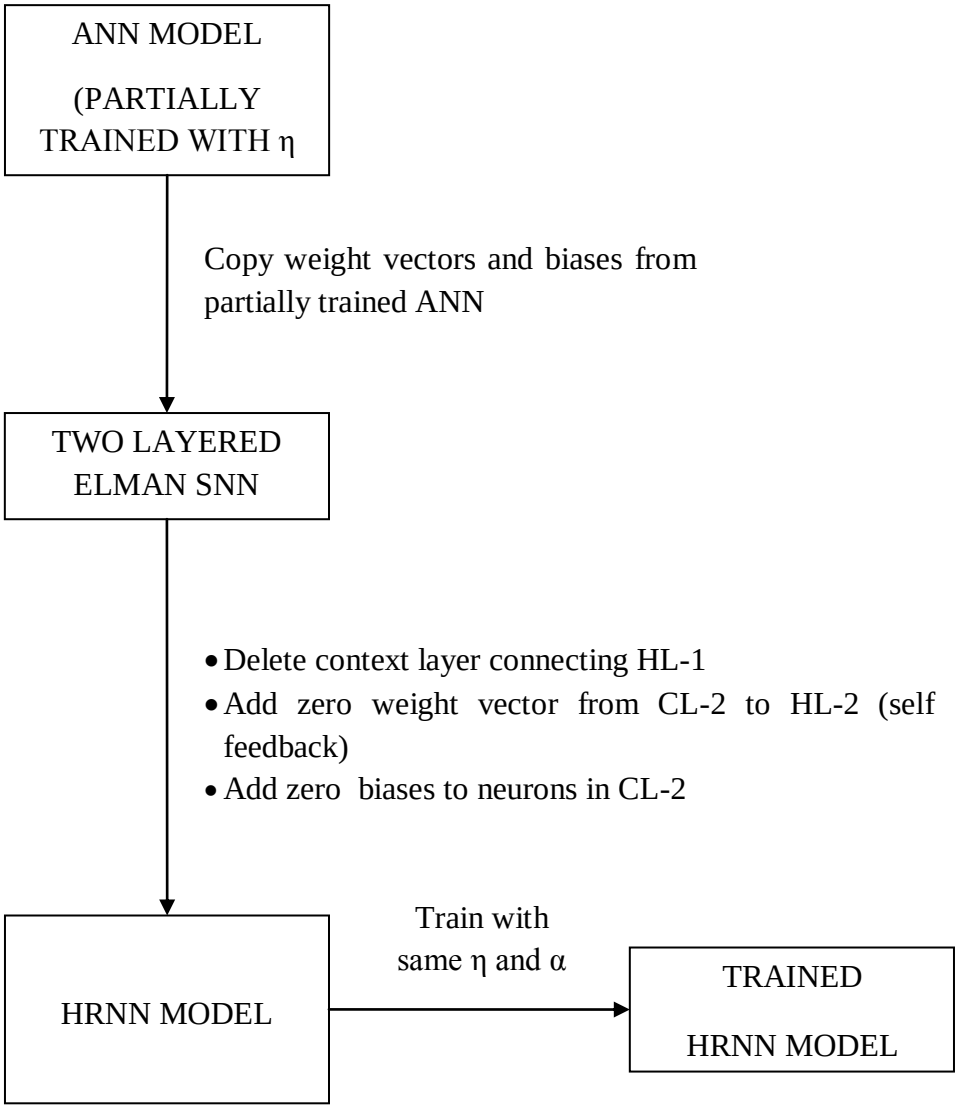

Figure 8.3 Formulation of HRNN model

Table 8.1 Experimental data on Al-4.5Cu-5TiB_2 composite mushy state rolled in as cast and pre-hot rolled conditions (Herbert 2007).

Specimen Description	Liquid Volume Fraction	As cast Al-4.5Cu-5TiB_2 Composite samples subjected to mushy state rolling		Pre hot rolled Al-4.5Cu-5TiB_2 Composite samples subjected to mushy state rolling	
		Grain size (μm)		Grain size (μm)	
		Large	Small	Large	Small
As cast		50 ± 8			
Hot rolled				52 ± 15	28 ± 9
2.5% thickness reduction	f_l ~ 0.1	62 ± 14	27 ± 12	43 ± 16	27 ± 13
	f_l ~ 0.2	58 ± 18	33 ± 11	42 ± 18	26 ± 11
	f_l ~ 0.3	66 ± 15	37 ± 10	47 ± 20	25 ± 11
5% thickness reduction	f_l ~ 0.1	54 ± 16	25 ± 9	42 ± 16	26 ± 11
	f_l ~ 0.2	51 ± 11	31 ± 10	41 ± 15	25 ± 12
	f_l ~ 0.3	55 ± 14	32 ± 10	46 ± 17	24 ± 11
7.5% thickness reduction	f_l ~ 0.1	62 ± 20	32 ± 13	40 ± 15	26 ± 10
	f_l ~ 0.2	48 ± 19	26 ± 12	39 ± 15	25 ± 11
	f_l ~ 0.3	53 ± 18	27 ± 13	45 ± 17	24 ± 09
10% thickness reduction	f_l ~ 0.1	49 ± 17	29 ± 11	47 ± 18	32 ± 13
	f_l ~ 0.2	47 ± 14	30 ± 12	43 ± 16	25 ± 11
	f_l ~ 0.3	54 ± 12	26 ± 11	45 ± 16	27 ± 12

The formulation of a Hybrid Recurrent Neural Network (HRNN) is demonstrated in the following subsection by taking the example of a partially trained FFNN for prediction of grain sizes of mushy state rolled Al-4.5Cu-5TiB_2 composite when rolled in as cast as well as from pre hot rolled condition. For this purpose, two Elman SRN architectures have been selected:

a) Elman SRN with 4 input neurons corresponding to material type, % thickness reduction, % liquid volume fraction and % TiB_2 respectively, 7 and 4 neurons in the first and second hidden layers, and 2 output neurons corresponding to large and small grain sizes respectively. This architecture is denoted as 4-7-4-2 architecture.

b) The second architecture considered for demonstration of HRNN is the one containing 4 neurons in the input layer, 9 neurons each in the first and second hidden layer and 2 neurons in the output layer. This architecture is denoted as 4-9-9-2 architecture.

8.4.1 Modelling of HRNN with 4-7-4-2 architecture

The network was trained with learning rate parameter as 0.85 and momentum factor 0.65. Initially the network is trained as an ANN network. Table 8.2 gives the details of the error in prediction in terms of MSE existing at various stages of network training. The ANN network converges to a MSE of 0.000362612 after 15 lakh epochs. To obtain the HRNN, the ANN is now trained till 50000 epochs. The weights of this ANN are then borrowed in the input weights file for RNN training. The network is found to oscillate after it reaches a MSE of 0.00205. This happens, probably due to the fact that the ANN training up to 50000 epochs has not provided sufficient gradient descent on the MSE weights plane for the Hybrid RNN to further travel in the direction of negative gradient.

Table 8.2 Variation of MSE with number of epochs

Sr. No.	Number of epochs	MSE
1	1	0.329771
2	100000	0.00467185
3	200000	0.002215
4	300000	0.00153321
5	400000	0.0014147
6	500000	0.00129209
7	600000	0.00105979
8	700000	0.000684544
9	800000	0.00056784
10	1500000	0.000362612

Further to this, the ANN was trained up to 100000 epochs and the weights were borrowed in the input weights file for RNN training. The results were better than the first case, but the convergence was found to be slow. After training for 150000 epochs, the MSE is found to be 0.0013. Hence in the next step the ANN is trained for 500000 epochs and subsequently, the weights are borrowed in the input file for RNN

training. It was found that after further training of HRNN for around 227000 epochs, the network converged satisfactorily.

The results of the HRNN predictions of grain sizes after being trained from partially trained ANN of 4-7-4-2 architecture are compared with the parent ANN having same architecture after being trained for 1500000 epochs and are listed in Table 8.3. In the material type column, numeral 1 denotes as cast condition of Al-4.5Cu-5TiB_2 composite, while numeral 2 indicates its pre hot rolled condition.

It is seen that the maximum error is |0.58|% at 5 % thickness reduction with 10 % liquid volume fraction in the as cast composite for small grain size, while for large grain size it is also at the same location. However in the majority of the cases, the error with hybrid RNN is within |0.5|%. The HRNN is modelled after borrowing the weights from partially trained ANN after 5 lakh epochs. Further, the HRNN converged nicely to a MSE of 0.000362612. Thus to achieve the same degree of convergence HRNN has consumed 776000 lesser epochs as compared to that of parent ANN, thus giving a saving of 51.7 % of computational time, which is quite substantial. Furthermore, the error in predictions too is quite insignificant in comparison with the parent ANN predictions for the same data.

8.4.2 HRNN with 4-9-9-2 architecture

Here, the network is formulated with 4 input neurons, 9 neurons each in second and third layer and 2 output neurons. The number of input vectors is taken as 240, just to emphasize that the number of input vectors has no great bearing on the convergence of Hybrid RNN. The ANN network is first trained until 50000 epochs and then hybrid RNN is constructed by borrowing weights of trained ANN. The network is further trained for 85000 epochs as it gave the same MSE as that of parent ANN when trained to 277356 epochs.

Table 8.3 Comparison of grain sizes by ANN and Hybrid RNN after 2.24 lakh epochs of HRNN and 15 lakh epochs of ANN

Sr. No.	Input			Output					
				Grain Sizes					
				Large			Small		
	Mat/ Pro.	% TR*	%LVF**	ANN	RNN	% Error over ANN	ANN	RNN	% Error over ANN
1	1	2.5	10	61.21	61.10	0.190139	28.12	28.03	0.307209
2	1	2.5	20	58.33	58.32	0.026569	33.37	33.36	0.018879
3	1	2.5	30	66.01	65.97	0.054232	36.22	36.2	0.064047
4	1	5	10	54.53	54.23	0.54335	23.87	23.73	0.578546
5	1	5	20	50.53	50.52	0.023745	28.84	28.84	0.004854
6	1	5	30	55.64	56.66	-1.83923	29.86	29.86	0.024776
7	1	7.5	10	61.72	61.62	0.168968	31.65	31.58	0.21482
8	1	7.5	20	47.58	47.58	0.007986	26.49	26.49	-0.01057
9	1	7.5	30	53.17	53.13	0.060559	27.75	27.75	0.022696
10	1	10	10	48.36	48.36	0.004135	31.30	31.30	0.002236
11	1	10	20	48.28	48.27	0.010149	28.31	28.31	-0.00671
12	1	10	30	52.63	52.60	0.057751	27.88	27.87	0.020085
13	2	2.5	10	43.25	43.21	0.085769	27.89	27.88	0.047323
14	2	2.5	20	43.18	43.19	-0.01343	27.26	27.27	-0.0154
15	2	2.5	30	47.31	47.30	0.018177	26.77	26.77	-0.00486
16	2	5	10	41.21	41.20	0.032511	26.38	26.37	0.013267
17	2	5	20	41.05	41.05	-0.02168	25.33	25.34	-0.02566
18	2	5	30	44.99	44.99	0.021111	25.37	25.38	-0.01025
19	2	7.5	10	41.79	41.79	-0.00885	26.30	26.30	-0.01369
20	2	7.5	20	39.70	39.71	-0.0267	24.06	24.07	-0.03282
21	2	7.5	30	44.71	44.70	0.022366	24.92	24.92	-0.01163
22	2	10	10	46.25	46.25	-0.00757	30.49	30.49	-0.00394
23	2	10	20	42.35	42.35	-0.01983	26.46	26.46	-0.02381
24	2	10	30	45.59	45.58	0.025658	25.61	25.61	-0.00781

% TR* - % ThicknessReduction
1 – as cast
Mat – Material

% LVF** - %Liquid Volume Fraction
2 – Pre hot rolled
Pro. - Process

The comparison of predictions between the parent ANN with 4-9-9-2 architecture and its Hybrid RNN is given in Table8.4 below for a MSE of 0.0001762 achieved by parent ANN after being trained using 277356 epochs. The HRNN was trained with 240 patterns to emphasize that the data set available for training has no bearing on the implementation of the model. The total number of epochs of HRNN coupled with those of partially trained ANN works out to 135000 epochs, thus giving a saving in computation time in excess of 50 %. It can be seen that the error in estimation with hybrid RNN with respect to Parent ANN is within 7 %, while in majority of the cases the error is within 1 %.

Table 8.4 Comparison of grain size predicted by ANN & Hybrid RNN after MSE = 0.0001762

Sr. No.	Input			Output					
				Grain Size (µm)					
				Large			Small		
	Mat / Process	% TR*	%LVF**	ANN	RNN	% Error over ANN	ANN	RNN	% Error over ANN
1	1	2.5	10	54.1	54.2	-0.0369	29.52	29.4	0.1355
2	1	2.5	20	52.6	52.6	-0.057	34.10	34.0	0.0293
3	1	2.5	30	59.9	59.9	-0.0835	37.50	37.7	-0.6667
4	1	5	10	51.0	51.0	-0.0392	29.04	29.0	0.0689
5	1	5	20	46.2	45.6	1.2967	30.67	30.6	-0.0326
6	1	5	30	52.2	52.2	-0.0957	33.61	31.3	6.7539
7	1	7.5	10	49.4	49.4	-0.0202	29.47	29.4	0.0679
8	1	7.5	20	43.8	43.8	0	29.43	29.4	0
9	1	7.5	30	49.2	49.2	-0.0813	28.09	28.3	-0.7832
10	1	10	10	49.0	49.0	0	30.59	30.5	0.0981
11	1	10	20	43.7	43.7	-0.0229	29.91	29.9	0.0334
12	1	10	30	49.1	49.4	-0.6923	27.39	27.5	-0.6572
13	2	2.5	10	44.8	44.8	0.0669	24.6	24.5	0.122
14	2	2.5	20	42.8	42.8	0	26.55	26.5	0
15	2	2.5	30	48.2	48.3	-0.0414	26.74	26.9	-0.7479
16	2	5	10	43.5	43.5	0.023	24.99	24.9	0
17	2	5	20	39.5	39.5	0	25.13	25.1	-0.0398
18	2	5	30	43.7	43.7	-0.0458	24.72	24.9	-0.7282
19	2	7.5	10	43.6	43.6	0.0229	26.26	26.2	0.0381
20	2	7.5	20	38.8	38.8	0.0257	25.38	25.3	0

21	2	7.5	30	42.8	42.8	0.0233	25.04	25.0	0
22	2	10	10	44.9	44.9	0.0445	28.19	28.1	0.0709
23	2	10	20	40.3	40.3	0.0248	26.95	26.9	0.0371
24	2	10	30	44.3	44.3	-0.0451	26.661	26.7	-0.4081

% TR* - % Thickness Reduction Mat - Material % LVF** - % Liquid Volume Fraction

8.4.3 Statistical testing of RNN model predictions

In this section it is proposed to assess statistically the predictions of RNN. To be able to perform the statistical testing, the predictions of parent ANN and HRNN are compared with the actual values of grain sizes as well as amongst themselves. The resulting errors are then statistically checked using the following statistical tools.

In the statistical analysis carried out (refer APENDIX III), the following three tests were being used:

1. Testing the quality of two means using the two sample student_t test.
2. Testing whether the population has standard mean normal distribution using one sample Kolmogorov – Smirnov test.
3. Testing if the two populations belong to the same continuous distribution using two samples Kolmogorov – Smirnov test.

K-S test for single sample and two samples were used to test the normality of the distribution of errors in prediction of large and small grain sizes as predicted by ANN and HRNN with different architectures mentioned at 8.4.1 and 8.4.2 above. The errors were calculated between the predicted values obtained from ANN and actual values and also between the predicted values obtained from HRNN and actual values. A third type of error was calculated between the values predicted by HRNN and ANN. Further to this, two sample student t_test was performed for testing the equality of means of populations representing the errors between ANN and HRNN predictions for large grain size and small grain size. To be able to analyze the data more meaningfully, the population of errors was divided into errors in predictions for as cast Al-4.5Cu-5TiB_2 composite and pre hot rolled Al-4.5Cu-5TiB_2 composite. For the

purpose of statistical analysis of the performance of HRNN with the fully trained parent ANN, the following terminology of errors is defined.

a. Error (a): Error in prediction of large grain size and small grain size by ANN with 4-7-4-2 architecture over the target values.
b. Error (b); Error in prediction of large grain size and small grain size by HRNN with 4-7-4-2 architecture over the target values.
c. Error(c); Error in prediction of large grain size and small grain size by ANN with 4-9-9-2 architecture over the target values.
d. Error (d); Error in prediction of large grain size and small grain size by HRNN with 4-9-9-2 architecture over the target values.

8.4.3.1 Testing of equality of means

Table 8.5 gives the results of the two sample student t test performed on the error population deduced from the predictions of HRNN and ANN with different architectures. It can be seen that the means of the errors from HRNN prediction populations are comparable to the mean values of populations obtained from ANN predictions for similar architectures. Furthermore, the standard deviation values also are comparable for similar architectures of ANN and HRNN.

In testing of hypothesis, the strength of the conclusion is decided by level of significance α. The popular value of α is 0.05. The decision about the test is based on the value of the test statistics obtained from the sample and the benchmark value of appropriate test statistics obtained from the tables, using α and degrees of freedom (which can always be obtained from the size of sample).

However, while reporting the conclusion, the value of test statistic obtained is never reported. As a result, closeness of this test value obtained from the sample and the bench mark value of appropriate test statistic also does not get reported.

This difficulty is overcome when p value of test is indicated. The p value indicates the probability of obtaining a test statistic as extreme as the one actually observed, assuming that the null hypothesis is true.

Table 8.5 Results of two sample student t test.					
Architecture		Large grain size **(HRNN) Error Population 1**		Small grain size **(ANN) Error Population 2**	
		As cast	Pre hot rolled	As cast	Pre hot rolled
4-7-4-2	Mean:	-0.0334	0.0034	-0.0136	0.0047
	St.dev:	0.0401	0.0068	0.0244	0.0026
4-9-9-2	Mean:	-0.0201	-0.0134	-0.0053	0.0052
	St.dev:	0.0099	0.0073	0.0022	0.0015

St. dev = standard deviation

8.4.3.2 Testing errors for standard normal distribution

Testing of the error distribution of ANN and HRNN predictions over target values of large grain sizes and small grain sizes was carried out using one sample Kolmogorov – Smirnov test. For this purpose, the various errors as defined in section 8.4.3 were considered. The results of the test are tabulated in Table 8.6. It can be seen that with a significance level of 5% ($\alpha = 0.05$), used for the test, all the error distributions i.e. Error (a) to Error (d) are accepted as standard normal distributions. Table 8.6 gives the p values for all the error distributions. H_0 indicates that the error population has normal distribution, while H_1 indicates that the error population does not have normal distribution.

Table 8.6 Results of one sample Kolmogorov – Smirnov test.					
Test No.	**α**	**Errors**	**p value**		**Conclusion**
			Large grain size	Small grain size	
A	0.05	Error(a)	0.7366	0.8174	H_0: Accepted
B	0.05	Error(b)	0.8174	0.0940	H_0: Accepted
C	0.05	Error(c)	0.1879	0.1860	H_0: Accepted
D	0.05	Error(d)	0.1983	0.1901	H_0: Accepted

8.4.3.3 Testing of equality of continuous distributions using two samples Kolmogorov – Smirnov test

Here the distribution of errors between ANN predicted values for grain sizes using 4-7-4-2 and 4-9-9-2 architectures over target values of grain sizes were checked with their counterparts predicted by HRNN with similar architectures, for equality. The results of this test are presented in Table 8.7. H_0 indicates that the two error distributions under test are equal, while H_1 indicates that they are not equal.

Table 8.7 Results of two samples Kolmogorov – Smirnov test.

Test No.	Population of errors tested	α	p value		Conclusion
			Large grain size	Small grain size	
A	Error(a) v/s Error(b)	0.05	0.9999	0.1094	H_0: Accepted
B	Error(c) v/s Error(d)	0.05	0.9999	0.9999	H_0: Accepted

From the discussions carried out in this and the previous two sections, namely 8.4.3.1 and 8.4.3.2, it is seen that the predictions done by the trained parent ANN and the HRNN formulated from the partially trained parent ANN are statistically equivalent. This lends us with an important decision making criterion to select HRNN as a possible mathematical model to compliment ANN modelling using FFNN architectures, especially when the training of FFNN becomes a cumbersome process in terms of problems related to its convergence. Thus the equivalence of HRNN model with ANN model is well established, in addition to lesser training time for HRNNs.

Discussion on HRNN models for prediction of different parameters of mushy state rolling of Al-4.5Cu-5TiB_2 composite and their comparison with the corresponding ANN models are presented below.

8.5 MODELLING OF HRNN FOR PREDICTION OF GRAIN SIZES

The hybrid RNN will now be modelled afresh for prediction of grain sizes using architecture similar to that which was used for ANN model for grain size predictions. In other words, the HRNN now proposed to be modelled is formulated by borrowing the weights from a partially trained parent ANN used in chapter 4 for prediction of grain sizes. The architecture used for the parent ANN of chapter 4 had the designation 3-7-4-2. This ANN was trained with $\eta = 0.85$ and $\alpha = 0.65$ till steep downward gradient is witnessed on the MSE weights plane, which can be witnessed from the programme execution on the computer screen. Such steep decrease was observed at 500000 lakh epochs where the MSE was found to be 0.00128. At this point HRNN with same architecture was formulated by borrowing the weights from parent ANN. The weights in the context layers were kept as zero (i.e. unbiased). The network was then trained with same values of η and α. After training for a further 2 lakh iterations, the network converged very well with a MSE of 0.000236682.

8.5.1 Comparison of prediction of grain sizes by ANN and HRNN for mushy state rolled as cast Al-4.5Cu-5TiB_2 composite

Table 8.8 lists down the values of large grain sizes and small grain sizes (μm) predicted by ANN and HRNN respectively along with the error in prediction of grain sizes by HRNN over ANN.

Table 8.8 ANN & HRNN comparison of grain sizes for Al-4.5Cu-5TiB_2 composite rolled in mushy state in as cast condition.

Sr. No.	Input		Output					
			Grain Sizes (μm)					
			Large			Small		
	% Th. Red	%Liq. Vol. Fraction	ANN	RNN	% Error	ANN	RNN	% Error
1	0	0	49.9944	49.99	0.0088	49.8947	49.89	0.0094
2	2	17	61.5498	61.48	0.1134	30.2633	30.26	0.0109
3	2.5	5	66.7204	66.64	0.1205	27.2855	27.31	-0.0898
4	2.5	10	60.7838	60.7	0.1379	27.4532	27.46	-0.0248
5	2.5	20	59.338	59.28	0.0977	33.8438	33.82	0.0703
6	2.5	30	64.776	64.72	0.0865	35.8221	35.84	-0.05

7	2.5	35	66.6396	66.64	-0.0006	30.0602	30.06	0.0007
8	5	5	69.5573	69.49	0.0968	27.2271	27.25	-0.0841
9	5	10	55.6733	55.59	0.1496	25.8852	25.9	-0.0572
10	5	20	49.9853	49.95	0.0706	29.4956	29.48	0.0529
11	5	30	55.5784	55.53	0.0871	33.4465	33.45	-0.0105
12	5	35	61.1633	61.17	-0.011	28.4914	28.48	0.04
13	6	7	66.9744	66.89	0.126	28.032	28.01	0.0785
14	6	17	48.496	48.47	0.0536	25.793	25.8	-0.0271
15	6	33	56.3759	56.38	-0.0073	28.2583	28.25	0.0294
16	7.5	5	71.394	71.39	0.0056	32.4656	32.49	-0.0752
17	7.5	10	61.5025	61.45	0.0854	30.92	30.91	0.0323
18	7.5	20	47.299	47.23	0.1459	27.3059	27.26	0.1681
19	7.5	30	52.922	52.91	0.0227	26.4012	26.4	0.0045
20	7.5	35	56.2987	56.32	-0.0378	24.2107	24.19	0.0855
21	10	5	48.5162	48.52	-0.0078	30.514	30.52	-0.0197
22	10	10	49.2457	49.26	-0.029	30.5459	30.54	0.0193
23	10	20	48.0792	48.07	0.0191	30.494	30.49	0.0131
24	10	30	54.1504	54.17	-0.0362	26.2361	26.22	0.0614
25	10	35	59.3253	59.36	-0.0585	21.9236	21.88	0.1989
26	11.5	17	47.0124	47	0.0264	30.4498	30.44	0.0322
27	12.5	5	46.7048	46.69	0.0317	30.4369	30.43	0.0227
28	12.5	10	46.7111	46.69	0.0452	30.4372	30.44	-0.0092
29	12.5	20	46.7789	46.76	0.0404	30.44	30.43	0.0329
30	12.5	30	46.8364	46.83	0.0137	30.391	30.38	0.0362
31	12.5	35	48.8614	48.87	-0.0176	29.249	29.23	0.065

It can be seen from Table 8.8 that the maximum error of 0.1496 % in prediction is observed in the as cast composite. This maximum error is observed when composite is mushy state rolled with 5 % thickness reduction from temperature corresponding to 10 % liquid volume fraction. The lowest error in large grain size prediction is observed as -0.0585 % with 10 % thickness reduction when rolled at temperature corresponding to 35 % volume fraction of liquid. A maximum error of 0.1989 % is witnessed in case of small grain size prediction when the composite is mushy state rolled with 35 % liquid volume fraction to 10% thickness reduction. A minimum error of -0.0898 % occurs in small grain size predictions at 2.5 % thickness reduction rolled from temperature corresponding to 5 % volume fraction of liquid.

Table 8.9 Comparison of grain sizes predictions by ANN and HRNN for Al-4.5Cu-5TiB_2 composite rolled in mushy state in Pre Hot Rolled condition.

Sr. No.	Input		Output					
			Grain Sizes (μm)					
			Large			Small		
	% Th. Red	%Liq. Vol. Fraction	ANN	RNN	% Error	ANN	RNN	% Error
1	0	0	51.985	51.97	0.0289	28.51	28.53	-0.0537
2	2	17	42.619	42.62	-0.0023	25.46	25.47	-0.035
3	2.5	5	43.635	43.63	0.0115	25.40	25.41	-0.0209
4	2.5	10	42.282	42.28	0.0047	25.38	25.39	-0.0189
5	2.5	20	42.475	42.48	-0.0118	25.52	25.53	-0.0235
6	2.5	30	47.616	47.64	-0.0504	24.55	24.57	-0.0472
7	2.5	35	47.731	47.78	-0.1027	23.81	23.82	-0.0273
8	5	5	42.016	42.02	-0.0095	25.27	25.28	-0.0142
9	5	10	40.908	40.91	-0.0049	25.23	25.24	-0.019
10	5	20	40.675	40.68	-0.0123	25.30	25.31	-0.0387
11	5	30	45.474	45.51	-0.0792	24.34	24.37	-0.085
12	5	35	46.701	46.76	-0.1263	23.60	23.62	-0.0597
13	6	7	41.136	41.14	-0.0097	25.24	25.26	-0.0499
14	6	17	40.569	40.58	-0.0271	25.22	25.23	-0.0131
15	6	33	46.718	46.77	-0.1113	23.80	23.82	-0.0542
16	7.5	5	47.096	47.08	0.034	30.34	30.33	0.0349
17	7.5	10	40.752	40.76	-0.0196	25.33	25.34	-0.0103
18	7.5	20	40.501	40.51	-0.0222	25.21	25.22	-0.0337
19	7.5	30	45.184	45.21	-0.0575	24.37	24.39	-0.0771
20	7.5	35	46.729	46.79	-0.1305	23.51	23.53	-0.0851
21	10	5	46.703	46.69	0.0278	30.43	30.42	0.0329
22	10	10	46.687	46.66	0.0578	30.41	30.40	0.0477
23	10	20	42.093	42.05	0.1022	26.52	26.49	0.1293
24	10	30	44.7634	44.78	-0.0371	26.82	26.83	-0.0373
25	10	35	45.7546	45.81	-0.1211	24.42	24.44	-0.0708
26	11.5	17	46.6799	46.66	0.0426	30.41	30.41	0.0266
27	12.5	5	46.699	46.68	0.0407	30.43	30.42	0.0411
28	12.5	10	46.692	46.67	0.0471	30.42	30.42	0.0289
29	12.5	20	46.7	46.67	0.0642	30.43	30.41	0.0851
30	12.5	30	46.716	46.70	0.0342	30.42	30.42	0.0164
31	12.5	35	46.526	46.53	-0.0086	29.60	29.6	0.0169

8.5.2 Comparison of prediction of grain sizes by ANN and HRNN for mushy state rolled Al-4.5Cu-5TiB_2 composite in pre hot rolled condition

Table 8.9 shows the values of large and small grain sizes predicted by ANN and HRNN for pre hot rolled composite rolled in mushy state to different thickness reductions ranging from 2 to 12.5 % and from mushy state temperatures corresponding to 5 to 35 % volume fractions of liquid in the composite. From Table 8.9, it can be seen that maximum error of 0.1022 % occurs in prediction of large grain size when pre hot rolled composite is rolled to 10 % thickness reduction in mushy state with 20 % volume fraction of liquid in the pre hot rolled composite. Minimum error in prediction of -0.1305 % is witnessed with 7.5 % thickness reduction when mushy state rolled from 35 % liquid volume content in the composite. In case of small grain size prediction by HRNN, maximum and minimum errors of prediction of HRNN over ANN are 0.1293 and -0.0851 % at 10 and 7.5 % thickness reduction and corresponding to 20 and 35 % liquid volume fractions respectively.

From Table 8.8 it is seen that the HRNN model predicts grain sizes for as cast composite rolled from mushy state within an error of |0.2|% over ANN model predictions. Also Table 8.9 shows that the HRNN model predicts large and small grain sizes within an error of |0.1305|% over corresponding ANN model predictions. Moreover, the time required for training is significantly lower than that for ANN model. Thus the ANN model can be replaced by a HRNN model, especially in cases where there is dynamic feedback of changing process parameters usually associated with smart manufacturing systems.

8.6 MODELLING OF HRNN FOR PREDICTION OF HARDNESS

In chapter 5, modelling of ANN for prediction of hardness of mushy state rolled Al-4.5Cu-5TiB_2 composite was discussed. The architecture of the four layer perceptron used for prediction of hardness was 5-5-3-1. It was found to converge satisfactorily after 325000 iterations with an MSE of 0.0000975. The formulation of HRNN was done from a parent ANN containing 5 input nodes (corresponding to material type, % thickness reduction, % liquid volume fraction, large grain size and small grain size of

the composite), 5 and 3 nodes in first and second hidden layers respectively and one output node for hardness. After training the network for 50000 iterations a steep gradient was observed on the MSE v/s Weights plane. At this point, the weights from this partially trained ANN were borrowed into the architecture of RNN to formulate HRNN. The HRNN was then further trained. After a further training of 200000 iterations, the network converged to the same MSE as obtained from ANN having 5-5-3-1 architecture. Thus the total saving in time of around 23.07 % is achieved using HRNN formulation. The results of hardness prediction by HRNN as against that by ANN for mushy state rolled composite rolled in as cast as well pre hot rolled condition are discussed in the forthcoming sub sections at 8.6.1 and 8.6.2 respectively.

8.6.1 Comparison of hardness predictions made by HRNN with ANN predicted values of hardness for Al-4.5Cu-5TiB_2 composite rolled from mushy state in as cast condition

Table 8.10 shows the values of hardness predicted by HRNN and ANN modelled for predicting hardness of Al-4.5Cu-5TiB_2 composite, mushy state rolled in as cast condition to various thickness reductions ranging from 2 to 12.5 % and at mushy state temperatures corresponding to 5 to 35 % liquid volume fractions.

Table 8.10 RNN predicted values of hardness of as cast Al-4.5Cu-5TiB_2 composite samples subjected to mushy state rolling with ANN predicted values

Specimen description		Hardness (Hv)			Error (%)	
		Experimental	ANN	RNN	RNN over ANN	RNN over Experimental
As cast		78	77.66	78.12	-0.5923	-0.1538
*2 % Thickness Reduction	*f1~ 0.17	94	92.662	97.18	-4.8758	-3.383
2.5% Thickness Reduction	f_l~ 0.05	-------	83.212	84.41	-1.4397	-------
	[a]f_l ~ 0.1	90	87.89	90.95	-3.4816	-1.0556
	[a] f_l ~ 0.2	105	105.45	103.3	2.0389	1.619
	[a] f_l ~ 0.3	88	90.144	86.28	4.2865	1.9545
5% Thickness Reduction	[a] f_l ~ 0.1	101	100.13	100.78	-0.6492	0.2178
	[a] f_l ~ 0.2	112	112.28	111.68	0.5344	0.2857
	[a]f_l ~ 0.3	96	93.473	99.96	-6.94	-4.125

*6% Thickness reduction	*f_1~ 0.07	89	88.22	92.18	-4.4888	-3.573
	*f_1~0.17	114	112.18	112.06	0.107	1.7018
	*f_1~0.33	92	92.431	84.11	9.0024	8.5761
7.5% Thickness Reduction	af_l ~ 0.1	105	104.63	107.13	-2.3894	-2.0286
	af_l ~ 0.2	117	116.31	117.10	-0.6792	-0.0855
	afl ~ 0.3	103	101.05	102.17	-1.1084	0.8058
10% Thickness Reduction	af_l ~ 0.1	118	117.15	115.6	1.3231	2.0339
	af_l ~ 0.2	121	121.14	121.59	-0.3715	-0.4876
	af_l ~ 0.3	106	104.63	106.99	-2.2556	-0.934
* 11.5% Thickness Reduction	*f_1 ~ 0.17	123	122.4	123.05	-0.531	-0.0407
12.5% Thickness Reduction	f_l ~ 0.05	-------	117.79	116.37	1.2055	-------
	f_l ~ 0.1	-------	121.72	120.37	1.1091	-------
	f_l~ 0.2	-------	122.86	124.71	-1.5058	-------
	f_l ~ 0.3	-------	102.3	118.54	-	-------
	f_l ~ 0.35	-------	103.73	102.44	1.2436	-------

It can be seen from Table 8.10 that the error in prediction of hardness by RNN compared to that by ANN within the range of experimentation is within |6.95|% while that of RNN over target values is within |8.58|%. However, the maximum error in prediction by the model is -15.8749 % corresponding to rolling with 12.5 % and with composite mushy state rolled from temperature corresponding to 30 % volume fraction of liquid. Thus it appears that the model is ideally suited for making predictions within the data set for which the HRNN is trained with certain constraints for extrapolation. Moreover, while extracting the results of the HRNN for values outside the range of training data, error in excess of 40 % was observed corresponding to 2.5 % thickness reduction with 35 % liquid volume fraction, as compared to the ANN predictions. Thus the HRNN model proposed for hardness predictions for mushy state rolled Al-4.5Cu-5TiB_2 composite is definitely suitable for interpolating the data for hardness within the range for which the HRNN is trained. Furthermore, it can be observed from Table 8.10, that the error observed between validation experiment results of hardness and HRNN predicted results is within |8.6|%. Kusiak and Kuziak (2002) have reported a maximum error of 8 % in ANN predictions, while Jiahe *et al.* (2003) reported a maximum error of 5.7 % in grain size predictions using ANN. Hence it can be concluded that the model, in addition to prediction of hardness

within the training data range can also extrapolate results within the range of experiments conducted to validate the ANN model i.e. from 2 to 11.5 % thickness reduction and 7 to 33 % liquid volume fraction.

Figure 8.4 through 8.7 show the plots of variation of hardness of Al-4.5Cu-5TiB_2 composite mushy state rolled in as cast condition, predicted by HRNN and by ANN with different thickness reductions, with rolling initiated from mushy state temperatures corresponding to 10, 17, 20 and 30 % volume fractions of liquid in the as cast composite. It can be seen from the plots of Figure 8.4 to Figure 8.6 that the prediction curves of HRNN closely follow the curves of predictions by ANN. However, as can be seen from Figure 8.7, when as cast Al-4.5Cu-5TiB_2 composite containing 30 % volume fraction of liquid is rolled in mushy state, the predictions of hardness by HRNN seem to diverge from predictions made by ANN beyond 11.5 % thickness reduction, clearly indicating that, beyond 11.5 % thickness reduction, the model loses its capability to predict hardness within an acceptable level of accuracy as discussed earlier in this section.

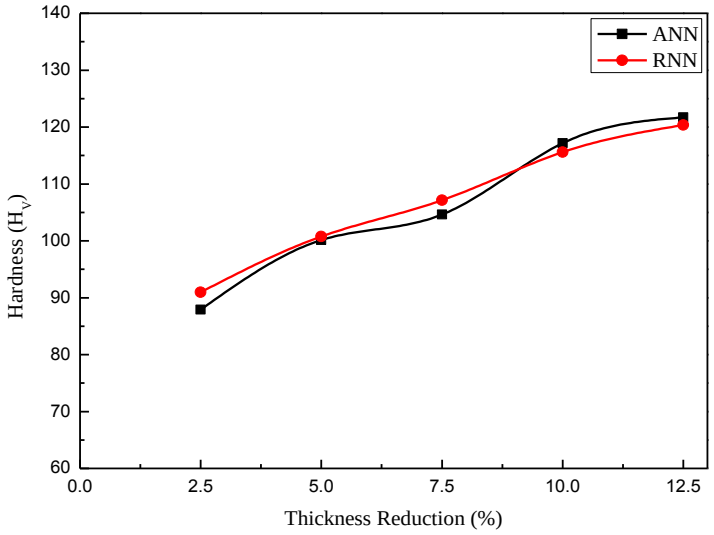

Figure 8.4 Plot showing comparison of predictions of hardness made by ANN and RNN when as cast Al-4.5Cu-5TiB_2 composite is rolled to varying thickness reductions in mushy state with 10% liquid volume fraction.

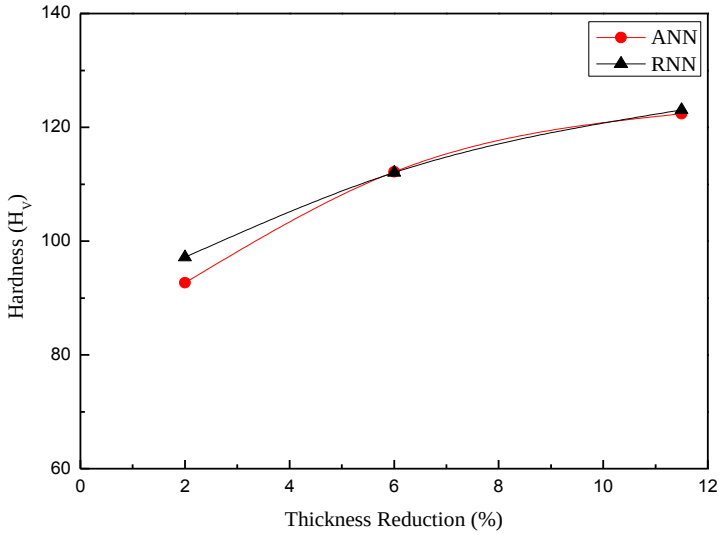

Figure 8.5 Plot showing comparison of predictions of hardness made by ANN and RNN when as cast Al-4.5Cu-5TiB_2 composite is rolled to varying thickness reductions in mushy state with 17% liquid volume fraction.

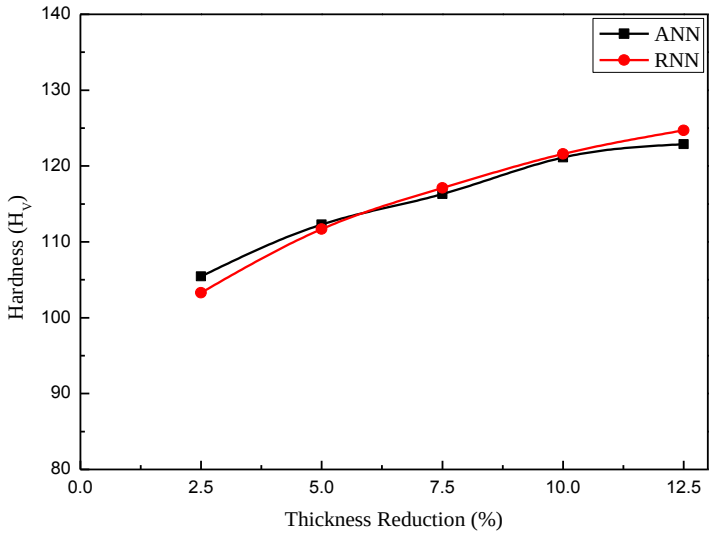

Figure 8.6 Plot showing comparison of predictions of hardness made by ANN and RNN when as cast Al-4.5Cu-5TiB_2 composite is rolled to varying thickness reductions in mushy state with 20% liquid volume fraction.

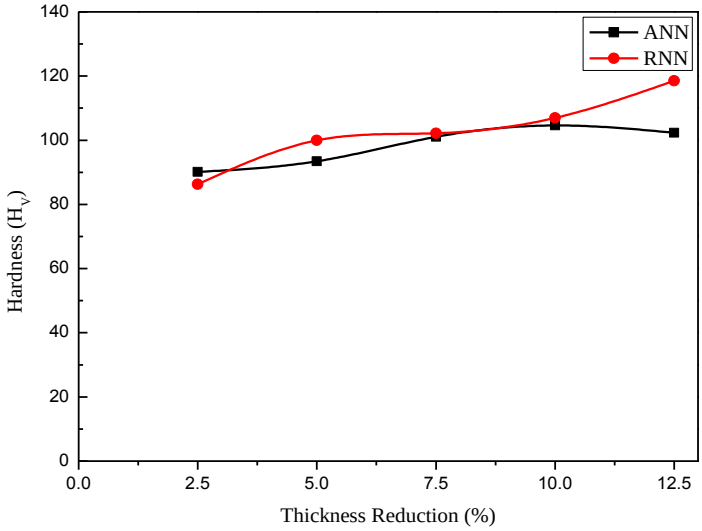

Figure 8.7 Plot showing comparison of predictions of hardness made by ANN and RNN when as cast Al-4.5Cu-5TiB_2 composite is rolled to varying thickness reductions in mushy state with 30% liquid volume fraction.

Table 8.11 RNN predicted values of hardness of pre hot rolled Al-4.5Cu-5TiB_2 composite samples subjected to mushy state rolling with ANN predicted values.

Specimen description		Hardness (Hv)			Error (%)	
		Experimental	ANN	RNN	RNN over ANN	RNN over Experimental
Hot rolling		85	85.264	84.37	1.0585	0.7412
* 2% thickness reduction	*f1~0.17	102	103.49	101.36	2.0582	0.6275
2.5% thickness reduction	fl ~ 0.05	-------	90.7	93.38	-2.9548	-------
	af$_l$ ~ 0.1	95	95.93	96.34	-0.4274	-1.4105
	af$_l$ ~ 0.2	106	105.01	104.9	0.1048	1.0377
	af$_l$ ~ 0.3	88	88.114	88.81	-0.7899	-0.9205
5% thickness reduction	af$_l$ ~ 0.1	104	102.21	100.73	1.448	3.1442
	af$_l$ ~ 0.2	112	111.92	112.29	-0.3306	-0.2589
	af$_l$ ~ 0.3	99	100.15	98.77	1.3779	0.2323
* 6% thickness reduction	*f$_l$ ~ 0.07	101	99.724	104.52	-4.8093	-3.4851
	*f$_l$ ~ 0.17	114	115.57	113.19	2.0594	0.7105
	*f$_l$ ~ 0.33	101	103.3	94.84	14.211	12.2574

7.5% thickness reduction	[a]f_l ~ 0.1	110	110.33	110.74	-0.3716	-0.6727
	[a]f_l ~ 0.2	116	117.27	117.62	-0.2985	-1.3966
	[a]f_l ~ 0.3	108	108.12	105.85	2.0995	1.9907
10% thickness reduction	[a]f_l ~ 0.1	116	116.44	115.16	1.0993	0.7241
	[a]f_l ~ 0.2	121	120.44	121.55	-0.9216	-0.4545
	[a]f_l ~ 0.3	113	112.35	113.3	-0.8456	-0.2655
* 11.5% thickness reduction	*f_l ~ .17	122	122.31	122.53	-0.1799	-0.4344
12.5% thickness reduction	f_l ~ 0.05	-------	115.95	115.49	0.3967	-------
	f_l ~ 0.1	-------	121.18	119.67	1.2461	-------
	f_l ~ 0.2	-------	123.06	124.25	-0.967	-------
	f_l ~ 0.3	-------	112.64	117.91	-4.6786	-------
	f_l ~ 0.35	-------	113.9	104	8.6918	-------

8.6.2 Comparison of hardness predictions made by HRNN with the ANN predicted values for Al-4.5Cu-5TiB_2 composite rolled from mushy state in pre hot rolled condition

The hardness values of pre hot rolled Al-4.5Cu-5TiB_2 composite rolled in mushy state with thickness reductions ranging from 2 to 12.5 % and at mushy state temperatures corresponding to 5 to 35 % volume fraction predicted by HRNN and ANN are presented in Table 8.11. It can be seen from Table 8.11 that maximum error in prediction of HRNN over ANN within the range of data used for training the HRNN lies within |2.1|%. The maximum error is witnessed when the pre hot rolled composite is rolled at mushy state temperature corresponding to 30 % volume fraction of liquid with 7.5 % thickness reduction. Predictions outside the data used for network training result in a maximum error of 8.6918 % when mushy state rolled to 12.5 % thickness reduction with 35 % liquid volume fraction in the composite. For an extrapolation with 6 % thickness reduction and 33% liquid volume fraction, an error of 14.21 % over ANN and 12.25 % over experimental results are observed. From Table 8.11 it can also be seen that in most of the cases the error in prediction over ANN predicted values is within |3|%. Further while testing the network for extrapolation of hardness, it is observed that with 2.5, 5 and 7.5 % thickness reduction of the composite rolled in

mushy state with 35 % liquid volume fraction in the composite, the error in prediction is of the order of 30 %. Therefore, it can be inferred that the HRNN model proposed can supplement the ANN in predictions of hardness of mushy state rolled Al-4.5Cu-5TiB_2 composite rolled to 2 % to 12.5 % thickness reductions and at mushy state temperatures corresponding to 5 to 33 % liquid volume fraction.

Figure 8.8 to Figure 8.11 show the plots of variation of hardness with respect to thickness reduction during mushy state rolling of pre hot rolled Al-4.5Cu-5TiB_2 composite rolled from constant mushy state temperatures corresponding to 10, 17, 20 and 30 % volume fractions of liquid in the composite. It can be seen from plots of Figure 8.8 to Figure 8.10, that the hardness prediction plot of HRNN closely follows that of ANN. In Figure 8.11, it is seen that plot of hardness prediction by HRNN tends to deviate from ANN predictions beyond 12.5 % thickness reduction when the composite is mushy state rolled from temperature corresponding to 30 % volume fraction of liquid. Thus it is clear that prediction beyond 30 % liquid volume fraction the accuracy in prediction deteriorates. However from Table 8.11 it is seen that error of 8.57 % at 33 % liquid volume fraction is reasonable. Kusiak and Kuziak (2002) reported an error of 8 % in the prediction of ultimate stress in steel using neural networks. Plot in Figure 8.9 relates to the predictions made by HRNN with ANN predictions for the data used for validation of NN model. This plot is for variation of hardness with respect to thickness reduction per roll pass when the pre hot rolled composite containing 17 % liquid fraction is rolled in mushy state. The plots of hardness predictions by HRNN are seen to closely match the predictions by ANN. Thus the plots from Figure 8.8 to Figure 8.11 communicate the usefulness of HRNN model in prediction of hardness of pre hot rolled Al-4.5Cu-5TiB_2 composite rolled at mushy state temperatures corresponding to 5 to 33 % liquid volume fractions and rolled to 2 to 11.5 % thickness reductions per pass.

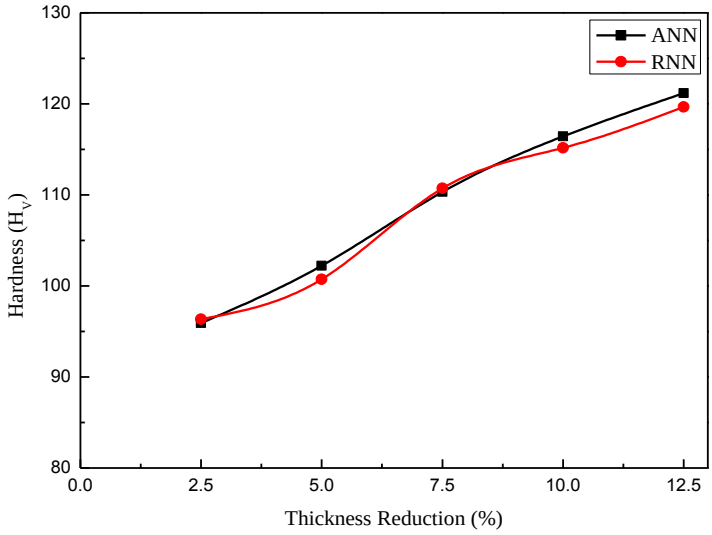

Figure 8.8 Plot showing comparison of predictions of hardness made by ANN and RNN when pre hot rolled Al-4.5Cu-5TiB_2 composite is rolled to varying thickness reductions in mushy state with 10% liquid volume fraction.

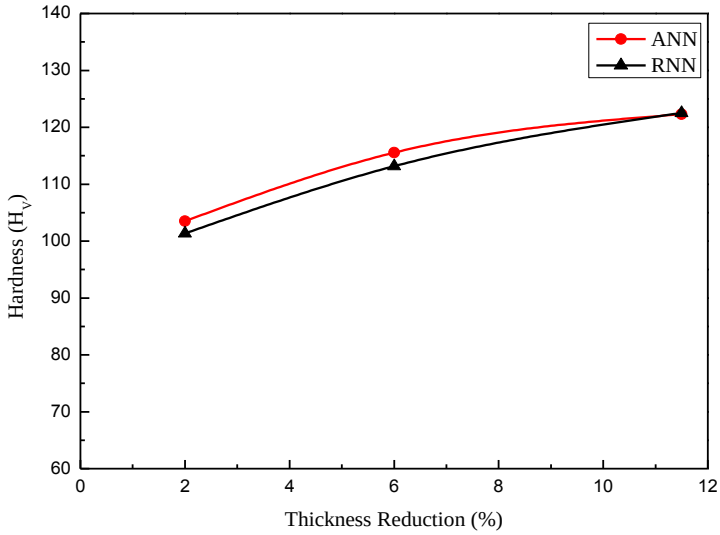

Figure 8.9 Plot showing comparison of predictions of hardness made by ANN and RNN when pre hot rolled Al-4.5Cu-5TiB_2 composite is rolled to varying thickness reductions in mushy state with 17% liquid volume fraction.

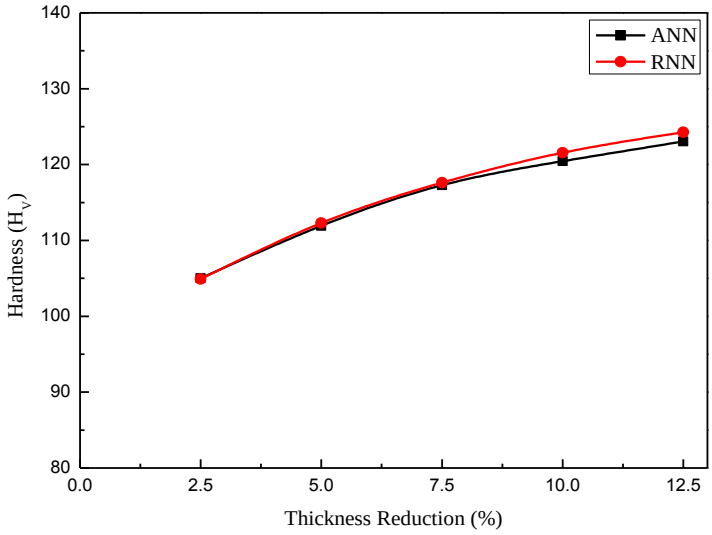

Figure 8.10 Plot showing comparison of predictions of hardness made by ANN and RNN when pre hot rolled Al-4.5Cu-5TiB_2 composite is rolled to varying thickness reductions in mushy state with 20 % liquid volume fraction.

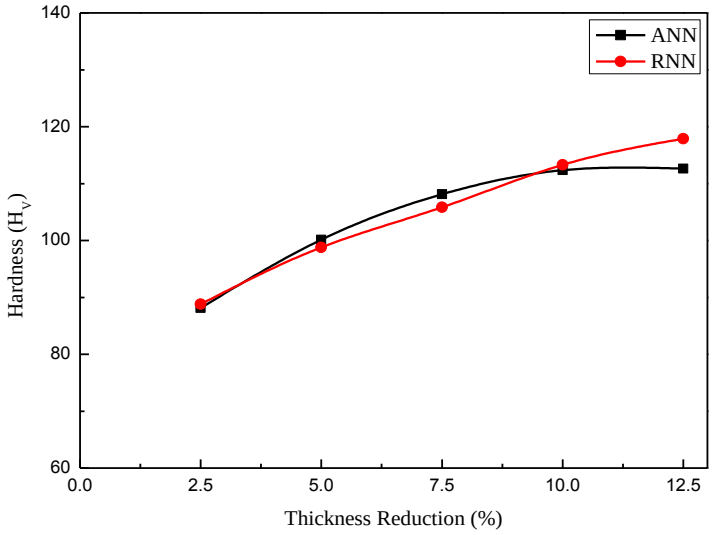

Figure 8.11 Plot showing comparison of predictions of hardness made by ANN and RNN when pre hot rolled Al-4.5Cu-5TiB_2 composite is rolled to varying thickness reductions in mushy state with 30% liquid volume fraction.

8.7 MODELLING OF HRNN FOR PREDICTION OF TENSILE PROPERTIES

The FFNN modelled for prediction of tensile properties had 7-9-6-3 architecture. The HRNN proposed for prediction of tensile properties is constructed from the same basic architecture. Initially, the ANN with 7 input nodes (corresponding to material type, % thickness reduction, % liquid volume fraction, % TiB_2, large and small grain sizes and hardness), 9 and 6 nodes in first and second hidden layers respectively and 3 output nodes (corresponding to yield strength, UTS and pct. elongation) is considered for partial training, till a steep downward gradient in MSE is observed. The fully trained ANN of the same architecture converged clearly after 4,90,000 iterations with an MSE of 0.00017 using the values of η and α as 0.85 and 0.7, respectively. Now, for formulating the HRNN, the ANN network was trained partially and weights of this partially trained parent ANN were borrowed in the HRNN network of similar architecture as that of parent ANN. The HRNN then was further trained till the MSE was comparable to that obtained with fully trained ANN. The training of HRNN with η=0.85 and α=0.7 was stopped when MSE reached a value of 0.000137. In the forthcoming subsections the performance of HRNN is compared with ANN model in terms of values of yield strength, ultimate tensile strength and pct. elongation predicted by them.

8.7.1 Comparison of prediction of tensile properties by HRNN with ANN predictions

The predictions of yield and ultimate tensile strength for Al-4.5Cu alloy and Al-4.5Cu-5TiB_2 composite obtained by using trained HRNN and those obtained using ANN model of Chapter 6 are presented in Table 8.12.

Table: 8.12 Predicted values of tensile properties with HRNN and ANN for as cast Al-4.5Cu alloy and Al-4.5Cu-5TiB_2 composite rolled in mushy state in as cast and pre hot rolled condition.								
Mat. Type	**% Th. Red.**	**% Liq. Vol. Fraction**	**Yield Strength (MPa)**			**UTS (MPa)**		
			ANN	**RNN**	**Error (%)**	**ANN**	**RNN**	**Error (%)**
Al-4.5Cu alloy	0	0	118.9	118.91	-0.0084	166.96	166.9	0.0359
	2.5	30	120.4	120.2	0.1661	176.58	176.24	0.1925
	5	30	99.4	99.18	0.2213	145.48	145.17	0.2131
As cast Al-4.5Cu-5TiB_2	0	30	175.8	175.6	0.1138	238.28	238.1	0.0755
	2.5	30	197.9	197.92	-0.0101	260.32	260.31	0.0038
	5	30	223.4	223.36	0.0179	278.24	278.2	0.0144
Pre-hot rolled Al-4.5Cu-5TiB_2	5	10	185.1	185.1	0	242.93	242.8	0.0535
	5	20	220.6	220.5	0.0453	273.3	273.3	0
	5	30	215.2	215.24	-0.0186	271.21	271.23	-0.0074

From Table 8.12, it can be seen that the errors in prediction are very low and within 0.23 % for yield strength predictions and within 0.22 % in case of UTS predictions. This indicates that the generalisation of relationships by HRNN are of nearly the same order as that by ANN for predicting yield strength and UTS for Al-4.5Cu alloy and Al-4.5Cu-5TiB_2 composite when mushy state rolled from as cast as well as from pre hot rolled condition.

Table 8.13 gives the predictions of pct. elongation obtained from HRNN and ANN. It can be seen from the table that the maximum error of 0.1953 % in prediction occurs in case of mushy state rolled Al-4.5Cu alloy containing 30 % liquid volume is rolled to 5 % thickness reduction per pass. The errors in prediction seen in Table 8.12 are less than the errors reported in use of NN models for predictions. Selvakumar *et al.* (2007) have reported a maximum error of 5 % in the prediction of axial stress, hoop stress , hydrostatic stress and the axial strain in their work on modelling the effect of particle size and iron content on forming of Al-Fe preforms using ANN. The prediction errors when the predicted pct. elongation is expressed within two decimal places are found

to be very small (infinitesimal in most cases), indicating that the HRNN has generalised the relationship of inputs and output to the same order as that of ANN.

Table: 8.13 Predicted values of pct. elongation with HRNN and ANN for as cast Al-4.5Cu alloy and Al-4.5Cu-5TiB_2 composite rolled in mushy state in as cast and pre hot rolled condition.

Mat. Type	% Th. Red.	% Liq. Vol. Fraction	Pct elongation		Error (%)
			ANN	RNN	
Al-4.5Cu alloy	0	30	6.95	6.947	0.0432
	2.5	30	6.39	6.39	0
	5	30	5.12	5.11	0.1953
As cast Al-4.5Cu-5TiB_2	0	30	10.44	10.43	0.0958
	2.5	30	11.83	11.83	0
	5	30	14.1	14.1	0
Pre-hot rolled Al-4.5Cu-5TiB_2	5	10	11.52	11.52	0
	5	20	14.34	14.34	0
	5	30	13.6	13.59	0.0735

Thus from Table 8.12 and 8.13 it can be concluded that the performance of HRNN and ANN model are identical in terms of predictions of strength and elongation of Al-4.5Cu alloy and Al-4.5Cu-5TiB_2 composite rolled in mushy state within the range of data for which these models have been trained.

8.8 MODELLING OF HRNN FOR PREDICTION OF WEAR PROPERTIES

Hybrid recurrent neural network is constructed from a parent ANN having the same architecture as that was modelled for prediction of wear rate. The FFNN modelled for predicting wear rate of Al-4.5Cu-5TiB_2 composite rolled from mushy state had architecture of 7 neurons in input layer (corresponding to material type, % thickness reduction, % liquid volume fraction, large and small grain sizes, hardness and normal load), 7 and 4 neurons in first and second hidden layer respectively and one output node representing wear rate. The HRNN for wear rate predictions was trained and modelled in a manner similar to that obtained for grain size, hardness and tensile properties predictions. The training of the HRNN for wear rate predictions was stopped when an MSE of 2.92 x 10^{-5} was achieved using $\eta = 0.5$ and $\alpha = 0.5$. In the

subsection to follow, the prediction of wear rate by HRNN is compared with that by the fully trained ANN modelled for wear rate predictions in chapter 7.

8.8.1 Comparison of predictions of wear rate by HRNN and ANN

The wear rate predictions by HRNN and ANN when Al-4.5Cu-5TiB_2 composite is rolled in mushy state with different thickness reductions per pass, and at different mushy state temperatures are listed in Table 8.14. The last column of the table shows the error in prediction of HRNN over the values predicted by ANN. It can be observed from Table 8.14 that the maximum prediction error equaling -10% occurs in prediction of wear rate by HRNN with 7.5% thickness reduction when pre hot rolled Al-4.5Cu-5TiB_2 composite is mushy state rolled at temperature corresponding to 30 % volume fraction of liquid with a normal load of 19.6N. In the case of as cast composite, the maximum error in prediction is -2.931 % with 2.5 % thickness reduction, 30 % liquid volume fraction and a normal load 58.8N. It can also be observed from Table 8.14 that majority of errors are within |5|%.The prediction errors of HRNN model are comparable with the errors reported in literature. Mandal *et al*. (2007) in their paper reported a Gaussian distribution of % error of prediction within ±10 % in prediction of flow stress using Resilient Propagation algorithm which is reported to perform better than Back Propagation algorithm.

Table 8.14 Wear rate predicted by HRNN &ANN for mushy state rolled Al-4.5Cu-5TiB_2 composite in as cast and pre hot rolled condition.

Material	Thickness reduction (%)	Liquid volume fraction (%)	Load (N)	Wear rate			Error of RNN over ANN (%)
				Experimental	ANN	RNN	
As cast Al-4.5Cu-5TiB2 Composite	2.5	30	19.6	0.00392	0.0038	0.00391	-2.8947
			39.2	0.00525	0.0052	0.00524	-0.7692
			58.8	0.00595	0.0058	0.00597	-2.931
			78.4	0.00651	0.0064	0.00655	-2.3438
	5.0	30	19.6	0.00360	0.0036	0.00360	0
			39.2	0.00421	0.0042	0.00424	-0.9524
			58.8	0.00539	0.0053	0.00536	-1.1321
			78.4	0.00601	0.006	0.00595	0.8333

Pre hot rolled Al-4.5Cu-5TiB2 Composite	2.5	30	19.6	0.00308	0.003	0.00315	-5
			39.2	0.00517	0.005	0.00514	-2.8
			58.8	0.00574	0.0058	0.00577	0.5172
			78.4	0.00605	0.0059	0.00619	-4.9153
	5.0	30	19.6	0.00298	0.003	0.0028	6.6667
			39.2	0.00407	0.004	0.00413	-3.25
			58.8	0.00518	0.0052	0.00502	3.4615
			78.4	0.00592	0.0059	0.006	-1.6949
	7.5	10	19.6	0.0027	0.0027	0.0026	3.7037
			39.2	0.00454	0.0045	0.00456	-1.3333
			58.8	0.00516	0.0051	0.00518	-1.5686
			78.4	0.00644	0.0064	0.00654	-2.1875
		20	19.6	0.00217	0.0021	0.00215	-2.381
			39.2	0.00263	0.0028	0.00262	6.4286
			58.8	0.00401	0.0039	0.00391	-0.2564
			78.4	0.00501	0.005	0.00515	-3
		30	19.6	0.00233	0.0022	0.00242	-10
			39.2	0.00405	0.0038	0.00405	-6.5789
			58.8	0.00444	0.0044	0.00461	-4.7727
			78.4	0.00581	0.0056	0.00591	-5.5357

Figure 8.12 shows the plots of variation of wear rate (mm^3/km) predicted by HRNN and ANN when Al-4.5Cu-5TiB_2 composite in as cast state is rolled in mushy state at 632°C with respect to normal load (N) with 2.5 and 5 % thickness reductions. It can be seen that the curves with both thickness reductions follow each other quite closely.

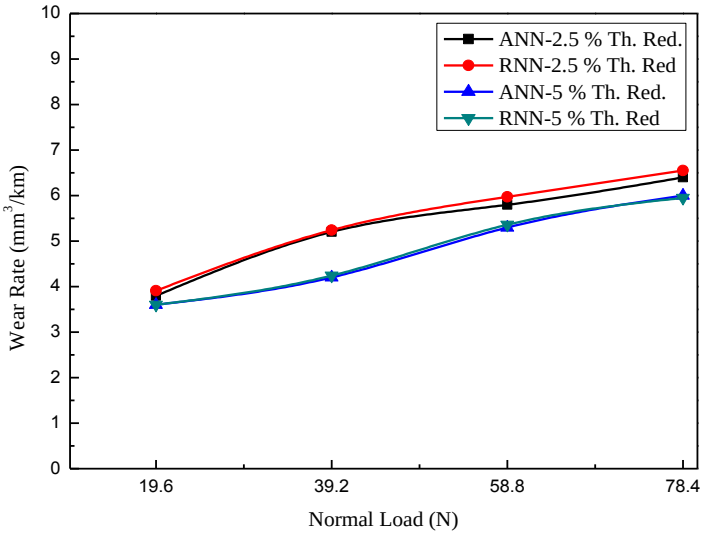

Figure 8.12 Plot showing comparison of predictions of wear rate by HRNN and ANN with respect to normal load when as cast Al-4.5Cu-5TiB_2 composite containing 30 % volume fractions of liquid is mushy state rolled to 2.5 and 5 % thickness reduction per pass.

Similarly plots in Figure 8.13 show variations in wear rate predicted by HRNN and ANN for pre hot rolled composite under same conditions as in Figure 8.12. Here too, it can be seen that the predictions match closely with the curves being almost similar. However, the curve for HRNN predictions with 2.5 % thickness reduction seems to diverge beyond normal load of 78.4N. Plots in Figure 8.14 show the variation of wear rate predictions by HRNN in comparison to that by ANN when pre hot rolled Al-4.5Cu-5TiB_2 composite is rolled in mushy state at temperatures 610°C, 626°C and 632°C (corresponding to 10, 20 and 30 % liquid volume fraction) to 7.5 % thickness reduction. It is observed that the predictions made by both the models are quite similar with the curves closely following each other in all the three cases. From the foregoing discussion on the performance of the HRNN modelled for prediction of wear rate of mushy state rolled Al-4.5Cu-5TiB_2 composite, it can be concluded that HRNN model predictions are comparable to that of ANN within an overall error of prediction of |10|% over ANN model predictions.

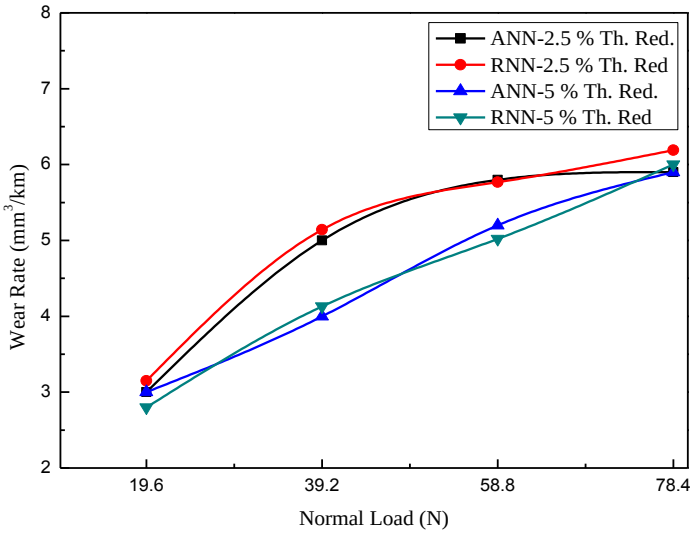

Figure 8.13 Plot showing comparison of predictions of wear rate by HRNN and ANN with respect to normal load when pre hot rolled Al-4.5Cu-5TiB_2 composite containing 30% volume fractions of liquid is mushy state rolled to 2.5 and 5 % thickness reduction per pass.

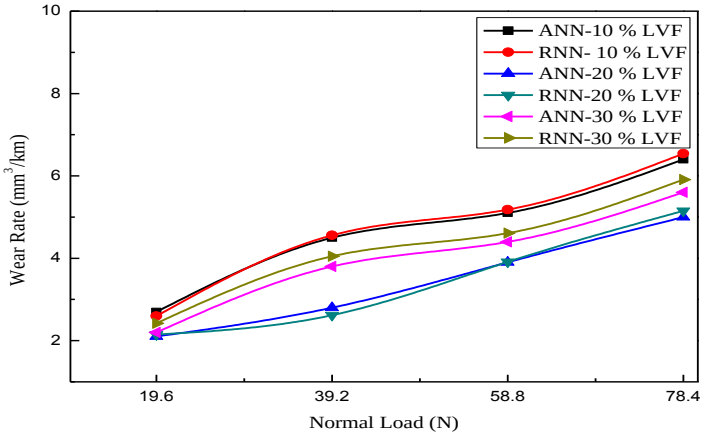

Figure 8.14 Plot showing comparison of predictions of wear rate by HRNN and ANN with respect to normal load when pre hot rolled Al-4.5Cu-5TiB_2 composite containing 10, 20 and 30% volume fractions of liquid is mushy state rolled to 7.5% thickness reduction per pass.

8.9 SUMMARY

1. Elman simple neural network (SRN) was found to have issues relating to convergence when trained for prediction of grain size (large and small) for application relating to mushy state rolling of Al-4.5Cu-5TiB_2 composite. Three layered as well as four layered extended Elman recurrent networks were tried out with different combinations of neurons per hidden layer and learning rate parameter (η) and momentum term (α). The network was found to oscillate in local minimums and subsequently stopped learning with three layered SRN. The four layered extended Elman recurrent neural network fared slightly better, but was unable to map the input output relationships as there was no learning possible beyond a certain stage of training.
2. The problem of convergence of extended Elman recurrent neural network was overcome by constructing a hybrid recurrent neural network (HRNN) by borrowing weights from a partially trained FFNN having same architecture as that of extended Elman recurrent neural network (minus context or temporal layers), when steep downward gradient is observed on the MSE v/s. Weights plane. Further training of such HRNN resulted in fast learning. The overall training time was found to reduce significantly.
3. The statistical study of errors done using two sample student t test and one sample and two sampled Kolmogorov – Smirnov test indicated that the means of the errors in prediction of both the HRNN and ANN models calculated over target values are comparable and the statistical distribution of the two errors is equivalent. Thus the statistical analysis inferred that the error distributions of both the models are statistically equivalent.
4. The HRNN model for grain size prediction predicted large and small grain sizes of Al-4.5Cu-5TiB_2 composite rolled in mushy state in as cast and pre hot rolled condition, containing 5 to 35 % liquid volume fraction with 2 to 12.5 % thickness reduction per pass within an error of |0.2|% of the corresponding values predicted by ANN model.
5. The HRNN model for hardness predictions of the mushy state rolled composite rolled in as cast as well as pre hot rolled form predicted the hardness within an

error of |6.58|% within the range of data used for training the network and within |14.2|% within the data used for validating the ANN. However, the predictions were observed to diverge beyond 33 % liquid volume fractions with all cases of thickness reductions considered. Therefore, the HRNN model for hardness predictions are valid from 5 to 33 % volume fractions of liquid in the composite rolled to 2 to 12.5 % thickness reductions only. Thus HRNN model can be used for interpolating the data as well as for extrapolation with small constraints.

6. The predictions of HRNN modelled for prediction of tensile properties of mushy state rolled Al_4.5Cu alloy and Al-4.5Cu-5TiB_2 composite matched the predictions done by ANN model.
7. The wear rates of as cast as well as pre hot rolled Al-4.5Cu-5TiB_2 composite rolled from mushy state that were predicted by HRNN were within an error of 10 % of the values predicted by the ANN model for wear rate predictions.
8. This leads to an inference that HRNN models, being similar in performance to the ANN (FFNN) models in terms of prediction capabilities and the time required for training of HRNN being significantly reduced, they are superior to ANN models.

Chapter 9

CONCLUSIONS AND SCOPE FOR FUTURE WORKS

9.1 CONCLUSIONS

1. Artificial neural network models were successfully formulated to predict the grain sizes, hardness, wear properties and tensile properties of Al-4.5Cu-5TiB_2 composite rolled in mushy state in as cast and pre hot rolled condition, with varying thickness reductions ranging from 2 to 12.5 % and at various temperatures corresponding to 5 % to 35 % volume fraction of liquid in the composite with a fair degree of accuracy.
2. The large and small grain sizes predicted by the ANN model for grain size predictions were found to be within ±6.1 pct. over the target values of large and small grain sizes. The ANN models for hardness, tensile properties and wear rate are found to predict within an error of ±2.65 pct, ±7.65 pct and ±6.5 pct respectively. Majority of the predictions done by the ANN model for tensile properties are within ±2.3 pct, while those by ANN model for wear properties are within ±3.6 pct. Thus, the ANN models successfully represent the relationships between the mushy state rolling parameters and the properties for which they have been modelled. The ANN models have been validated by conducting experiments on mushy state rolling of Al-4.5Cu-5TiB_2 composite with predefined mushy state conditions i.e. (a) with thickness reduction of 2% at 619°C, (b) with 6% thickness reduction at 598°C, 619°C and 633°C, respectively and (c) 11.5% thickness reduction at 619°C. The grain size model predicts the large and small grain sizes within an error of ± 3.4 pct. for the composite rolled in as cast as well as pre hot rolled conditions. The hardness model exhibits an error of ±2.8 pct. over the validation target values of hardness. The wear properties model is validated within an error of ±5.51 pct. The ANN models for grain size, hardness and wear properties predictions extrapolate beyond the range of data used for

training within a small error of ±2.5 pct. The validity of the model to predict the grain sizes, hardness, wear and tensile properties of mushy state rolled Al-4.5Cu-5TiB_2 composite has therefore been established.

3. The grain size model reveals that the variation of grain sizes following rolling carried out at different mushy state temperatures corresponding to required liquid volume fractions in the composite does not show any definite trend with respect to % thickness reductions. The study of variation of hardness of mushy state composite predicted by hardness model (within the range of data used to train the model), with respect to reduction in thickness at any given liquid volume fraction indicates that the highest value of hardness of the composite lies in the range of 10 % thickness reduction and 20 % liquid volume fraction. Outside the training data range, higher values of hardness are found with 12.5 % thickness reduction when the composite is mushy state rolled at around 18 % liquid volume fraction. The variation of wear rate analysed using the ANN model for wear properties indicates that the wear rate and specific wear rate decrease with increase in thickness reduction for any given volume fraction of liquid in composite, with variation more pronounced at lower values of normal loads. The variation of wear rate and specific wear rate is found to be insignificant at higher values of normal loads. The variation of specific wear rate with normal loads indicates lower values of specific wear rate when the composite is mushy state rolled from range of temperatures corresponding to around 20 % liquid volume fraction in the composite. The ANN model for tensile properties indicates that maximum strength and elongation of the composite rolled from mushy state in as cast and pre hot rolled condition to 5 % thickness reduction lies in the region containing 20 to 30 % liquid volume fraction.
4. The optimization of the hardness and wear properties has been obtained by interfacing the ANN models for hardness and wear property predictions with available GUI / API libraries. The model predicts the maximum hardness and wear rate of mushy state rolled Al-4.5Cu-5TiB_2 composite and also provide mushy state rolling parameters to achieve these optimum values.

5. Elman simple recurrent neural network (SRN) was found to have issues relating to convergence when trained as evidenced by different configurations discussed earlier. The problem of convergence of extended Elman recurrent neural network was overcome by constructing a novel hybrid recurrent neural network (HRNN) by borrowing weights from a partially trained FFNN having same architecture as that of extended Elman recurrent neural network (devoid of context or temporal layers), when steep downward gradient is observed on the MSE vs. Weights plane. Further training of such HRNN resulted in fast learning.
6. The statistical study of errors indicates that the means of the errors in prediction of both the HRNN and ANN models calculated over target values are comparable and the statistical distribution of the two errors is equivalent. Thus the ANN and HRNN models are equivalent in terms of prediction capability, provided that the HRNN model is constructed from the parent ANN model having similar architecture as that of HRNN (devoid of the temporal layers). The overall training time for an HRNN constructed by borrowing weights from a partially trained ANN is found to reduce significantly as compared to a fully trained ANN having the same prediction capability

The unique feature of the current research is the development of an HRNN model which performs faster predictions than corresponding FFNNs with same levels of accuracy. This HRNN model has been developed through a novel approach of borrowing weights from a partially trained FFNN model, to be fed into an extended Elman Simple Recurrent Neural Network.

9.2 SCOPE FOR FUTURE WORK

The HRNN model due to its faster learning ability scores over ANN. The present day industrial processes involve a lot of in process monitoring and control. Any subtle changes in the output(s) of the process are fed back into the process control mechanism. The mechanism then takes appropriate corrective action, resets the process parameters and brings back the process output(s) to the desired state. The

developed HRNN model, due to its faster processing could be embedded as part of such controller strategy in mushy state rolling process in future.

The HRNN model developed could be customised to suit many other processes because of its generality in coding and flexibility. The generality of coding allows the user to select the any area ranging from finance to engineering and meteorological applications. The flexibility of the code written allows the user to select any number of input parameters and desired number of output parameters. The code also provides flexibility and generality in selection of learning rate parameter, momentum term and number of neurons in each hidden layer.

Appendix I

Extract of code used for training the Feed Forward Neural Network and computation of the outputs from the Network.

```
main()
{
        cout << "       Prediction of Grainsize, Hardness and Wear Properties of " <<
endl;
        cout << "           Mushy State rolled Al-4.5Cu-TiB2 Composite" << endl;
   cout << "          using Feed Forward and Recuurent Neural Networks" << endl;

        cout << "                          by" << endl;
        cout << "                  Akshay V. Nigalye, (ME08p03) " << endl;
        cout << "          National Institute of Technology Karnataka, Surathkal" <<
endl;
   cout << endl;
        cout << endl << "Enter your Network preference" << endl;
        cout << "1. Feed Forward Neural Network" << endl;
        cout << "2. Recurrent Neural Network" << endl;

        fchoise = getch();
        if (fchoise != '1' && fchoise != '2' ) { return 0; }
        else  for(;;) {
                char choice;
                cout << endl << "Enter the Training or Prediction preference" << endl;
                cout << "1. load data" << endl;
                cout << "2. learn from data" << endl;
                cout << "3. compute output pattern" << endl;
```

```
cout << "4. make new data file" << endl;
cout << "5. save data" << endl;
cout << "6. print data" << endl;
cout << "7. change learning rate and momentum factor" << endl;
cout << "8. exit" << endl << endl;
cout << "Enter your choice (1-8)";

do { choice = getch(); }
while (choice != '1' && choice != '2' && choice != '3' && choice != '4' && choice != '5' && choice != '6' && choice != '7' && choice != '8');
switch(choice) {
    case '1':{ if (file_loaded == 1) clear_memory();
               get_file_name();
               file_loaded = 1;
               if (fchoise=='2') {recurrent_load_data(filename); }
               else {load_data(filename); }
    }
    break;
    case '2': learn();
    break;
    case '3': compute_output_pattern();
    break;
    case '4': make();
    break ;
    case '5':{ if (file_loaded == 0)
               {
```

```
                                        cout << endl << "there is no data loaded into
memory" << endl;
                                        break;
                                        }
                                cout << endl << "enter a filename to save data to: ";
                                cin >> filename;
                                save_data(filename); }
                        break;
                        case '6': print_data();
                        break;
                        case '7': change_learning_rate_and_momentum();
                        break;
                        case '8': return 0;
                };
        }
}
void initialize_net()
{
        int x;
        input = new double * [number_of_input_patterns];
        if(!input) { cout << endl << "memory problem!"; exit(1); }
        for(x=0; x<number_of_input_patterns; x++)
        {
                input[x] = new double [input_array_size];
                if(!input[x]) { cout << endl << "memory problem!"; exit(1); }
        }

        hidden1 = new double [hidden_array_1_size];
```

```
        if(!hidden1) { cout << endl << "memory problem!"; exit(1); }

        if (fchoise==2) { rhidden1 = new double [rhidden_array_1_size];
                        if(!rhidden1) { cout << endl << "memory problem!"; exit(1);
}}

        hidden2 = new double [hidden_array_2_size];
        if(!hidden2) { cout << endl << "memory problem!"; exit(1); }

        if (fchoise==2) { rhidden2 = new double [rhidden_array_2_size];
                        if(!rhidden2) { cout << endl << "memory problem!"; exit(1);
}}

        output = new double * [number_of_input_patterns];
        if(!output) { cout << endl << "memory problem!"; exit(1); }
        for(x=0; x<number_of_input_patterns; x++)
        {
                output[x] = new double [output_array_size];
                if(!output[x]) { cout << endl << "memory problem!"; exit(1); }
        }
        target = new double * [number_of_input_patterns];
        if(!target) { cout << endl << "memory problem!"; exit(1); }
        for(x=0; x<number_of_input_patterns; x++)
        {
                target[x] = new double [output_array_size];
                if(!target[x]) { cout << endl << "memory problem!"; exit(1); }
        }

        bias = new double [bias_array_size];
```

```
if(!bias) { cout << endl << "memory problem!"; exit(1); }

weight_i_h = new double * [input_array_size];
if(!weight_i_h) { cout << endl << "memory problem!"; exit(1); }
for(x=0; x<input_array_size; x++)
{
        weight_i_h[x] = new double [hidden_array_1_size];
        if(!weight_i_h[x]) { cout << endl << "memory problem!"; exit(1); }
}
oldweight_i_h = new double * [input_array_size];
if(!oldweight_i_h) { cout << endl << "memory problem!"; exit(1); }
for(x=0; x<input_array_size; x++)
{
        oldweight_i_h[x] = new double [hidden_array_1_size];
        if(!oldweight_i_h[x]) { cout << endl << "memory problem!"; exit(1); }
}

if (fchoise==2) { rweight_h1 = new double * [rhidden_array_1_size];
if(!rweight_h1) { cout << endl << "memory problem!"; exit(1); }
for(x=0; x<rhidden_array_1_size; x++)
{
        rweight_h1[x] = new double [hidden_array_1_size];
        if(!rweight_h1[x]) { cout << endl << "memory problem!"; exit(1); }
}}
weight_h_h = new double * [hidden_array_1_size];
if(!weight_h_h) { cout << endl << "memory problem!"; exit(1); }
for(x=0; x<hidden_array_1_size; x++)
{
```

```
            weight_h_h[x] = new double [hidden_array_2_size];
            if(!weight_h_h[x]) { cout << endl << "memory problem!"; exit(1); }
        }

        oldweight_h_h = new double * [hidden_array_1_size];
        if(!oldweight_h_h) { cout << endl << "memory problem!"; exit(1); }
        for(x=0; x<hidden_array_1_size; x++)
        {
            oldweight_h_h[x] = new double [hidden_array_2_size];
            if(!oldweight_h_h[x]) { cout << endl << "memory problem!"; exit(1);
}
        }


        if (fchoise==2) { rweight_h2 = new double * [rhidden_array_2_size];
        if(!rweight_h2) { cout << endl << "memory problem!"; exit(1); }
        for(x=0; x<rhidden_array_2_size; x++)
        {
            rweight_h2[x] = new double [hidden_array_2_size];
            if(!rweight_h2[x]) { cout << endl << "memory problem!"; exit(1); }
        }}

        weight_h_o = new double * [hidden_array_2_size];
        if(!weight_h_o) { cout << endl << "memory problem!"; exit(1); }
        for(x=0; x<hidden_array_2_size; x++)
        {
            weight_h_o[x] = new double [output_array_size];
            if(!weight_h_o[x]) { cout << endl << "memory problem!"; exit(1); }
```

```
        }

        oldweight_h_o = new double * [hidden_array_2_size];
        if(!oldweight_h_o) { cout << endl << "memory problem!"; exit(1); }
        for(x=0; x<hidden_array_2_size; x++)
        {
                oldweight_h_o[x] = new double [output_array_size];
                if(!oldweight_h_o[x]) { cout << endl << "memory problem!"; exit(1);
}
        }

        errorsignal_hidden1 = new double [hidden_array_1_size];
        if(!errorsignal_hidden1) { cout << endl << "memory problem!"; exit(1); }

        errorsignal_hidden2 = new double [hidden_array_2_size];
        if(!errorsignal_hidden2) { cout << endl << "memory problem!"; exit(1); }

        errorsignal_output = new double [output_array_size];
        if(!errorsignal_output) { cout << endl << "memory problem!"; exit(1); }

        return;
}
void learn()
{
        if (epochstat==0) epoch=0;
        if (file_loaded == 0)
        {
                cout << endl << "there is no data loaded into memory" << endl;
```

```
                return;
        }
        cout << endl << "learning..." << endl << "press a key to return to menu" <<
endl;


        register int y;


        if (fchoise==1)
        {
        while(!kbhit()) {
      cout << "FFNN learning    ";
                for(y=0; y<number_of_input_patterns; y++) {
                        forward_pass(y);
                        backward_pass(y);
                        }
                if(compare_output_to_target()) {
                        cout << endl << "Feed forward learning successful" << endl;
                        return;
                        }
                epoch++;
                epochstat=1;
                }
        }
        else
        {
        while(!kbhit()) {
      cout << "RNN learning     " ;
                for(y=0; y<number_of_input_patterns; y++) {
```

```
                recurrent_forward_pass(y);
                recurrent_backward_pass(y);
                }
            if(compare_output_to_target()) {
                cout << endl << "Recurrent learning successful" << endl;
                return;
                }
            epoch++;
            epochstat=1;
            }
        }
        cout << endl << "learning not successful yet" << endl;
        return;
}

void forward_pass(int pattern)
{
        register double temp=0;
        register int x,y;
// INPUT -> HIDDEN1
        for(y=0; y<hidden_array_1_size; y++) {
            for(x=0; x<input_array_size; x++)
            {
                temp += (input[pattern][x] * weight_i_h[x][y]);
            }
            hidden1[y] = (1.0 / (1.0 + exp(-1.0 * (temp + bias[y]))));
            temp = 0;
        }
```

```
// HIDDEN1 -> HIDDEN2
        for(y=0; y<hidden_array_2_size; y++) {
                for(x=0; x<hidden_array_1_size; x++)
                {
                        temp += (hidden1[x] * weight_h_h[x][y]);
                }
                hidden2[y] = (1.0 / (1.0 + exp(-1.0 * (temp + bias[y + hidden_array_1_size]))));
                temp = 0;
        }


// HIDDEN2 -> OUTPUT
        for(y=0; y<output_array_size; y++) {
                for(x=0; x<hidden_array_2_size; x++)
                {
                        temp += (hidden2[x] * weight_h_o[x][y]);
                }
                output[pattern][y] = (1.0 / (1.0 + exp(-1.0 * (temp + bias[y + hidden_array_1_size + hidden_array_2_size]))));
                temp = 0;
        }
        return;
}
void backward_pass(int pattern)
{
        register int x, y;
        register double dweight_h_o = 0.0 , dweight_h_h = 0.0, dweight_i_h = 0.0, temp = 0.0;
// COMPUTE ERRORSIGNAL FOR OUTPUT UNITS
```

```
for(x=0; x<output_array_size; x++)
{
    errorsignal_output[x] = ((target[pattern][x] - output[pattern][x]) * output[pattern][x] * (1- output[pattern][x])) ;
}
// ADJUST WEIGHTS OF CONNECTIONS FROM HIDDEN LAYER 2 TO OUTPUT UNITS
for(x=0; x<hidden_array_2_size; x++) {
    for(y=0; y<output_array_size; y++) {
        dweight_h_o = weight_h_o[x][y] - oldweight_h_o[x][y];
        weight_h_o[x][y] += ((learning_rate * errorsignal_output[y] * hidden2[x]) + (momentum * dweight_h_o));
    }
}
for(x=0; x<hidden_array_2_size; x++)
    for(y=0; y<output_array_size; y++)
        oldweight_h_o[x][y] = weight_h_o[x][y];

// ADJUST BIASES FOR OUTPUT UNITS
for(x=(hidden_array_1_size+hidden_array_2_size); x<bias_array_size; x++) {
    bias[x] += (learning_rate * errorsignal_output[x]);
}
// COMPUTE ERRORSIGNAL FOR HIDDEN LAYER 2 UNITS
for(x=0; x<hidden_array_2_size; x++) {
    for(y=0; y<output_array_size; y++) {
        temp += (errorsignal_output[y] * weight_h_o[x][y]);
    }
    errorsignal_hidden2[x] = hidden2[x] * (1-hidden2[x]) * temp;
    temp = 0.0;
```

```
        }
// ADJUST WEIGHTS OF CONNECTIONS FROM HIDDEN LAYER 2 TO HIDDEN LAYER 1
        for(x=0; x<hidden_array_1_size; x++) {
                for(y=0; y<hidden_array_2_size; y++) {
                        dweight_h_h = weight_h_h[x][y] - oldweight_h_h[x][y];
                        weight_h_h[x][y] += ((learning_rate * errorsignal_hidden2[y] * hidden1[x]) + (momentum * dweight_h_h));
                }
        }
        for(x=0; x<hidden_array_1_size; x++)
                for(y=0; y<hidden_array_2_size; y++)
                        oldweight_h_h[x][y] = weight_h_h[x][y];
// ADJUST BIASES OF HIDDEN LAYER 2 UNITS
        for(x=hidden_array_1_size; x<(bias_array_size-hidden_array_2_size); x++) {
                bias[x] += (learning_rate * errorsignal_hidden2[x]);
        }
   // COMPUTE ERRORSIGNAL FOR HIDDEN LAYER 1 UNITS
        for(x=0; x<hidden_array_1_size; x++) {
                for(y=0; y<hidden_array_2_size; y++) {
                        temp += (errorsignal_hidden2[y] * weight_h_h[x][y]);
                }
                errorsignal_hidden1[x] = hidden1[x] * (1-hidden1[x]) * temp;
                temp = 0.0;
        }

// ADJUST WEIGHTS OF CONNECTIONS FROM INPUT TO HIDDEN LAYER 1 UNITS
        for(x=0; x<input_array_size; x++) {
```

```
                for(y=0; y<hidden_array_1_size; y++) {
                        dweight_i_h = weight_i_h[x][y] - oldweight_i_h[x][y];
                        weight_i_h[x][y] +=((learning_rate * errorsignal_hidden1[y]*input[pattern][x]) + (momentum*dweight_i_h));
                }
        }
        for(x=0; x<input_array_size; x++)
                for(y=0; y<hidden_array_1_size; y++)
                        oldweight_i_h[x][y] = weight_i_h[x][y];

// ADJUST BIASES OF HIDDEN LAYER 1 UNITS
        for(x=0; x<hidden_array_1_size; x++) {
                bias[x] += (learning_rate * errorsignal_hidden1[x]);
        }
        return;
}
void compute_output_pattern()
{
        if (file_loaded == 0)
        {
                cout << endl << "there is no data loaded into memory" << endl;
                return;
        }
        char choice;
        cout << endl << endl << "1. load trained input pattern into network" << endl;
        cout << "2. load custom input pattern into network" << endl;
        cout << "3. go back to main menu" << endl << endl;
        cout << "Enter your choice (1-3)" << endl;
```

```
	do { choice = getch(); } while (choice != '1' && choice != '2' && choice != '3');
	switch(choice) {
		case '1': test();
		break;
		case '2': if (fchoise==2) rcustom();
			else custom();
		break;
		case '3': return;
	};
}
void test()
{
	int x;
	double y;
   pattern = 0;
	while(pattern == 0) {
		cout << endl << endl << "There are " << number_of_input_patterns << " input patterns in the file," << endl << "enter a number within this range: ";
		cin >> pattern;
	}

	if(pattern > number_of_input_patterns) {
		cout << "Pattern number entered exceeded the limit" << number_of_input_patterns << endl;
		return;
	}

	pattern--;
```

```
        if (fchoise==2)
                recurrent_forward_pass(pattern);
        else
                forward_pass(pattern);
        output_to_screen();
    return;
}

void output_to_screen()
{
        int x;
        double y, z ;
        double diff= maxnum - minnum;
        cout << endl << "Output pattern:" << endl;
        for(x=0; x<output_array_size; x++) {
     y= ((( output[pattern][x] - 0.1 ) * diff ) / 0.8 ) + minnum;
                cout << endl << (x+1) << " Tested Output: " << y ;
        }
        cout << endl;
        return;
}

void custom()
{
   double temp=0;
        int x,y,z,fload=0;
        int num_patterns;
        double **custom_input;
```

```
        char cusfile[128],
      outfile[128];

        cout << endl << "enter the number of patterns in the file" << endl;
        cin >> num_patterns;

  custom_input = new double *[num_patterns];
        if(!custom_input) { cout << endl << "memory problem!"; return;    }
        for(x=0; x<num_patterns; x++)
        {
                custom_input[x] = new double [input_array_size];
                if(!custom_input[x]) { cout << endl << "memory problem!"; exit(1); }
        }

        double *custom_output = new double [output_array_size];
        if(!custom_output) { delete [] custom_input; cout << endl << "memory problem!"; return; }

        double *custom = new double [input_array_size];
        if(!custom_output) { delete [] custom_input; cout << endl << "memory problem!"; return; }

        char cchoice;
        cout << endl << endl << "1. load custom input pattern individually" << endl;
        cout << "2. load custom inputs patterns file" << endl;
        cout << "3. go back to main menu" << endl << endl;
        cout << "Enter your choice (1-3)" << endl;
```

```
   do { cchoice = getch(); } while (cchoice != '1' && cchoice != '2' && cchoice != '3');
          switch(cchoice) {
                  case '1': {
           cout << " load the custom input"<< endl;
           for(x = 0; x < input_array_size; x++)          cin >> custom_input[0][x];
           }
                  break;
                  case '2': {
           cout << endl << endl << "enter file that contains test input pattern: ";
                 cin >> cusfile;
                 ifstream in(cusfile);
                 if(!in) { cout << endl << "failed to load data file" << endl; return; }

                 for(z=0; z<num_patterns; z++)
                                for(x = 0; x < input_array_size; x++)          in                    >> custom_input[z][x];
           in.close();
           }
                  break;
                  case '3': return;
          };

  for(z=0; z<num_patterns; z++) {

      double diff= maxnum-minnum;

      for (x = 0; x < input_array_size; x++)
                  {
```

```
custom[x]= (((custom_input[z][x]- minnum)*0.8)/diff)+0.1;
}

for(y=0; y<hidden_array_1_size; y++) {
for(x=0; x<input_array_size; x++) {
temp += (custom[x] * weight_i_h[x][y]);
}
hidden1[y] = (1.0 / (1.0 + exp(-1.0 * (temp + bias[y]))));
temp = 0;
}

for(y=0; y<hidden_array_2_size; y++) {
for(x=0; x<hidden_array_1_size; x++) {
temp += (hidden1[x] * weight_h_h[x][y]);
}
hidden2[y] = (1.0 / (1.0 + exp(-1.0 * (temp + bias[y + hidden_array_1_size]))));
temp = 0;
}

for(y=0; y<output_array_size; y++) {
for(x=0; x<hidden_array_2_size; x++) {
temp += (hidden2[x] * weight_h_o[x][y]);
}
custom_output[y] = (1.0 / (1.0 + exp(-1.0 * (temp + bias[y + hidden_array_1_size + hidden_array_2_size]))));
temp = 0;
}
```

```
                if(cchoice=='2'){ if(fload!=1){
        cout << " enter the name of the file to save the predicted outputs from input file " << cusfile << endl;
                cin >> outfile;
        fload=1;}
        }

        cout << endl << "Input pattern:" << "[" << (z+1) << "]" << endl;
                for(x = 0; x < input_array_size; x++) {
                        cout << (x+1) << ": " << ((((  custom[x] - 0.1 ) * diff ) / 0.8 ) + minnum) <<endl;
                }

                cout << endl << endl << "Output pattern:";
                for(x=0; x<output_array_size; x++) {
                        cout << endl << (x+1) << ": " << ((((  custom_output[x] - 0.1 ) * diff ) / 0.8 ) + minnum)<< endl ;
                        }

        ofstream out;
                out.open(outfile, ofstream::app);
                if(!out) {cout << endl << " failed to save custom output file" << endl; return;}
                for(x=0; x<output_array_size; x++) {
                        out << "[" << (z+1) << "]" << "[" << (x+1) << "]  " << ((((  custom_output[x] - 0.1 ) * diff ) / 0.8 ) + minnum) << ' ' ;
                        out <<endl;
                        }
        out.close();
```

```
        delete [] custom_output;
                delete [] custom;
                cout << endl;
        }

        for(x=0; x<num_patterns; x++)
        {
                delete [] custom_input[x];
        }
        delete [] custom_input;
        fload=0;
        return;
}
```

Appendix II

A2.1 Code written in Computational file of Microsoft SilverLight API for the Manual computation of hardness.

```
#region Hardness

    #region Manual

    private void tabItemANNHardnessManualbutton1_Click(object sender,
RoutedEventArgs e)
    {
      double maxnum = 121.824;
      double minnum = 0;
      const int input_array_size = 5;
      const int hidden_array_1_size = 4;
      const int hidden_array_2_size = 3;
      const int output_array_size = 1;

      double[,] weight_i_h = new double[input_array_size, hidden_array_1_size]
      {
        {-15.7427, -22.9999, -0.829085, 16.5365},
        {18.3658, -2.87572, -0.153679, -8.11444},
        { 16.9694, -24.8862, 3.89563, -32.8081},
        {4.1756, -2.44843, 5.32811, -1.04068},
        {8.8315, 0.381159, 6.73193, -2.6118}
      };

      double[,] weight_h_h = new double[hidden_array_1_size,
hidden_array_2_size]
      {
        {10.934, 10.8556, 2.61835},
        {-3.66757, -13.9818, 1.7814},
        {1.05747, -4.92797, 1.7347},
        {-1.29822, 11.3375, 2.37397}
      };

      double[,] weight_h_o = new double[hidden_array_2_size, output_array_size]
      {
        {-2.94166},
        {4.93686},
        {-0.174129}
      };
```

```
        double[] bias = new double[]
        {
           -8.83525, 12.7545, -5.1725, 10.2617,
           0.33406, 0.69, 0.65,
           0.68
        };

        // generate the input patterns
        double[] inputPattern = new double[input_array_size];
        inputPattern[0] =
float.Parse(tabItemANNHardnessManualInputtextBox5.Text);
        inputPattern[1] =
float.Parse(tabItemANNHardnessManualInputtextBox1.Text);
        inputPattern[2] =
float.Parse(tabItemANNHardnessManualInputtextBox2.Text);
        inputPattern[3] =
float.Parse(tabItemANNHardnessManualInputtextBox4.Text);
        inputPattern[4] =
float.Parse(tabItemANNHardnessManualInputtextBox3.Text);

        // create normalized input and output arrays
        double[] normInputPattern = new double[input_array_size];
        double[] normOutputPattern = new double[output_array_size];

        // create hidden arrays
        double[] hidden1 = new double[hidden_array_1_size];
        double[] hidden2 = new double[hidden_array_2_size];

        double temp = 0;
        double diff = maxnum - minnum;

        // normalize inputs
        for (int x = 0; x < input_array_size; x++)
        {
           normInputPattern[x] = (((inputPattern[x] - minnum) * 0.8) / diff) + 0.1;
        }

        // inputs -> hidden1
        for (int y = 0; y < hidden_array_1_size; y++)
        {
           for (int x = 0; x < input_array_size; x++)
           {
              temp += (normInputPattern[x] * weight_i_h[x, y]);
           }
           hidden1[y] = (1.0 / (1.0 + Math.Exp(-1.0 * (temp + bias[y]))));
           temp = 0;
```

```
        }

        // hidden1 -> hidden2
        for (int y = 0; y < hidden_array_2_size; y++)
        {
            for (int x = 0; x < hidden_array_1_size; x++)
            {
                temp += (hidden1[x] * weight_h_h[x, y]);
            }
            hidden2[y] = (1.0 / (1.0 + Math.Exp(-1.0 * (temp + bias[y +
hidden_array_1_size]))));
            temp = 0;
        }
        // hidden2 -> output
        for (int y = 0; y < output_array_size; y++)
        {
            for (int x = 0; x < hidden_array_2_size; x++)
            {
                temp += (hidden2[x] * weight_h_o[x, y]);
            }
            normOutputPattern[y] = (1.0 / (1.0 + Math.Exp(-1.0 * (temp + bias[y +
hidden_array_1_size + hidden_array_2_size]))));
            temp = 0;
        }
        tabItemANNHardnessManualOutputtextBox2.Text =
((((normOutputPattern[0] - 0.1) * diff) / 0.8) + minnum).ToString();
        }

    #endregion
```

A2.2 Code is written in Computational file of Microsoft SilverLight API for obtaining the Line plot of hardness at varying small grain size.

```
#region Line Plot

    private void ANNHardnessLineplotInputradbut3_Click(object sender,
RoutedEventArgs e)
    {
        if ((bool)ANNHardnessLineplotInputradbut1.IsChecked)
        {
            ANNHardnessLineplotInputtextBox1.Visibility =
System.Windows.Visibility.Visible;
            ANNHardnesseLineplotTB1.Visibility =
System.Windows.Visibility.Visible;
            ANNHardnessLineplotInputtextBox2.Visibility =
System.Windows.Visibility.Visible;
```

```
            ANNHardnessLineplotInputtextBox3.Visibility =
System.Windows.Visibility.Visible;
            ANNHardnesseLineplotTB2.Visibility =
System.Windows.Visibility.Collapsed;
            ANNHardnessLineplotInputtextBox4.Visibility =
System.Windows.Visibility.Collapsed;
            ANNHardnessLineplotInputtextBox5.Visibility =
System.Windows.Visibility.Visible;
            ANNHardnesseLineplotTB3.Visibility =
System.Windows.Visibility.Collapsed;
            ANNHardnessLineplotInputtextBox6.Visibility =
System.Windows.Visibility.Collapsed;
            ANNHardnessLineplotInputtextBox7.Visibility =
System.Windows.Visibility.Visible;
            ANNHardnesseLineplotTB4.Visibility =
System.Windows.Visibility.Collapsed;
            ANNHardnessLineplotInputtextBox8.Visibility =
System.Windows.Visibility.Collapsed;
            ANNHardnessLineplotInputtextBox9.Visibility =
System.Windows.Visibility.Visible;
            ANNHardnesseLineplotTB5.Visibility =
System.Windows.Visibility.Collapsed;
            ANNHardnessLineplotInputtextBox10.Visibility =
System.Windows.Visibility.Collapsed;
        }
        else if ((bool)ANNHardnessLineplotInputradbut2.IsChecked)
        {
            ANNHardnessLineplotInputtextBox1.Visibility =
System.Windows.Visibility.Visible;
            ANNHardnesseLineplotTB1.Visibility =
System.Windows.Visibility.Collapsed;
            ANNHardnessLineplotInputtextBox2.Visibility =
System.Windows.Visibility.Collapsed;
            ANNHardnessLineplotInputtextBox3.Visibility =
System.Windows.Visibility.Visible;
            ANNHardnesseLineplotTB2.Visibility =
System.Windows.Visibility.Visible;
            ANNHardnessLineplotInputtextBox4.Visibility =
System.Windows.Visibility.Visible;
            ANNHardnessLineplotInputtextBox5.Visibility =
System.Windows.Visibility.Visible;
            ANNHardnesseLineplotTB3.Visibility =
System.Windows.Visibility.Collapsed;
            ANNHardnessLineplotInputtextBox6.Visibility =
System.Windows.Visibility.Collapsed;
            ANNHardnessLineplotInputtextBox7.Visibility =
System.Windows.Visibility.Visible;
```

```
            ANNHardnesseLineplotTB4.Visibility =
System.Windows.Visibility.Collapsed;
            ANNHardnessLineplotInputtextBox8.Visibility =
System.Windows.Visibility.Collapsed;
            ANNHardnessLineplotInputtextBox9.Visibility =
System.Windows.Visibility.Visible;
            ANNHardnesseLineplotTB5.Visibility =
System.Windows.Visibility.Collapsed;
            ANNHardnessLineplotInputtextBox10.Visibility =
System.Windows.Visibility.Collapsed;
        }
        else if ((bool)ANNHardnessLineplotInputradbut4.IsChecked)
        {
            ANNHardnessLineplotInputtextBox1.Visibility =
System.Windows.Visibility.Visible;
            ANNHardnesseLineplotTB1.Visibility =
System.Windows.Visibility.Collapsed;
            ANNHardnessLineplotInputtextBox2.Visibility =
System.Windows.Visibility.Collapsed;
            ANNHardnessLineplotInputtextBox3.Visibility =
System.Windows.Visibility.Visible;
            ANNHardnesseLineplotTB2.Visibility =
System.Windows.Visibility.Collapsed;
            ANNHardnessLineplotInputtextBox4.Visibility =
System.Windows.Visibility.Collapsed;
            ANNHardnessLineplotInputtextBox5.Visibility =
System.Windows.Visibility.Visible;
            ANNHardnesseLineplotTB3.Visibility =
System.Windows.Visibility.Collapsed;
            ANNHardnessLineplotInputtextBox6.Visibility =
System.Windows.Visibility.Collapsed;
            ANNHardnessLineplotInputtextBox7.Visibility =
System.Windows.Visibility.Visible;
            ANNHardnesseLineplotTB4.Visibility =
System.Windows.Visibility.Visible;
            ANNHardnessLineplotInputtextBox8.Visibility =
System.Windows.Visibility.Visible;
            ANNHardnessLineplotInputtextBox9.Visibility =
System.Windows.Visibility.Visible;
            ANNHardnesseLineplotTB5.Visibility =
System.Windows.Visibility.Collapsed;
            ANNHardnessLineplotInputtextBox10.Visibility =
System.Windows.Visibility.Collapsed;
        }
        else if ((bool)ANNHardnessLineplotInputradbut3.IsChecked)
        {
```

```
            ANNHardnessLineplotInputtextBox1.Visibility =
System.Windows.Visibility.Visible;
            ANNHardnesseLineplotTB1.Visibility =
System.Windows.Visibility.Collapsed;
            ANNHardnessLineplotInputtextBox2.Visibility =
System.Windows.Visibility.Collapsed;
            ANNHardnessLineplotInputtextBox3.Visibility =
System.Windows.Visibility.Visible;
            ANNHardnesseLineplotTB2.Visibility =
System.Windows.Visibility.Collapsed;
            ANNHardnessLineplotInputtextBox4.Visibility =
System.Windows.Visibility.Collapsed;
            ANNHardnessLineplotInputtextBox5.Visibility =
System.Windows.Visibility.Visible;
            ANNHardnesseLineplotTB3.Visibility =
System.Windows.Visibility.Visible;
            ANNHardnessLineplotInputtextBox6.Visibility =
System.Windows.Visibility.Visible;
            ANNHardnessLineplotInputtextBox7.Visibility =
System.Windows.Visibility.Visible;
            ANNHardnesseLineplotTB4.Visibility =
System.Windows.Visibility.Collapsed;
            ANNHardnessLineplotInputtextBox8.Visibility =
System.Windows.Visibility.Collapsed;
            ANNHardnessLineplotInputtextBox9.Visibility =
System.Windows.Visibility.Visible;
            ANNHardnesseLineplotTB5.Visibility =
System.Windows.Visibility.Collapsed;
            ANNHardnessLineplotInputtextBox10.Visibility =
System.Windows.Visibility.Collapsed;
        }
        else if ((bool)ANNHardnessLineplotInputradbut5.IsChecked)
        {
            ANNHardnessLineplotInputtextBox1.Visibility =
System.Windows.Visibility.Visible;
            ANNHardnesseLineplotTB1.Visibility =
System.Windows.Visibility.Collapsed;
            ANNHardnessLineplotInputtextBox2.Visibility =
System.Windows.Visibility.Collapsed;
            ANNHardnessLineplotInputtextBox3.Visibility =
System.Windows.Visibility.Visible;
            ANNHardnesseLineplotTB2.Visibility =
System.Windows.Visibility.Collapsed;
            ANNHardnessLineplotInputtextBox4.Visibility =
System.Windows.Visibility.Collapsed;
            ANNHardnessLineplotInputtextBox5.Visibility =
System.Windows.Visibility.Visible;
```

```
            ANNHardnesseLineplotTB3.Visibility =
System.Windows.Visibility.Collapsed;
            ANNHardnessLineplotInputtextBox6.Visibility =
System.Windows.Visibility.Collapsed;
            ANNHardnessLineplotInputtextBox7.Visibility =
System.Windows.Visibility.Visible;
            ANNHardnesseLineplotTB4.Visibility =
System.Windows.Visibility.Collapsed;
            ANNHardnessLineplotInputtextBox8.Visibility =
System.Windows.Visibility.Collapsed;
            ANNHardnessLineplotInputtextBox9.Visibility =
System.Windows.Visibility.Visible;
            ANNHardnesseLineplotTB5.Visibility =
System.Windows.Visibility.Visible;
            ANNHardnessLineplotInputtextBox10.Visibility =
System.Windows.Visibility.Visible;
        }
    }

    private void ANNHardnessLinePlotinputbutton1_Click(object sender,
RoutedEventArgs e)
    {
        if ((bool)ANNHardnessLineplotInputradbut5.IsChecked)
            UpdateANNHardnessTypeLineplot();
        else if ((bool)ANNHardnessLineplotInputradbut1.IsChecked)
            UpdateANNHardnessThicknessReductionLineplot();
        else if ((bool)ANNHardnessLineplotInputradbut2.IsChecked)
            UpdateANNHardnessLiqVolFracLineplot();
        else if ((bool)ANNHardnessLineplotInputradbut4.IsChecked)
            UpdateANNHardnessLargeGrainLineplot();
        else if ((bool)ANNHardnessLineplotInputradbut3.IsChecked)
            UpdateANNHardnessSmallGrainLineplot();
        else
            MessageBox.Show("Nothing selected");
    }

    const int ANN_Hardness_MaxPoints = 500;

    double[,] inputPatternsANNHardness = new double[ANN_Hardness_MaxPoints,
5];
    double[,] outputPatternsANNHardness = new
double[ANN_Hardness_MaxPoints, 1];

    private void UpdateANNHardnessSmallGrainLineplot()
    {
        // get the values from the GUI
        float fixedType = float.Parse(ANNHardnessLineplotInputtextBox9.Text);
```

```
        float fixedthickness = float.Parse(ANNHardnessLineplotInputtextBox1.Text);
        float fixedLiqVolFrac =
float.Parse(ANNHardnessLineplotInputtextBox3.Text);
        float fixedLargeGrain =
float.Parse(ANNHardnessLineplotInputtextBox7.Text);
        float SmallGrainLow =
float.Parse(ANNHardnessLineplotInputtextBox5.Text);
        float SmallGrainHigh =
float.Parse(ANNHardnessLineplotInputtextBox6.Text);
        int numPoints = int.Parse(ANNHardnessLineplotInputtextBox11.Text);

        // calculate the independent and dependent values
        List<Item> series1 = new List<Item>();
        LineSeries plottable1 = new LineSeries();

        Style noPointstyle = new System.Windows.Style(typeof(Control));
        noPointstyle.Setters.Add(new Setter() { Property = TemplateProperty, Value =
null });

        // calculate the step size for the points
        float stepSize = (SmallGrainHigh - SmallGrainLow) / (numPoints - 1);

        // generate the input patterns
        for (int i = 0; i < numPoints; i++)
        {
            inputPatternsANNHardness[i, 0] = fixedType;
            inputPatternsANNHardness[i, 1] = fixedthickness;
            inputPatternsANNHardness[i, 2] = fixedLiqVolFrac;
            inputPatternsANNHardness[i, 3] = fixedLargeGrain;
            inputPatternsANNHardness[i, 4] = SmallGrainLow + i * stepSize;
        }

        // create array for output patterns
        //double[] outputPatterns = new double[numPoints];

        double maxnum = 121.824;
        double minnum = 0;
        const int input_array_size = 5;
        const int hidden_array_1_size = 4;
        const int hidden_array_2_size = 3;
        const int output_array_size = 1;

        // create normalized input and output arrays
        double[] normInputPattern = new double[input_array_size];
        double[] normOutputPattern = new double[output_array_size];

        // create hidden arrays
```

```
        double[] hidden1 = new double[hidden_array_1_size];
        double[] hidden2 = new double[hidden_array_2_size];

        double temp = 0;

        double[,] weight_i_h = new double[input_array_size, hidden_array_1_size]
        {
           {-15.7427, -22.9999, -0.829085, 16.5365},
           {18.3658, -2.87572, -0.153679, -8.11444},
           { 16.9694, -24.8862, 3.89563, -32.8081},
           {4.1756, -2.44843, 5.32811, -1.04068},
           {8.8315, 0.381159, 6.73193, -2.6118}
        };

        double[,] weight_h_h = new double[hidden_array_1_size,
hidden_array_2_size]
        {
           {10.934, 10.8556, 2.61835},
           {-3.66757, -13.9818, 1.7814},
           {1.05747, -4.92797, 1.7347},
           {-1.29822, 11.3375, 2.37397}
        };

        double[,] weight_h_o = new double[hidden_array_2_size, output_array_size]
        {
           {-2.94166},
           {4.93686},
           {-0.174129}
        };

        double[] bias = new double[]
        {
           -8.83525, 12.7545, -5.1725, 10.2617,
           0.33406, 0.69, 0.65,
           0.68
        };

              for (int z = 0; z < numPoints; z++)
        {
           double diff = maxnum - minnum;

           // normalize inputs
           for (int x = 0; x < input_array_size; x++)
           {
              normInputPattern[x] = (((inputPatternsANNHardness[z, x] - minnum) *
0.8) / diff) + 0.1;
           }
```

```
            // inputs -> hidden1
            for (int y = 0; y < hidden_array_1_size; y++)
            {
                for (int x = 0; x < input_array_size; x++)
                {
                    temp += (normInputPattern[x] * weight_i_h[x, y]);
                }
                hidden1[y] = (1.0 / (1.0 + Math.Exp(-1.0 * (temp + bias[y]))));
                temp = 0;
            }

            // hidden1 -> hidden2
            for (int y = 0; y < hidden_array_2_size; y++)
            {
                for (int x = 0; x < hidden_array_1_size; x++)
                {
                    temp += (hidden1[x] * weight_h_h[x, y]);
                }
                hidden2[y] = (1.0 / (1.0 + Math.Exp(-1.0 * (temp + bias[y +
hidden_array_1_size]))));
                temp = 0;
            }
            // hidden2 -> output
            for (int y = 0; y < output_array_size; y++)
            {
                for (int x = 0; x < hidden_array_2_size; x++)
                {
                    temp += (hidden2[x] * weight_h_o[x, y]);
                }
                normOutputPattern[y] = (1.0 / (1.0 + Math.Exp(-1.0 * (temp + bias[y +
hidden_array_1_size + hidden_array_2_size]))));
                temp = 0;
            }

            outputPatternsANNHardness[z, 0] = ((((normOutputPattern[0] - 0.1) * diff)
/ 0.8) + minnum);

            series1.Add(
                new Item()
                {
                    Independent = inputPatternsANNHardness[z, 4],
                    Dependent = outputPatternsANNHardness[z,0]
                }
            );

        }
```

```
            ANNHardnessLineplot.Series.Clear();

            if ((bool)ANNHardnessLinePlotinputCkbox1.IsChecked)
            {
                // update the plot
                plottable1.ItemsSource = series1;
                plottable1.IndependentValueBinding = new
System.Windows.Data.Binding("Independent");
                plottable1.DependentValueBinding = new
System.Windows.Data.Binding("Dependent");
                plottable1.DataPointStyle = noPointstyle;

                ANNHardnessLineplot.Series.Add(plottable1);
            }

        }
```

A2.3 Code written in Computational file of Microsoft SilverLight API for the Bar plot of hardness (used to optimise hardness of mushy state rolled composite) by varying each input parameter.

```
#region Bar Plot

    // paste here and change names accordingly
    List<Item1> Hardness;
    ColumnSeries plotHardness;
    bool HardnessBarPlotLoaded = false;

    private void ANNHardnessBarplot_Loaded(object sender,RoutedEventArgs e)
    {
       if (HardnessBarPlotLoaded)
          return;

       Hardness = new List<Item1>();
       Hardness.Add(new Item1() { Independent = String.Empty, Dependent = 20 });
       ANNHardnessBarplot.Axes.Clear();

       ANNHardnessBarplot.Axes.Add(new CategoryAxis()
       {
          Orientation = AxisOrientation.X
       });

       ANNHardnessBarplot.Axes.Add(new LinearAxis()
       {
          Orientation = AxisOrientation.Y,
          Minimum = 40,
          Maximum = 140,
          Interval = 20
       });

       plotHardness = new ColumnSeries()
       {
          Title = "Hardness",
          ItemsSource = Hardness,
          IndependentValueBinding = new
System.Windows.Data.Binding("Independent"),
          DependentValueBinding = new
System.Windows.Data.Binding("Dependent"),
          Visibility = System.Windows.Visibility.Collapsed
       };


       ANNHardnessBarplot.Series.Clear();
```

```
            ANNHardnessBarplot.Series.Add(plotHardness);

            ToolTipService.SetToolTip(ANNHardnessTypeSlider,
ANNHardnessTypeSlider.Minimum.ToString("F0"));
            ToolTipService.SetToolTip(ANNHardnessthickSlider,
ANNHardnessthickSlider.Minimum.ToString("F2"));
            ToolTipService.SetToolTip(ANNHardnessLVFSlider,
ANNHardnessLVFSlider.Minimum.ToString("F2"));
            ToolTipService.SetToolTip(ANNHardnessLGSSlider,
ANNHardnessLGSSlider.Minimum.ToString("F2"));
            ToolTipService.SetToolTip(ANNHardnessSGSSlider,
ANNHardnessSGSSlider.Minimum.ToString("F2"));

            HardnessBarPlotLoaded = true;
        }

        private void ANNHardnessBarplotinputbutton1_Click(object sender,
RoutedEventArgs e)
        {
            if (!HardnessBarPlotLoaded)
                return;

            UpdateANNHardnessBarPlot();

            if ((bool)ANNHardnessBarplotinputCkbox1.IsChecked)
                plotHardness.Visibility = System.Windows.Visibility.Visible;
            else
                plotHardness.Visibility = System.Windows.Visibility.Collapsed;

        }
        // Fromm Here
        private void UpdateANNHardnessBarPlot()
        {
            double maxnum = 121.824;
            double minnum = 0;
            const int input_array_size = 5;
            const int hidden_array_1_size = 4;
            const int hidden_array_2_size = 3;
            const int output_array_size = 1;

            double[,] weight_i_h = new double[input_array_size, hidden_array_1_size]
            {
                {-15.7427, -22.9999, -0.829085, 16.5365},
                {18.3658, -2.87572, -0.153679, -8.11444},
                { 16.9694, -24.8862, 3.89563, -32.8081},
                {4.1756, -2.44843, 5.32811, -1.04068},
                {8.8315, 0.381159, 6.73193, -2.6118}
```

```
        };

        double[,] weight_h_h = new double[hidden_array_1_size,
hidden_array_2_size]
        {
           {10.934, 10.8556, 2.61835},
           {-3.66757, -13.9818, 1.7814},
           {1.05747, -4.92797, 1.7347},
           {-1.29822, 11.3375, 2.37397}
        };

        double[,] weight_h_o = new double[hidden_array_2_size, output_array_size]
        {
           {-2.94166},
           {4.93686},
           {-0.174129}
        };

        double[] bias = new double[]
        {
           -8.83525, 12.7545, -5.1725, 10.2617,
           0.33406, 0.69, 0.65,
           0.68
        };

        // generate the input patterns
        double[] inputPattern = new double[input_array_size];
        inputPattern[0] = (ANNHardnessTypeSlider.Value >= 1.5) ? 2 : 1;
        inputPattern[1] = (ANNHardnessthickSlider.Value);
        inputPattern[2] = (ANNHardnessLVFSlider.Value);
        inputPattern[3] = (ANNHardnessLGSSlider.Value);
        inputPattern[4] = (ANNHardnessSGSSlider.Value);

        // create normalized input and output arrays
        double[] normInputPattern = new double[input_array_size];
        double[] normOutputPattern = new double[output_array_size];

        // create hidden arrays
        double[] hidden1 = new double[hidden_array_1_size];
        double[] hidden2 = new double[hidden_array_2_size];

        double temp = 0;
        double diff = maxnum - minnum;

        // normalize inputs
        for (int x = 0; x < input_array_size; x++)
        {
```

```
            normInputPattern[x] = (((inputPattern[x] - minnum) * 0.8) / diff) + 0.1;
        }

        // inputs -> hidden1
        for (int y = 0; y < hidden_array_1_size; y++)
        {
            for (int x = 0; x < input_array_size; x++)
            {
                temp += (normInputPattern[x] * weight_i_h[x, y]);
            }
            hidden1[y] = (1.0 / (1.0 + Math.Exp(-1.0 * (temp + bias[y]))));
            temp = 0;
        }

        // hidden1 -> hidden2
        for (int y = 0; y < hidden_array_2_size; y++)
        {
            for (int x = 0; x < hidden_array_1_size; x++)
            {
                temp += (hidden1[x] * weight_h_h[x, y]);
            }
            hidden2[y] = (1.0 / (1.0 + Math.Exp(-1.0 * (temp + bias[y +
hidden_array_1_size]))));
            temp = 0;
        }

        // hidden2 -> output
        for (int y = 0; y < output_array_size; y++)
        {
            for (int x = 0; x < hidden_array_2_size; x++)
            {
                temp += (hidden2[x] * weight_h_o[x, y]);
            }
            normOutputPattern[y] = (1.0 / (1.0 + Math.Exp(-1.0 * (temp + bias[y +
hidden_array_1_size + hidden_array_2_size]))));
            temp = 0;
        }

        Hardness.ElementAt(0).Dependent = ((((normOutputPattern[0] - 0.1) * diff) /
0.8) + minnum);

        plotHardness.Refresh();
    }
private void ANNhardnessSlider_ValueChanged(object sender,
RoutedPropertyChangedEventArgs<double> e)
    {
        if (sender.Equals(ANNHardnessTypeSlider))
```

```
            ToolTipService.SetToolTip(ANNHardnessTypeSlider,
(ANNHardnessTypeSlider.Value >= 1.5) ? "2" : "1");
        else if (sender.Equals(ANNHardnessthickSlider))
            ToolTipService.SetToolTip(ANNHardnessthickSlider,
ANNHardnessthickSlider.Value.ToString("F2"));
        else if (sender.Equals(ANNHardnessLVFSlider))
            ToolTipService.SetToolTip(ANNHardnessLVFSlider,
ANNHardnessLVFSlider.Value.ToString("F2"));
        else if (sender.Equals(ANNHardnessLGSSlider))
            ToolTipService.SetToolTip(ANNHardnessLGSSlider,
ANNHardnessLGSSlider.Value.ToString("F2"));
        else if (sender.Equals(ANNHardnessSGSSlider))
            ToolTipService.SetToolTip(ANNHardnessSGSSlider,
ANNHardnessSGSSlider.Value.ToString("F2"));
        else
            return;

        UpdateANNHardnessBarPlot();
    }

    #endregion
```

Appendix III

One-Sample and two sample Kolmogorov-Smirnov test

The One-Sample Kolmogorov-Smirnov Test procedure is a statistical analysis technique that compares the observed cumulative distribution function for a variable with a specified theoretical distribution, which may be normal, uniform, Poisson, or exponential. The Kolmogorov-Smirnov *Z* is computed from the largest difference (in absolute value) between the observed and theoretical cumulative distribution functions. This goodness-of-fit test tests whether the observations could reasonably have come from the specified distribution. In the present work the error distributions mentioned from (a) to (d) in section 8.4.3 are compared with a standard normal distribution.

In a manner, one sample KS test is a nonparametric test for the equality of continuous, one-dimensional probability distributions a two sample KS test is used to compare two samples. The Kolmogorov–Smirnov statistic quantifies a distance between the empirical distribution function of the sample and the cumulative distribution function of the reference distribution, or between the empirical distribution functions of two samples. The null distribution of this statistic is calculated under the null hypothesis that the samples are drawn from the same distribution in the case of two sample test or that the sample is drawn from the reference distribution in the one-sample case. In each case, the distributions considered under the null hypothesis are continuous distributions but are otherwise unrestricted.

Student_t Test

An unpaired t-test (also known as the student's t-test) and the paired t-test both assume that analysed data is from a normal distribution. In an unpaired t-test, the test is applied to two independent representative groups of a distribution. The sample sizes from the two groups may or may not be equal. In addition to the assumption that the data is from a normal distribution, it is also assumed that the standard deviations are

approximately same in both the groups. Then the t-test compares the means of the two groups of data. The test determines whether the data has come from the same population or not. The mean difference is then calculated which could be positive or negative. The mean difference is calculated with a 95% confidence interval or 5% significance. A p-value is calculated where p is the probability of a false-positive event.

In a paired t-test, the data is derived from study subjects who have been measured at two time points (each individual has two measurements). The two measurements generally are before and after a cause and effect relationship. Then a 95% confidence interval is derived from the difference between the two sets of paired observations.

Appendix IV

The data used for validation of the ANN with feed forward architectures are actually the unseen data, as the network modelling was done prior to conduct of validation experiments. Therefore, the generalisation of the ANN models proposed is implied by the small errors in prediction that have been cited in the thesis (Table 4.4, 4.5, 5.4, 5.5, 6.3 and 7.2). However, the generalisation capability of the ANN model (i. e. The architecture used for prediction of grain sizes, hardness etc.) can be demonstrated by picking up a similar data and training the network for this data and checking:

i. Convergence characteristics
ii. Error in prediction

Generalisation capability of the ANN model for grain size prediction

The generalisation capability of the ANN model for prediction of grain sizes is presented by considering the case of mushy state rolling of as cast Al-4.5Cu-5TiC composite which is different from the material tried out in our study. The data has been taken from the work of Herbert (2007). The input parameters for the network are initial material of the Al-4.5Cu-5TiC composite (which is kept constant = 1), % Thickness reduction and % Liquid volume fraction in the composite. The outputs of the network are large and small grain sizes. The network is trained with the available 12 input-output patterns. Same architecture as that was used for the prediction of grain sizes for Al-4.5Cu-5TiB_2 composite is used for training this network. Similarly the learning rate and momentum term was also not changed. The network converged nicely to a MSE of 0.00016 after around 18.8 lakh epochs. Table 4.6 gives the comparison of literature data with the ANN predictions in terms of percentage error in prediction over the literature data.

TABLE A.1 Comparison of values of grain sizes of as cast Al-4.5Cu- 5TiC composite samples subjected to mushy state rolling with ANN predicted values. (Herbert 2007)

Specimen descriptions		Literature		ANN		%Error	
		Grain size(μm)		Grain size (μm)		Grain size	
		Large	Small	Large	Small	Large	Small
2.5% Thickness Reduction	$f_l \sim 0.1$	78	40	77.93	40.21	0.09	-0.53
	$f_l \sim 0.2$	75	38	73.70	39.05	1.73	-2.76
	$f_l \sim 0.3$	84	47	83.88	46.92	0.14	0.17
5% Thickness Reduction	$f_l \sim 0.1$	71	39	70.99	38.04	0.01	2.46
	$f_l \sim 0.2$	70	41	69.62	40.35	0.54	1.59
	$f_l \sim 0.3$	76	42	77.47	40.55	-1.93	3.45
7.5% Thickness Reduction	$f_l \sim 0.1$	70	44	70.49	44.61	-0.7	-1.39
	$f_l \sim 0.2$	69	48	71.69	48.05	-3.9	-0.1
	$f_l \sim 0.3$	82	49	81.24	49.37	0.93	-0.76
10.5% Thickness Reduction	$f_l \sim 0.1$	68	48	68.34	47.87	-0.5	0.27
	$f_l \sim 0.2$	67	44	66.14	44.84	1.28	-1.91
	$f_l \sim 0.3$	79	44	78.75	44.66	0.32	-1.5

It can be seen from Table 4.6 that the ANN model predicts the large grain sizes within ± 1.93%. Similarly, the small grain sizes are predicted by the network within an error of ± 3.45%. Thus it is seen that for a given kind of model processing, be it mushy state rolling, mushy state forging or any other mushy state forming process, same ANN model can be used to predict the grain sizes.

Generalisation capability of the ANN model for hardness prediction

The data for demonstrating the generalisation capability of the ANN model for hardness prediction is taken from the work of Herbert (2007). The part of the work of Herbert (2007) used here involved the study on the hardness characteristics of mushy state rolled as cast Al-4.5Cu-5TiC composite. ANN model with 12 available patterns is trained with the same architecture, learning rate parameter and momentum factor as used for training the model for predicting hardness of Al-4.5Cu-5TiB_2 composite. The inputs to the network are initial material of the Al-4.5Cu-5TiC composite (which is kept constant = 1), % Thickness reduction and % Liquid volume fraction in the composite, large and small grain size. The output of the network is hardness. The network was found to excellently converge to a MSE of 2.4 x 10^{-5} after 6.3 lakh

epochs. Table A.2 shows the comparison of the literature values of hardness with the ANN predicted values of hardness.

Table A.2 Comparison of values hardness from literature for pre hot rolled Al-4.5Cu-TiC composite samples subjected to mushy state rolling with ANN predicted values.

Specimen descriptions		Experimental			ANN	%Error
		Grain size (μm)		Hardness (Hv)	Hardness (Hv)	Hardness
		Large	Small			
2.5% Thickness Reduction	f_l ~ 0.1	78	40	89	89.32	-0.36
	f_l ~ 0.2	75	38	92	91.14	0.93
	f_l ~ 0.3	84	47	85	84.55	0.53
5% Thickness Reduction	fl ~ 0.1	71	39	92	92.16	-0.17
	f_l ~ 0.2	70	41	95	94.3	0.74
	f_l ~ 0.3	76	42	88	89.29	-1.47
7.5% Thickness Reduction	f_l ~ 0.1	70	44	93	93.5	-0.54
	f_l ~ 0.2	69	48	96	96.2	-0.21
	f_l ~ 0.3	82	49	91	91.12	-0.13
10.5% Thickness Reduction	f_l ~ 0.1	68	48	95	94.79	0.22
	f_l ~ 0.2	67	44	98	97.83	0.17
	f_l ~ 0.3	79	44	94	93.55	0.48

It can be seen from Table A.2 that the error in prediction for hardness over the entire range of data used for training the network is within ± 1.47 %. This demonstrates that the ANN model with a particular architecture can be used to model similar processes. This is because ANN models having similar architectures possess capabilities to generalise the subtle relationships that exist between the input-output data for similar processes. Moreover, the code that has been developed is generic in nature having flexibility in the selection of architectures, in terms of number of layers and number of neurons in each layer as well as associated coefficients. Due to this, the Hybrid RNN model developed may be easily adopted to any of the process prediction, following proper training.

REFERENCES

Ackley, D.H., Hinton, G.E., and Sejnowski, T.J. (1985). “A learning algorithm for Boltzman machines.” *Cognitive Science*, 9, 147-169.

Aikin, R. (1997). "The mechanical properties of in-situ composites." *JOM, Journal of the Minerals, Metals and Materials Society* 49(8), 35-39.

Amhold, V. and Muller-Schwelling, D. (1991). *SAE Technical Paper Series 910156*. SAE International, Warrendale, PA

Annavarapu, S. and Doherty, R.D. (1995). "Inhibited coarsening of solid-liquid microstructures in spray casting at high-volume fractions of solid." *Acta Metall. Mater.*, 43, 3207-3230.

Apaydin, N. Prabhakar, K.V. and Doherty, R.D. (1980). "Special grain boundaries in rheocast Al-Mg." *Mater. Sci. Eng. A.*, 46, 145-150.

Archard, J.F. (1953). “Contact and rubbing of flat surfaces”. *J. Appl. Phys.*, 24, 981-988.

Atkinson, H.V. (2005). "Modelling the semisolid processing of metallic alloys." *Prog. in Mater. Sci.*, 50, 341-412.

Attoh-Okine, N.O. (1999). “Analysis of learning rate and momentum term in backpropagation neural network algorithm trained to predict pavement performance.” *Adances in Engineering Software*, 30, 291-302.

Barnes, H.A., and Walters, K. (1985). "The Yield Stress Myth." *Rheol. Acta*, 24, 323-326.

Barnes, H.A., Hutton, J.F., and Walters, K. (1989). "An introduction to rheology." Amsterdam, The Netherlands: *Elsevier*, 27-31.

Bartels, C., Raabe, D Gottstein, G., Huber, U. (1997). "Investigation of the precipitation kinetics in an Al6061/TiB_2 metal matrix composite." *Mater Sci. Eng. A*, 237, 12-23.

Bengioy, Y., Simrad, P., and Frasconi, P. (1994). ‘Learning long time dependencies with gradient descent is difficult.” *IEEE Trans. Neural Netw.*, 5(2), 157-166.

Bergsma, S.C., Tolle, M.C., Kassner, M.E., Li, X., and E. Evangelista, (1997). "Semi-solid thermal transformations of Al-Si alloys and the resulting mechanical properties." *Mater. Sci. Eng. A*, 237, 24–34.

Bergsma, S.C. Li, X. Kassner, M.E. (2001). "Semi-solid thermal transformations in Al–Si alloys: II. The optimized tensile and fatigue properties of semi-solid 357 and modified 319 aluminum alloys." *Mater. Sci. Eng. A*, 297, 69-77.

Bezdek, J.C. (1992). "On the relationship between neural networks, pattern recognition and intelligence." *Int. J. Approx. Reasoning*, 6, 85-107.

Bhat Radhakrishna, B.V., Mahajan, Y.R., Roshan, H.M., Prasad, Y.U.R.K. (1992). "Processing map for hot working of powder metallurgy 2124 Al-20 vol. pct. SiC_p metal matrix composite". *Metall. Trans. A.*, 23, 2223-2230.

Blazek, K.E., Kelly, J.E., and Pottore, N.S. (1995). "The development of a continuous rheocaster for ferrous and high-melting point alloys." *ISIJ Int.*, 35, 813-818.

Blais, S., Loue, W., and Pluchon, C. (1996). "Structure Control by Electromagnetic Stirring and Reheating at Semi-solid State." *Proc. 4th Int. Conf. on Semi-Solid Processing of Alloys and Composites*, Kirkwood DH, Kapranos P, eds., Sheffield, UK, June 1996, University of Sheffield, 187-192.

Braccini, M., Salvo, L., Suery, M., Brechet, Y. (1998). *Proc. 5th Int. Conf. on Semi-Solid Processing of Alloys and Composites*, Bhasin AK, Moore JJ, Young KP, Midson S, eds., Golden, Colorado, USA, June 1998. Golden, CO: Colorado School of Mines, USA, 371-378.

Cameron, S. H. (1960). "An estimate of the complexity requisite in a universal decision network.' *Wright Air Development Division*, report, 60-600.

Caracostas, C.A., Chiou, w.A., Fine, M.E. and Chung, H.S. (1992). "Wear mechanisms during lubricated sliding of XD^{TM} 2024 – Al-TiB_2 metal matrix composites against steel". *Scripta Metall. Mater.*, 27, 167-172.

Chen, C.Y., Sekhar, J.A., Backman, D.G. and Mehrabian, R. (1979). "Thixoforging of aluminium alloys." *Mater. Sci. Eng*, 40, 265-272.

Chen, D.S., and Jain, R.C. (1994). "A robust backpropagation algorithm for function approximation." IEEE Trans. *Neural Networks*, 5, 467-479.

Chen, T.J., Hao, Y., and Sun, J. (2002). "Microstructural evolution of previously deformed ZA27 alloy during partial remelting." *Mater. Sci. Eng. A*, 337, 73-81.

Cho, J.C., Cho, H.Y., Min, G.S., Park, H.J., and Choi, J.U. (1996). "A fundamental study on semi-solid forging with light and hardly formable materials." *J. Korean Soc. Prec. Eng.*, 13(7), 29-35.

Cho W.G., and Kang, C.G. (2000). "Mechanical properties and their microstructural evaluation in the thixoforming process of semisolid aluminium alloy." *J. Mater. Process. Tech.*, 105, 269-277.

Choi, J.C., and Park, H.J. (1998a). *Proc. 5th Int. Conf. on Semi-Solid Processing of Alloys and Composites,* Bhasin AK, Moore JJ, Young KP, Midson S, eds. Golden, Colorado, USA, June 1998. Golden, CO: Colorado School of Mines, USA, 457-464.

Choi, J.C., and Park, H.J. (1998b). "Microstructural characteristics of Aluminium 2024 by cold workingin the SIMA process." *J. Mater. Process. Tech.*, 82, 107-116.

Cibula, A. (1949). "The mechanism of grain refinement of sand castings in Al alloys." *J. Inst. Metals,* 76, 321-360.

Cibula, A. (1951). "The grain refinement of Al alloy castings by additions of Ti and B." *J. Inst. Metals,* 80, 1-16.

Cui, J. Lu, G. Dong, J. Xia, K. (2000). "Microstructures after casting and reheating in a continuously cast aluminium alloy 7075." *Proc. 6th Int. Conf. on Semi-Solid Processing of Alloys and Composites*, Chiarmetta GL, Rosso M, eds., Turin, Italy, Sept 2000, Brescia. Italy: Edimet Spa: (2000), 701-704.

Cumming, S. (1993). "Neural networks for monitoring of engine condition data." *Neural Computing and applications*, 1, 96-102.

Das, A**.,** Ji, S., and Fan, Z. (2002). "Morphological development of solidification structures under forced fluid flow: a Monte-Carlo simulation." *Acta Mater.*, 50(18), 4571-4585.

Das, A**.,** and Fan, Z. (2004). "A Monte Carlo simulation of solidification structure formation under melt shearing." *Mater. Sci. Eng. A.*, 365(1-2), 330-335.

DeFreitas, E.R., Ferracini Jr., E., and Ferrante, M. (2004). "Microstructure and rheology of an AA2024 aluminium alloy in the semisolid state, and mechanical properties of a back extruded part." *J. Mater. Process. Tech.*, 146**,** 241–249.

Deuis, R.L., Subramanian, C. and Yellup, J.M. (1997). "Dry sliding wear of aluminium composites – A review". *Compos. Sci. Tech.*, 57, 415-435.

Dobrazanski, L.A.,Maniara, R., Sokolowski, J.H., and Krupinski, M. (2007). "Modelling of mechanical properties of Al-Si-Cu cast alloys using the neural network." *J. Achievements in Materials and Manufacturing Engineering,* 20(1-2), 347-350.

Doherty, R.D., Lee, H.I., and Feest, E.A. (1984). "Microstructure of stir-cast metals." *Mater. Sci. Eng. A.*, 65, 181-189.

Easton, M., and St. John, D. (1999a). "Grain refinement of Aluminum Alloys: Part I: the Nucleant and Solute paradigms- A review of the Literature." *Metall. Trans. A,* 30, 1613-1623.

Easton, M. St. John, D. (1999b). "Grain refinement of Aluminum Alloys: Part II: Confirmation of, and a Mechanism for, the Solute Paradigm." *Metall. Trans.* A, 30, 1625-1633.

Elias L., Kirkwood, D.H., and Sellars, C.M. (1988). *Proc 2nd World Basque Congress, Conference on New Structural Materials,* Bilbao, Spain (Servicio Central de Publicaciones del Gobeierno Vasco), 285–295.

Elman, J.L. (1990). "Finding structure in time." *Cognitive Science,* 14, 179-211.

Elman, J.L. (1991). "Distributed representations, simple neural networks and grammatical structures." *Machine Learning,* 7, 195-225.

Fan, Z., Bevis, M.J., and Ji, S. (1999a). "Method and apparatus for producing semisolid metal slurries and shaped components." Patent PCT/WO/O1/21343A1, 1999.

Fan, Z., Bevis, M.J., and Ji, S. (1999b). "Process and apparatus for manufacturing castings from immiscible metallic liquids." PCT/WO 01/23124 Al (1999).

Fan, Z., Ji, S., and Bevis, M.J. (2001a). "Semi-solid processing of engineering alloys by a twin-screw rheomoulding process*." Mater. Sci. Eng. A,* 299, 210–217.

Fan, Z., Ji, S., and Zhang, J., (2001b). "Processing of immiscible metallic alloys by rheomixing process." *Mater. Sci. Technol.,* 17, 837-842.

Fan, Z. (2002). "Semisolid metal processing*." Int. Mat. Rev.,* 47(2), 49-85.

Ferrante, M., and DeFreitas, E. (1999). "Rheology and microstructural development of Al-4%Cu alloy in the semisolid state." *Mater. Sci. Engg, A,* 271, 172-180.

Flemings, M. C. (1991). "Behaviour of Metal alloys in semisolid state." *Metall. Trans. A,* 22, 957-981.

Flemings, M.C. (1991). "Behaviour of metals in semisolid state." Metall. Trans. A, 22, 957-981.

Flemings, M.C., Chen, S.F., Diewwanit, I., and Cornie, J. A. (1992). "Rheology and structure of some Aluminium base composites." *Proc. 2nd Int. Conf. on Semi-Solid Processing of Alloys and Composites,* Brown SB, Flemings MC, eds.,Cambridge, MA, USA. Warrendale, TMS (1992), 202-210.

Flemings, M C., Martinez, R.A., Figuredo, A., and Yurko, J.A. (2003). "Metal alloy compositions and Process." United States Patent No. 6645323, November 11, 2003.

Flemings M.C., and Martinez, R.A. (2006). "Principles of Microstructural Formation in Semi-Solid Metal Processing." *Solid state Phenomena,* 116-117, 1-8.

Frasconi, P., Gori, M. and Soda, G. (1992). “Local feedback multilayered networks”. *Neural Computation,* 120-130.

Fraser, M.C. (2000). “Neural networks literature review from a statistical perspective.” California State University, Hayward.

Fukuoka, S., and Kiuchi, M. (1974). "A study on plastic working of alloys in their mushy state.” *Proc. 15th Int. Conf. on Machine Tool Design and Research.* Tobias, S.A., Koenigsberger, F. eds., Birmingham, 18-20 September (1974), 423.

Gabathuler, J.P., Barras, D., Krahenbuhl, Y., and Weber, J.C. (June 1992). "Evaluation of various processes for the production of billets with Thixotropic properties." *Proc. 2nd Int. Conf. on Semi-Solid Processing of Alloys and Composites,* Brown SB, Flemings MC, eds., Cambridge, MA, USA. Warrendale, TMS (1992), 33-46.

Gabathuler, J.P., Huber, H.J., and Erling, J. (1993). "Specific properties of produced parts using the thixocasting process." *Proceedings of the International Conference on Aluminium Alloys: new process technologies.* Associazonne Italiana Metallurgia. Italy: Ravenna, 169-180.

Gebelin,J.C., Suery, M., and Favier, D. (1999). "Characteriztion of the rheological behavior in the semisolid solid state of grain refined AZ91 magnesium alloys." *Mater. Sci. Eng. A,* 272, 134-144.

Giles, C., Miller C., Chen, D., Chen, H., Sun, G. And lee, Y. (1992). “Learning and extracting Finite state automats with second order recurrent neural networks.”, *Neural Computations,* 4, 393-405.

German, S., and Bienenstock, E. (1992). “Neural networks and the bias/variance dilemma.” *Networks and Neural Computation,* 4 (1), 1-54.

Gormann, R.P., and Sejnowski, T.J. (1988). “Analysis of hidden units in a layered network trained to classify sonar targets.” *Neural Networks,* 1(1), 75-89.

Gruning, A. (2006). “Stack-like and que-like dynamics in recurrent neural networks.” *Connection Sci.,* 18(1), 23-42.

Gruning, A. (2007) “Elman backpropagation as reinforcement of simple recurrent neural networks.” *Neural computation,* 19(11), 3108-3131.

Guler, N.F., Ubeyli E.D. and Guler I. (2005). “Recurrent neural networks employing Lyapunov exponents for EEG signals classification”. *Expert systems with applications,* 29, 506-514.

Hamilton, R. W., Zhu, Z., Dashwood, R. J., and Lee, P. D. (2003). "Direct semi-solid forming of a powder SiC-Al PMMC: flow analysis, Compos." *Part A Appl. Sci. Manuf.,* 34(4), 333-339.

Haque, M.E. and Sudhakar (2002). “ANN Back Propagation Model for fracture toughness in microalloy steel”. *Int. Jour. of Fatigue,* 24, 1003-1010.

Hardy, S.C., and Voorhes, P.W. (1988). "Ostwald ripening in a system with a high volume fraction of coarsening phase.' *Metall. Trans. A,* 19, 2713-2721.

Hartnett, J.P., and Hu, R.Y.Z. (1989). "Technical Note: The Yield Stress - An Engineering Reality." *J. Rheol.,* 33, 671-679.

Hartley, P., and Pillinger, I. (2006). “Numerical simulation of the forging process.” *Comp. Methods Appl. Mech. Engrg.,* 195, 6676-6790.

Hellawell, A. (1996). "Grain Evolution in Conventional and Rheocastings, Proc. 4th Int Conf on Semi-solid Processing of Alloy and Composites.” *Proc. 4th Int. Conf. on Semi-Solid Processing of Alloys and Composites,* Kirkwood DH, Kapranos P, eds., Sheffield, UK, June 1996, University of Sheffield, 60-65.

Herbert, M.A., Sarkar, C., Mitra, R., and Chakraborty, M. (2006). “Microstructural evolution, hardness and alligatoring in the mushy state rolled cast Al-4.5Cu Alloy and in-situ Al-4.5Cu-5tiB_2 composite.” *Metall. Mater. Trans. A,* 38, 2110-2143.

Herbert, M.A. (2007) “Some studies on the mushy state rolling of Al-4.5Cu alloy base *in situ* composites reinforced with TiB_2 or TiC particles.” Ph.D. thesis, Indian Institute of Technology, Kharagpur, India.

Herbert, M.A., Maiti, R., Mitra, R., and Chakraborty, M. (2008). “Wear behaviour of cast and mushy state rolled Al-4.Cu alloy and in-situ al-4.5Cu-5TiB_2 composite.” *Wear,* 265, 1306-1618.

Herbert, M.A., Das, A.G., Maiti, R., Chakraborty, M., and Mitra, R., (2010). “Tensile properties of cast and mushy state rolled Al-4.Cu alloy and *in-situ* al-4.5Cu-5TiB_2 composite*.” Inter. J. Cast Metal, Res,* 23(4), 216-224.

Hirt, G., Cremer, T., Witulski, R., and Tinius, H.C. (1997). "Lightweight near net shape components produced by thixofroming." *Materials and Design,* 18(4/6), 315-321.

Hong, T.W., Kim, S.K., Ha, H.S., Kim, M.G., Lee, D.B., Kim, Y.J. (2000). "Microstructural evolution and semisolid forming of SiC particulate reinforced AZ91HP magnesium composites." *Mater. Sci. Technol.,* 16, 887-892.

Hopfield, J.J. (1982). “Neural networks and physical systems with emergent collective computational capabilities.” *Proc. National Academy of Sciences,* USA, 79, 2554-2558.

Hopfield J.J. (1984). “Neurons with graded responses have collective computational properties like those of two-state neurons.” *Proc. National Academy of Sciences,* USA, 81, 3088-3092.

Hornik, K. (1993). “Some new results on neural network approximation.”*Neural Networks,* 6(8), 1069-1072.

Ilegbusi, O.J., and Szekely, J. (1988). "Mathematical Modelling of the Electromagnetic Stirring of Molten Metal Solid Suspensions." *Trans. Iron Steel Inst. Jpn.,* 28, 97-103.

Ito, Y., Flemings, M.C., and Corne, J.A. (1992). “Rheological behaviour and microstructure of. Al-6wtpcSi”, *Nature and properties of semi-solid materials,* Sekhar J. A., and Dantzig, J. A. eds., Warrcndale, PA, TMS (1992), 3–17.

Jiahe, A., Jiang, X., Huiju, G., Yaohe, H., and Xishan, X. (2003). “Artificial neural network for prediction of the microstructure of 60Si2MnA rod based on its controlled rolling and cooling process parameters.” *Mater. Sci. and Engg.* A, 344, 318-322.

Joly, P. A. and Mehrabian, R. (1976). "The rheology of a partially solid alloy." *J. of Materials Science,* 11**,** 1393-1418.

Jones, G. P., and Pearson, J. (1976). "Factors affecting the grain refinement of Al using Ti and B additives." *Metall. Trans. B,* 7, 223-234.

Jordan, M. (1992). “Constrained supervised learning.” *J. Math. Psychol.,* 36, 396-425.

Jordan, M. I. (1995). “The organization of action sequences: evidence from a relearning task.” *J. Motor behaviour,* 27, 179-192.

Jorstad, J.L., Pan, Q. Y., and Apelian, D. (2005). "Solidification microstructure affecting ductility in semisolid cast products." *Mater. Sci. Engg.* A, 413-414, 186-191.

Jung, H.K., and Kang, C. G. (2002). "Induction heating process of an Al-Si aluminum alloy for semi-solid die casting and its resulting microstructure.” *J. Mater. Process. Tech.,* 120, 355-364.

Kahermann, W., Sachragner, R., Young, K.P. (1996). “Free standing raw material production system for SSM recycling.*” Proc. 4th Int. Conf. on Semi-Solid Processing of Alloys and Composites,* Kirkwood, D.H., Kapranos P., eds., Sheffield, UK, June 1996, University of Sheffield, 154-158.

Kamat, S.V., Hirth, J.P., and Mehrabian, R. (1989). "Mechanical properties of particulate reinforced Aluminium matrix composites." *Acta Metall.,* 37(9), 2395-2402.

Kang, C.G., and Ku, G.S. (1995). "An experimental investigation on infiltration limit and mechanical properties of Al_2O_3 short fiber reinforced metal matrix composites fabricated by squeeze casting.*" J. Comp. Mater.,* 29(4), 444-462.

Kang, J.Y. and Song, J.H. (1998). “Neural network applications in determining the fatigue crack opening load.” *Int. J. Fatigue,* 20(1), 57-69.

Kapranos, P., Ward, P.J., Atkinson, H.V., and Kirkwood, D.H. (2000). “Near net shaping by semi-solid metal processing." *Materials and Design*, 21**,** 387-394.

Kapranos, P., Kirkwood, D.H., Atkinson, H.V., Rheinlander, J.T., Bentzen, J.J., Toft, P.T., Debel, C.P., Laslaz, G., Maenner, L., Blais, S., Rodriguez-Ibabe, J.M., Lasa. L., Giordano, P., Chiarmetta, G., and Giese, A. (2003). "Thixoforming of an automotive part in A390 hypereutectic Al–Si alloy." *J. Mater. Process. Tech.*, 135**,** 271–277.

Kattamis, T.Z., and Piccone, T.J. (1991). "Rheology of semisolid Al–4.5%Cu–1.5%Mg alloy." *Mater. Sci. Eng. A*, 131**,** 265–272.

Kaufmann, H., Wabusseg, H., Uggowitzer, P.J. Wabusseg, H., and Uggowitzer, P.J. (2000a). “Metallurgical and processing aspects of the NRC semi-solid casting technology.” *Aluminium*, 76, 70-75.

Kaufmann, H., Wabusseg, H., and Uggowitzer, P.J (2000b). “Casting of light metal wrought alloys by New Rheocasting.” *Proc. 6th Int. Conf. on Semi-Solid Processing of Alloys and Composites*, Chiarmetta GL, Rosso M, eds., Turin, Italy, Sept 2000, Brescia. Italy: Edimet Spa: 457-462.

Kenney, M.P., Courtois, J.A., Evans, R.D., Farrior, G.M., Kyonka, C.P., Koch, A.A., and Young, K.P. (1988). *Metals handbook*, 9th ed., ASM International, Metals Park, OH, USA, 15, 327–338.

Kim, J.W., Weistroffer, H.R., and Redmond, R.T. (1993). “Expert systems for bond rating: a comparative analysis of statistical, rule-based and neural network systems”, *Expert Systems*, 10, 167-172.

Kirkwood, D.H., and Kapranos, P. (1989). "Semisolid Processing of Alloys." *Met. Mater.*, 5(1), 16-19.

Kirkwood, D.H. (1994). "Semi-solid metal processing." *Int. Mat. Rev.*, 39(5), 173-189.

Kiuchi, M., and Fukuoka, S. (1979). "Study on flow stress of alloys in mashy state." *Journal of Japan Society for Technology of Plasticity*, 20**,** 826-833.

Kiuchi, M., Sugiyama S. (1982). "Investigation into mashy state processing and working of particle reinforced composite metals." *J. Jap. Soc. for Technol. of Plast.*, 23, 915-923.

Kiuchi, M. (1987). "Application of mashy state working processes to production of metal ceramic composites." *Annals of CIRP*, 36(1), 173-176.

Kiuchi, M. (1989). *"Metal forming in mushy state in Plasticity and Modern metal forming technology."* Blazynski, T.Z. ed., Elsivier Applied Science., London & New York, 289-313.

Kiuchi, M., and Sugiyama, S. (1991). "Mushy state rolling of Aluminium alloys and Cast irons." *Annals of the CIRP*, 40, 259-261.

Kiuchi, M., and Sugiyama, S. (June 1992). "*Application of mashy metal processing and forging technologies to manufacturing fiber reinforced metals."* Proc. 2nd Int. Conf. on Semi-Solid Processing of Alloys and Composites, Brown SB, Flemings MC, eds., Cambridge, MA, USA. Warrendale, TMS (1992), 382-389.

Koike, S. (2002). "A class of adaptive size control algorithms for adaptive filters." *IEEE Trans. Signal Processes,* 50(6), 1315-1326.

Koke, J., and Modigell, M. (2003). "Flow behaviour of semisolid metal alloys." *Jour. Non-Newtonian Fluid Mech.,* 112, 141–160.

Kopp, R. (1996). "Some current developments in metal forming technology." *J. Mater. Process. Tech.,* 60, 1-9.

Kopp, R., Neudenberger, D., and Winning, G. (2001). "Different concepts of thixoforging and experiments for rheological data." *J. Mater. Process. Tech.,* 111, 48–52.

Kremer, S.C. (1995). "On the computational power of Elman style neural networks." *IEEE Trans. Neural Netw.,* 6, 1000-1004.

Kuan, C.M., Hornik,K., and White, H. (1994). "A convergence result for learning in recurrent neural networks." *Neural Computation,* 420-444.

Kusiak, J., and Kuziak, S. (2002). "Modelling of microstructure and mechanical properties of steel using artificial neural networks." *J. Mater. Process. Tech.,* 127, 115-121.

Lakshmi,S., Lu, L. and Gupta, M. (1998) "*In situ* preparation of TiB_2 reinforced Al based composites". *J. Mater. Process. Tech.,* 73, 160-166.

Lang, K.J., Waibet, A.H. and Hinton, G.E. (1990). "A time-delay neural network architecture for isolated word recognition". *Neural Networks,* 3, 23-44.

Lapedes, A., and Farber, R. (1988). "How neural network works." *Neural Network Processing Systems,* Anderson, and D. Z. eds., (Denver), American Institute of Physics, New York, 442-456.

Lapkowski, W. Sinczak, J. Rusz, S. (1997). "Feasibility of metal forming in semisolid state." *J. Mater. Process. Tech.,* 63, 260-264.

Lapkowski, W. (1998). "Some studies regarding thixoforming of metal alloys." J*our. Mater. Process. Technol.*, 80-81, 463-468.

Larkiola, J., Myllykeski, P., Nylander, J., and Korhonen, A.S. (1996). "Prediction of rolling force in cold rolling by using physical models and neural computing." *J. Mater. Process. Tech.*, 60(1-4), 381-386.

Larkiola, J., Myllykeski, P., Korhonen, A.S., and Cser, L. (1998). "The role of neural networks in optimisation of rolling processes." *J. Mater. Process. Tech.*, 80-81, 16-23.

Leatham, A., Ogilvy, A., Chesney, P., and Wood, P. (1989). "Osprey process-production flexibility in material manufacture." *Metals and Materials*, 5, 140-143.

Lee, H.I., Doherty, R.D. E.A. Feest, and Titchmarsh, J.M. (1983). "Structure and segregation of stir-cast aluminum alloys." *Proc. Int. Conf. on Solidification Technology in the Foundry and Cast house*, Warwick, Coventry, 1980 (The Metals Society, London (1983)), 119-125.

Lee,D.K., Jung, H.K., and Kang, C.G. (1994). "Filling Limitation in Intelligent Thixoforging Processing of Metal Matrix Composites and their Mechanical Properties." *Proc. 3rd Int. Conf. on Semi-Solid Processing of Alloys and Composites*, Kiuchi M, editor., Tokyo, Japan, June 1994. Tokyo Institute of Industrial Science (1994), 731-738.

Lehuy, H., Masounave, J. and Blain, J. (1985). "Rheological behaviour and microstructure of stir-casting zinc-aluminium alloys." *Mater. Sci.*, 20, 105–113.

Li, X., Chen, G, Chen, Z. And Yuan, Z. (2002). "Chaotifying linear Elman networks." *IEEE Trans. Neural Netw.*, 13(5), 11193-1199.

Li, M., Liu, X., Xiong, A. (2002). "Prediction of Mechanical properties of forged TC11 titanium alloy by ANN". *J. Mater. Process. Tech.*, 121, 1-4

Light, W.A. (1992). "Some aspects of radial basis function approximation." *Proc.,approximation Theory, Spline Functions and Applications*, Singh, S.P eds., NATO, ASI, Baston: Kluwer Academic Publishers, 256, 163-190.

Lippman, R.P. (1987). "An introduction to computing with neural nets." *IEEE ASSP Magazine*, 4, 4-22.

Liu, D., Atkinson, H.V., Kapranos, P., Jirattiticharoean, W., and Jones, H. (2003). "Microstructural evolution and tensile mechanical properties of thixoformed high performance aluminium alloys." *Mat. Sc. and Engg A.*, 361, 213-224.

Loue, W.R., Suery, M., Lquerbes, J. (June 1992). "Microstructure and rheology of partially remelted Al-Si alloys." *Proc. 2nd Int. Conf. on Semi-Solid Processing of Alloys and Composites*, Brown SB, Flemings MC, eds., Cambridge, MA, USA. Warrendale, TMS (1992), 266-275.

Loue, W.R., and Suery, M. (1995). "Microstructural evolution during partial remelting of Al-Si7Mg alloys." *Mater. Sci. Eng. A.,* 203, 1-13.

Mada, M., and Ajersch, F., (1996). "Rheological model of semisolid A356-SiC composite alloys. Part I. Dissociation of agglomerate Structures during shear." *Mater. Sci. Eng. A,* 212, 157–170.

Mada,M., and Ajersch, F. (1996). "Rheological model of semisolid A356-SiC composite alloys. Part II. Reconstitution of agglomerate structures at rest." *Mater. Sci. Eng. A,* 212, 171–177.

Maier, H.E., and Dandy, G.C. (1999). "Empirical comparison of various methods for training feed-Forward neural networks for salinity forecasting." *Water Resources Research,* 35, 2591-2596.

Mandal, A., Maiti, R., Chakraborty, M. and Murty, B.S. (2004). "Effect of TiB_2 particles on aging response of Al-Cu alloy". *Mater. Sci. and Eng. A.,* 386, 296-300.

Mandal A., (2007). "Studies on synthesis and characterisation of Al based *in situ* composites reinforced with TiB_2 particles". Ph.D. Thesis, Indian Institute of Technology, Kharagpur, India.

Mandal, S., Sivaprasad, P.V., Venugopal, S., and Murthy, K.P.N. (2009). "Artificial neural network modelling to evaluate and predict the deformation behaviour of stainless steel type AISI 304L during hot torsion." *Applied Soft Computing,* 9, 237-244.

Martinez, R.A., Figuredo, A., Yurko, J.A., and Flemings, M C. (2001). "Efficient formation of structures suitable for semi-solid forming." *Transactions of the 21st Intl. Die casting Congress (2001),* 47-54.

Martin, C.L., Kumar, P., and Brown, S.B. (1994). "Constitutive modeling and characterization of the flow behaviour of semisolid metal alloy slurries - 2. Structural evolution under shear deformation." *Acta. Metall. Mater.,* 42, 3603-3614.

Martinez, R.A. (2001) "A new technique for the formation of semi-solid structures." MS Thesis. Massachusetts Institute of Technology, Cambridge, MA.

Martinez, R.A., Karma, A., and Flemimgs, M C. (2006). "Spheroidal particle stability in semisolid processing." *Metall. Mater. Trans. A.,* **17,** 2807 –2815.

Mathur, P., Apelian, D., and Lawley, A. (1989). "Analysis of spray deposition process." *Acta Metall.,* 37(2), 429-443.

McCartney, D. G. (1989). "Grain refining of Aluminum and its alloys using inoculants." *Int. Mater. Rev.*, 34, 247-260

McLelland, A.R.A., Atkinson, H.V., Kapranos, P., and Kirkwood, D.H. (1991). "Thixoforming spray-formed aluminum silicon-carbide metal matrix composites." *Mater. Lett.*, 11(1-2), 26-30.

McCulloh, W.S., Pitts, W. (1943). "A logical calculus of the ideas immanent in nervous activity." *Bulletin of Mathematical biophysics,* 5, 115-133.

Mclelland, A.R.A., Henderson, N.G., Atkinson, H.V., Kirkwood, D.H. (1997). "Anomalous rheological behaviour of semi-solid alloy slurries at low shear rates." *Mater. Sci. Eng. A,* 232, 110–118.

Minsky, M.L. (1954). "Theory of neural analog reinforcement systems and its application to the brain model problem." Ph.D. thesis, Princeton University, Princeton, NJ, USA.

Minsky, M.L. (1961). "Steps towards artificial intelligence." *Proc. IRE,* 49, 5-30.

Minsky, M.L., Papert S.A. (1969). "*Perceptrons*." Cambridge: MA, MIT Press, 68-81.

Minghetti, T., Stone-hope, K., Nastran, M., Kuzman, K., Gullo, G.C., and Uggowitzer, P.J. (2001). "Advanced forming techniques for aluminum based metal matrix of composites." *Proc. Proc. 4th Int. Conf. ESAFORM Conference on material Forming,* Liege (B), 23-25.

Mirchandani, G., and Cao, W. (1989). "On hidden nodes for neural nets." IEEE *Trans. Circuits and systems*, 36(5), 661-664.

Miwa, K., Takashi, I., and Ohashi, T. (June 1992). "Fabrication of SiC whisker reinforced aluminium alloy matrix composites by compocasting process." *Proc. 2nd Int. Conf. on Semi-Solid Processing of Alloys and Composites,* Brown SB, Flemings MC, eds., Cambridge, MA, USA, J Warrendale, TMS (1992), 398-405.

Modigell, M., Koke, J., and Petera, J. (1999). "Time-dependent rheological properties of semisolid metal alloy." *Mech. Time-Depend. Mater.*, 3, 15–30.

Modigell, M., Koke, J., Kopp,R., Nuedenburger, D., Sahm, P.R., and Klaassen, O. (2000). "Comparison of rheological measurement methods for semi-solid alloys." *Proc. 6th Int. Conf. on Semi-Solid Processing of Alloys and Composites,* Chiarmetta GL, Rosso M, eds., Turin, Italy, Sept 2000, Brescia. Italy: Edimet Spa; (2000), 605-609.

Moon, H.K., Cornie, J.A., and Flemings, M.C. (1991). "Rheological behavior of SiC particulate (Al-6.5wt-percent-Si) composite slurries at temperatures above the liquidus and within the liquid + solid region of the matrix." *Mater. Sci. Engg, A,* 144, 253-265.

Moschini, R. (1996). "Mass production of Fuel Rails by pressure die casting in the semi liquid state." *In: Proc. 4th Int. Conf. on Semi-Solid Processing of Alloys and Composites,* Kirkwood DH, Kapranos P, eds., Sheffield, UK, June 1996, University of Sheffield, 248–250.

Mousavi Anijdah, S.M., Madaah-Hosseini, H., and Baharami, A. (2007). "Flow stress optimisation for 304 stainless steel under cold and warm compression by Artificial neural networks and genetic algorithm." *Materials and Design,* 28, 609-615.

Mullis, A.M. (1999). "Growth induced dendritic bending and rosette formation during solidification in a shearing flow." *Acta Mater.,* 47, 1783-1789.

Murty, B.S. Kori, S.A. Chakraborty, M. (2002). "Grain refinement of Al and its alloys by heterogeneous nucleation and alloying." *Int. Mater, Rev.,* 47(1), 3-29.

Nafisi, S., and Ghomashchi, R. (2005). "Semi-solid metal processing routes: An overview." *Can. Metall. Q.,* 44(3), 289-304.

Naidermaier, F., Langgarther, J., Hirt, G. And Niedic I. (1998). "Horizontal continuous casting of SSM Billets." *Proc. 5th Int. Conf. on Semi-solid Processing of Alloys and Composites,* Bhasin, AK, Moore, J.J., young K.P., Midson, S. eds., Golden Colrado, USA, June 1998, Golden CO; Colrado, Scool of Mines, USA(1998), 407-414.

Narendra, K. and Parthasarathy, K. (1990)"Identification and control of dynamical systems using neural networks". *IEEE Trans. Neural Netw.,* 1 (1), 4-27.

Nozer, M. (1993). "Neural net architectures for temporal sequence processing." *Predicting the failure and understanding the part,* Weigend, A., Gershenfeld, N. eds., Redwood city, CA: Addison-Wesley.

Pasternak, L., Carnahan, R., Decker, R., and Kilbert, R. (1992a). "Semi-solid production processing of magnesium alloy by Thixomoulding." *Proc. 2nd Int. Conf. on Semi-Solid Processing of Alloys and Composites,* Brown, S.B., Flemings, M.C., eds., Cambridge, MA, USA, June 1992, Warrendale, TMS, 398-405.

Pasternak, L., Carnahan, R., Decker, R., and Kilbert, R. (1992b). "Semisolid production processing of magnesium alloys by Thixomoulding." *Proc. 2nd Int. Conf. on semisolid processing of alloys and Composites,* Brown, S.B., Flemings, M.C., eds. Cambridge, MA. USA, June 1992, Warrendale, TMS, 159-169.

Patuwo, E., Hu, M.Y., and Hung, M.S. (1993). “Two-group classification using neural networks.” *Decision Sciences,* 24(4), 825-845.

Peng, H., Wang, S.P., Wang, N., and Wang, K.K. (1994). "Rheomolding – Injection Molding of Semi-Solid Metals." *Proc. 3rd Int. Conf. on Semi-Solid Processing of Alloys and Composites,* Kiuchi M, editor., Tokyo, Japan, June 1994. Tokyo Institute of Industrial Science (1994) 191–200.

Peng, H., and Wang, K.K. (1996). “Steady-state and transient rheological behavior of a semi-solid tin–lead alloy in simple shear flow." *Proc. 4th Int. Conf. on Semi-Solid Processing of Alloys and Composites,* Kirkwood D.H., Kapranos P, eds., Sheffield, UK, June 1996, University of Sheffield, 2-9.

Peng, H. Hsu, W.M. (September 2000). "Development on rheomolding of magnesium parts." *In: Proc. 6th Int. Conf. Semi Solid Processing of Alloys and Composites,* Chiarmetta GL, Rosso M, eds. Turin, Italy, Edimet Spa, 313–317.

Peng, Z., Yun-hui, D., Xing, S., Zhang, L., Zeng, D. and Li-min, B. (2002). “Semi-solid Processing of Steel-Al-7 Graphite Binding plate”. *J. of Wuhan Univ. of Tech.-Mater. Sci. Ed.,* 17(3), 46-49.

Plett, G.L. (2003). “Adaptive inverse control of linear and non linear systems using dynamic neural networks.” *IEEE Trans. Neural Netw.,* 14(2), 360-376.

Poppe, T., Obradevic, D., and Schlang, M. (1995). “Neural networks: reducing energy and raw materials requirements*.” Siemens review – R&D Special*, Fall (1995), 24-27.

Potzinger,R., Kaufmann, H., and Uggowitzer, P.J., (2000). "Magnesium New Rheocasting - A Novel Approach To High Quality Magnesium Castings." *Proc. 6th Int. Conf. on Semi-Solid Processing of Alloys and Composites,* Chiarmetta GL, Rosso M, eds., Turin, Italy, Sept 2000, Brescia. Italy: Edimet Spa: (2000), 85-90.

Powell, B.J.D. (1985). “Radial basis functions for multivariable interpolation: A review.’ *Proc. IMA Conference on algorithms for the approximation of Functions and Data* RMCS, Shrevenhem, England, 143-167.

Quaak, C. J., Horsten, M. G., and Kool, W. H. (1994). "Rheological behaviour of partially solidified aluminium matrix composites." *Mater. Sci. Engg, A,* 183, 247-256.

Quaak, C. J., Katgerman,, L., and Kool, W.H. (1996). "Viscosity evolution of partially solidified aluminium slurries after a shear rate jump.” *Proc. 4th Int. Conf. on Semi-Solid Processing of Alloys and Composites,* Kirkwood DH, Kapranos P, eds., Sheffield, UK, June 1996, University of Sheffield, 35–39.

Rachmat, R.S., Takano, H., Ikeya, N., Kamado, S., and Kojima,Y. (2000). "Application of semi-solid forming to 2024 and 7075 wrought aluminum billets fabricated by the EMC process." *Mater. Sci. Forum,* 329(3), 487-492.

Raj, R., Ashby, M.F. (1971). "On grain boundary sliding and diffusional creep". *Metall. Trans.,* 2, 1113-1127.

Rao, K.P., and Prasad, Y.K.D.V. (1995). "Neural network approach to flow stress evaluation in hot deformation." *J. Mater. Process. Tech.,* 53(3-4), 552-566.

Rao, B.P.C., Raj, B., Jayakumar, T., and Kalyanasundaram, P. (2002). "An artificial neural network for eddy current testing of austenitic stainless steel welds.' *NDT & E International,* 35, 393-398.

Reddy, N.S. (2004). "Study of some complex metallurgical systems by Computational Intelligence techniques." Ph.D. thesis, Indian Institute of Technology, Kharagpur, India.

Reddy, N.S., Prasad Rao, A.K., Chakraborty, M., and Murty, B.S. (2005). "Prediction of grain size of Al_7Si alloy by neural networks." *Mater. Sci. and Eng. A,* 391, 131-140.

Reddy N.S., Lee Y. H., Park C. H., Lee S. C. (2008). "Prediction of flow stress in Ti-6Al- 4V alloy with an equiaxed α + β microstructure by artificial neural networks." *Mater. Sci. and Engg. A,* 492(1-2), 276-282.

Rice, C. S., and Mendez, P.F. (2001). *"Slurry based semisolid die casting." Adv. Mater. Proc.,* 159(10), 49-52.

Ripley, B.D. (1994). "Neural networks and related methods for classification." *Journal of the Royal Statistical society, series B, Methodological,* 56(3), 409-456.

Rosenblatt, F. (1958). "The Perceptron: A probabilistic model for information storage and organisation in the brain." *Psychological Review,* 3, 461-483.

Rovira,M.M., Lancini,B.C., and Robert, M.H. (1999). *"Thixo-forming of Al-Cu alloys." J. Mater. Process. Tech.,* 92-93, 42-49.

Roy, B.M. Venkataraman, V.V. Bhanuprasad, Y.R. Mahajan, G., Sundararajan. (1992). "The effect of particulate reinforcement on the sliding wear behaviour of aluminium matrix composites." *Metall. Mater. Trans. A,* 23, 2833–2847.

Rumelhart, D.E., MeClelland J.C. (1986*).* In: *Parallel distributed processing: Explorations in the Microstructure of Cognition*, vol. 1, Cambridge, MA: MIT Press.

Rumelhart, D.E., Hinton, G.E., and Williams R.J. (1986a). "Learning internal representations by error propagation." In *Parallel distributed processing: Explorations in the Microstructure of Cognition*, vol. 1, Rumelhart, D.E., MeClelland J.C. and the PDP Reasearch group, eds., Cambridge, MA: MIT Press, 318-362.

Sahoo, P. and Koczak, J. (1991). "Microstructure Property – Relationships of in situ reacted TiC/Al-Cu metal Matrix composites". *Mate. Sci. and Eng. A,* 131, 69-76

Salvo, L., Loue, W.R., and Suery, M. (1995). "Influence of prior solidification conditions on the structure and rheological behaviour of partially remelted Al-Si alloys." *ISIJ Intl.,* 35, 798-804.

Sano, H., Tosiane, N., Chikubo, Y. *et al.* (1992). "Spray formed aluminium alloy components for automotive applications.' *Proc. 2nd Int. Conf. Spray Forming, Osprey Metals,* Neath, UK, 363-375.

Sannes, S., Gjestland, H., Arnberg, L., and Solberg, J.K. (1994a). "Microstructure Coarsening of Semi-Solid Mg Alloys." *Proc. 3rd Int. Conf. on Semi-Solid Processing of Alloys and Composites,* Kiuchi M, ed., Tokyo, Japan, June 1994. Tokyo Institute of Industrial Science, 75-84.

Sannes,S., Gjestland ,H., Arnberg, L., and Solberg, J.K. (1994b). "Yield Point Behaviour of Semi-Solid Mg. Alloys." *Proc. 3rd Int. Conf. on Semi-Solid Processing of Alloys and Composites,* Kiuchi M, ed., Tokyo, Japan, June 1994. Tokyo Institute of Industrial Science, 271-280.

Seconde, J.F., and Suery, M. (1984). "Effect of solidification conditions on deformation-behaviour of semi-solid Sn-Pb alloys." *J. Mater. Sci.,* 19, 3995-4006.

Selvakumar, N., Ganesan P., Radha, P., Narayanasamy, P. and Pandey, K. (2007). "Modelling the effect of particle size and iron content on forming of Al–Fe composite preforms using neural network".*Materials and Design,* 28, 119-130.

Sevan-Schreiber, D., Cleeremans, A., and MeClelland, J. (1988). Carnegie, Mellon Univ. Tech. Rep. CMV-CS-88-193.

Sharda, R. and Patil (1994). "Neural Networks for the OR/MS Analyst: An Application Bibliography." *Interfaces,* 24, 116-130.

Sherby, O.D., Wadsworth, J.D. (1989). "Superplasticity – recent advances and future directions." *Prog. Mater. Sci.,* 33, 169-221

Siddhalingeshwar, I.G. (2011). "Microstructure-Property relationship in mushy state rolled in-situ Al-4.5Cu-5TiB_2 composite." Ph.D. thesis, Indian Institute of Technology, Kharagpur, India.

Siegert, K., Wolf, A., and Baur, J. (2000). "Thixoforging of Aluminium and Brass." *Production Engineering* (Annals of the German Academic Society for Production Engineering, VII/1, 21 – 24.

Sigworth, G.K. (1996). "Rheological properties of metal alloys in the semi-solidstate." *Can. Metall. Q.*, 35, 101-122.

Skolianos, S. and Kattamis, T.Z. (1993) "Tribological properties of cast SiC_p reinforced Al-4.5%Cu-1.5% Mg alloy." *Mater. Sci. Eng. A.,* 163, 107-114.

Skolianos, S. (1996) "M.echanical behavior of cast SiC_p reinforced Al-4.5%Cu-1.5% Mg alloy." *Mater. Sci. Eng. A.,* 369, 76-82.

Song, Q., Spall, J., Soh, Y.C., and Ni, J. (2008). "Robust neural network tracking controller using simultaneous perturbation stochastic approximation." *IEEE Trans. Neural Netw.,* 19(5), 817-835.

Song, Q., Wu, Y.L., and Soh, Y.C. (2008a). "Robust adaptive gradient descent training algorithm for recurrent neural networks in discrete time domain." *IEEE Trans. Neural Netw.,* 19(11), 1841-1853.

Song, Q., Soh, Y.C., and Zhao, L. (2009). "A robust extended Elman backpropagation algorithm" In: *Proc., Int. Joint Conf. Neural Netw.,* Atlanta, Georgia, USA, 2971-2977.

Song, Q. (2010). "On the weight convergence of Elman networks." *IEEE Trans. Neural Netw.,* 21(3), 463-480.

Spencer, D. Mehrabian, B. R., and Fleming, M. C. (1972). "The rheological behaviour of Sn-15Pb in the crystallization range." *Metall. Trans. A,* 3, 1925-1932.

Srinivasan, V., Valsan, M., Rao, K.B.S., Mannan, S.L., and Raj, B. (2003). "Low cycle and creep interaction behaviour of 316L(N) stainless steel and life prediction by artificial neural network approach." *Int. J. Fatigue,* 25, 1327-1338.

Stern, H.S. (1996). "Neural networks in applied statistics." *Techno Metrics,* 38, 205-214.

Su, J., Li, H., Liu, P., Dong, Q., and Li, A. (2007). "Aging process for a copper alloy considering hardness and electrical conductivity." *Comp. Mater. Sci.,* 38, 697-701.

Subramanian, V., Hung, M.S., and Hu, M.Y. (1993). "An experimental evaluation of neural networks for classification." *Computers and Operations research,* 20(7), 769-782.

Suery, M., Martin,C.L., and Salvo, L. (1996*). "Overview of the rheological behaviour of globular and dendritic slurries." Proc. 4th Int. Conf. on Semi-Solid Processing of Alloys and Composites,* Kirkwood DH, Kapranos P, eds., Sheffield, UK, June 1996, University of Sheffield, 21-29.

Sukimoto, M., Iwai, I. and I. Murase. (1986). In Aluminium Technology '86: *Proceedings of the International Conference,* Institute of Metals, London (1986) 557-564.

Sukumaran, K. Pai, B.C. Chakraborty, M. (2004). "The effect of isothermal stirring on an Al-Si alloy in the semisolid condition*." Mater. Sci. Eng. A,* 369, 275-283.

Sun, X., Chang, C., Liu, X., Wang, G., and Yu, B. (1995). *Iron and Steel (China),* 30(11), 26-29.

Taha, M.A., Elmahallawy, N.A., and Assar, A.M. (1988). "Control of the continuous rheocasting process. 1. Heat flow model 2. Rheological behaviour analysis." *J. Mater. Sci.,* 23, 1379–1390.

Tan, W., Liu, Z., Wu, D., and Wang, G. (2009). "Artificial neural network modelling of microstructure during C-Mn and HSLA plate rolling." *J. Iron and Steel,* 16(2), 80-83.

Teasauro, G.,Touretzky, G. and Leen, T. (1995). *"An experimental comparison of Recurrent Neural Networks".* MIT Press, 697-704.

Tietmann, A., Bremer, T., Hirt, G., and Kopp, R. (1992). "Preliminary results in thixoforging aluminum wrought alloys." *Proc. 2nd Int. Conf. on Semi-Solid Processing of Alloys and Composites,* Brown SB, Flemings MC, eds., Cambridge, MA, USA, June 1992. Warrendale, TMS, 170-179.

Turng, L.S., and Wang,K.K. (1991). "Rheological behaviour and modelling of semi-solid Sn-15 Pb alloy." *J. Mater. Sci.,* 26, 2173–2183.

Turczyn, S., and Malinowski, Z. (1996a). *"Split ends and central burst defects in rolling materials processing defects."* Elsevier, Ghosh, S.K., and Predeleance, M., eds., 401-416.

Turkeli,A., and Akbas,, N. (1996). "Formation of non-dendritic structure in 7075 wrought aluminum alloy by SIMA process and effect of heat treatment." *Proc. 4th Int. Conf. on Semi-Solid Processing of Alloys and Composites,* Kirkwood DH, Kapranos P, eds., Sheffield, UK, June 1996, University of Sheffield, 1–74.

Tzimas, E., and Zavaliangos, A. (1999). "Mechanical behaviour of alloys with equiaxed microstructure in the semisolid state at high solid content." *Acta Mater.,* 47(2), 517-528.

Tzimas, E., and Zavaliangos, A., (2000a). "Evaluation of volume fraction of solid in alloys formed by semisolid processing." *J. Mater. Sci.,* 35, 5319-5329.

Tzimas, E., and Zavaliangos, A. (2000b). "Evolution of near-equiaxed microstructure in the semisolid state." *Mater. Sci. Eng. A.,* 289, 228-240.

Valer, J., Meneses, J.P., Antonin, F.S., and Suery, M. (1999). "Microstructural and mechanical characterization of an Al-21.8 wt.% Ge brazing alloy with a globular morphology of the primary Al-rich phase." *Mater. Sci. Eng. A.,* 272, 342-350.

Vives,C. (1992). "Elaboration of semisolid alloy by means of new electro magnetic rheocasting processes." *Metall. Trans.* B, 23(2), 189-205.

Vives, C., Bas,J., Beltran, G., and Fontaine, G. (1993). "Fabrication of metal-matrix composites using a helical induction stirrer." *Mater. Sci. Eng. A.,* 173, 239-242.

Vogel, A., and Cantor, B. (1977). "Stability of a spherical particle growing from a stirred melt." *J. Cryst. Growth,* 37, 309-316.

Vogel, A. (1977). PhD Thesis, University of Sussex, U.K.

Vogel, A., Doherty, R.D., and Cantor, B. (1979). "Stircast microstructure and slow crack growth." In: Proc. Int. Conf. on Solidification and casting of Metals, *The Metals Society,* London (1979), 518-525.

Wabbuseg, H., Kaufmann, H., and Uggowitzer, P.J. (2000). "Struktur und Eigenschaften von New Rheocasting-Bauteilen." *Giesserei* 87, 39-43.

Waluka, D., LeBeau, S., Prewitt, N., and Decker, R. (2000). "Thixomoulding technology opportunities and practical uses." *Proc. 6th Int. conf. Seemi Solid processing of Alloys and Composites,* Chiarmetta Gl, Rosso M, eds., Turin, Italy, September 2000: Edimet Spa, 109-114.

Wan, G., Witulski, T., and Hirt, G. (1993). "Thixoforming of Al alloys using modified chemical grain refinement for billet production." *Proc. Int. Conf. on aluminium alloys, New Process Technologies,* Marine di Ravenna, Italy, Assiciazona di Metallurgia, 3-4 June, 129-141.

Wang, D.H., Liu, Z.Y., Wank, G.D., Zhang, Q., Jiang, H.S., and Wang, H.S. (1995). "Predicting mechanical properties of hot rolled strip using neural network." *Iron and Steel (China),* 30(1), 28-31.

Wang, N. Peng, H., and Wang,K.K. (1996). "Assessment of porosity level in rheomolded parts." In: *Proc. 4th Int. Conf. on Semi-Solid Processing of Alloys and Composites.* Kirkwood DH, Kapranos P, eds., Sheffield, UK, June 1996, University of Sheffield, 342-346.

Wang, H., and Xu, J. (2006). "Semisolid casting of automotive component, Water pump lid." *Solid state phenomena*, 116-117, 88-91.

Wang, H. Davidson, C.J. St. John, D. H. (2000a). "The semisolid shear properties and casting behaviour of Al7Si0.3Mg alloys produced by low temperature pouring." *Proc. 6th Int. Conf. on Semi-Solid Processing of Alloys and Composites*, Chiarmetta GL, Rosso M, eds., Turin, Italy, Sept 2000, Brescia. Italy: Edimet Spa: 149-154.

Wang, H., St. John, D. H., Davidson, C.J., and Couper, M.J. (2000b). "Characterization and shear behaviour of semi solid Al-7Si-0.35Mg alloy microstructures." *Aluminium Trans.*, 2, 57-66.

Wang, H. St. John, D. H. Davidson, C.J. Couper, M.J. (2000c). "Comparison of the semisolid shear behaviour of Al-7Si-0.35Mg alloys produced by two casting method." *Mater. Sci. Forum.*, 329-330, 449-454.

Ward, P.J., Atkinson, H.V., Anderson, P.R.G., Elias, L.G., Garcia, B., Kahlen, L., and Rodriguez-Ibabe, J.M. (1996). "Semi-solid processing of novel MMCs based on hypereutectic aluminium-silicon alloys." *Acta Metall. et Mater.*, 44, 1717–1727.

Widrow, B., Hoff, M.E. (1960). "Adaptive switching circuits." *Proc. IRE Wescon Convention Record*, 4, 96-104.

Widrow, B., Rumelhart D.E., and Lehr, M.A. (1994). "Neural Networks: Applications in industry, business and science." *Communication of the ACM*, 37, 93-105.

Wood, J.V., Davies, P. and Kellie, J.L.F. (1993) "Properties of reactively cast Aluminium-TiB_2 alloys". *Mater. Sci. Tech.*, 9, 833-840.

Worgotter, F., and Porr, B. (2005). "Temporal sequence learning, prediction and control – A review of different models and their relation to biological mechanisms." *Neural Computation*, 17(2), 245-319.

Xia, K., and Tausig, G., (1998). "Liquidus casting of a wrought aluminum alloy 2618 for thixoforming." *Mater. Sci. Eng. A.*, 246, 1-10.

Xie, L., Xu, J., Yang, B., Zhang, Z., and Shi, L. (2006). "Thixoforming and Industrial applications of semisolid alloy Al-6Si-2Mg." *Solid state phenomena*, 116-117, 72-75.

Yang, L.J. (2003). "Wear coefficient equation for aluminium based matrix composites against steel disc'. *Wear*, 255, 579-592.

Yoon, Y., Swales, G., and Margario, T.M. (1993). "A comparison of discriminant analysis versus artificial neural networks." *Journal of Operational Research Society*, 44, 51-60.

Youn, S. W., Kang, C. G. and Seo, P. K. (2002). “Mechanical characteristics evaluation of hollow shape part with metal matrix composites fabricated by thixoforging process.” *J. Mater. Process. Tech.*, 130-131**,** 574-580.

Young, K.P., Kyonka,C., and Courtois, F. (1983). "Fine grained metal composition." United States Patent No. 4415374, November 15 (1983).

Young, K.P., Tyler, D.E., Cheskis, H.P., and Watson, W.G. (1984). "Process and apparatus for continuous slurry casting." United States Patent No. 4482012, November 13 (1984).

Yurko, J.A., Niu, X.P., and Pinwill, I. (1999). "Thixocasting of a near-liquidus cast Al-Mg based alloy." *J. Mater. Sci. Lett.*, 18, 1869-1870.

Yurko, J.A., Martinez, R.A., and Flemings, M C. (2003). “Commercial development of the Semi-Solid Rheocasting (SSR)." *Transactions of the 21st Intl. Die casting Congress,* 379-384.

Zhang, H., and Wang, J.N. (2001). "Thixoforming of spray-formed 6066Al/SiCp composites*." Compos. Sci. and Technol.,* 61, 1233–1238.

Zhicago, S., He, Y. and Ze, T. (2010). “Microstructural evolution model of TA15 titanium alloy based on BP neural network method and application in isothermal deformation”. *Computational Material Science*, 50, 308-318.

Zillgen, M., and Hirt, G. (1996). "Microstructural Effects of Electro-magnetic Stirring in Continuous Casting of Various Aluminum Alloys." *Proc. 4th Int. Conf. on Semi-Solid Processing of Alloys and Composites,* Kirkwood DH, Kapranos P, eds., Sheffield, UK, June 1996, University of Sheffield, 180-186.

Zoqui, E. J., and Robert, M. H. (1998). "Structural modification in rheocast Al-Cu alloys by heat treatment and implications on mechanical properties." *J. Mater. Process. Tech.*, 78, 198-203.

Zoqui, E., and J. Robert, M. H. (2001). "Contribution to the study of mechanisms involved in the formation of rheocast structure." *J. Mater. Process. Tech.*, 109, 215-219.

Zoqui, E.J., Shehata, M.T., Paes, M., Kao, V., Es-Sadiqi, E. (2002). “Morphological evolution of A356 during partial remelting.” *Mater. Sci. Eng. A.,* 325, 38-53.

Zoqui, E. J. (2003). "Morphological analysis of SSM Al-4.5wt % Cu measured by the rheocast quality index." *J. Mater. Process. Tech.*, 135-144, 195-201.

Zu Lijjun and Luo Shoujing (2001). "Study on the powder mixing and semi-solid extrusion forming process of SiCp/2024Al composites." *J. Mater. Process. Tech.,* 114(3), 189-193.

ASM Handbook. (1992), "Friction, lubrication and wear". 18, 785-794 & 801-811.

ASM Handbook, (1992). Vol. 3, ASM International, Materials Park, OH, USA, 4, 1.23 & 1.24.

ASM Handbook, (1997). *Heat treating,* ASM International, Materials Park, OH, USA, 4, 841-887.

Annual Book of ASTM standards. (2003). ASTM standard E 112-96^{e2}, Philadelphia, PA, United States.

Berry, M.J.A., and Linoff, G. (1997). "*Data mining techniques for marketing sales and customer support*." John Wiley and Sons, New York.

Bezdek, J.C. (1994). "Computational Intelligence: Imitating Life." Zurada, J.M., Marks II, R.J., Robinson, IEEE Press.

Dieter, G.E. (1986). *"Mechanical Metallurgy".* Third Edition, McGraw Hill Book Co., New York, NY, 586.

Haykin, S. (2004). "*Neural Networks: A comprehensive Foundation."* Pearson Education (Singapore) Pte. Ltd., 482, F.I.E., Patparganj, Delhi.

Hebb, D.O. (1949). "*The organisation of behaviour: A neuropsychological Theory*." Wiley, New York.

Hecht-Nielsen, R. (1991). "*Neurocomputing."* Addison Wesley Publishing Company, Inc., USA.

Jordan, M. (1986). "Serial order: A parallel distributed processing approach." *Advances in Connectionist Theory: Speech,* Elman, J.L., Rumelhart, D.E., eds., New Jersey, Erlbaum, Hillsdale.

Kolen, G.F. (2001). *"A Field Guide to Dynamical Recurrent Networks."* New York, IEEE Press.

Mandic, D.P., and Chambers, A. (2001). *"Recurrent neural networks for prediction: Learning, Algorithms, Architecture and Stability."* Chichester UK: Wiley.

McCullagh, P.C., and Nelder, J.A. (1989). "*Generalised Linear Models."* Chapman & Hall, London.

Metals handbook, 10th ed., ASM International, Metals Park, OH, USA, 2 (1990).

Muller, B. and Reinhardt, J. (1991). "Neural Network: An Introduction." *Physics of Neural Networks,* Springer-Verlag, New York.

Muroga, S. (1971). "*Threshold Logic and its Application."* Wiley Interscience, New York.

Pedriyez, W. (1998). "*Computational Intelligence An Introduction*." CRS Press, Boca Raton, New York.

Rabinowicz, E. (1965). *"Friction and wear of materials".* John Wiley and sons, New York, USA, 168-169.

Sutton, R.S., and Barto, A.G. (2002). "*Reinforcement learning: An Introduction."* Bradford Books, MIT Press, Cambridge.

Swingler, K. (1996). "*Applying Neural Networks: A Practical Guide."* Academic Press, Harcourt, Brace and Company, Publishers, London.

Szezepaniak, P.S. (1999). "*Computational Intelligence and applications."* Physica-Verlag, Springer-Verlag, Heidelberg, New York.

Yegnanarayana, B. (2008). *"Artificial Neural Networks."* PHI Pvt. Ltd., New Delhi, India.

Zurada, J.M., Marks II, R.J., and Robinson, C.J. (1994). eds. *"Computational Intelligence Imitating Life"*. IEEE Press.

Zurada, J. (2003). *"Introduction to Artificial Neural Systems".* Jaico Publishing House, Mumbai, India.

Potts, W.J.E. (2000) Neural Network modelling course notes, Cary, NC, SAS institute.

LIST OF PUBLICATIONS

International Journal Papers:

1. "Convergence of Recurrent Neural Networks Using Partially Trained ANN." *International Journal of Engineering Research and Technology (IJERT)*, Vol. 1, No. 5, 1-14.
2. "Prediction of Bimodal Grain Size in Mushy State Rolled Al - 4.5Cu - 5 TiB_2 Composite Using Artificial Neural Networks." *Materials and Design"*, Under review.

International Conferences:

1. "*Correlation of Grain Size with process parameters and Wt. % TiB_2 in Al - 4.5(wt. %) Cu - 5 (wt. %) TiB_2 Composite Using Artificial Neural Networks."* 4th International Conference on Advances in Mechanical Engineering, S.V. National Institute of Technology, Surat, Gujrat, Sept, 2010.
2. *"Prediction of grain size and hardness in pre hot rolled Al-4.5(wt. %) Cu-5(wt. %) TiB_2 composite using artificial neural networks."* International Conference on Reliability, Infocom Technology and Optimization 2010, Lingaya's University, Nov, 2010.
3. *"Correlation of hardness, microstructural properties and phase parameters with wear properties during the mushy state rolling of Al-4.5Cu-5TiB_2 composite, using Artificial Neural Networks."* International Conference on Mathematical Modelling and Applications to Industrial Problems, NIT Calicut, March, 2011.

RESUME

The author Akshay V. Nigalye was born on 22nd October 1964 at Vasco – Da - Gama, Goa. He obtained his primary education in Government Primary School, Vaddem, Vasco – Da -Gama, Goa. He completed his secondary and higher secondary education in St. Joseph's Institute and M.E.S. Higher Secondary school, Vasco – Da - Gama, Goa respectively. He secured his Bachelors degree in Mechanical Engineering from Bombay University in the year 1988 with First Class (Honours). He worked with M/s Goa Auto Accessories Ltd., Goa for a brief period of one year as Graduate Engineer Trainee and then worked as Assistant Production Engineer with M/s United Lead Oxide Products (Pvt.) Ltd., for 3 years. He later joined Institute of Shipbuilding Technology, Goa as lecturer in Mechanical Engineering. He obtained his Masters degree in Machine Design from Bombay University in the year 1998 securing First Class with Distinction. He became Head of Department (Mechanical Engineering) at Institute of shipbuilding Technology, Goa in the year 1999 and then took over as Principal in the year 2005. Presently he is working as a teaching faculty in Department of Mechanical Engineering of Goa College of Engineering.

The author is a member of Society of Automobile Engineers India. He is also the advisor for the Students' Chapter **SAEINDIA** at Goa College of Engineering, Farmagudi, Ponda, Goa.

The author has published a part of his research work in the form of papers in three International Conferences and one paper in an International Journal. The papers in International Conferences have been presented at SVNIT Surat, NIT Calicut and Lingaya's University, Faridabad, Harayana. The author also has submitted a paper to an International Journal which is presently under review.

The author has been associated with testing of materials. He has expertise in the use of Universal Testing Machines, Brinell and Rockwell Hardness Testing Machine and universal Impact Testing machine. His research interests include Neural Network modelling of mushy state forming processes and conventional high temperature forming processes.